

ROLE OF CELL MATRIX ADHESION IN REGULATING GOLGI ORGANIZATION AND FUNCTION

A THESIS

SUBMITTED IN PARTIAL FULFILLMENT OF THE REQUIREMENTS

OF THE DEGREE OF

DOCTOR OF PHILOSOPHY

BY

VIBHA SINGH

20123177

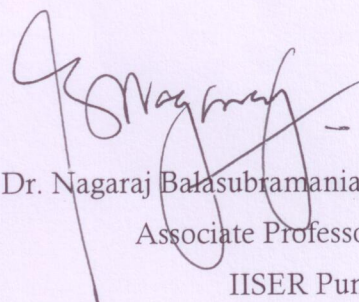


**INDIAN INSTITUTE OF SCIENCE EDUCATION AND RESEARCH
PUNE**

2018

CERTIFICATE BY SUPERVISOR

I certify that the thesis entitled "**Role of cell-matrix adhesion in regulating Golgi organization and function**" presented by **Ms. Vibha Singh** represents her original work which was carried out by her at IISER, Pune under my guidance and supervision during the period from **August 1st 2012** to **March 5th 2018**. The work presented here or any part of it has not been included in any other thesis submitted previously for the award of any degree or diploma from any other University or institutions. I further certify that the above statements made by her in regard to her thesis are correct to the best of my knowledge.



Dr. Nagaraj Balasubramanian
Associate Professor
IISER Pune

Date: **MAR 5, 2018**

DECLARATION

I declare that this written submission represents my idea in my own words and where others' ideas have been included; I have adequately cited and referenced the original sources. I also declare that I have adhered to all principles of academic honesty and integrity and have not misrepresented or fabricated or falsified any idea/data/fact/source in my submission. I understand that violation of the above will be cause for disciplinary action by the Institute and can also evoke penal action from the sources which have thus not been properly cited or from whom proper permission has not been taken when needed.

Vibha Singh

Vibha Singh

Reg. No. 20123177

Date: 05/03/2018

Acknowledgments

First and foremost I would like to thank my Ph.D. supervisor Dr. Nagaraj Balasubramanian for giving me the opportunity to pursue my graduate studies in his laboratory. I thank him to provide the liberty to do experiments of my choice and at the same time, guided and streamlined those as addition to the story. Perhaps the most valuable lesson that I have learned from Nagaraj is the scientific approach: how to think and design experiments and evaluate the work of others. I also would like to thank him for teaching how to communicate research ideas and findings in person and on paper.

I thank members of my Research Advisory Committee - Dr. Thomas Pucadyil (IISER Pune), Dr. Richa Rikhy (IISER Pune) and Dr. Deepa Subramanyam (NCCS Pune) for their timely inputs and suggestion which help better planning of the project.

I thank management and authorities at IISER Pune for providing excellent infrastructure and the necessary equipment and resources and Wellcome-DBT India Alliance for funding the research in the lab. I thank Sujaya Ingale at Venture Center NCL for help with flow cytometry studies. I acknowledge microscopy facility at IISER for providing a smooth access and technical help with the confocal microscopes. I also thank all the faculty and colleagues at Biology department at IISER Pune for help with reagents and technical assistance and their time in discussing the project.

I thank my fellow lab mates in Cell adhesion group Trupti, Archana, Siddhi, Natasha, Neha and Keerthi who contributed immensely at my personal and professional time at IISER. The group has been a source of support and a great help in troubleshooting experiments, discussion during lab meetings.

My time at IISER was made enjoyable and fun at large part by my friends and I am extremely thankful to Trupti, Aditi, Shubhankar, Ankitha, Neha, and Ayantika who all have been very supportive in a very special way and I have learned a lot from them.

A special thanks to Harshini and Manawa for their immense support, advice, and encouragement. I thank my old friend Poornima for her best wishes.

This thesis would have been difficult without the constant support and well wishes of my family. I dedicate this thesis to my parents for their unconditional love, patience, and blessings to see this achievement come true. My brothers, parent in laws, sister in laws have been equally supportive and understanding and I thank all of them. And most of all I owe a tremendous thanks to my extremely supportive husband Manish for being so appreciative and helpful during the final stages of my Ph.D.

Vibha Singh

March 2018

Contents

<u>Sr. No.</u>	<u>Title</u>	<u>Page Number</u>
	Essential abbreviations	
	Abstract	
	Synopsis	
	Chapter 1: Introduction and Review of literature.....	28
1.1	Integrins: Role and regulation.....	29
1.1.1	What are integrins?	29
1.1.2	How do integrins work?	31
1.1.3	Cellular functions regulated by integrins.....	34
1.1.4	Integrin dependent membrane trafficking.....	37
1.2	The Golgi apparatus.....	40
1.2.1	Golgi apparatus Discovery and early perspective.....	40
1.2.2	Structural components of the Golgi apparatus.....	42
1.2.3	Regulators holding up the Golgi.....	46
1.2.4	Golgi Endoplasmic reticulum connection.....	52
1.3	Cellular functions regulated by the Golgi.....	56
1.3.1	Golgi mediated Cellular functions.....	56
1.3.2	Trafficking through Secretory pathway.....	57
1.3.3	Glycosylation	62
1.3.4	Golgi trafficking and glycosylation in disease condition.....	64
1.4	Golgi fragmentation in normal cellular function and disease.....	65
1.4.1	Golgi fragmentation during mitosis.....	65
1.4.2	Regulators of mitotic Golgi fragmentation.....	68
1.4.3	Golgi fragmentation during meiosis, apoptosis.....	70
1.4.4.	Golgi fragmentation in disease conditions.....	71
1.5	Hypothesis and Objectives of the thesis.....	73

	Chapter 2: Materials and Methodology	74
2.1	Materials	75
2.1.1	Reagents.....	75
2.1.2	Antibodies.....	75
2.1.3	Plasmids.....	76
2.2	Methods commonly used throughout the study	77
2.2.1	Cell culture and transfections.....	77
2.2.2	Suspension and re-adhesion of cells.....	78
2.2.3	GM1 labeling of cells with CTxB.....	80
2.2.4	Measuring Cell volume using surface GM1 labelled suspended and re-adherent cells.....	80
2.2.5	Binding of fibronectin and poly L-Lysine coated beads to cells.....	80
2.2.6	Spatial Golgi localization relative to the cell-bound fibronectin coated bead.....	81
2.2.7	Inhibitors studies.....	82
2.2.8	Arf1 activity assay.....	82
2.2.9	Detection of Dynein bound with Active Arf1.....	83
2.2.10	Immunofluorescence detection of the cis-Golgi marker, GM130.....	84
2.2.11	Confocal Microscopy.....	84
2.2.12	Deconvolution of Z stacks and object analysis.....	85
2.2.13	Determining the Golgi distribution profile in a cell population.....	86
2.2.14	Co-localization analysis.....	86
2.2.15	Cell membrane lectin labeling and quantitation by flow cytometry.....	87
2.2.16	Statistical analysis.....	88
	Chapter 3: Study the effect of cell-matrix adhesion on Golgi organization	90
3.1	Rationale	91
3.2	Results	93
3.2.1	Cell-matrix adhesion regulates signaling/endocytosis.....	93
3.2.2	Localization of Golgi markers in cell lines used.....	96
3.2.3	Adhesion regulate Golgi organization in mouse embryonic fibroblast cells.....	98
3.2.4	Adhesion regulate Golgi organization in human fibroblast, endothelial and breast	

epithelial cells	109
3.2.5 Differential regulation of Golgi compartments by adhesion.....	114
3.2.6 Integrin clustering/activation could restore Golgi organization in non-adherent WT-MEF.....	118
3.2.7 No spatial predisposition of Golgi organization from cell-matrix binding site....	122
3.2.8 Cell-matrix adhesion regulated Golgi organization occurs independently of growth factors.....	124
3.3 Summary.....	127
3.4 Conclusion.....	128

Chapter 4: Study the regulation of Golgi organization by cell-matrix adhesion.

4.1 Rationale.....	130
4.2 Results.....	132
4.2.1 Cytoskeletal elements are structurally intact and functional in suspended and re- adherent cells.....	132
4.2.2 Intact microtubule and not actin network is essential for integrin-mediated adhesion regulated Golgi organization.....	135
4.2.3 Cell-matrix adhesion regulate activation of small GTPase Arf1.....	142
4.2.4 Cell matrix adhesion dependent Arf1 activation controls Golgi organization..	144
4.2.5 BIG1/2 is the predominant Arf1 specific GEF downstream adhesion mediated Golgi organization.....	155
4.2.6 Microtubule depolymerization does not affect Arf1 activity to block adhesion- mediated Golgi re-organization.....	157
4.2.7 Adhesion-dependent activation of Arf1 recruits motor protein dynein for Golgi organization.....	160
4.3 Summary.....	165
4.4 Conclusion.....	165

**Chapter 5: Compare loss of adhesion mediated Golgi disorganization to Golgi
fragmentation.....**

5.1	Rationale	167
5.2	Results	168
5.2.1	Cell-matrix mediated disorganized Golgi remains separate from Endoplasmic reticulum.....	168
5.2.2	BFA mediated Arf1 inhibition results in fragmentation of Golgi, which is structurally distinct from Golgi disorganization.....	170
5.2.3	BFA inhibited Arf1 in suspended cells causes the disorganized Golgi to fall back into Endoplasmic reticulum.....	177
5.3	Summary	181
5.4	Conclusion	182

Chapter 6: Study the effect of adhesion-dependent Golgi disorganization on Golgi function.....

6.1	Rationale	184
6.2	Results	186
6.2.1	Loss of cell-matrix adhesion increases global cell surface glycosylation in WT-MEFs.....	186
6.2.2	Restoration of Golgi organization in non-adherent cells abolishes the increase in surface glycosylation.....	190
6.2.3	Golgi disorganization is functionally different from Golgi fragmentation.....	194
6.3	Summary	197
6.4	Conclusion	198

Chapter 7: Study Adhesion dependent regulation of Golgi organization in anchorage-independent cancer cells.....

7.1	Rationale	200
7.2	Results	202
7.2.1	Golgi organization in cancer cell lines.....	202
7.2.2	Anchorage-independent activation of Arf1 retains an organized Golgi in non-	

	adherent T24 cells.....	205
7.3	Summary	209
7.4	Conclusion	209
	Chapter 8: Discussion	210
	Conclusion	226
	References	228

Essential abbreviations.

μM	micromolar
μL	microliter
μg	microgram
ECM	Extra cellular matrix
ER	Endoplasmic Reticulum
BFA	Brefeldin A
GCA	Golgicide A
NOC	Nocodazole
LatA	Latrunculin A
CB	Ciliobrevin D
Arf1	ADP-ribosylation factor-1
GEF	Guanine nucleotide exchange factors
GAP	GTPase-activating proteins
GM130	Golgi Matrix Protein 130
Man II	Mannosidase-II
GalTase	beta-1,4-galactosyltransferase

ABSTRACT

Cell-matrix adhesion regulates membrane trafficking to control anchorage-dependent signaling. While a dynamic Golgi complex can contribute to this pathway, its control by adhesion remains untested. Loss of adhesion rapidly disorganizes the Golgi in mouse and human fibroblast cells, its integrity restored rapidly on re-adhesion to fibronectin (but not poly-l-lysine coated beads) along the microtubule network. Adhesion regulates the trans-Golgi more prominently than the cis /cis-medial Golgi, though they show no fallback into the ER making this reorganization distinct from known Golgi fragmentation. This is controlled by an adhesion-dependent drop and recovery of Arf1 activation, mediated through the Arf1 GEF BIG1/2 over GBF1. Constitutively active Arf1 disrupts this regulation and prevents Golgi disorganization in non-adherent cells. Adhesion regulates active Arf1 binding to the microtubule minus-end motor protein dynein to control Golgi reorganization, which ciliobrevin blocks. This regulation by adhesion controls Golgi function, promoting cell surface glycosylation on the loss of adhesion that constitutively active Arf1 blocks. This study hence identifies cell-matrix adhesion to be a novel regulator of Arf1 activation, controlling Golgi organization and function in anchorage-dependent cells.

SYNOPSIS

Introduction.

Cell adhesion to extracellular matrix is vital for cell proliferation and growth and is shown to regulate cellular processes like migration, cell spreading, polarity, cytoskeletal re-arrangement and membrane trafficking (endocytosis and exocytosis). The architecture of the Golgi apparatus is subject to many variables and directly contributes to Golgi inheritance and function (Emr et al., 2009; Marsh and Howell, 2002). In mammalian cells, the Golgi is made up of a series of flattened cisternal stacks that are not homogeneous and contain different resident proteins that allow the Golgi to be divided into cis, medial, and trans regions (Dunphy and Rothman, 1985; Shorter and Warren, 2002). The cis Golgi receives newly synthesized proteins and lipids from the ER, while cargo exits the Golgi at the trans side (Glick and Luini, 2011). The Golgi apparatus undergoes dramatic fragmentation during cell division (Colanzi and Corda, 2007; Colanzi et al., 2003), apoptosis (Hicks and Machamer, 2005) and disease conditions like neuronal degeneration (Nakagomi et al., 2008) and cancer (Petrosyan, 2015a). This fragmentation is at times reversible and seen to play a role in Golgi function (Colanzi and Corda, 2007). Cell adhesion to the extracellular matrix is a vital regulator of many of the above cellular processes and disease conditions (LaFlamme et al., 2008; Reverte et al., 2006; Wu and Reddy, 2012). While a role for cell adhesion in regulating membrane trafficking to support anchorage-dependent signalling is known (Balasubramanian et al., 2007; Caswell et al., 2009; Pawar et al., 2016), no such regulatory crosstalk between cell adhesion and the Golgi organization has been identified.

Two major set of observations from literature, **(1)** Cell-matrix adhesion regulates membrane trafficking and cell cycle, and **(2)** the Golgi regulates membrane trafficking and cell cycle progression, undergoing reversible fragmentation during mitosis. Using these known observations the hypothesis was proposed that cell-matrix adhesion could control Golgi organization and hence function in a cell. Thesis have been divided into following sub-aims and to attempt to address the central question.

- I.** Study the effect of cell-matrix adhesion on Golgi organization.
- II.** Study the regulation of Golgi organization by cell-matrix adhesion.
- III.** Compare loss of adhesion mediated Golgi disorganization to Golgi fragmentation.
- IV.** Study the effect of adhesion-dependent Golgi disorganization on Golgi function.
- V.** Study if and how this pathway is deregulated in anchorage-independent cancer cells.

.....

I. Study the effect of cell-matrix adhesion on Golgi organization.

In this study, effect loss of cell-matrix adhesion and re-adhesion to fibronectin (in the absence of serum growth factors) have on the Golgi organization was tested. Serum starved wild-type mouse embryonic fibroblasts (WT-MEFs) on the loss of adhesion rapidly disorganize their cis-Golgi (detected with GM130), cis-medial Golgi (detected with Mannosidase II-GFP) and most prominently the trans-Golgi (detected with GalTase-RFP). Re-adhesion of cells to fibronectin for just 5 mins (or less) while not significantly affecting cell shape and volume, dramatically restores cis, cis-medial and trans-Golgi organization. This is reflected in a

significant reduction in the number of Golgi objects in re-adherent cells relative to when they are suspended. Percentage distribution of the organized vs disorganized trans-Golgi phenotype when compared in the cell population further confirms the disorganized phenotype to be prominent in suspended cells, reversed rapidly on re-adhesion. This adhesion-dependent regulation of the Golgi organization was also observed in anchorage-dependent human endothelial cells and human foreskin fibroblasts. A similar and significant change in Golgi object numbers was observed in these cells when they are suspended and re-adherent.

The kinetics of Golgi reorganization in WT-MEFs when tested for cis, cis-medial and trans-Golgi, showed their dispersal and re-organization to both be very rapid. Following their detachment, in the time it takes to process and fix cells (5' suspension) the Golgi is seen to disorganize. This reflects in Golgi object numbers being high at the 5 min suspension, showing a modest but significant increase over the next 90 to 120 mins. Re-adhesion of cells for 5 mins shows a dramatic re-organization of the Golgi with a significant drop in the number of cis, cis-medial and trans-Golgi objects. This suggests regulation of Golgi organization to be rather sensitive to the loss and recovery of cell-matrix adhesion. It was also observed that adhesion regulates cis/cis-medial Golgi differentially than trans-Golgi. This was evident in the extent of disorganization and relative localization of these compartments in a suspended cell. Next, it was tested and found that binding of fibronectin-coated beads to suspended cells could also restore the integrity of the cis and trans-Golgi significantly better than poly L-lysine coated beads. Percentage distribution of the organized vs disorganized trans-Golgi phenotype when compared across the bead-bound cell population further confirms the prominent disorganized phenotype in suspended cells to be reversed on the binding of fibronectin-coated

bead but not by poly L-lysine beads. The position of the reorganized Golgi when analysed did not show any spatial predisposition towards the fibronectin-coated bead or coverslip. This suggests the adhesion-dependent regulatory signal is carried rapidly to the Golgi to drive its reorganization.

II. Study the regulation of Golgi organization by cell-matrix adhesion.

Knowing the role cytoskeletal networks have in mediating cell adhesion-dependent signalling and Golgi organization (Egea et al., 2006; Sandoval et al., 1984; Sütterlin and Colanzi, 2010), its role was tested in this pathway. Loss of adhesion and re-adhesion did not significantly affect the organization of the microtubule network and MTOC or the actin cytoskeletal network in cells. Both networks are functionally active in non-adherent cells, as Nocodazole and Latrunculin A treatment distinctly affected endocytic trafficking of GM1-CTxB on the loss of adhesion. On nocodazole treatment, GM1 is endocytosed into the cell cortex but not trafficked to the recycling endosome (Balasubramanian et al., 2007), while Latrunculin A treatment blocks GM1 endocytosis. WT-MEFs suspended for 90 mins and treated with Nocodazole (10 μ M) for another 30 mins showed the cis-medial Golgi (Man II GFP) to be further disorganized with a significant increase in the number of discontinuous Golgi objects detected per cell. The trans-Golgi (Galtase RFP), which on the loss of adhesion is already extensively disorganized, did not show such a distinct change. On re-adhesion however, Nocodazole-treated cells failed to reorganize both the cis-medial and trans-Golgi. Interestingly, disrupting the actin cytoskeleton with Latrunculin A (0.5 μ M) did not affect cis-medial or trans-Golgi organization in suspended and re-adherent cells. This provides evidence that disorganized Golgi in suspended cells is held along microtubule network and

also it differs for cis/cis-medial and trans-Golgi compartment. In the presence of intact microtubule network, cis and cis-medial Golgi compartment appeared similar, as reflected in an incomplete dispersal of Golgi objects in the cell. This hence suggests the adhesion-dependent organization of the Golgi is mediated exclusively along the microtubule network.

Small GTPase, Arf1, localizes to Golgi, and has been implicated in regulating Golgi organization during mitosis (Altan-Bonnet et al., 2003). Inactivation of Arf1, and hence its dissociation from Golgi membranes during onset of mitosis resulted in Golgi fragmentation in mammalian cell. It was hence asked if adhesion could regulate Arf1 activation (like it regulates Arf6) (Balasubramanian et al., 2007) to control Golgi organization. Active Arf1 pulled down using GST conjugated GGA3 Arf effector binding domain reveals loss of adhesion to significantly reduce Arf1 activation (by ~60%), restored on re-adhesion to fibronectin. To test the role this drop has in mediating Golgi disorganization on the loss of adhesion GFP tagged constitutively active Arf1 (Q71L) in WT-MEFs was expressed and it was found that it prevents disorganization of the trans-Golgi (Galactose-RFP) in suspended cells. GFP-WT-Arf1 expressing MEFs behaved like control cells, with a distinctly disorganized Golgi phenotype on the loss of adhesion. This is further reflected in a significant decrease in the number of trans-Golgi objects per cell in suspended Q71L-Arf1 expressing cells relative to WT-Arf1 and untransfected cells. The distribution profile of organized versus disorganized phenotype in suspended and re-adherent WT-Arf1 and Q71L-Arf1 expressing cell populations further confirm this regulation. Active Arf6 (T157A) similarly expressed in cells did not have this effect further confirming this regulation to be Arf1 specific.

Further, if re-adhesion mediated recovery of Arf1 activation is needed for Golgi reorganization was explored, by inhibiting Arf1 using a dominant negative mutant (GFP tagged T31N Arf1) or inhibitor Brefeldin A (BFA). Cells suspended for 90 mins were incubated with BFA for an additional 30 mins and then re-plated on fibronectin. Both treatments while not further disrupting the disorganized trans-Golgi phenotype (GalTase-RFP) in suspended cells (120' SUSP) did prevent the Golgi from reorganising on re-adhesion to fibronectin. This is reflected in Golgi object numbers in re-adherent cells being comparable to those seen in suspended cells. The distribution profile of organized versus disorganized phenotype in BFA treated suspended and re-adherent cell populations confirming the same. Binding of fibronectin-coated beads to suspended BFA treated cells (BFA+FN-Bead) failed to restore Golgi integrity unlike untreated cells bound to FN beads. Golgi object numbers accordingly stayed significantly high in treated cells. The distribution profile of the organized versus disorganised phenotype in BFA treated cells further confirming its effect. Together these studies reveal loss of adhesion mediated drop and re-adhesion mediated recovery in Arf1 activation to control Golgi organization. The differential effect BFA (inhibits Arf1-GEF BIG1/2 and GBF1), but not Golgicide (inhibits Arf1-GEF GBF1), has on re-adhesion mediated Golgi organization also supports a role for Arf1-GEF, BIG1/BIG2 over GBF1 along this pathway.

Further, Active Arf1 (GTP bound) recruits microtubule motor protein dynein through Golgin160 to Golgi membranes to controls it's organization. Dynein facilitates the movement of Golgi membranes to the microtubule minus end, its dissociation from the Golgi promoting its disorganization (Yadav et al., 2012). It was hence explored if adhesion

regulated Arf1 activity also uses dynein to control Golgi organization. Indeed it was observed that less dynein was pulled down with active Arf1 fraction in suspended cells than re-adherent cells, while the total dynein levels remain same. This led us to ask if impairment of dynein function affects adhesion mediated re-organization of Golgi. Ciliobrevin D mediated inhibition of dynein function in cells suspended for 90 mins (Golgi disorganized by the loss of adhesion), while not significantly affecting trans-Golgi organization and Golgi object numbers in suspended cells did prevent the reorganization of the Golgi on re-adhesion. The percentage distribution of the organized versus disorganized phenotype in treated re-adherent cells further confirming this regulation. Arf1 activation on re-adhesion was not affected by ciliobrevin treatment, suggesting Arf1 activation is upstream and recruits dynein in this pathway. These studies provide evidence that on re-adhesion, BIG1/2 mediated Arf1 activation recruits functional dynein that works along the microtubule network to reorganize the Golgi.

III. Compare loss of adhesion mediated Golgi disorganization to Golgi fragmentation.

BFA mediated inhibition of Arf1 in earlier studies is shown to cause β COPI mediated fall back of the cis/medial Golgi membrane to the endoplasmic reticulum (ER), leading to Golgi fragmentation (Mardones et al., 2006). In non-adherent cells, the disorganized cis-Golgi (GM130) and cis-medial Golgi (Man II-GFP) were both seen to not localize with the ER (detected using KDEL-RFP). BFA treatment of suspended cells, while not affecting the disorganized trans-Golgi, did cause the cis-medial Golgi (Man II GFP) to fragment and redistribute to the ER (KDEL-RFP). This reflects in a significant increase in their co-localization along line plots and in cellular Pearson's coefficient. While on the loss of

adhesion Arf1 activity drops by ~60% (relative to stable adherent cells), BFA treatment of suspended cells reduces it further by ~60%, causing a net ~85% drop (relative to stable adherent cells). This suggests the differential effect on Arf1 activation variably affects Golgi organization causing the Golgi to “disorganize” on the loss of adhesion and further “fragment” as Arf1 activation drops on BFA treatment. This led us to ask if the loss of adhesion mediated Golgi disorganization affects Golgi function and how this could be similar or different from BFA mediated Golgi fragmentation.

IV. Study the effect of adhesion-dependent Golgi disorganization on Golgi function.

A major read out of Golgi function in cells is their ability to glycosylate and deliver protein and lipids at the cell surface. Both *N*- and *O*-glycosylation involve a series of enzymatic reactions catalyzed by glycan-processing enzymes across the cis, medial and trans-Golgi compartments (Freeze and Ng, 2011; Roth, 2002; Stanley, 2011; Varki, 1998). Changes in Golgi architecture does affect processing and trafficking of glycosylated proteins and lipids (Koreishi et al., 2013; Pokrovskaya et al., 2011; Xiang et al., 2013) and can be detected using lectins that selectively recognize glycan epitopes (Sharon and Lis, 2004). Using flow cytometry, quantitation of the cell surface binding of fluorescently tagged lectins, Concanavalin A (ConA) (mannose-binding), wheat germ agglutinin (WGA) (Galactose/*N*-acetylgalactosamine binding), peanut agglutinin (PNA) (*N*-acetylglucosamine binding) and ulex europaeus agglutinin (UEA) (Fucose binding), on loss of adhesion was done. Cells held in suspension for 120 mins showed increased cell surface binding of all four lectins relative to their levels when detached (5 min SUSP). A gradual increase in cell surface glycosylation over time, when compared 5', 10', 20', 30', 60', 90', and 120' suspension time points were

observed. Further, similar increase in cell surface glycosylation was observed when the synthesis of new proteins was blocked. This suggests loss of adhesion promotes Golgi processing and/or trafficking to increase cell surface glycosylation levels.

To confirm if this is indeed the result of Golgi disorganization on the loss of adhesion, it was tested if active Arf1 mediated restoration of Golgi integrity in suspended cells affects this glycosylation. Cherry tagged WT-Arf1 and active Q71L-Arf1 expressing cells selected by flow cytometry when compared showed a modest but insignificant change in basal cell membrane ConA and UEA binding (5' SUSP). Active Arf1 did, however, block the increase in cell surface glycosylation observed in control and WT Arf1 expressing 120' SUSP cells. This confirms the loss of adhesion mediated regulation of Arf1 and resulting Golgi disorganization affects Golgi function. BFA mediated fragmentation of the Golgi in suspended cells did not support such an increase in surface glycosylation (detected by ConA binding) confirming the fragmented Golgi to also be functionally distinct.

V. Study if and how this pathway is deregulated in anchorage-independent cancer cells.

Finally, if “cell matrix adhesion – Golgi” pathway exist in anchorage-independent cancer cells and if Arf1 plays a role in it was explored. Various studies have identified Golgi to be present in the fragmented form in many different types of cancers (Egea et al., 1993; Kellokumpu et al., 2002a; Migita and Inoue, 2012a; Petrosyan, 2015b). Trans-Golgi organization by expressing GalTase-RFP was screened in pancreatic cancer cell lines MIA-PaCa-2 (K-RAS G12V) and CFPAC-1 (K-RAS G12V), fibrosarcoma cell line HT-1080 (N-RAS G12V) and bladder cancer cell line T-24 (H-RAS G12V). It was observed that MIA-

PaCa-2, CFPAC-1, and HT-1080 cells display disorganized Golgi when cells were adherent and also on when the cells were suspended and re-adherent on fibronectin. However, T24 cell line showed a compact organized Golgi when adherent and interestingly non-adherent cell retained the organized Golgi phenotype. T24 re-adherent cells on fibronectin also displayed organized Golgi. This led us to test Arf1 active levels in T24 suspended cells and it was found that Arf1 is active in an anchorage-independent manner. Since fibroblasts, endothelial and epithelial cells tested earlier provided evidence that decrease in Arf1 active levels downstream of cell-matrix adhesion resulted in Golgi disorganization, it was asked what effect inhibition of Arf1 activity could have on Golgi organization in T24 cells. Arf1 inactivation was achieved by Brefeldin-A (BFA), Golgicide-A (GCA) and by expressing dominant negative Arf1 mutant (T31N-Arf1-GFP) in T24 cells. All three treatment resulted in robust disorganization of Golgi in non-adherent T24 cells. These studies suggest "cell-matrix adhesion-Golgi" is deregulated in bladder cancer T24 cells, and the cells retain the Golgi integrity as Arf1 is anchorage independent.

Summary.

Taken together these studies identify cell-matrix adhesion as a novel regulator of Golgi organization and function in anchorage-dependent cells. Cell-matrix adhesion regulates Arf1 activity which recruits motor protein dynein along microtubule network to organize Golgi. The rapid and reversible nature of this regulation suggests cells could use this pathway to actively tune Golgi function. This could, in turn, regulate processing and delivery of receptors at the cell surface. Glycosylation of membrane receptors is seen to affect receptor signalling (J., 2012) and is significantly altered in anchorage-independent cancer cells. In many cancers,

the Golgi is inherently fragmented to drive this change. Most important cell adhesion proteins, integrins are also glycosylated, which affects their dimerization and ability to interact with other receptors (Janik et al., 2010). It will be of interest to test if and how changes in surface glycosylation on the loss of adhesion compare to those seen on oncogenic transformation (Kellokumpu et al., 2002b; Pokrovskaya et al., 2011). Cell-matrix adhesion is also known to regulate cell cycle progression, helping determine spindle orientation and axis in a dividing cell (Matsumura et al., 2016). Furthermore, Arf1 inactivation is necessary for mitotic Golgi fragmentation which is integral to its inheritance by daughter cells and cell cycle progression. Loss of cell-matrix adhesion contributes to mitotic cell rounding (Suzuki and Takahashi, 2003). This leads to a speculation that alteration in cell-matrix adhesion and signaling could regulate Arf1 to drive Golgi disorganization and eventual fragmentation in a mitotic cell. Loss of adhesion mediated differential reorganization of the cis/medial vs trans-Golgi could also provide a novel system for testing their role in the secretory pathway in cells. A comprehensive characterization of regulation of Golgi organization and glycosylation in T24 bladder cancer cells will provide a better understanding of how cancer cells overcome this regulation.

REFERENCES.

- Altan-Bonnet, N., Phair, R.D., Polishchuk, R.S., Weigert, R., and Lippincott-Schwartz, J.** (2003). A role for Arf1 in mitotic Golgi disassembly, chromosome segregation, and cytokinesis. *Proc. Natl. Acad. Sci.* *100*, 13314–13319.
- Balasubramanian, N., Scott, D.W., Castle, J.D., Casanova, J.E., and Schwartz, M.A.** (2007). Arf6 and microtubules in adhesion-dependent trafficking of lipid rafts. *Nat. Cell Biol.* *9*, 1381–1391.
- Caswell, P.T., Vadrevu, S., and Norman, J.C.** (2009). Integrins: masters and slaves of endocytic transport. *Nat. Rev. Mol. Cell Biol.* *10*, 843–853.

- Colanzi, A., and Corda, D.** (2007). Mitosis controls the Golgi and the Golgi controls mitosis. *Curr. Opin. Cell Biol.* *19*, 386–393.
- Colanzi, A., Suetterlin, C., and Malhotra, V.** (2003). Cell-cycle-specific Golgi fragmentation: how and why? *Curr. Opin. Cell Biol.* *15*, 462–467.
- Dunphy, W.G., and Rothman, J.E.** (1985). Compartmental organization of the Golgi stack. *Cell* *42*, 13–21.
- Egea, G., Francí, C., Gambús, G., Lesuffleur, T., Zweibaum, A., and Real, F.X.** (1993). cis-Golgi resident proteins and O-glycans are abnormally compartmentalized in the RER of colon cancer cells. *J. Cell Sci.* *105 (Pt 3)*, 819–830.
- Egea, G., Lázaro-Diéguez, F., and Vilella, M.** (2006). Actin dynamics at the Golgi complex in mammalian cells. *Curr. Opin. Cell Biol.* *18*, 168–178.
- Emr, S., Glick, B.S., Linstedt, A.D., Lippincott-Schwartz, J., Luini, A., Malhotra, V., Marsh, B.J., Nakano, A., Pfeffer, S.R., Rabouille, C., et al.** (2009). Journeys through the Golgi—taking stock in a new era. *J. Cell Biol.* *187*, 449–453.
- Freeze, H.H., and Ng, B.G.** (2011). Golgi glycosylation and human inherited diseases. *Cold Spring Harb. Perspect. Biol.* *3*, a005371.
- Glick, B.S., and Luini, A.** (2011). Models for Golgi traffic: A critical assessment. *Cold Spring Harb. Perspect. Biol.* *3*.
- Hicks, S.W., and Machamer, C.E.** (2005). Golgi structure in stress sensing and apoptosis. *Biochim. Biophys. Acta - Mol. Cell Res.* *1744*, 406–414.
- J., B.** (2012). The Role of Glycosylation in Receptor Signaling. In *Glycosylation*, (InTech), p.
- Janik, M.E., Lityńska, A., and Vereecken, P.** (2010). Cell migration—The role of integrin glycosylation. *Biochim. Biophys. Acta - Gen. Subj.* *1800*, 545–555.
- Kellokumpu, S., Sormunen, R., and Kellokumpu, I.** (2002a). Abnormal glycosylation and altered Golgi structure in colorectal cancer: dependence on intra-Golgi pH. *FEBS Lett.* *516*, 217–224.
- Kellokumpu, S., Sormunen, R., and Kellokumpu, I.** (2002b). Abnormal glycosylation and altered Golgi structure in colorectal cancer: dependence on intra-Golgi pH. *FEBS Lett.* *516*, 217–224.
- Koreishi, M., Gniadek, T.J., Yu, S., Masuda, J., Honjo, Y., and Satoh, A.** (2013). The Golgin Tether Giantin Regulates the Secretory Pathway by Controlling Stack Organization within Golgi Apparatus. *PLoS One* *8*, e59821.
- LaFlamme, S.E., Nieves, B., Colello, D., and Reverte, C.G.** (2008). Integrins as regulators of the mitotic machinery. *Curr. Opin. Cell Biol.* *20*, 576–582.
- Mardones, G.A., Snyder, C.M., and Howell, K.E.** (2006). Cis-Golgi matrix proteins move directly to endoplasmic reticulum exit sites by association with tubules. *Mol. Biol. Cell* *17*, 525–538.
- Marsh, B.J., and Howell, K.E.** (2002). Timeline: The mammalian Golgi — complex debates. *Nat. Rev. Mol. Cell Biol.* *3*, 789–795.
- Matsumura, S., Kojidani, T., Kamioka, Y., Uchida, S., Haraguchi, T., Kimura, A., and Toyoshima, F.** (2016). Interphase adhesion geometry is transmitted to an internal regulator for spindle orientation via caveolin-1. *Nat. Commun.* *7*, ncomms11858.
- Migita, T., and Inoue, S.** (2012a). Implications of the Golgi apparatus in prostate cancer.

Int. J. Biochem. Cell Biol. *44*, 1872–1876.

Migita, T., and Inoue, S. (2012b). Implications of the Golgi apparatus in prostate cancer. Int. J. Biochem. Cell Biol. *44*, 1872–1876.

Nakagomi, S., Barsoum, M.J., Bossy-Wetzell, E., Sütterlin, C., Malhotra, V., and Lipton, S.A. (2008). A Golgi fragmentation pathway in neurodegeneration. Neurobiol. Dis. *29*, 221–231.

Pawar, A., Meier, J.A., Dasgupta, A., Diwanji, N., Deshpande, N., Saxena, K., Buwa, N., Inchanalkar, S., Schwartz, M.A., and Balasubramanian, N. (2016). Ral-Arf6 crosstalk regulates Ral dependent exocyst trafficking and anchorage-independent growth signalling. Cell. Signal. *28*, 1225–1236.

Petrosyan, A. (2015a). Onco-Golgi: Is Fragmentation a Gate to Cancer Progression? Biochem. Mol. Biol. J. *1*.

Petrosyan, A. (2015b). Onco-Golgi: Is Fragmentation a Gate to Cancer Progression? Biochem. Mol. Biol. J. *1*.

Pokrovskaya, I.D., Willett, R., Smith, R.D., Morelle, W., Kudlyk, T., and Lupashin, V. V (2011). Conserved oligomeric Golgi complex specifically regulates the maintenance of Golgi glycosylation machinery. Glycobiology *21*, 1554–1569.

Reverte, C.G., Benware, A., Jones, C.W., and LaFlamme, S.E. (2006). Perturbing integrin function inhibits microtubule growth from centrosomes, spindle assembly, and cytokinesis. J. Cell Biol. *174*, 491–497.

Roth, J. (2002). Protein N-glycosylation along the secretory pathway: relationship to organelle topography and function, protein quality control, and cell interactions. Chem. Rev. *102*, 285–303.

Sandoval, I. V, Bonifacino, J.S., Klausner, R.D., Henkart, M., and Wehland, J. (1984). Role of microtubules in the organization and localization of the Golgi apparatus. J. Cell Biol. *99*, 113s–118s.

Sharon, N., and Lis, H. (2004). **History of lectins: from hemagglutinins to biological recognition molecules.** Glycobiology *14*, 53R–62R.

Shorter, J., and Warren, G. (2002). Golgi Architecture and Inheritance. Annu. Rev. Cell Dev. Biol. *18*, 379–420.

Stanley, P. (2011). Golgi glycosylation. Cold Spring Harb. Perspect. Biol. *3*, a005199.

Sütterlin, C., and Colanzi, A. (2010). The Golgi and the centrosome: building a functional partnership. J. Cell Biol. *188*, 621–628.

Suzuki, K., and Takahashi, K. (2003). Reduced cell adhesion during mitosis by threonine phosphorylation of beta1 integrin. J. Cell. Physiol. *197*, 297–305.

Varki, A. (1998). Factors controlling the glycosylation potential of the Golgi apparatus. Trends Cell Biol. *8*, 34–40.

Wu, X., and Reddy, D.S. (2012). Integrins as receptor targets for neurological disorders. Pharmacol. Ther. *134*, 68–81.

Xiang, Y., Zhang, X., Nix, D.B., Katoh, T., Aoki, K., Tiemeyer, M., and Wang, Y. (2013). Regulation of protein glycosylation and sorting by the Golgi matrix proteins GRASP55/65. Nat. Commun. *4*, 1659.

Yadav, S., Puthenveedu, M.A., and Linstedt, A.D. (2012). Golgin160 Recruits the Dynein Motor to Position the Golgi Apparatus. Dev. Cell *23*, 153–165.

Chapter 1: Introduction and review of Literature

1.1 Integrins: Role and regulation.

1.1.1 What are integrins?

1.1.1.1 Introduction.

Integrins are the family of heterodimeric trans-membrane cell surface receptors that are crucial for the metazoan cell to exist. The name “integrin” was given when Hynes and colleagues in 1987, when it first showed the trans-membrane protein identified to be able to physically integrate between extracellular matrix (ECM), fibronectin and intracellular cytoskeleton, actin (Tamkun et al., 1986).

In last three decades, since the first characterization, an enormous amount of diverse research has been performed and has led to great understanding for integrins structure and cellular functions (Campbell and Humphries, 2011; Hynes, 2004; Pan et al., 2016). Functionally, it has been demonstrated that integrins clustering and activation at the cell surface, through specific extracellular matrix ligand interaction regulates diverse cellular processes like cell adhesion, migration, cell growth and proliferation, cell polarity, cytoskeleton re-arrangement, membrane trafficking (Berrier and Yamada, 2007; Caswell et al., 2009; Danen and Yamada, 2001).

1.1.1.2 The Integrin Family: Structure.

In mammalian cells, till date, 24 canonical integrin heterodimer resulting from the different pairing of 18- α subunits and 8- β subunits have been reported (Hynes, 2002). These

heterodimers have also been shown to be expressed in tissue-specific manners and bind to different ligands to carry out its diverse functions (Barczyk et al., 2010).

Each α and β -subunits have a single membrane-spanning domain, short and unstructured cytoplasmic tail. Size of the subunits vary, but typically α -subunits are 1000 and β -subunits are 750 amino acids long respectively (Hynes, 2002).

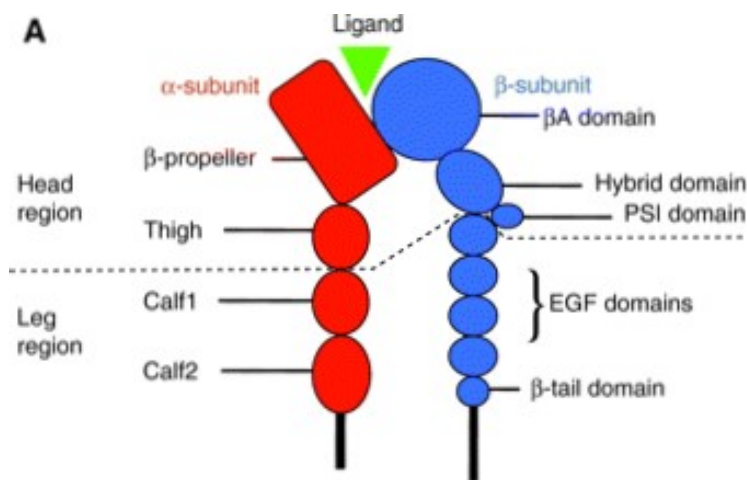


Figure 1.1. Schematic of Integrin Structure. The α -subunit (Red) and β -subunit (Blue) of one integrin heterodimer adopt a “head region” on the extracellular side and “leg” region on the intracellular side of the cell surface. Ligand (Green) Binding takes place at the interface of β -propeller and β A domain of α and β subunits. (Reproduced from Askari et al., JCS 2009).

The overall structure (**Figure 1.1**) in most of the integrins is a “head region” (amino terminus of α and β subunits, the β -propeller and β A domain respectively, assemble by non-covalent interaction) providing a ligand binding site and “leg region” (calf1 and calf2 domains in α -subunit, and EGF domains in β -subunit).

1.1.2 How do integrins work?

1.1.2.1 Ligand Binding.

Integrin-ligand binding has been classified into four major groups, based on the type of molecular interaction (**Figure 1.2**). Based on the different extracellular domains of different α and β subunits, integrins can be classified as **(1)** RGD tripeptide motif recognizing integrins ($\alpha 5\beta 1$, $\alpha V\beta 1$, $\alpha V\beta 3$, $\alpha V\beta 5$, $\alpha V\beta 6$, $\alpha V\beta 8$, and $\alpha IIb\beta 3$), **(2)** collagen binding integrins ($\alpha 1\beta 1$, $\alpha 2\beta 1$, $\alpha 3\beta 1$, $\alpha 10\beta 1$, and $\alpha 11\beta 1$), **(3)** laminins binding integrins ($\alpha 1\beta 1$, $\alpha 2\beta 1$, $\alpha 3\beta 1$, $\alpha 6\beta 1$, $\alpha 7\beta 1$, and $\alpha 6\beta 4$) **(4)** leukocytes integrins ($\alpha L\beta 2$, $\alpha M\beta 2$, $\alpha X\beta 2$, and $\alpha D\beta 2$) (Hynes, 1987; Plow et al., 2000).

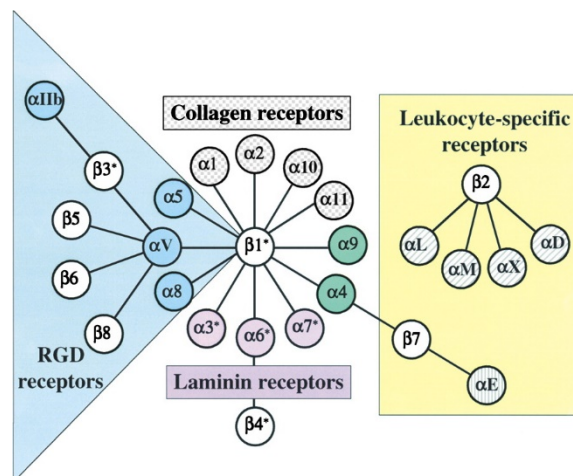


Figure 1.2. Classification of integrin-based on ligand binding. Integrins are broadly divided into 4 groups based on the type of ligand it binds. (Reproduced from Hynes et al., Cell 2002).

Apart from the above-mentioned ligands, integrins have metal ion-dependent adhesive (MIDAS) motif, “I domain” (in α -subunit), and “I domain-like structure” (in β subunit).

Mg^{2+} , Ca^{2+} , and Mn^{2+} divalent cations coordinate the ligand binding to integrins for its binding and subsequent activation (Humphries et al., 2003; Lee et al., 1995).

1.1.2.2 Activation and Bi-directional signaling.

Integrin-ligand binding would be meaningful to the cell only if this interaction relays the signal in order to modulate a cellular function. Ligand binding to its specific integrin receptor results in integrin clustering (formation of hetero-oligomers) and activation by bringing in a conformational change in the structure of the protein, which is referred to as the activated state.

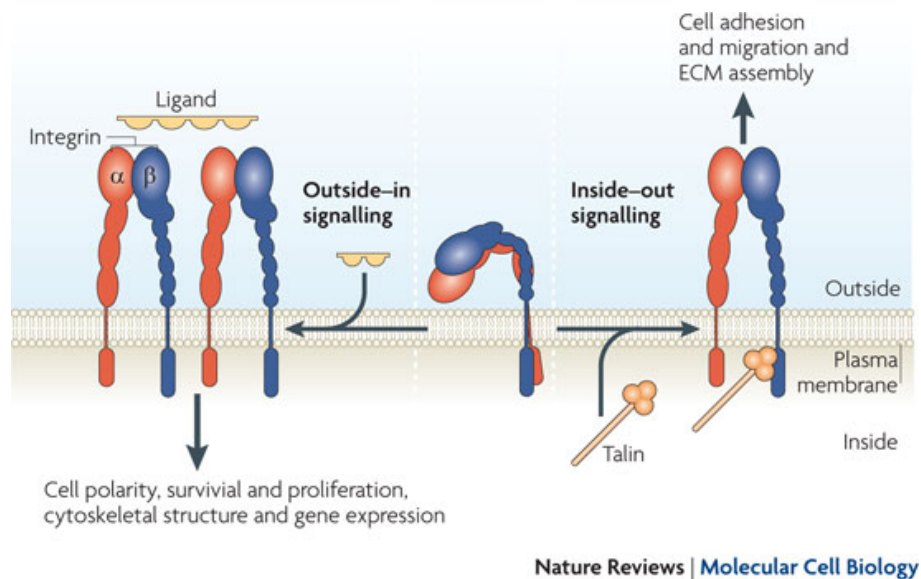


Figure 1.3. Model of Integrin bi-directional signaling. (Adapted from Shattil et al., Nature Reviews Molecular Cell Biology 2010).

Unlike many other receptor-mediated signaling, integrins can regulate functions in two directions (**Figure 1.3**), **(i)** Outside-in signaling (low-affinity ligand state), **(ii)** Inside-out signaling (high-affinity ligand state) (Arnaout et al., 2005; Humphries et al., 2003; Hynes, 2002). Most adherent cells that are attached to a basement membrane have a basal level of activated integrins, while freely circulating platelets and leukocytes have basal inactivated integrins.

Outside-in signaling.

The extracellular ligand binds to integrin receptor brings about integrin clustering at the cell surface, the formation of tight focal adhesion complexes, leading up to interaction of cytoplasmic domain of integrin with proteins like talin, and finally resulting into actin reorganization (Arnaout et al., 2005; Hynes, 2002). As this mode of signaling travels from outside to the inside of the cell, it is referred to as outside-in signaling of integrin.

Outside-in signaling results in recruitment of proteins like talin, vinculin, and activation of tyrosine protein kinase (Focal adhesion kinase), which results in activation of signaling pathways to regulate cell proliferation, survival, and migration. Outside-in signaling also brings in actin reorganization by triggering Arp2/3 branching at actin filaments, and activation of Rac, Cdc42, and Rho GTPase, which plays a key role in lamellopodium formation and cell migration (Barczyk et al., 2010; Huvneers and Danen, 2009).

Inside-out signaling.

Inside-out signaling as the name suggests, transmits the signal from inside to outside of a cell. This mode of integrin signaling is particularly important for cells, like blood cells or immune cells, where cells and ligands are in close proximity, but the interaction takes place only when the integrin receptor gets activated in response to some external cue, such as injury to vascular cells or inflammatory response. Talin and Kindlin, cytoplasmic proteins that physically interact with integrins, have been demonstrated to bind and activate integrins to carry out inside-out signaling (DeMali et al., 2003; Lawson and Schlaepfer, 2012; Vinogradova et al., 2002).

Although it's viewed as two separate events, these bi-directional signalings are often linked and set feedback loop to modulate certain processes.

1.1.3 Cellular functions regulated by integrins.

Integrins regulate various diverse cellular functions by sensing the many aspects of ECM components, as well as biochemical cues. As illustrated in **Figure 1.4**, cell extracellular matrix and integrin interaction results in scaffolding of many downstream proteins (Talin, vinculin, Kindlin, Tensin) and regulates signaling kinases (Src, JNK, MEK, ERK) (Schwartz, 2001), and ultimately affects cell adhesion, cell proliferation (Schwartz, 2001), cell cycle (Danen and Yamada, 2001), cell survival (Stupack and Cheresch, 2002), cell polarity (Cox et al., 2001), migration (Huttenlocher and Horwitz, 2011), actin cytoskeleton (DeMali et al., 2003), membrane trafficking (endocytosis and exocytosis) (Caswell et al., 2009; Wickström and Fässler, 2011).

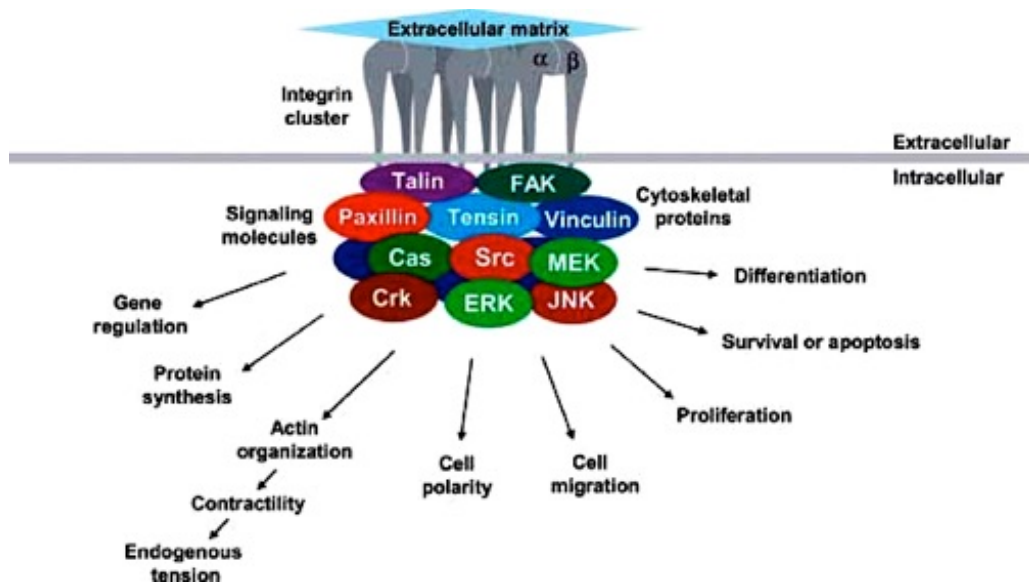


Figure 1.4. Model for integrin and cell-extracellular interaction and their downstream regulation. Integrins heterodimer at the cell surface recruits cytoplasmic molecules in response to extracellular cues, and interaction with downstream signaling molecules it regulates many aspects of cellular function. (Reproduced from Yamada et al., *Journal of cellular physiology*, 2007).

Integrin-mediated cell adhesion.

Cell adhesion to extracellular components through integrins plays an important role in the organization, maintenance, and repair of several tissues. This interaction has been shown to be necessary for a variety of physiological processes, including embryonic mesoderm development, epithelial morphogenesis, neural tube development, maintenance of muscle tissue integrity (De Arcangelis and Georges-Labouesse, 2000)(references within this review).

Integrin-mediated cell adhesion takes place through formation of “focal adhesion”, where scaffolding of signaling molecules such as integrin-linked-kinase (ILK), Focal adhesion kinase (FAK), phospholipase C, and Rho-GTPase family proteins occurs (Lawson and Schlaepfer,

2012; Lawson et al., 2012). These focal adhesion structures are complex in terms of their components and regulation, with ~ 150 different molecules associated (Geiger and Yamada, 2011; Geiger et al., 2009). These signaling molecules are in fact act upstream in pathways that regulate certain cellular processes.

Migration.

Cell migration is a dynamic physiological process wherein there is a balanced interaction between cell and its substratum (to which it is attached and over which it migrates). Cell migration is particularly important to study during leukocyte trafficking in immune cells (Radi et al.), tissue regeneration and repair (Koivisto et al., 2014), embryonic morphogenesis (Zhu et al., 2002), and also during disease conditions like cancer invasion and metastasis (Desgrosellier and Cheresch, 2010; Seguin et al., 2015).

Integrins aids two major aspects during cell migration: **(i)** It produces traction force between the cell and the substratum by linking ECM to the actin cytoskeleton **(ii)** It scaffolds various signaling molecules that are necessary to initiate and carry out the migration. Integrins have been shown to drive this complicated yet tightly regulated process, where it generates high traction force at the front edge of the cell, literally pushing the cell forward, and simultaneously pulling the rear edge. There is a continuous assembly and disassembly of adhesion sites, which is again regulated by Rho, Rac and Cdc42 GTPase activity, actin polymerization, with the help of myosin motor protein activity (Caswell and Norman, 2006; Ridley, 2011; Rottner and Stradal, 2011).

Cell cycle and mitosis.

Although growth factors were normally considered to be the main regulators of cell cycle progression, it is well established now that all anchorage-dependent cells require integrin-ECM regulation to progress through the cell cycle (Benaud and Dickson, 2001; LaFlamme et al., 2008). Integrin-mediated adhesion to ECM is essential for activation of MEK1, expression of cyclin-D1 and progression through a G1-S phase of cell cycle (Reverte et al., 2006; Schwartz and Assoian, 2001; Schwartz and Ginsberg, 2002). Resting interphase cells have large focal adhesions which are disassembled at the onset of mitosis with changes in cell morphology, as cells adopt a round shape (Ezratty et al., 2005; Geiger et al., 2001; Maddox and Burridge, 2003). Furthermore, cells fail to undergo cytokinesis, resulting in binucleated cells, when held in suspension (loss of integrin-mediated signaling) (Ben-Ze'ev and Raz, 1981; Kanada et al., 2005; Pellinen et al., 2008; Pugacheva et al., 2006). There are reports suggesting reduced cell adhesion during mitosis is brought about by threonine phosphorylation of $\beta 1$ integrin at 788-789 residues. This phosphorylation results in the inability of the integrins to interact with the actin cytoskeleton (Suzuki and Takahashi, 2003). Taken together, these studies provide evidence that integrin-mediated adhesion is required and necessary for mitotic progression.

1.1.4 Integrin dependent membrane trafficking.

Integrin-mediated membrane Endocytosis.

Integrin-mediated cell adhesion via FAK and Src kinase triggers caveolar and Raft endocytosis as illustrated in **Figure 1.5**. When cells are detached from the substratum, it

triggers internalization of caveolae and subsequent removal of active Rac bound to the plasma membrane, eventually downregulating growth signaling pathways such as Akt and Erk (Pelkmans et al., 2005; del Pozo et al., 2004, 2005).

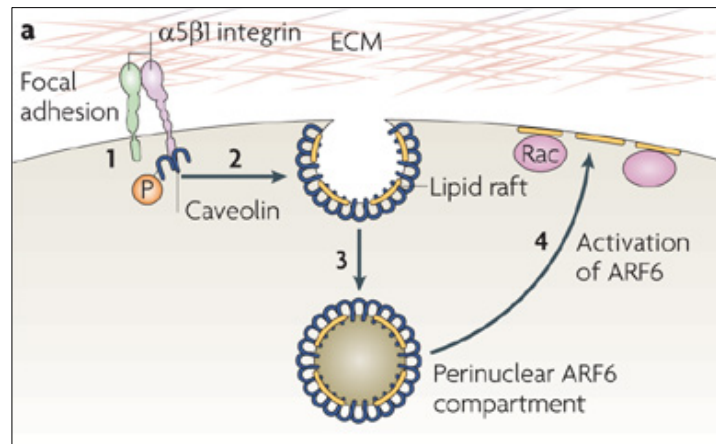


Figure 1.5. Role of integrins in controlling lipid raft trafficking. When cells are adherent, integrin engagement with fibronectin leads to the retention of phosphorylated caveolin in focal adhesions (1), which opposes the endocytosis of lipid rafts. Cell detachment triggers the release of phosphorylated caveolin from focal adhesions (2), thus allowing its association with caveolae to induce the endocytosis of lipid rafts (3). Re-engagement of $\alpha 5 \beta 1$ integrin (1) reverses this process, both by sequestering phosphorylated caveolin to shut down lipid raft internalization and by activating ADP-ribosylation factor-6 (ARF6) to promote rapid recycling of lipid rafts, which recruits active Rac to the plasma membrane (4). (Adapted from Patrick T. Caswell et al., *Nature Reviews Molecular Cell Biology* 2009).

Recent literature indicates that apart from regulating raft microdomains endocytosis, integrin-mediated adhesion acts as a global regulator of endocytosis such as bacterial products (Marre et al., 2010; Martchenko et al., 2010), EGF and Transferrin by HeLa cells (Collinet et al., 2010).

Integrin-mediated membrane Exocytosis.

Integrin-mediated cell adhesion has also been shown to control the secretion of soluble and membrane-associated proteins, such as TGF- β (Ortega-Velazquez et al., 2004), VEGF (Wang et al., 2011) and insulin (Kragl and Lammert, 2010).

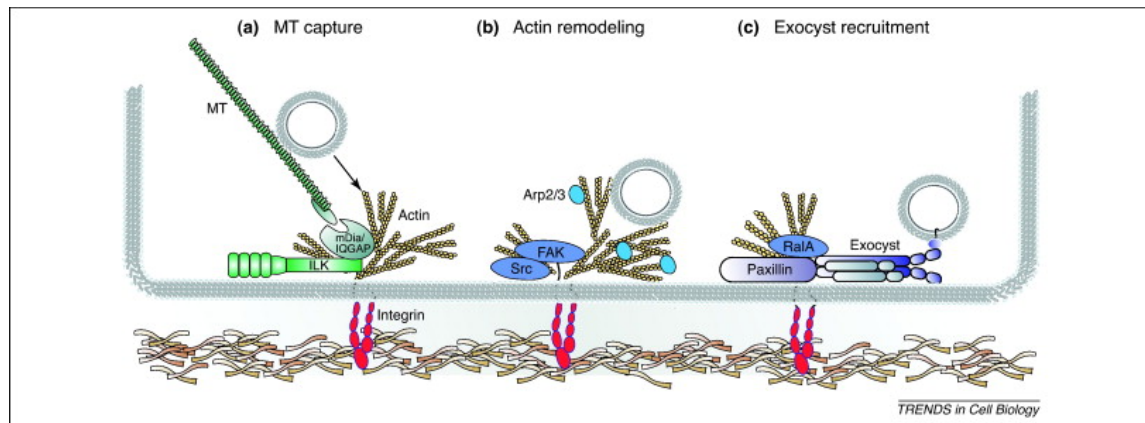


Figure 1.6. Role of integrins in exocytosis. Integrin signaling regulates exocytosis on various levels. (a) Integrin signaling through the scaffold protein Integrin-linked kinase, ILK (b) through the activity of the integrin-associated kinases FAK and Src. (c) through paxillin and RalA GTPase during exocyst assembly and activation. (Adapted from Sara A wickstrom et al., Trends in Cell Biology 2011).

As shown in **Figure 1.6**, integrins controls exocytosis by three major pathways, via integrin-linked kinase ILK (Tucker et al., 2008), or through FAK and Src kinase activity (Palazzo et al., 2004), or via exocyst complex targeted by Ral and Arf6 GTPase (Balasubramanian et al., 2007, 2010; Pawar et al., 2016).

Integrin regulates plasma membrane order.

Integrin clustering on ligand binding has been shown to make the plasma membrane into an ordered state. Membrane order of mature focal adhesion sites represents the highly ordered state. The ordered state of the plasma membrane is crucial in physiology as the specialized microdomain can act as a platform for downstream trafficking and signaling (Gaus et al., 2006; Lingwood and Simons, 2010; van Zanten et al., 2009).

In summary, cell-matrix adhesion through integrins regulates endo-and exocytosis, as well as recycling of physiologically important molecules. However, only a few regulatory and signaling pathways, receptors or membrane compartment have been studied thoroughly so far. Thus, identification of cell-adhesion dependent trafficking and its extension into the identification of new regulatory pathways and mechanism will be an exciting area of future research.

1.2 The Golgi apparatus.

1.2.1 Golgi apparatus Discovery and early perspective.

1.2.1.1 Endomembrane system.

In a eukaryotic cell, membrane-bound organelles like the nucleus, mitochondria, endoplasmic reticulum, Golgi apparatus, and lysosomes perform specific functions which are dictated by their unique architecture. A typical eukaryotic cell comprises of a complex set of sub-cellular compartments collectively called as “endomembrane system”, which are distinct in structure and function, and function in a coordinated manner (Jékely, 2007; Wideman et al., 2014).

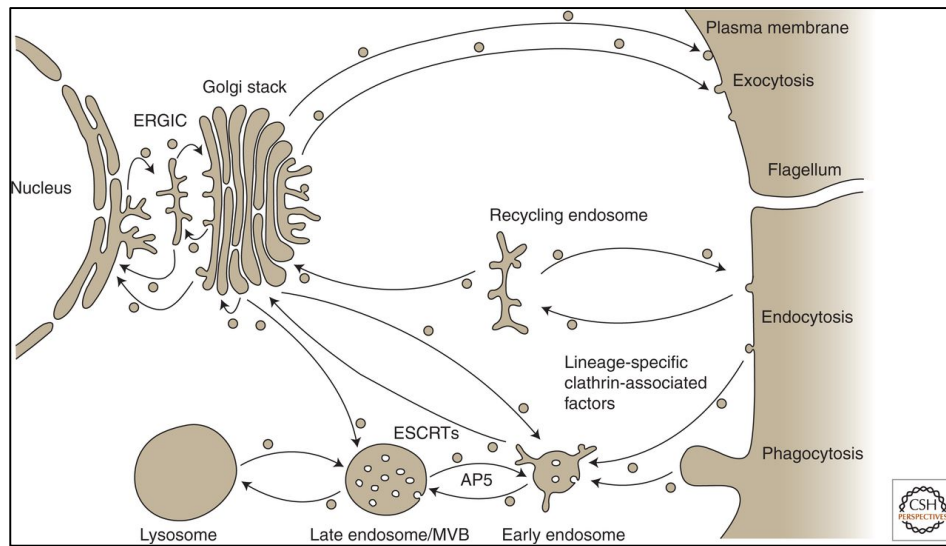


Figure 1.7. Schematic of a eukaryotic cell showing Endomembrane organelles and membrane trafficking. (Reproduced from Wideman JG et al., Cold Spring Harb Perspect Biol. 2014).

As depicted in the schematic, **Figure 1.7**, endomembrane system consists of membrane-bound organelles such as the endoplasmic reticulum (ER), the Golgi, peroxisomes, lysosomes, early and late endosomes, as well as carry out processes such as phagocytosis, endocytosis, and membrane recycling. As this thesis is focused on regulation of Golgi organization and function, I will mainly focus on what is known about Golgi (role and regulation) in the field so far.

1.2.1.2 Golgi apparatus: A Brief History.

In 1898, Camillo Golgi communicated his discovery to Medical-Surgical Society of Pavia , which was regarding a complex staining procedure that led him observe the presence of perinuclear structure in the mouse nerve cell, which he referred to as “apparato reticulare interno”

(Golgi et al., 2001) (translation of the original article by Camillo Golgi). At present this cellular organelle, which is present ubiquitously in all eukaryotic cells, as “Golgi apparatus”, “Golgi complex”, or sometimes just “Golgi”, all the terms are often interchangeable. It’s now known and accepted that Golgi is an independent cellular organelle, involved in various cellular processes, such as protein secretion, glycosylation etc. However, many decades following its discovery Golgi’s existence was challenged by many researchers, and considered to be an artifact of the staining procedure.

The debate was finally answered around the 1950s, mostly due to work by Dalton and Felix (in 1954, 1956), when electron microscopic images unquestionably established the presence of Golgi cisternae (then called lamellae structure) in a cell, and it was generally accepted in the field (Dalton and Felix, 1954; DALTON and FELIX, 1956).

1.2.2 Structural components of the Golgi apparatus.

The Golgi apparatus is the most complex and elaborate sub-cellular organelle in the cell (Farquhar and Palade, 1981). Typically, a eukaryotic Golgi consists of continuous flat membranous sacs, called “cisternae” which are generally arranged into polarized stacks (Ladinsky et al., 1999; Rambourg and Clermont, 1997), with some unstacked cisternae in ancestral eukaryotes (Mowbrey and Dacks, 2009). A number of cisternae in a Golgi stack are variable depending on the organism and cell type, and it may range from 3-20 (Becker and Melkonian, 1996; Rambourg and Clermont, 1997). Lower vertebrates have one Golgi stack in a cell, but higher vertebrates have evolved the Golgi to form a lateral link between

individual stacks, which finally appear as a continuous “ribbon” like structure (Klumperman, 2011; Marsh et al., 2001).

Remarkably, regardless of variation in the number of cisternae, presence/absence of stacks, and a number of stacks, Golgi functions with the conserved method in diverse eukaryotes like yeasts, plant and animal cells (Duden and Schekman, 1997; Hawes, 2004; Klute et al., 2011). Golgi is located at a pericentriolar region near microtubule organizing center (MTOC) of the cell (Sütterlin and Colanzi, 2010), and cytoskeleton is closely related in maintaining its structural identity (this regulation is discussed in greater detail later).

1.2.2.1 How many classes of Golgi cisternae exist?

Within a Golgi stack, cisternal membranes differ in terms of its composition, protein content, and localization and function (Day et al., 2013; Farquhar, 1985; Munro, 2005; Papanikou and Glick, 2009). This classification of the organization of Golgi cisternae was explored with a combination of classical electron microscopy and enzyme-activity based cyto-chemically staining the Golgi and many different cell types were documented.

Although many different types of methods have been utilized to highlight various Golgi features over decades, there is a general consensus about the general compartmental organization. Based on the presence of different set of resident structural and processing enzymes, a typical Golgi is divided into four distinct compartments (*i*) *cis*, (*ii*) *medial*, (*iii*) *trans* and (*iv*) *trans Golgi network* as described in **Figure 1.8** (Klumperman, 2011; Papanikou and Glick, 2014).

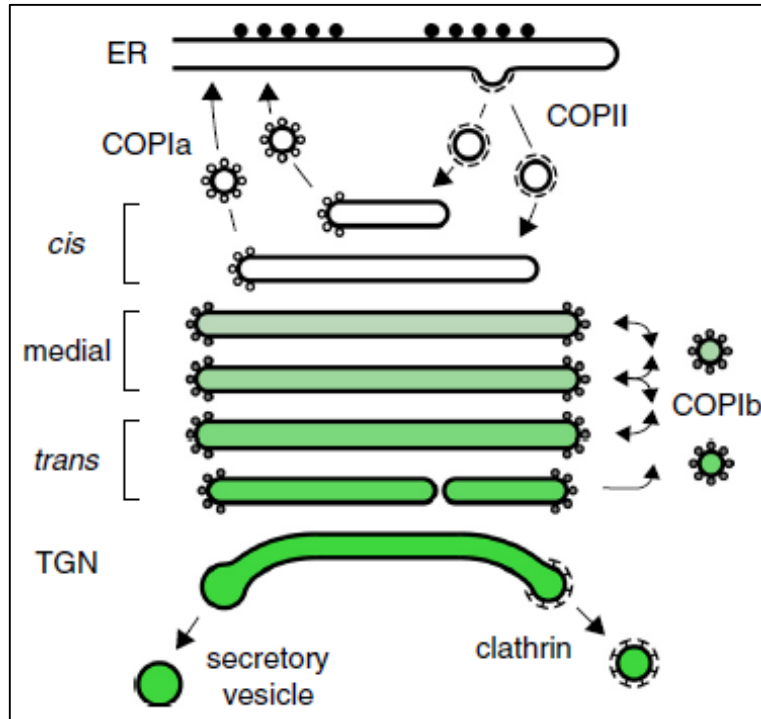


Figure 1.8. Schematic representation of the Golgi cisternal compartments. (Adapted from Effrosyni Papanikou and Benjamin S Glick, *Current Opinion in Cell Biology* 2014).

Many Golgi stacks are then laterally connected to give rise to a compound ribbon-like appearance (Trucco et al., 2004). The mammalian cell consists of an additional compartment, ER-Golgi-Intermediate-Compartment (ERGIC), which is associated with ER exit sites (Appenzeller-Herzog et al., 2006; Lippincott-Schwartz et al., 2000). ERGIC derived vesicles move along the microtubules towards Golgi ribbon and dock at cis-Golgi cisternae (Bannykh and Balch, 1997). At the trans side, *trans-Golgi network* segregates and delivers the processed cargoes which were trafficked through the Golgi to various destinations like, plasma membrane, endosomes, or secretes outside the cell (Bannykh et al., 1998; De Matteis and Luini, 2008). Cisternae in different parts of the stack recruit a different set of coatomer

complex proteins, COP1 and COPII to mediate vesicle biogenesis. Vesicle-mediated inter Golgi transport helps in retaining cisternae resident proteins and enzymes and regulates dynamic anterograde and retrograde trafficking pathways (Orci et al., 1998; Rabouille and Klumperman, 2005).

1.2.2.2 The *cis* side of the Golgi.

Proteins enter the secretory pathway from endoplasmic reticulum which is destined for secretion or various intracellular compartments. Numerous lines of evidence have now established bi-directional transport cycles between ER, ERGIC, and cis-Golgi compartments, which is essential for their structural integrity and functioning (Ben-Tekaya et al., 2005; Lippincott-Schwartz et al., 1997; Scales et al., 1997). Coatamer protein complex COPII is responsible for anterograde transport (from ER to cis Golgi), while COPI for retrograde transport. Sec12, an integral ER membrane protein activates Sar1 GTPase, which drives COPII assembly at ER membranes. COPII coated vesicles, ~ 60 to 100 nm in diameter, triggers vesicles biogenesis and formation with help of downstream recruitment of Sec23 and Sec31 effector proteins. COPII vesicles eventually fuse and uncoat to the ERGIC compartment, which is en route to cis Golgi (Barlowe, 2003; Barlowe et al., 1994).

1.2.2.3 The *trans* side of the Golgi.

Structurally, *trans-Golgi network* (TGN) is different from the rest of the Golgi cisternae, as it is tubular and branched reticular structure which is in continuation with trans-cisternae of Golgi stack (Geuze and Morré, 1991; De Matteis and Luini, 2008). This change from tubular to reticular morphology is the result of protein and lipid composition being different at TGN

membranes. Most prominent dissimilarity at TGN membranes, which is responsible for its appearance and function different from the rest of the Golgi is the presence of clathrin (Pearse and Robinson, 1990). Unlike COP coats, Clathrin coats are thicker and spiky in morphology and form clathrin-coated buds at curved TGN tubules which exit for further destination into the cell (Ladinsky et al., 2002; Mogelsvang et al., 2004).

Trans side of the Golgi, TGN is the hub of sorting of proteins and lipids post Golgi trafficking, and post-translational modification. Anterograde route of these cargoes is apical and basolateral plasma membrane, recycling endosomes, late endosomes, secretory granules (De Matteis and Luini, 2008). Additionally, retrograde transport from TGN to Golgi stacks takes place simultaneously to maintain the dynamic flux of membranes and proteins (Johannes and Popoff, 2008). Each destination route could be having a different type of carrier, and active research is going on to understand the TGN sorting mechanism.

1.2.3 Regulators of Golgi apparatus organization.

1.2.3.1 Cytoskeleton.

Microtubules. As MTOC is the main microtubule organizing center and is localized very closely with Golgi apparatus in a cell, its regulation on Golgi structure has been explored. Now, it's been known for a long time that structural integrity of Golgi is dependent on microtubules (Sandoval et al., 1984). Depolymerization of microtubules network results in disconnection of cisternal stacks and dispersal into cytoplasm with swollen cisternae and few surrounding vesicles. This altered Golgi, however, remains functional with only moderate effect on protein secretion (Van De Moortele et al., 1993; Robin et al., 1995).

MTOC (Centrosome): An interesting study revealed that disconnecting Golgi and centrosome connection affects the Golgi structure, and prevents directed cell migration (Hurtado et al., 2011).

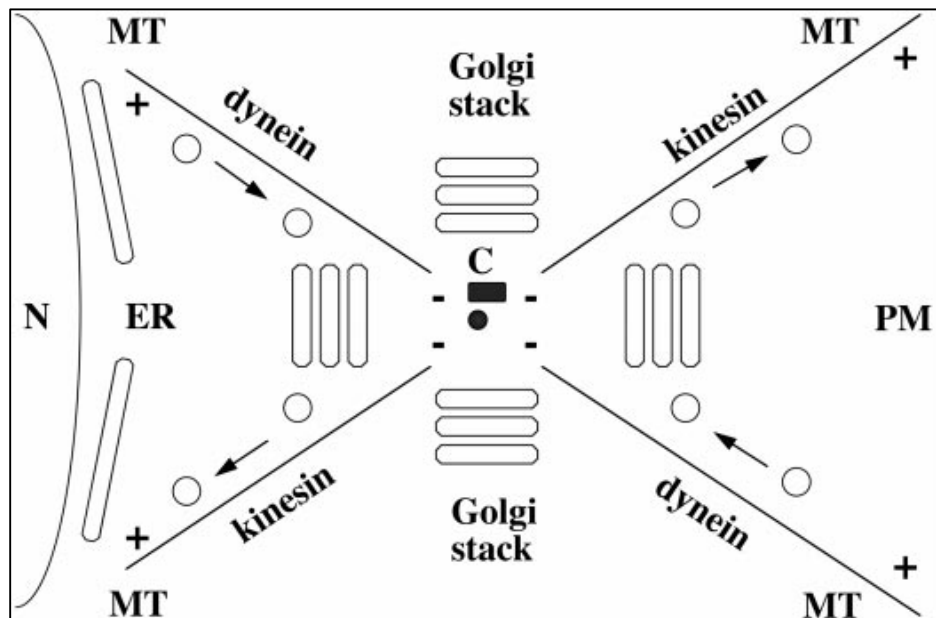


Figure 1.9. Schematic of the role of the microtubule motor proteins cytoplasmic dynein and kinesin in membrane transport to and from the Golgi complex. The plus and minus ends of microtubules are indicated. C, centrosome; ER, endoplasmic reticulum; MT, microtubules; N, nucleus; PM, plasma membrane. (Reproduced from Johan Thyberg et.al, Experimental Cell Research 1999).

Actin is required for biogenesis of Golgi-derived transport carriers and maintains the unique flat shape of Golgi cisternae (Egea et al., 2006; Valderrama et al., 1998). Actin microfilaments also support retrograde transport from Golgi to ER (Valderrama et al., 2001).

Motor Proteins. A range of cytoskeletal motor proteins associated with Golgi and are involved in trafficking to and through Golgi. This includes myosin-II, V and VI (actin-

associated motor), kinesin1, 2, and 3 (+ end microtubule-associated motor), and cytoplasmic dynein-1 (- end microtubule-associated motor) proteins. As illustrated in **Figure 1.9**, Kinesin-1, 2 and 3 mediate traffic away from Golgi, while dynein-1 is responsible for carrying cargo towards the MTOC (Brownhill et al., 2009; Burkhardt, 1998a). Role of Dynein-1 has been studied relatively in more detail, and its absence causes Golgi to fragment and disperse in the cell. It is required for correct pericentriolar position and integrity of Golgi (Corthésy-Theulaz et al., 1992; Harada et al., 1998).

1.2.3.2. Golgins and GRASPS.

Several studies have revealed the presence of detergent-insoluble proteinaceous scaffold towards the cytoplasmic face of the Golgi, which is known as **Golgi matrix, Figure 1.10 (a)** (Slusarewicz et al., 1994). Various Golgi matrix proteins have been classified which includes GRASP (GRASP-55, GRASP-65), Golgins (GM130, p115, Golgin-84, Golgin-97, Golgin-160 etc.) (Xiang and Wang, 2011). These Golgi matrix proteins have characteristic long coiled-coil domains and they are fiber-like connections between two cisternae or between a vesicle and cisternae, **Figure 1.10 (b)**.

Golgins.

Different **Golgins** are localized at distinct regions in a Golgi stack. For instance, GM130, Golgin-160, GMAP-210 are *cis* Golgins, while Golgin-97, Golgin-245 are *trans*-Golgins, and Giantin, Golgin-84 are localized at Golgi rims. Most of the Golgins have the domain which binds with Rab or Arl GTPase and contributes in regulating membrane traffic within and to/from the Golgi (Munro, 2011). As an example, GM130 interacts with another Golgin,

p115, which is required for formation of COPII vesicles to fuse with cis-Golgi membranes (Nakamura et al., 1997).

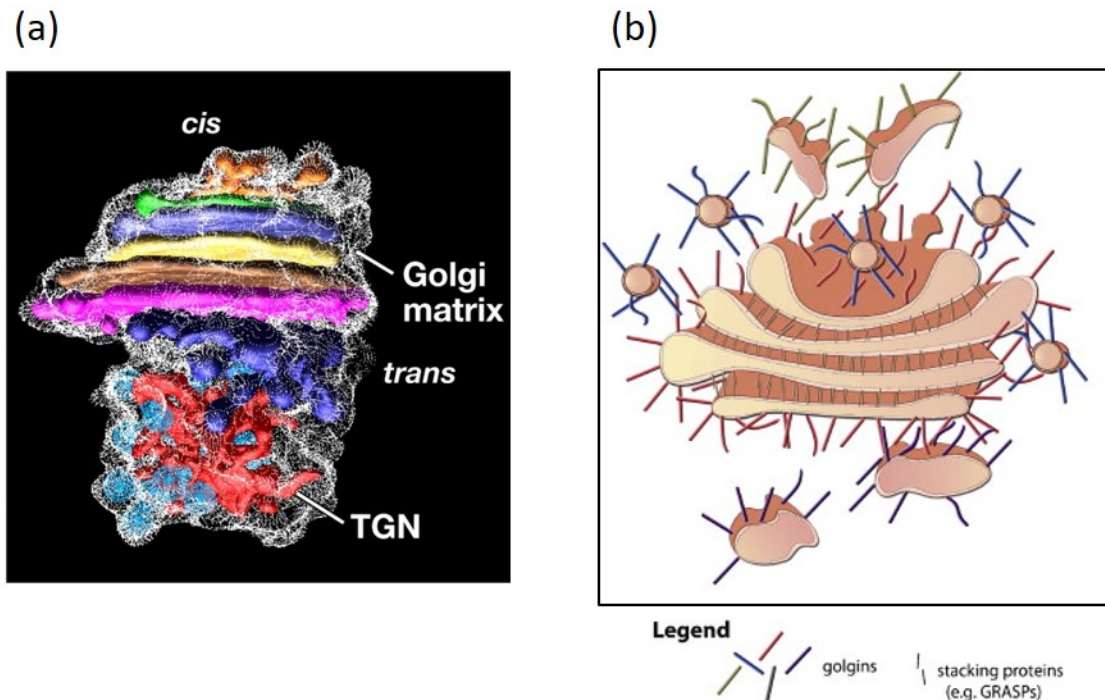


Figure 1.10. (a) Electron tomographic model of Golgi stack and its surrounding Golgi matrix. (Adapted from Stachelin LA and Kang BH, Plant Physiol. 2009). **(b) Schematic of Golgins and GRASPs surrounding and stacking the Golgi cisternae.** (Adapted from Ramirez IB and Lowe M, Seminars in Cell & Developmental Biology, 2009).

GRASP.

There are two types of GRASP (Golgi Reassembly and Stacking Proteins) in a mammalian cell, termed as GRASP-55 and GRASP-65. Both the proteins are quite similar in amino acid sequence and domain arrangements but differ in localization, with GRASP-65 being

restricted to cis, and GRASP-55 present around medial cisternae. Another difference lies in their interacting partners, GRASP-65 binds to GM130, while GRASP-55 binds to Golgin-45. GRASPs, as they have been named connects cisternae within a Golgi stack (such as cis to medial), and also make lateral connections between cis to cis or medial to medial (from two Golgi stacks) giving rise to Golgi ribbon-like shape (Barinaga-Rementeria Ramirez and Lowe, 2009).

1.2.3.3. Small GTPase.

Small GTPases are a family of proteins, with Mol. Wt. ~ 21 kDa (hence termed small), which are involved in various cellular processes ranging from organelle homeostasis, cytoskeletal dynamics, vesicle trafficking, migration etc. Small GTPase cycles between GDP, “inactive”, and GTP, “active” bound form, where activation is regulated by GEF (Guanine exchange factor) and inactivation by GAP (GTPase-activating protein) (Cherfils and Zeghouf, 2013).

As illustrated in **Figure 1.11**, four classes of small GTPase, Ras, Rho, Rab, and Arf, are localized on Golgi and regulates signaling, trafficking, and maintaining the integrity of the organelle. There exist a crosstalk between these small GTPases to exert its regulatory role at Golgi (Baschieri and Farhan, 2012).

Ras GTPase regulates many cellular processes like cell proliferation, differentiation, and apoptosis. The crucial signaling pathway that Ras GTPase activates is Raf-MEK-ERK mitogen-activated protein kinase cascade. RasGRP1 (GEF) activates Ras at Golgi and downstream of this ERK response is elicited (Chiu et al., 2002).

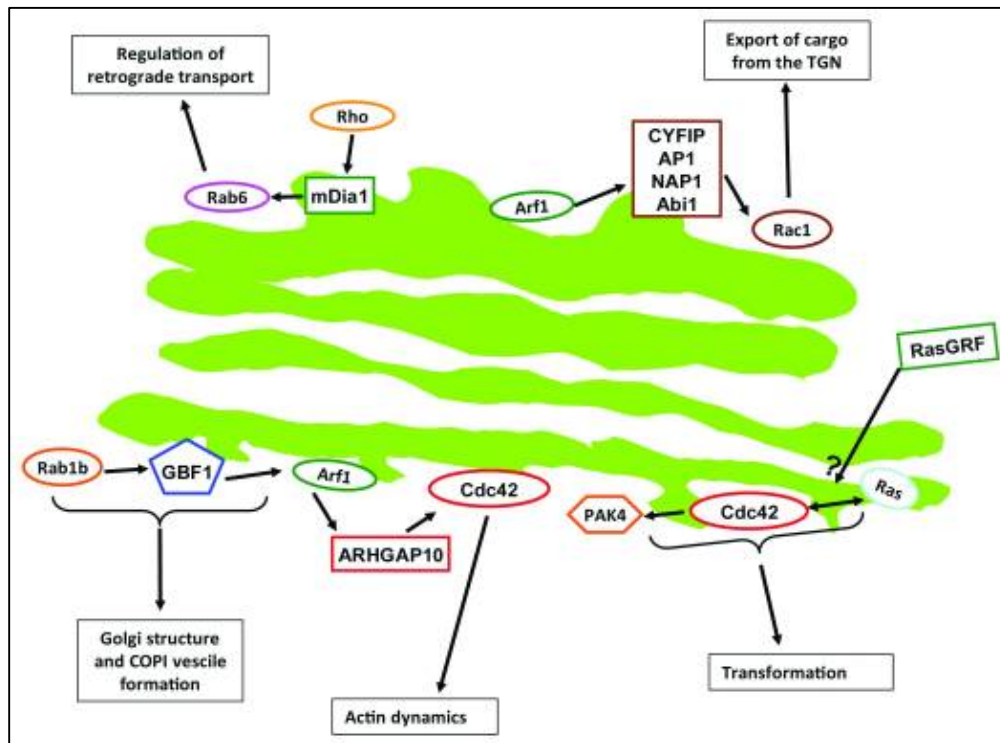


Figure 1.11. Schematic of the crosstalk of small GTPase at Golgi to maintain its architecture and function. (Reproduced from Baschieri F. and Farhan H., Small GTPases, 2012).

Rho GTPase, comprises of Rho, Rac and Cdc42 groups are the central cytoskeletal regulator, and by this means controls cell migration, vesicle trafficking, and cytokinesis. In particular, Cdc42 plays an active role at Golgi by regulating bidirectional COPI transport and exerts cell polarity independent of plasma membrane pool of Cdc42 (Farhan and Hsu, 2016; Park et al., 2015).

Rab GTPase is the largest family of Ras-related proteins and play a crucial role in membrane trafficking at different endomembrane structures, and importantly at Golgi. It does so by regulating directed carrier movement and also tethering at the target membranes (Pfeffer, 1999).

Arf GTPase (ADP-ribosylation factor) family of small GTPase has been strongly implicated in membrane traffic and organelle architecture (D'Souza-Schorey and Chavrier, 2006; Donaldson et al., 2005). In mammalian cells, Arfs are divided into 3 classes: class I, composed of Arf 1 and 3, class II, composed of Arf 4 and 5, and class III, composed only of Arf6, which is the most different protein of this family (LI et al., 2004). Sar1 and ~ 20 Arf-like proteins (ARLs) are also included in Arf GTPase family. Arf1 plays an important role in the maintenance of the Golgi structure, its inactivation results in disassembly of the Golgi structure. Double knockdown of Arf1 and Arf4 results in disassembly of Golgi. Arf1, Arf4, and Arf5 are involved in COPI biogenesis and budding, and trafficking from Golgi to ER (Volpicelli-Daley et al., 2005). Recent studies provide evidence of the role of Arf1 in the formation of bi-directional tubules from the Golgi (Bottanelli et al., 2017).

1.2.3.4. Protein Kinases:

Many mitogen-activated protein kinases such as MEK1 (mitogen-activated protein kinase 1), plk1 (polo-like kinase 1), cdk1 (cyclin-dependent kinase 1), Erk1 are potentially involved in regulation of Golgi structure in various cellular conditions (Chia et al., 2012a).

1.2.4 Golgi – Endoplasmic reticulum connection.

1.2.4.1 Endoplasmic reticulum:

Endoplasmic reticulum (ER) is a single copy number, membrane-enclosed organelle, which is connected to the nuclear envelope (NE), and fundamental to many cellular functions (Baumann and Walz, 2001). ER acts as the starting point of the secretory pathway in the cell. Proteins are translocated into ER for folding, post-translational modification, which then gets

exported into lipid coated vesicles. It acts as Ca^{2+} storage, regulates calcium homeostasis and is also involved in the synthesis of lipid molecules, phospholipids, and steroids. Furthermore, it can act as the acceptor organelle for retrograde vesicles (Baumann and Walz, 2001; Levine and Rabouille, 2005).

Although various functions have been attributed to ER in great detail, molecules that create this structure have been explored only recently. Few major structural contributors being, reticulons which are responsible for the high curvature of ER tubule, atlastin which provides the polygonal structure to ER sheets (Rismanchi et al., 2008); several proteins like p180, CLAMP-63, and kinectin give rise the typical sheet-like structure (Klopfenstein et al., 2001). The combined effect of many factors eventually gives rise to the dynamic morphology of ER. These include the interplay between ER and microtubules, membrane fusion and fission events, and the above mentioned structural proteins. It has been acknowledged for a long time now that ER undergoes dynamic morphological alterations which have a consequence on its function; however, the structure-function relationship needs to be defined at a molecular level.

Even though a vast amount of work has been done on Golgi and endoplasmic reticulum (ER) structure, function, and its inheritance, there still exist a debate if Golgi biogenesis is dependent on ER or not. Till late 80's it was assumed that Golgi is a stable organelle for its biogenesis, maintaining its structure and regulation of function. In this section, I would present how ER and Golgi are connected and what are the recent advances in our understanding so far.

1.2.4.2 Is Golgi an independent organelle?

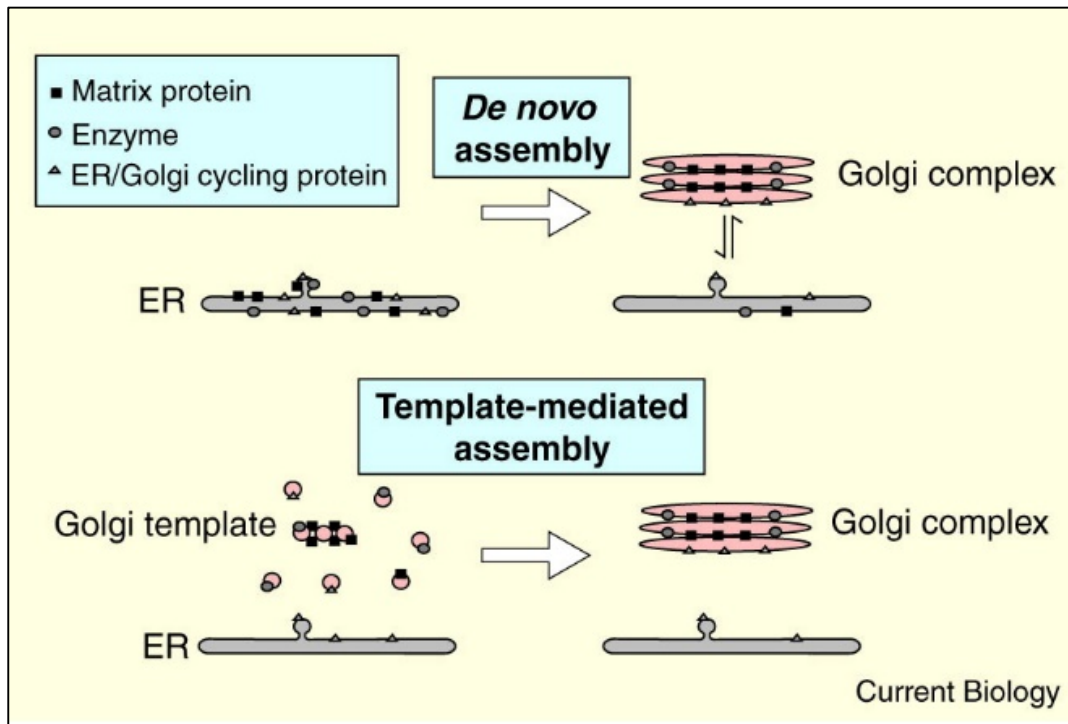


Figure 1.12. Models for Golgi biogenesis. (Reproduced from Martin Lowe, Current Biology, 2002).

Two different models have been proposed to explain Golgi biogenesis in a mammalian cell, **(i) de novo assembly** **(ii) template mediated assembly**. According to the **de novo assembly**, Golgi apparatus is self-organized after Golgi proteins/components present in ER exits. The main feature of this model is this process is independent of ER, making Golgi an independent organelle. **Template mediated assembly** describes the formation of Golgi apparatus on the pre-existing template and this views Golgi to be in constant dynamic equilibrium with ER, making it dependent organelle on ER (Lowe, 2002). The first indication that challenged Golgi

as an independent organelle came when a fungal metabolite, Brefeldin A (BFA) which blocks ER to Golgi transport, results in re-distribution of Golgi enzymes into ER (Fujiwara et al., 1988; Lippincott-Schwartz et al., 1989).

Cells expressing dominant negative Sar1 (Sar1 DN), GTPase required for ER exit, showed mixing of Golgi enzymes into ER (Girod et al., 1999). Furthermore, studies with Sar1 DN claimed that in an interphase cell all the Golgi enzymes visit ER with $t_{1/2} \sim 1$ hour (Miles et al., 2001). Nocodazole (microtubule depolymerizing agent) induced fragmentation of Golgi was also proposed to be the result of recycling of Golgi proteins into ER (Storrie et al., 1998). Golgi enzymes of cells undergoing cell division, where microtubules have been shown to depolymerize, was also shown to re-distribute to ER (Altan-Bonnet et al., 2006). These reports definitely provide evidence that Golgi enzymes have the capacity to re-distribute to ER under an artificial condition or secretory pathway is affected. More extensive research is needed regarding the fate of Golgi enzymes when the secretory pathway is not perturbed?

Nonetheless, another set of idea considers Golgi to be an autonomous organelle and inherited independently of ER. Studies in support of this model came from experiments using ER trapping Golgi enzymes and claims that Golgi membranes remain separate from ER under normal conditions, such as protein secretion (Villeneuve et al., 2017a), or cell division (Pecot and Malhotra, 2004, 2006) in mammalian cells.

1.3 Cellular functions regulated by the Golgi.

1.3.1 Golgi mediated Cellular functions.

As the central organelle in the secretory pathway Golgi apparatus is very crucial to many diverse cellular functions (Cancino and Luini, 2013; Corda et al., 2012; Wilson et al., 2011), which includes:

- a) Post-translational modification of proteins and lipids (for example glycosylation),
- b) Trafficking (to and from the Golgi)
- c) Sorting of proteins and lipids (to different destinations in the cell)
- d) Secretion outside the cell
- e) Lipid homeostasis
- f) Centre for Microtubule nucleation
- g) Acts as Calcium store.
- h) Golgi as a signaling hub, mainly the Ras, Src and Cdc42 signaling pathways
- i) Organelle based cell cycle checkpoint (This is discussed in detail in section 1.4).

The complex architecture of Golgi narrates to its function. Recent advances in the field have provided evidence that intact and organized Golgi structure and positioning in the cell is crucial for trafficking and direction of secretion, glycosylation, cell polarization, cell migration (Millarte and Farhan, 2012; Rios and Bornens, 2003; Wilson et al., 2011; Yadav and Linstedt, 2011). Here I will discuss mainly Golgi function in the context of trafficking and glycosylation.

1.3.2 Trafficking through the Secretory Pathway.

Protein and lipid sorting within the secretory pathway begins at the endoplasmic reticulum (ER), and at Golgi, it reaches a high level of complexity yet tightly regulated. Newly synthesized proteins and lipids are distinctly directed to multiple destinations, which includes the ER, various endosomes, plasma membrane and extracellular secretion (Bonifacino and Rojas, 2006; Rodriguez-Boulan and Müsch, 2005). The forward flow of cargo from ER to Golgi (anterograde transport) is balanced by recycling of components back to Golgi and ER (retrograde transport).

1.3.2.1 Various types of trafficking through the Secretory Pathway.

Trafficking through secretory pathway can be subdivided into three parts: (a) ER to Golgi transport (b) Intra-Golgi transport, and (c) Golgi to Plasma membrane transport. A lot of work has been done to address all types of above-mentioned transport pathways in the secretory pathway which has provided insights into trafficking and organelle biogenesis.

(a) ER to Golgi transport.

The first step in the anterograde transport is the packaging of newly synthesized proteins in the ER into COPII coated vesicles, and they form the ER Golgi intermediate compartment (ERGIC). COPII coat is characteristic of vesicles generating from ER which assembles in response to activation of Sar1 GTPase (Stinchcombe et al., 1995).

(b) Intra-Golgi transport.

Intra Golgi transport has been the most debated in the field, and there exist different views on how this process works. Few models of trafficking through Golgi have been proposed, which differ fundamentally but provide insight towards understanding the mechanism and regulation of protein trafficking through Golgi. The lack of conclusive experimental evidence has polarized the field to view the process as two models, which are vesicular shuttle model and the cisternal maturation/progression model, as explained in **Figure 1.13** (Glick and Luini, 2011).

The **vesicular shuttle model (Figure 1.13 A)** explains the cisternae are “static compartments”. Golgi enzymes are stably distributed within different compartments which are long-lived structures. This model implies the anterograde movement (cis-to-trans) of cargo by means of COPI/COPII vesicles that bud from one compartment and fuse with another. However, this model does not explain the mechanism of transport of cargoes which are too large to fit into transport vesicles.

The **cisternal maturation model (Figure 1.13 B)** depicts that individual Golgi cisternae are “transient compartments”. According to this model secretory cargo protein never leaves the individual cisternae, while cisternae mature from cis to trans compartment. New cisternae are continuously formed from ER-to-Golgi transport vesicles at the cis-face of Golgi and gradually disperse from trans face as post-Golgi vesicles. According to this model, COPII mediates transport from ER to Golgi and there exists a COPI mediated retrograde transport

(trans-to-cis) of Golgi structural proteins and enzymes, in order to retain them within Golgi compartments.

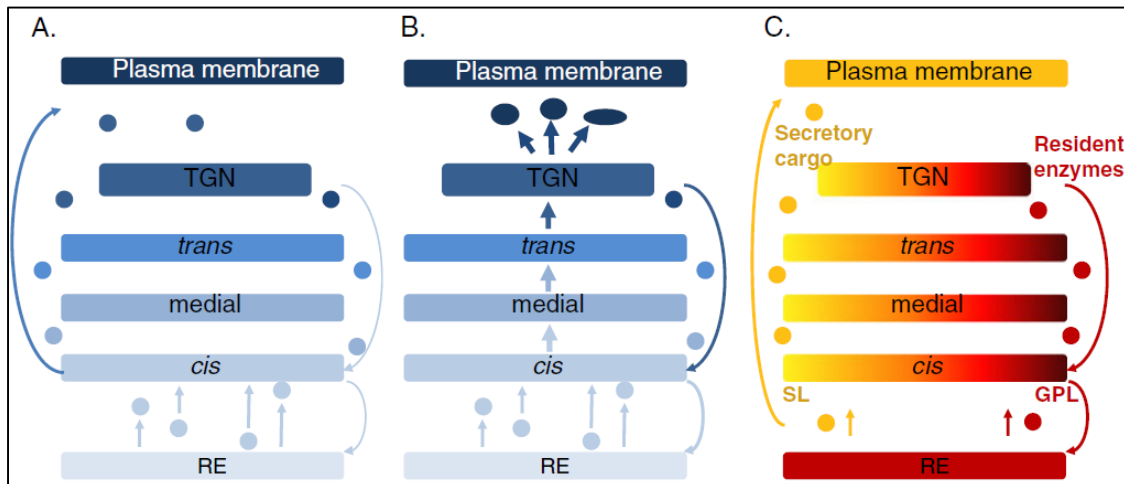


Figure 1.13. Models for Intra Golgi Traffic. (A) Vesicle shuttle model, and (B) Cisternal maturation model. (C) Rapid partitioning model. Reproduced from Rosnoblet C et al., Glycoconjugate, 2013. (This is a modified scheme from Benjamin S. Glick and Akihiko Nakano, Annu Rev Cell Dev Biol. 2009).

Experimental evidence exists in support of cisternal maturation model which came from labs of Benjamin Glick (Losev et al., 2006) and Akihiko Nakano (Matsuura-Tokita et al., 2006), where both the studies used live-cell fluorescence microscopy to directly observe cisternal maturation in Golgi of *Saccharomyces cerevisiae*. Although consensus has reached cisternal maturation model best defines the mechanism of Golgi trafficking, there is still debate over whether or not all cargo proteins follow the same route.

Patterson *et al.*, in 2008 (Patterson et al., 2008) demonstrated that some cargo proteins travel through the Golgi much slower than the rates at which cisternae matures, and describes another model for intra-Golgi trafficking, “**rapid partitioning model**” (Figure 1.13 C).

According to this model Golgi exists as a single compartment, with processing and export domains, which are established by different lipid composition. The two-phase system of membranes governs the transport of cargo proteins and Golgi enzymes. Golgi resident enzymes are brought back through retrograde route and follows GPL (Glycerophospholipids) gradient, whereas cargo proteins travel through cisternae via (Sphingolipids) SL gradient in the anterograde route.

(c) Golgi to Plasma membrane transport.

Trans-Golgi Network (TGN) acts as the central to endocytic and exocytosis processes and is extremely dynamic and tightly regulated. A cascade of signaling events takes place at TGN, where Diacylglycerol recruits by Ser/Thr kinase proteins (PKD), with the help of heterotrimeric G-proteins, catalyze the fission of vesicles from TGN (Malhotra and Campelo, 2011). Some aspects of protein trafficking through Golgi are better understood now, however, there are still unresolved issues within the field. For instance, do different cargoes follow different routes through the Golgi? If cisternae stacking is fundamentally important for its function, how trafficking still take place in plants and *S. cerevisiae* (where Golgi is not stacked and dispersed)?

1.3.2.2 Factors affecting trafficking through the Secretory Pathway.

Alteration in Golgi structure (referred to as Golgi fragmentation (discussed in section 1.4) in normal cells or diseased conditions could affect trafficking through the secretory pathway.

Alteration in trafficking in Normal cells.

Knock-down of Golgi proteins (structural and matrix) results in Golgi fragmentation and have a varied alteration in anterograde and retrograde trafficking depending on the protein that has been depleted. **GRASP-55/65** proteins are the cisternae stacking Golgi structural proteins and its depletion results in Golgi fragmentation. This also resulted in accelerated anterograde transport, that is, transport of proteins (CD8, VSVG) from ER to Golgi and Golgi to the plasma membrane and vesicle formation (Xiang et al., 2013).

Another Golgi matrix protein, **Giantin**, is important in Golgi architecture and function. Depletion of Giantin results in the formation of Golgi mini-stacks, without changing the size of cisternae. This altered Golgi structure is responsible for increased anterograde transport from Golgi to Plasma membrane (Koreishi et al., 2013). Depletion of **COG** complex protein results in mislocalization of β and ϵ -COP proteins and inhibition of retrograde transport (Smith et al., 2009).

Nocodazole-induced microtubule depolymerization mediated Golgi fragmentation has varied effects on anterograde and retrograde transport in a cell. Microtubule depolymerization had a very little effect on retrograde transport from Golgi to ER. On the other hand, anterograde transport from ER to Golgi gets blocked as these pre-Golgi intermediates require microtubule and dynein motor for protein translocation which gets disrupted on nocodazole treatment (Cole et al., 1996). Kinetics of Golgi to cell surface transport on microtubule depolymerization in these cells remains unaffected (Hirschberg et al., 1998). These studies indicated that microtubule strands are used for ER and Golgi transport only when these organelles are separate in a cell. Once the Golgi enzymes were re-

distributed in ER on microtubule de-polymerization, this requirement for transport was overridden.

Another Golgi fragmentation agent, **Brefeldin A**, results in dissociation of β -COPI and Arf1 proteins from Golgi membranes resulting in accelerated retrograde transport and redistribution of Golgi enzymes into ER. There is evidence that anterograde transport on BFA treatment is not affected, vesicles bud out of ER, but as there is no Golgi membrane to act as acceptor, it recycles back to ER (Lippincott-Schwartz et al., 1990).

Golgi fragmentation takes place in a reversible sequential process when the mammalian cell enters **mitosis**. During mitotic Golgi fragmentation, anterograde transport (ER to Golgi) has been reported to be blocked, while recycling back to the ER was observed (Farmaki et al., 1999; Villeneuve et al., 2017b). Golgi fragmentation caused by DNA damage was shown to block anterograde transport (Farber-Katz et al., 2014).

1.3.3 Glycosylation.

Glycosylation is the most important post-translational modification of proteins and lipids which occurs at Golgi. A variety of enzymes which carry out the transfer of glycan molecules, such as glycosyltransferases, glycosidases, and nucleotide sugar transporters are located in cis, medial and trans-Golgi membranes in an ordered manner and give rise to a final glycoconjugate before exiting trans Golgi network, **Figure 1.14** (Stanley, 2011).

The significance of glycosylation modification of proteins and lipids are vast, from the correct folding of proteins, regulation of thermostability of proteins, protein-protein interaction and

acting as a site of ligand binding on receptors resulting in a biological response (Dwek, 1998; Li and d'Anjou, 2009; Shental-Bechor and Levy, 2008).

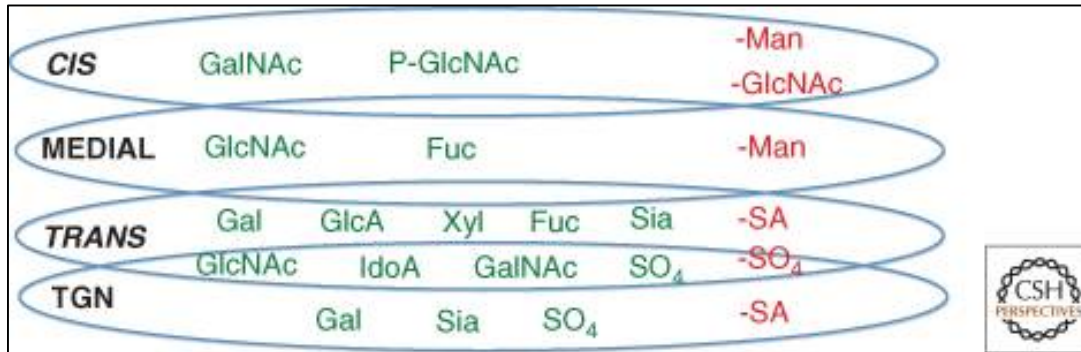


Figure 1.14. Golgi compartments showing where a specific glycosylation takes place. (Reproduced from Pamela Stanley, Cold Spring Harb Perspect Biol. 2011).

Thus, a lot of cellular processes are controlled by cell surface membranes and receptors, which in turn are regulated by correct functioning of Golgi.

1.3.3.1 Factors affecting Glycosylation.

Many factors could alter glycosylation in a cell which includes, luminal Golgi environment (Golgi pH) (Maeda and Kinoshita, 2010), Golgi structure and organization (Zhang and Ten Hagen, 2010), expression and correct functioning of enzymes catalyzing glycosylation, and proteins of conserved oligomeric Golgi (COG) complex (acts as a scaffold for Golgi membrane structure and tethering of retrograde vesicles) (Reynders et al., 2011).

1.3.3.2 Alteration in glycosylation in Normal cells.

Golgi fragmentation resulting from depletion of cisternae stacking protein, GRASP resulted in a decrease in cell surface N-glycosylation (Xiang et al., 2013). Giantin depletion mediated

Golgi fragmentation resulted in increased cells surface binding of WGA lectin, but not of ConA and PNA (Koreishi et al., 2013). Change in glycosylation is context dependent, as in it differs with the cause of change in Golgi structure or perturbation in the secretory pathway.

1.3.4 Golgi trafficking and glycosylation in a disease condition.

1.3.4.1 Alteration in trafficking in disease conditions.

In **colorectal cancer** tissue sections, number of transport vesicles were significantly less around the fragmented Golgi as opposed to normal colorectal tissue (Kellokumpu et al., 2002). This implies inhibition of anterograde/retrograde transport in these tissue samples. In a cellular model of **Parkinson's disease**, Golgi is fragmented at the onset of the disease condition. Retrograde transport was blocked while anterograde transport was significantly accelerated in these cells (Rendón et al., 2013a). In a cellular model of **Alzheimer's disease**, Golgi fragmentation is associated with accelerated anterograde transport of amyloid beta peptide (Joshi et al., 2014).

1.3.4.2 Alteration in glycosylation in disease cells.

In many cancer types, Golgi is fragmented and is accompanied by altered glycosylation (increased sialylation and decreased sulfation) on the cell surface (shorter and less branched carbohydrate chains) (Egea et al., 1993; Migita and Inoue, 2012; Petrosyan, 2015). Conserved oligomeric Golgi (COG) complex, which is made up of 8 protein subunits, plays a role in regulating retrograde trafficking (Golgi to ER) in the cells. Mutations in these proteins have been reported in patients with congenital disorders of glycosylation and results

in Golgi fragmentations and impairment in trafficking and Glycosylation (Reynders et al., 2011). Depletion of proteins of COG complex (COG 2, 3, 4, 6, and 8) resulted in increased cell surface binding of PNA, GS-II and GNL lectins (Pokrovskaya et al., 2011).

In Summary, Golgi sorts and traffic several proteins and lipid cargoes glycosylate them and regulate correct pick-up and delivery to different destinations. Any change in Golgi structure due to mutation/depletion/nonfunctioning of Golgi proteins or in disease conditions affects trafficking and glycosylation.

1.4 Golgi fragmentation in normal cellular function and disease.

1.4.1 Golgi fragmentation during mitosis.

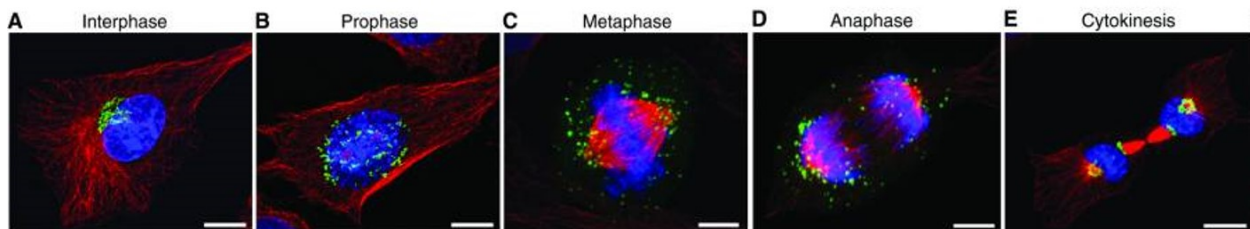


Figure 1.15. Morphology of the Golgi during the cell cycle in mammalian NRK cells. The continuous Golgi ribbon (*A*) is disassembled in early mitosis (*B*). The Golgi membranes concentrate at the spindle poles in metaphase cells (*C*). During anaphase (*D*), the Golgi membranes are partitioned and reform two ribbons on the opposite sides of the nucleus (*E*). Scale bar 10 μm (*A*, *B*, *E*); 5 μm (*C*, *D*). Images are z-projections of confocal image stacks where GM130 (green), α -tubulin (red), and DNA (Hoechst, blue). (Adapted from Yanzhuang Wang and Joachim Seemann, Cold Spring Harb Perspect Biol. 2011).

A very remarkable feature of Golgi physiology is its inheritance during the cell cycle. As the Golgi apparatus is a single copy organelle in a mammalian cell and restricted to pericentriolar localization, its inheritance to daughter cell during the cell division takes place by a dramatic morphological process known as “**Golgi fragmentation**”. During mitotic Golgi fragmentation, which is a reversible process, Golgi stacks get separated and broken down into smaller structures for its correct partitioning into daughter cells (Colanzi et al., 2003).

As described in **Figure 1.15**, at the onset of prophase mammalian Golgi gets converted into isolated stacks, which further gets fragmented in smaller structures at metaphase and becomes dispersed in the cytosol which is referred to as “Golgi haze”. By late anaphase, these fragmented Golgi structures start reassembling and become distributed as an organized and functional structure into the daughter cell. Golgi fragments are inherited into daughter cells during every cycle of cell division in all types of mammalian cells (Colanzi and Corda, 2007; Sütterlin et al., 2002). Interestingly, despite the dramatic alteration the mitotic Golgi haze retains cisternal polarity, that is, the cis-trans polarity of structural proteins and enzymes (Shima et al., 1997).

The reversible Golgi fragmentation in mammalian cells can be divided into three stages:

- a) Disassembly (consisting of ribbon unlinking, cisternal unstacking, and vesiculation).
- b) Partitioning
- c) Re-assembly of Golgi membranes

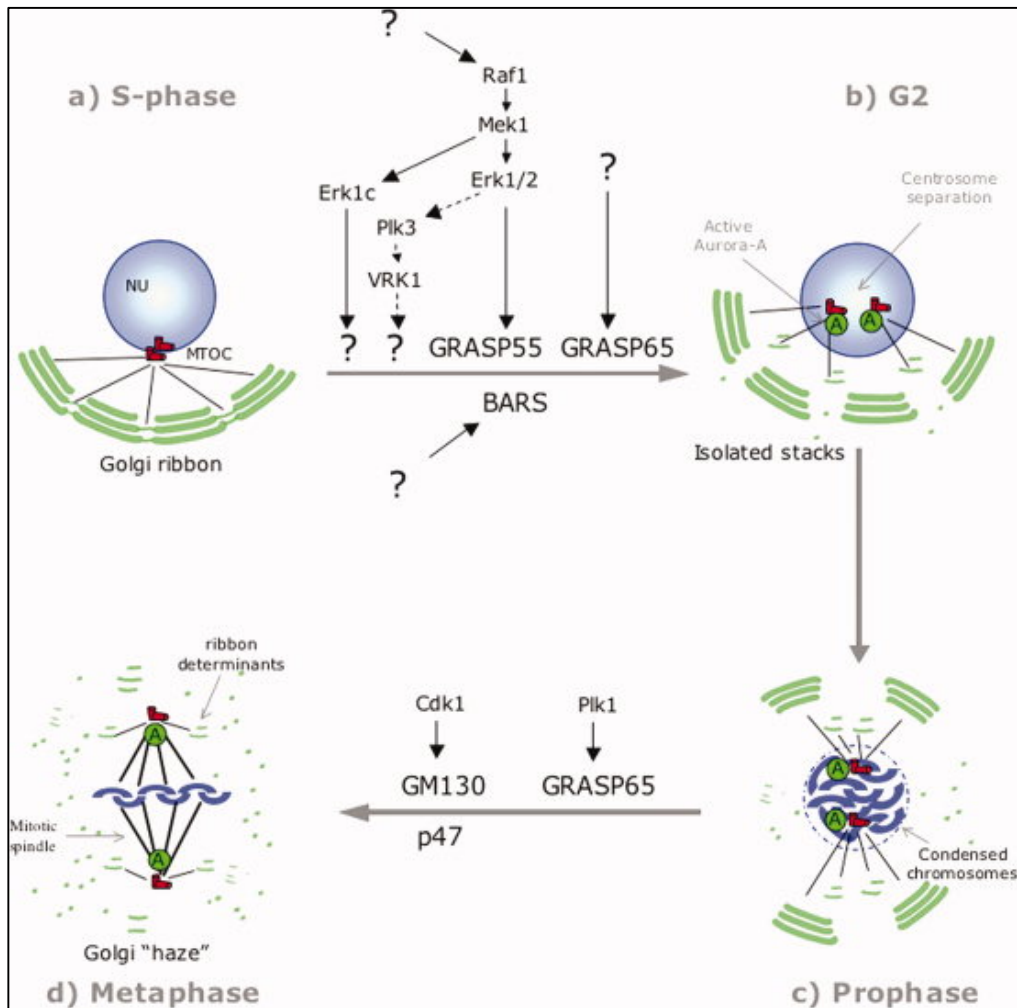


Figure 1.16. Schematic of Inheritance of the Golgi apparatus in mammalian cell displaying the regulators involved at different phases of mitosis. (Reproduced from Corda et al., IUBMB Life 2012).

(a) At the G2/M transition of cell cycle, lateral connections between individual Golgi stacks are detached and results in unlinking of the Golgi ribbon (**Figure 1.16 a, b**). This is followed by unstacking of cisternae in the isolated stacks (**Figure 1.16 c**) and subsequently fragmentation into vesicles (**Figure 1.16 d**). (b) These vesicles then get partitioned into newly forming daughter cells. (c) Golgi vesicles finally start to reassemble into a functional Golgi in both the daughter cells (Shorter and Warren, 2002).

1.4.2 Regulators of mitotic Golgi fragmentation.

1.4.2.1 Regulators involved in Sequential fragmentation.

Independent finding from several groups has defined the regulators of Golgi fragmentation, which are involved in controlling of mitotic entry of the cell, as demonstrated in **Figure 1.16**.

(a) Unlinking the Golgi ribbon.

During the late G2 phase of cell cycle, Membrane fission molecules (CtBP/BARS), Mitogen-activated kinases like Cdk1, MEK1, ERK, and Plk1 regulate unlinking of Golgi ribbon by severing the lateral connection between isolated stacks (Bisel et al., 2008; Feinstein and Linstedt, 2007). Mitogen-activated protein kinase (MEK)1 phosphorylates GRASP-55/65 to trigger unlinking of the ribbon which leads to the formation of isolated stacks (Tang et al., 2012).

(b) Unstacking of cisternae and vesiculation and partitioning.

GRASP-65, a protein involved in Golgi stacking, binds directly to GM130 and targets this complex to cis-Golgi. Cdc2 kinase phosphorylates GM130 at the onset of prophase, resulting in loss of interaction with p115, resulting in unstacking of cisternae (Lowe et al., 2000). Once the Golgi is unlinked, cisternal unstacking and conversion of Golgi membranes into vesicles, which happens simultaneously, takes place in a COPI dependent manner. Tethering of COPI vesicles happens by a ternary complex of Giantin-p115-GM130 complex and is regulated by small GTPase Rab1 (Moyer et al., 2001). Vesiculation is, in fact, a result of an imbalance of vesicle budding and fusion during mitosis.

Post unstacking and vesiculation Golgi is present in two separate pools. One being the vesicles, which is evenly distributed through the cytoplasm and second pool as clusters of

tubulo-vesicles, associated with spindles. As the mitosis progress, along with spindle, these structures gets partitioned into nascent forming daughter cells.

(c) Re-assembly of Golgi membranes.

Mechanistically, Golgi membranes re-assemble during telophase and cytokinesis, first formation of flat cisternae followed by its stacking. Eventually, Stacks come together to form two distinct Golgi ribbons on opposite sides of the nucleus as shown in **Figure 1.15 E**. Stacking and formation of ribbon requires tethering factor p115 and later GRASP proteins for re-assembly of Golgi membranes (Shorter and Warren, 1999).

1.4.2.2 Role of the microtubule.

Microtubules depolymerize when cell enter mitosis (at prophase) and as a consequence, therefore, Golgi stacks becomes small and disengage from each other and results in a perinuclear localization. At metaphase/anaphase, when spindle microtubules are aligned at the metaphase plate, Golgi cisternae disintegrate further and appear as Golgi-haze, dispersed throughout the cytoplasm. During telophase/cytokinesis, microtubules start polymerizing and driven by motor proteins, fragmented Golgi also reassembles to give two intact Golgi which gets segregated to each daughter cell (Burkhardt, 1998b).

1.4.2.3 Role of small GTPase, Arf1.

Furthermore, small GTPase, Arf1, has also been shown to be involved in mitotic Golgi fragmentation. Arf1 undergoes dynamic association-dissociation with Golgi membranes, and inactivation of Arf1 has been shown to precede and results in mitotic Golgi fragmentation (Altan-Bonnet et al., 2003). Active Arf1, GTP bound form, gets recruited to Golgi by Guanine

exchange factors (GEFs) and in turn recruits multiple cytosolic effectors to Golgi membranes that regulate protein sorting/trafficking (Donaldson and Jackson, 2000).

Research on mitotic Golgi fragmentation in past two decades led to the postulation of the organelle-specific checkpoint, known as “**Mitotic-Golgi checkpoint**”, which essentially monitors the structural integrity of the Golgi and regulate the cellular entry into mitosis. This checkpoint, however, differs from the conventional G2/M DNA damage checkpoint (Corda et al., 2012).

1.4.3 Golgi fragmentation during meiosis and apoptosis.

Apart from mitosis, various reports have identified fragmented Golgi structure during **meiosis**. Unlike mitosis, the outcome of meiosis is not an equal distribution of cytoplasmic content into daughter cells. During meiosis Golgi fuses with ER when fragmented and is not associated with the meiotic spindle. Once fertilization is committed, Golgi status does not control cytokinesis (Payne and Schatten, 2003).

During **apoptosis**, Golgi gets irreversibly fragmented, although whether it's a cause or effect remains unclear. There are certain similarities between mitotic and apoptotic Golgi fragmentation, such as the interconnected ribbon structure of the Golgi complex is lost, Golgi stacks no longer closely associated with the MTOC, individual cisternae further disassembled into clusters of vesicles and tubules dispersed throughout the cell. There is also an alteration in Golgi structural proteins Golgin-60, GRASP65, Giantin, GM130, p115. However, unlike mitosis, which is phosphorylation-mediated regulation, apoptotic Golgi fragmentation is

caspase-mediated cleavage of Golgi structural and regulatory proteins (Mukherjee et al., 2007)s.

1.4.4 Golgi fragmentation in disease conditions.

Golgi fragmentation has also been observed in many **neurodegenerative diseases**, including amyotrophic lateral sclerosis (ALS), Alzheimer's disease, Parkinson's disease, corticobasal degeneration, and Creutzfeldt-Jacob disease. However, the role of Golgi fragmentation in these conditions are poorly understood and have been addressed only now (Gonatas et al., 2006). In a cellular mimic model of Parkinson disease, Golgi fragmentation has been shown to precede the formation of inclusion bodies and is Rab and SNARE proteins dependent (Rendón et al., 2013b). Another study has highlighted the molecular mechanism and pathophysiological relevance of Golgi fragmentation during progressive motor neuropathy (neurodegenerative disorder), where crosstalk between Arf1 and TBCE (Golgi localized tubulin binding cofactor E) regulates Golgi fragmentation in this condition (Haase and Rabouille, 2015).

In many **cancer** conditions (prostate, colon, colorectal etc.) Golgi apparatus have been documented to be fragmented, however, researchers have begun to understand the role of Golgi fragmentation in the biology of cancer and tumors only recently (Petrosyan, 2015). Golgi functions such as trafficking and glycosylation are altered in different cancers, where Golgi is also fragmented (discussed in section 1.3 and 1.4). Further research is needed to understand the role and relevance of Golgi pathology in cancer.

Golgi fragmentation as a gate to cancer progression.

There is growing evidence in the field which describes Golgi fragmentation as a gate to cancer progression and metastasis which has been reviewed by Petrosyan A. (Petrosyan, 2015). In most cancers, the well-recognized alteration in glycosylation occurs as an increase in sialylation and is also reported to be associated with metastatic cell phenotype. This has been attributed as a consequence of dysregulation of glycosyltransferases and glycosidases. Further studies have provided evidence that inhibition of increased surface N-glycan and O-glycan in colon cancer cells could reverse its metastatic potential (Bresalier et al., 1991). Interestingly, studies post these findings also showed Golgi to be fragmented in these cancer cells, and likely be the reason to altered glycosylation (Egea et al., 1993; Kellokumpu et al., 2002).

Furthermore, the role of Ras superfamily of GTPase in cancer progression has been well studied for decades now. Role of Rab GTPases (which tightly associate and regulate Golgins to maintain Golgi organization and function) in cancer progression is also under investigation now. Rab GTPases, namely Rab6a (in prostate cancer) (Petrosyan et al., 2014) and Rab25 (in Breast and ovarian cancer) (Yin et al., 2012) have been linked to promoting Golgi fragmentation.

A recent report from Brad's group performed kinome- and phosphatome-wide RNAi screen in HeLa cells to investigate their role in Golgi structure and function (trafficking and glycosylation) (Chia et al., 2012b). A wide range of kinases came as a positive hit (in regulating Golgi architecture and processing), which is aberrantly downregulated in many cancers. These findings have opened up new areas for research where Golgi could be targeted for cancer therapy.

1.5 Hypothesis and Objectives of the thesis

1.5.1 Hypothesis: Can cell-matrix adhesion regulate Golgi organization and function?

This thesis tests the role of cell-matrix adhesion has in regulating Golgi organization and function. The hypothesis is built on two major observations from literature. **First**, cell-matrix adhesion (integrins) has been shown to regulate membrane trafficking and control cell cycle progression (with contribution from growth factors). Changes in cell adhesion seen to drive mitotic cell rounding. **Second**, Golgi is a vital organelle in the cells secretory pathway, is a major regulator of membrane trafficking in a cell. It is also seen to undergo a dramatic fragmentation as the cell enters mitosis. Despite this overlap, the role cell-matrix adhesion has on Golgi organization and function and its possible implications for the cell remain largely unexplored. The following objectives were designed to address this

Specific objectives of the thesis

- I. Study the effect cell-matrix adhesion has on Golgi organization.
- II. Study the regulation of Golgi organization by cell-matrix adhesion.
- III. Compare loss of adhesion mediated Golgi disorganization to Golgi fragmentation.
- IV. Study the effect of adhesion-dependent Golgi disorganization on Golgi function.
- V. Study if and how this pathway is deregulated in anchorage-independent cancer cells.

Chapter 2: Materials and Methodology

2.1 MATERIALS.

2.1.1 Reagents.

Fibronectin was purchased from Sigma (Cat. No. # F2006). Cholera toxin subunit B (CTxB) conjugated with Alexa 594 (C22843) or Alexa 488 (C34775) were purchased from Invitrogen molecular Probes and used at a 1:10000 dilution. Accutase was purchased from Sigma (Cat. No. # A6964). Lectin probes were purchased Invitrogen Molecular Probes, Concanavalin A-Alexa 488 (Cat. No. # C11252), PNA-Alexa-488 (Cat. No. # L21409), WGA-Alexa-488 (Cat. No. # W11261). UEA-FITC was purchased from Sigma (Cat. No. # L9006). Divinyl Polystyrene beads (Cat. No. # 42045A 1) were purchased from Thermo scientific. Nocodazole (Cat. No. # M1404), Latrunculin A (Cat. No. # L5163), Brefeldin A (Cat. No. # B7651), Golgicide A (Cat. No. # G0923), Cycloheximide (Cat. No. # C6255) were purchased from Sigma. Ciliobrevin D (Cat. No. # 250401) was purchased from Calbiochem. Fluoromount-G (Cat. No. # 0100-01) was purchased from Southern Biotech.

2.1.2 Antibodies.

Antibodies used for western blotting include mouse anti-Arf1 (clone 1D9, abcam, Cat. No. # ab2806) at a dilution of 1:500, Rabbit anti-Arf1 (clone EP442Y, abcam, Cat. No. # ab32524) at a dilution of 1:500, Mouse anti Dynein (clone 74.1, Millipore, Cat. No. # MAB1618) at a dilution of 1:2000, rabbit anti GFP (Santa Cruz, Cat. No. # GFP (FL): sc-8334) at a dilution of 1:700, Mouse anti β -tubulin (Clone E7, Developmental Studies Hybridoma Bank, Cat. No. #AB_2315513) at a dilution of 1:5000, mouse anti-HA.11 Epitope Tag Antibody (Clone 16B12, Covance, Cat. No. # MMS-101R) at a dilution of 1:2000,

Secondary antibodies conjugated with HRP were purchased from Jackson ImmunoResearch, and were used at a dilution of 1:10000.

Antibodies used for immunofluorescence include mouse anti-GM130 (BD transduction, clone 35, Cat. No. # 610822) at a dilution of 1:100, Mouse anti β -tubulin (Clone E7, Developmental Studies Hybridoma Bank, Cat. No. #AB_2315513) at a dilution of 1:1000, Anti-gamma Tubulin antibody (Abcam, Cat. No. # ab11317) at a dilution of 1:100, Rat anti-HA Epitope Tag Antibody (Clone 3F10, Roche, Cat. No. # 11867423001) at a dilution of 1:1000. Alexa Fluor 594 Phalloidin (Invitrogen ThermoFisher Scientific, Cat. No. # A12381) was used at a dilution of 1:100. Secondary antibodies with Alexa conjugate (488 or 594) were purchased from Invitrogen Molecular Probes (Cat. No. # A12379 and A12381) and were used at a dilution of 1:1000.

2.1.3 Plasmids.

HA-tagged (WT-Arf1, Q71L-Arf1, T31N-Arf1) and GFP-tagged (WT-Arf1 and T31N-Arf1) constructs were obtained from Dr. Satyajit Mayor (National Centre for Biological Sciences, Bangalore, India). GFP-tagged Arf1-Q71L construct was made by site-directed mutagenesis using GFP-Arf1-WT as a template and following primers:

(forward) 5'-GACGTGGGTGGCCTGGACAAGATCCGG-3' and

(reverse) 5'-CCGGATCTTGTCCAGGCCACCCACGTC-3'.

mCherry-tagged Arf1-WT and Arf1-Q71L constructs were made by releasing the Arf1 gene from GFP constructs (using Bgl II and BamHI sites) and cloning the same into an empty mCherry-N1 vector. Galtase-RFP, MannosidaseII-GFP, and KDEL-RFP constructs were all

obtained from Dr. Jennifer Lippincott Schwartz (NIH). All of the above-mentioned constructs were sequenced to confirm their identity before being used in our studies.

2.2 METHODS COMMONLY USED THROUGHOUT THE STUDY

2.2.1 Cell culture and transfections.

Mouse embryonic fibroblasts (MEFs) obtained from Dr. Richard Anderson (University of Texas Health Sciences Centre, Dallas TX) were cultured in complete Dulbecco's modified Eagle's medium (DMEM) (Invitrogen) with 5% fetal bovine serum (FBS) and penicillin-streptomycin (Invitrogen) at 37°C in a 5% CO₂ incubator. Human foreskin fibroblasts (BJ) Cells from ATCC and were cultured in complete Dulbecco's modified Eagle's medium (DMEM) (Invitrogen) with 10% fetal bovine serum (FBS) and penicillin-streptomycin (Invitrogen). Human umbilical vein endothelial cell line (EA.hy926) was a generous gift from Dr. Madhulika Dixit (IIT Madras). EA.hy926 cells were cultured for up to 4 passages in DMEM (Invitrogen) with 10% fetal bovine serum (FBS) supplemented with EGM-Plus SingleQuots (Lonza). MCF10A cells were obtained from Dr. Mayurika Lahiri (IISER Pune), and cells were grown in High Glucose DMEM without sodium pyruvate (Invitrogen) containing 5% horse serum (Invitrogen), 20 ng/mL EGF (Sigma), 0.5 µg/mL hydrocortisone (Sigma), 100 ng/mL cholera toxin (Sigma), 10 µg/mL insulin (Sigma) and 100 units/mL penicillin-streptomycin (Invitrogen) and were resuspended during sub-culturing in High Glucose DMEM without sodium pyruvate containing 20% horse serum and 100 units/mL penicillin-streptomycin (Invitrogen). 38B9 Pro-B cells and EL4-Pro-T cells were obtained from Dr. Jagan Pongubala (University of Hyderabad, India). 38B9 cells were cultured in RPMI+10% FBS+ 50 µM mercaptoethanol. E14 cells were cultured in DMEM+10% FBS.

WT-MEFs and BJ cells were transfected using LTX-PLUS (Invitrogen) and EA.hy926 cells using FuGENE (Promega) according to the manufacturer's protocol. Transfections were done in 6 cm dish using 4 μ g DNA for 6 hours (EA.hy926) or 12 hours (WT-MEFs and BJ cells). 36 hours after transfection cells were serum starved for 12 hours with DMEM containing 0.2% FBS.

2.2.2 Suspension and re-adhesion of cells.

WT-MEFs, Human Endothelial cells (EA.HY926s) or Human fibroblasts were all cultured in their respective growth medium in 60 mm dishes to ~ 75% confluency. Cells were serum starved (0.2% FBS) for 12 hours detached using Trypsin-EDTA (Invitrogen) or Accutase (Sigma) (for lectin labeling experiments), washed with 0.2% FBS containing DMEM, processed on the ice and an aliquot of cells collected as the 5 mins suspension time point. Cells were then held in suspension with 1% methylcellulose containing low serum DMEM (0.2% FBS) for increasing time (5 mins to 120 mins) as required (**Figure 2.1**). Post incubation cells were carefully washed twice with 0.2% FBS DMEM at 4^oC to avoid clumping and collected at the required time. These processed cells when needed were re-plated on coverslips coated with 2 μ g/ml fibronectin for the required time (5 mins, 15 mins, 4 hours for stable adherent cells). For confocal microscopy cells were fixed with 3.5% paraformaldehyde (PFA) for 15 mins at room temperature (RT), washed with PBS thrice, stained and mounted. For western blotting, suspended and re-adherent cells were lysed required amount of 1X Laemmli, heated at 95^oC for 5 mins and stored at -80^oC.

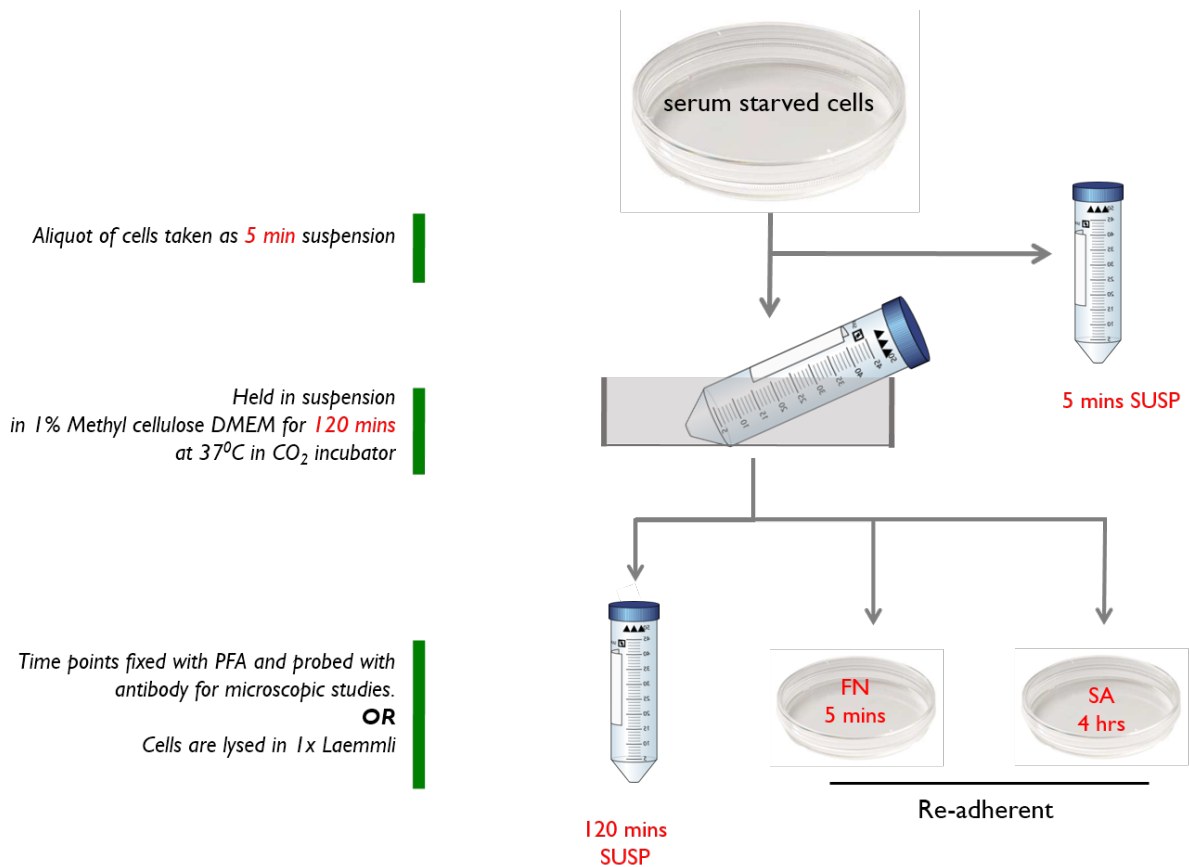


Figure 2.1 Schematic of the suspension assay. WT-MEFS or other cell types were cultured in their respective growth medium in 100 mm dishes to ~ 75% confluency. Cells were serum starved (incubated with medium containing 0.2% FBS) for 12 hours detached using Trypsin-EDTA (Invitrogen) or Accutase (Sigma) (for lectin labeling experiments), washed with 0.2% FBS containing DMEM, processed on the ice and an aliquot of cells collected. This processing takes about 5 mins and these detached cells are accordingly labeled as (detached 5'). Cells were then held in suspension with 1% methylcellulose containing low serum DMEM (0.2% FBS) for the required time. Post incubation cells were collected at the required time, carefully washed twice with 0.2% FBS DMEM at 4°C to avoid clumping. These processed cells when required were re-plated on coverslips coated with 2 µg/ml fibronectin for the required time (5 mins, 15 mins or 4 hours for stable adherent cells). For confocal microscopy suspended or re-adherent cells were fixed with 3.5% paraformaldehyde (PFA) for 15 mins at room temperature (RT), washed with PBS thrice, stained and mounted using fluoramount. For western blotting, suspended and re-adherent cells were lysed in the required amount of 1X Laemmli, heated at 95°C for 5 mins and stored at -80°C.

2.2.3 GM1 labeling of cells with CTxB.

Serum-starved WTMEFs detached with trypsin were labeled for 15min on ice with cholera toxin B subunit (CTxB) conjugated to Alexa 488 or Alexa 594. These cells were washed and fixed to look at surface GM1 labeling, to begin with, held in suspension for 120 mins to observe GM1 endocytosis. Cells were fixed with 3.5% PFA, mounted and observed. To test the role of the cytoskeleton in GM1 endocytosis adherent cells pre-treated with Nocodazole (10 μ M) or Latrunculin A (0.5 μ M) for one hour were detached, labeled and endocytosis similarly observed. Z stacks of surface GM1 labeled cells were deconvoluted and surface rendered to determine cell shape in suspended and re-adherent cells.

2.2.4 Measuring Cell volume using surface GM1 labeled suspended and re-adherent cells.

Z stacks of surface GM1 labeled cells were deconvoluted and surface rendered to determine cell shape in suspended and re-adherent cells. Threshold of 2% was set in order to completely fill the cell and hence giving a continuous structure. The average volume for suspended and re-adherent cells was then compared.

2.2.5 Binding of fibronectin and poly L-Lysine coated beads to cells.

8x10⁸ Divinyl polystyrene beads were re-suspended in 500 μ l PBS and sonicated for 30 seconds. Beads were washed thrice with cold 1X PBS (pH 7.4), centrifuged at 6000 rpm for 5 mins at 4°C and incubated with 500 μ l PBS containing 10 μ g/ml Fibronectin or 10 μ g/ml Poly-L-Lysine at 4°C overnight on a rotary shaker. Coated beads were centrifuged, washed with cold 1X PBS (pH 7.4) and blocked with 50 mg/ml BSA at 4°C for 3 hours on a rotary shaker. Beads were washed and re-suspended finally in 100 μ L of PBS (pH7.4). Adherent

WT-MEFs were labeled with CTxB-Alexa-594 on ice for 15 mins and then washed thoroughly to remove unbound probe. FN-coated beads (cells to bead ratio 1:10) were added and incubated for 15 mins at 37°C. Cells were then PFA fixed and mounted using Fluoromount-G. Cells with bound bead were then imaged.

Untransfected or GalTase RFP transfected serum-starved cells (2×10^5) were detached, held in suspension for 30 mins in 2 ml 0.2% FBS containing DMEM with 1% methylcellulose. 12.5 μ l FN or PLL coated bead suspension (2×10^6 beads) was added to the cells (cells: bead ration maintained at 1:10) mixed gently and incubated for 15 mins at 37°C. Cells were washed gently and fixed with 3.5% PFA for 15 mins and RT. Immunostaining of cells for GM130 was done as discussed later, with all washing steps done very carefully. Cells were then mounted using Fluoromount-G, allowed to dry for 24 hours and then imaged. Cells with bound beads were identified in the population and used for comparison.

2.2.6 Spatial Golgi localization relative to the cell-bound fibronectin coated bead.

Cross-sectional images of cells with a single attached FN bead were selected and an outline of the cell boundary with the location and outline of the bead made. The Golgi area was then mapped within the cell. These line drawings for cell outline + bead outline + mapped Golgi area for each cell were grouped together and the position of beads across cells was moved to cause them to overlap. The relative position of the Golgi for each cell while maintained relative to the bead was now comparable across cells and for bead position. This now allows us to generate a combined image for all cells with their cell perimeter and bead position being

identical and lets us look at Golgi position relative to the same. Golgi outlines are made transparent to allow us to see the overlap in localization.

2.2.7 Inhibitors studies.

For all the inhibitor studies, cells transiently expressing GalTase-RFP and ManII-GFP were serum starved with 0.2% FBS containing DMEM for 12 hours, trypsinized and held in suspension for 60 mins in 5ml of 1% methylcellulose containing DMEM. Cells were then treated with Nocodazole (10 μ M in DMSO), Latrunculin A (0.5 μ M in DMSO), BFA (10 μ g in MeOH), Ciliobrevin D (20 μ M in DMSO) and incubated for an additional 30 mins at 37°C. Control cells were treated with an equivalent volume of solvent (DMSO /MeOH). Cells were processed as described in suspension assay and suspension time point samples collected. Cells were re-plated on FN-coated coverslips with or without inhibitor for 5 mins, fixed, mounted and imaged using a confocal microscope.

2.2.8 Arf1 activity assay.

Cells serum starved with 0.2% FBS containing DMEM for 12 hours were detached using Trypsin-EDTA, held in suspension for 120 mins (120' SUSP), re-plated on fibronectin (10 μ g/ml) for 15 mins (15'FN) and for 4 hours to be stable adherent (SA). Cells were lysed and processed for Arf1 activity assay as described earlier (Balasubramanian et al., 2007). 30 μ L of WCL and all of the GGA3 pulldown sample were resolved by 12.5% SDS-PAGE gel and transferred to PVDF membrane (Millipore). Blots were blocked with 5% milk in Tris-buffered saline containing 0.1% Tween-20 (TBST) for 1 hour at RT and incubated with the anti-Arf1 antibody (Clone 1D9, Abcam) diluted 1:500 in 2.5% milk in TBST at 4°C overnight. Blots

were washed and incubated with anti-mouse HRP diluted 1:10000 in 2.5% milk in TBST at RT for an hour and developed with PICO chemiluminescence detection system (Thermo Scientific). LAS4000 (Fujifilm-GE) was used to image the blots and densitometric band analysis was done using Image J software (NIH).

To determine Percentage Arf1 activity, following calculation was used:

$$\text{Percentage Arf1 Activity} = \frac{\text{Pulldown Band Intensity} \times 100}{\text{Corresponding WCL Band Intensity} \times \text{Dilution factor}}$$

Dilution factor was calculated as the ratio of the amount of total cell lysate used for the pulldown (400 μ l) and the amount of this lysate loaded as representative of whole cell lysate (WCL) on SDS PAGE, (22.5 μ l WCL + 7.5 μ l 4 \times Laemmli). The dilution factor was hence $400 \div 22.5 = 17.77$. This ratio was kept constant in all the experiments in this study. Percentage active Arf1 levels thus calculated were compared between stable adherent, suspended and re-adherent cells.

Arf1 activity assay for inhibitor studies: For inhibitors studies (BFA, Ciliobrevin, and Nocodazole) percentage active Arf1 values for suspended or re-adherent cells were normalized to the control untreated cells and represented. Similarly, total Arf1 levels (Arf1/Actin in WCL samples) in inhibitor-treated cells were normalized to untreated controls and represented in every experiment.

2.2.9 Detection of Dynein bound with Active Arf1.

Active Arf1 was pulled down using the GST-GGA3 construct as described earlier for the activity assay. Pull down and whole cell lysate (WCL) samples were probed for mouse anti-

Arf1 antibody (clone 1D9, abcam, Cat. No. # ab2806) at a dilution of 1:500 and mouse anti Dynein antibody (clone 74.1, Millipore, Cat. No. # MAB1618) at a dilution of 1:2000. Arf1 and dynein levels in the pulldown were normalized to respective levels in the WCL, values thus obtained normalized to stable adherent cells and compared suspended and re-adherent cells.

Serum-starved 10×10^5 live WT MEF cells either treated with BFA (10 $\mu\text{g}/\text{mL}$ in MeOH) or MeOH as a control for 2 hours. Cells were lysed and immediately processed for pulldown of Active Arf1 using GST GGA3 beads as described earlier. Active Arf1 levels and dynein bound in pull-down fractions were detected by western blot and compared.

2.2.10 Immunofluorescence detection of the cis-Golgi marker, GM130.

Serum-starved cells held in suspension as described earlier or re-adherent were fixed with 3.5% paraformaldehyde (PFA), permeabilized with PBS containing 5% BSA and 0.05% Triton-X100 for 10 mins at RT. Cells were then blocked with 5% BSA in PBS for 30 mins at RT and then incubated with anti GM130 antibody diluted 1:100 in PBS with 5% BSA for an hour at RT. Cells were washed with PBS and incubated with 1:1000 diluted anti-mouse Alexa 488/ Alexa 568 antibody (as required) at RT for one hour. Suspended cells were similarly labeled in Eppendorf tubes and mixed regularly by tapping to prevent cells from settling. Cells were washed with 1X PBS and eventually reconstituted and mounted using flouromount-G.

2.2.11 Confocal Microscopy.

Cells were imaged using the Zeiss 710 or 780 laser scanning confocal microscopes using a 63X oil objective (NA 1.4). Acquisition settings were kept constant at: laser power = 2 %, 84

Pinhole = 1 AU, gain = 700 to 800 and images acquired at 1024 x 1024 resolution. Z-stacks were acquired at 0.2 μm interval thickness, deconvoluted and rendered as discussed below.

2.2.12 Deconvolution of Z stacks and object analysis.

All the images were processed and analyzed using the Huygens Professional version 16.10 (Scientific Volume Imaging, The Netherlands, <http://svi.nl>). De-convolution of confocal z-stack was optimized using the following settings. Average background value = 1, number of iterations = 30, signal to noise ratio (SNR) = 20, and quality change threshold = 0.0001. These settings were kept constant for all de-convoluted images discussed in this study. Theoretical point spread function (PSF) values were estimated for each z-stack and provide the minimal voxel size that the confocal microscope could resolve. This PSF value was then used in the software as garbage volume for surface rendering and object analysis. De-convoluted images were rendered either as a 3D maximum intensity projection (using the MIP Renderer plug-in) or surface rendered (using the Surface render plug-in with a 15% primary threshold). The top view of a MIP or surface rendered cell (zoomed 1.5X or 2.5X) was used to represent the Golgi phenotype. When needed a cross-sectional view along the Z-Axis of the MIP image was used to observe the localization of the Golgi in a re-adherent cell. Surface rendered images for GM1 labeled with CTxB were used to observe cell shape. When needed a movie representing the Golgi architecture was made using the deconvoluted 3D surface rendered image by processing it through the Huygens movie maker plugin.

The number of discontinuous Golgi objects in a 3D deconvoluted image was determined using the advanced object analysis plugin in the Huygens Professional software. The garbage

volume was set as calculated earlier, and a 15% threshold used to determine the number of discontinuous Golgi objects present in a cell. This was done for all cells in each treatment and the average number of Golgi objects determined. These were then compared between treatments to comment on the extent of the Golgi disorganization.

2.2.13 Determining the Golgi distribution profile in a cell population.

Cells were imaged using a confocal microscope and the structure of the Golgi observed and classified as organized or disorganized. An ***“Organized”*** Golgi was defined as one major compact object, plus 0-5 minor objects which were localized near to each other; ***“Disorganized”*** Golgi was defined combination of two phenotype: Partly disorganized (5-15) objects scattered in the cell, and disorganized (15-40) objects completely dispersed in the cell. A minimum of 50 (for bead experiments) and maximum of 200 randomly selected cells were observed in each population or treatment and their Golgi structure was classified as above. These numbers were then used to calculate percentage distribution of organized vs disorganized Golgi in each population. Representative cross-sectional confocal images of organized and disorganized Golgi from each population or treatment were acquired, deconvoluted, surface rendered.

2.2.14 Co-localization analysis.

The co-localization analysis was done using the Colocalization Analyzer Plug-in in the SVI Huygens Professional software (version 16.10). Deconvoluted cross-sections of a combination of Golgi markers were used to calculate Pearson’s coefficient. These values were then compared between suspended and re-adherent cells. De-convoluted z-stack of the entire cell

expressing cis-medial Golgi marker (Man II GFP) and ER marker (KDEL-RFP) were used to calculate Pearson coefficients. These values were then compared between untreated and BFA treated suspended cells. A line plot of the intensities for each marker was determined using the Huygens twin slicer plugin. Fluorescence intensities thus obtained for both markers were plotted using GraphPad Prism and the overlap in their intensities compared.

2.2.15 Cell membrane lectin labeling and quantitation by flow cytometry. (Specific to Chapter 6).

For studies on lectin binding, WTMEFs serum starved for 12 hours were detached using Accutase (Sigma), processed and then held in suspension for 120 mins. 10×10^5 live cells following detachment (5' SUSP) and after 120min in suspension, were incubated with Alexa-488 conjugated ConA ($0.025 \mu\text{g}/\mu\text{L}$), PNA ($0.025 \mu\text{g}/\mu\text{L}$), WGA ($0.0005 \mu\text{g}/\mu\text{L}$) and FITC-UEA ($0.1 \mu\text{g}/\mu\text{L}$) for 15 mins on ice in the dark in $200 \mu\text{l}$ PBS. Cells were gently mixed during incubation to avoid clumping. They were eventually washed with cold PBS, fixed with 3.5% PFA for 15 mins at RT and re-suspended in $200 \mu\text{L}$ PBS. Cells were analyzed using the BD LSRFortessa SORP cell analyzer. Unlabeled detached (5 min) and 120 mins suspended cells were analyzed to set forward and side-scatter profiles and this was then used to set a gate to classify autofluorescence and then lectin fluorescence was measured. 10000 events were recorded for each treatment and time point to obtain levels of bound lectins on the cell surface. This data was analyzed using the Flowing software 2.5.1 and median fluorescence intensity was calculated for each cell population. Median fluorescence intensities of 120 mins suspended cells were normalized to their respective 5 min suspension time points and compared.

Time Kinetics for Lectin binding.

For time kinetics studies, WTMEFs serum starved for 12 hours were detached using Accutase (Sigma), and 10×10^5 cells were held in suspension for 5, 10, 20, 30, 60 and 120 mins. Every time point was labeled with Alexa-488 conjugated ConA ($0.025 \mu\text{g}/\mu\text{L}$) for 15 mins on ice in the dark in $200 \mu\text{l}$ PBS. Rest of the protocol was followed as described in the previous section.

Cycloheximide for Lectin binding.

For cycloheximide studies, WT-MEFs serum starved for 8 hours were either mock treated or with $40 \mu\text{g}/\text{mL}$ cycloheximide (CHX) for 4 hours. Cells were then similarly subjected for ConA labelling at 5'SUSP and 120'SUSP time points as described earlier.

Lectin binding studies with Arf1 mutants.

WTMEFs transfected with empty CherryN1, WT-Arf1-CherryN1 and Q71L-Arf1-CherryN1 using LTX-PLUS transfection reagent (Invitrogen) were serum starved for 12 hours, detached (5' SUSP) using Accutase and held in suspension for 120 mins. 10×10^5 live cells (for each construct) were collected at both time points. Cells were surface labeled with Alexa-488 conjugated ConA ($0.025 \mu\text{g}/\mu\text{L}$), and FITC conjugated UEA ($0.1 \mu\text{g}/\mu\text{L}$) as described above. 7000 cells in the population gated for cherry fluorescence (Arf expression) were analyzed for lectin binding (Alexa 488/FITC). Flowing software 2.5.1 was used to determine median fluorescence intensity for bound lectin in cells suspended for 120 mins normalized to its respective 5 min suspension time point. Basal lectin levels (at 5 min suspension) were also compared across cells expressing Arf1 cherry constructs for WT-Arf1-Cherry and Q71L-Arf1-Cherry constructs.

2.2.16 Statistical analysis.

All the analysis was done using Prism Graphpad analysis software. Statistical analysis of data (number of Golgi objects, Arf1 activity, Pearson coefficient, and lectin studies) was done using the two-tailed unpaired Mann-Whitney t-test and when normalized to respective controls using the two-tailed single sample t-test. Statistical analysis for changes in distribution profile of Golgi phenotype was done using the two-tailed, Chi-square t-test. A minimum of 150 cells (from two or three independent experiments as stated) were counted and analyzed across experiments.

Chapter 3

**Study the effect of cell-matrix
adhesion on Golgi organization.**

3.1 RATIONALE.

Cell-matrix adhesion and its regulation of various cellular processes, signaling, migration, endocytosis, exocytosis, cytokinesis, cell polarity, have been explored in great depth. Formation of “focal adhesion”, where scaffolding of signaling molecules such as integrin-linked-kinase (ILK), focal adhesion kinase (FAK), Rho-GTPase family proteins, are the early steps in integrin-mediated adhesion regulation and has also been extensively studied (Geiger et al., 2001a; Lawson and Schlaepfer, 2012). Loss of cell-matrix adhesion regulates membrane trafficking by controlling FAK and Src kinase-dependent caveolar and membrane “raft” endocytosis which in turn triggers downregulation of growth signaling (Akt and Erk) (Pelkmans et al., 2005; del Pozo et al., 2004a, 2005). Integrin-mediated adhesion to ECM is essential for activation of MEK1, expression of cyclin-D1 and progression through a G1-S phase of cell cycle (Reverte et al., 2006; Schwartz and Assoian, 2001a; Schwartz and Ginsberg, 2002). Resting interphase cells have large focal adhesions which are disassembled at the onset of mitosis with changes in cell morphology, as cells adopt a round shape (Ezratty et al., 2005; Geiger et al., 2001b; Maddox and Burridge, 2003).

Furthermore, an intact organized Golgi appropriately positioned in a cell is crucial for glycosylation, trafficking, and directed secretion which will, in turn, affect processes like cell polarization and migration (Millarte and Farhan, 2012; Wilson et al., 2011; Yadav and Linstedt, 2011a). Proteins and lipids modified in the Golgi apparatus are directed to multiple destinations in the cell such as the endosomes, plasma membrane, and extracellular secretory pathways, in a tightly coordinated manner (Bonifacino and Rojas, 2006; De Matteis and

Luini, 2008). Interestingly, when the cell enters mitosis, “rounding up” of the cell (loss of adhesion to ECM connection) precede Golgi fragmentation (Maddox and Burridge, 2003; Suzuki and Takahashi, 2003). This raises the possibility that loss of adhesion event could have a role in mitotic Golgi fragmentation which remains unexplored. Additionally, in a migratory cell that is the adherent positioning of Golgi is regulated (Yadav and Linstedt, 2011b; Yadav et al., 2009), though if this is dependent on the Golgi organization and if and how adhesion controls the same remains largely unexplored.

This study, hence focussed on what happens to the Golgi organization in anchorage-dependent cells on their “loss of adhesion” and “restoration of adhesion” to fibronectin matrix. The aim of this chapter was to evaluate and characterize the Golgi organization phenotype in various anchorage-dependent cells under conditions where cells are just detached, held in suspension for increasing times and then re-plated on fibronectin (or fibronectin-coated beads) for increasing times.

- (1) Mouse embryonic fibroblasts (WT-MEF)
- (2) Human endothelial cells (EA.hy.926)
- (3) Human foreskin fibroblast cells (BJ)
- (4) Human breast epithelial cells (MCF10A)

These studies are done in these cells in low serum conditions to ensure that growth factor-mediated signaling is significantly reduced allowing us to look at this regulation by cell-matrix adhesion alone. Independently, the effect presence of serum growth factors have on the Golgi organization in these cells was also explored. These studies were done using distinct Golgi markers that label specific Golgi compartments (a) Cis, (b) Cis-Medial, (c) Trans Golgi, using antibody staining or transient expressing GFP/RFP tagged fusion proteins.

3.2 RESULTS.

3.2.1 Cell-matrix adhesion regulates signaling/endocytosis.

To evaluate if cell-matrix adhesion has any role in regulating Golgi organization, firstly time frame was established to test the hypothesis. As the aim is to compare organization of a membrane-bound organelle, which could be influenced by cell shape and size, the possibility of investigating this aim in cells which are adherent and completely spread out was ruled out on the coverslip. In order to negate the contribution growth factors and to be completely sure that cell-matrix adhesion is the primary cause of regulating Golgi organization, cells were serum starved for 12 hours (grown in medium with 0.2% serum).

Serum-starved WT-MEFs were labeled with Cholera toxin B subunit (CtXB-Alexa-594) on ice to label GM1 (lipid in raft microdomains on the cell surface). Cells were detached (5' SUSP) and held in suspension for 120 mins in 1% methyl cellulose (120' SUSP), and re-plated on fibronectin for 5 mins (5' FN). To examine the cell shape and volume in these time frames, cell shapes were visually compared and found it to be more or less spherical (Figure 3.1a). Next, volume of the entire cell was measured and observed no difference (Graph in Figure 3.1a). Next, the effect on downstream AKT activation in these time frames were evaluated. Immunoblots revealed that in suspension (120' SUSP) AKT phosphorylation was significantly reduced and it was rapidly triggered on just 5 mins of re-adhesion to fibronectin (Figure 3.1b). The endocytosis of GM1 which has been earlier reported to be regulated by cell-matrix adhesion (Balasubramanian et al., 2007) was also checked. GM1 as detected by

CTxB-Alexa-594 fluorescence labeled the cell surface in 5'SUSP, which was endocytosed and localized to recycling endosomes after 120'SUSP. On re-adhesion to fibronectin endocytosed GM1 could be seen moving towards cell periphery (Figure 3.1c). These data established the time frame that could be utilized to investigate the central question.

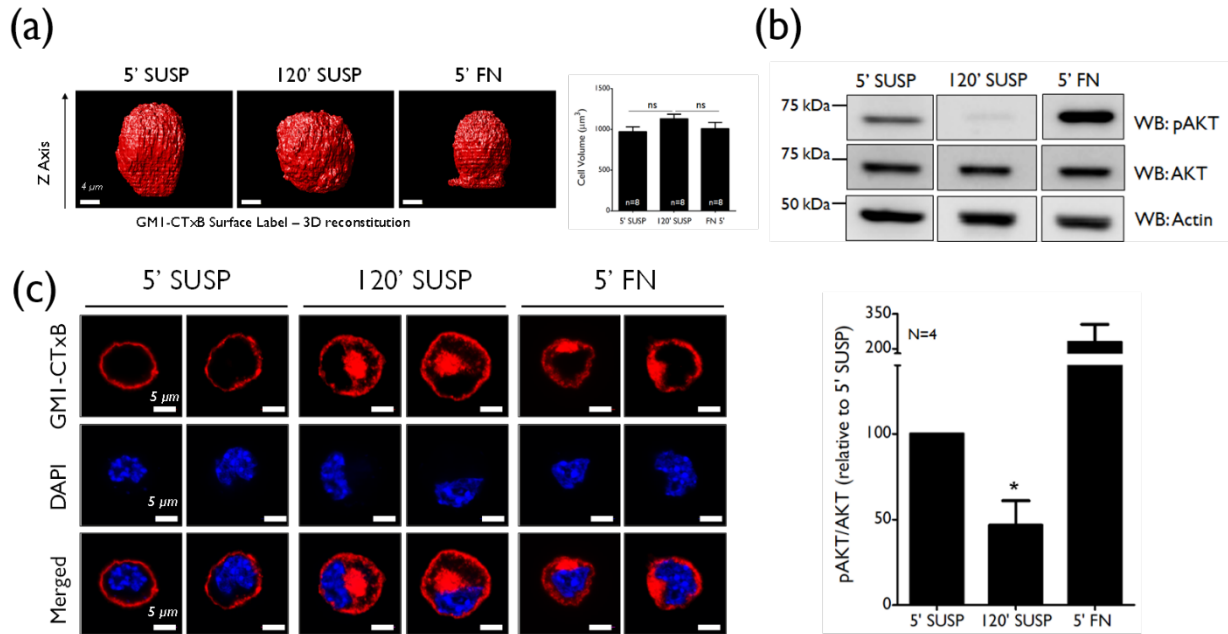


Figure 3.1 Selection of time points from suspension assay. (a) Stable adherent WT-MEFs pre-labeled with CTxB-Alexa 594 on ice for 15 mins were detached (5' SUSP) and held in suspension for 120 mins (120' SUSP), and re-plated on fibronectin for 5 mins (5' FN). Confocal Z stacks were deconvoluted, 3D reconstituted and the threshold set to fill the cell volume and observed along their Z-Axis. Scale bar in the images is set at 4 μm . The volume of such a cell was measured and represented as mean \pm SE from 8 cells from two independent experiments. (b) Western blot detection of phosphorylation on the serine 747 residues of AKT (S747), total AKT and actin in lysates from serum-starved WTMEFs stable adherent (SA), suspended for 120 mins (120' SUSP) and re-adherent on fibronectin for 5mins (5' FN). The ratio of pAkt/Akt was normalized to 5' SUSP and is represented in the graph as mean \pm SE from four independent experiments. (c) Stable adherent WT-MEFs pre-labeled with CTxB-Alexa 594 on ice for 15 mins were detached (5' SUSP) and held in suspension for 120 mins (120' SUSP), and re-plated on fibronectin for 5 mins (5' FN). Representative confocal cross-sections images of CTxB, DAPI and merged images are shown from 3 independent experiments. Scale bar in the images is set at 5 μm .

3.2.2 Localization of Golgi markers in cell lines used.

As a first step to address the hypothesis, localization of different Golgi markers in anchorage-dependent cell lines when they were completely adherent and well-spread (Figure 3.2) was checked. Mouse embryonic fibroblasts showed all the Golgi markers, cis-Golgi (by antibody staining for GM130), cis-medial Golgi (by expressing Mannosidase-II GFP) and trans-Golgi (by expressing GalTase-RFP) to be organized, perinuclear localization, as reported earlier in the literature (Figure 3.2 a-c). Similarly, human breast epithelial cells (MCF10A) cells revealed cis-Golgi (GM130) to be organized (Figure 3.2 d). Human foreskin fibroblast cells (BJ) (Figure 3.2 e, f) and human endothelial cells (EA.hy.926) (Figure 3.2 g, h) also displayed cis-medial (Man II GFP) and trans-Golgi (GalTase-RFP) to be organized and positioned perinuclearly.

These data established that Golgi in these cells, to begin with, was organized and positioned properly in adherent conditions.

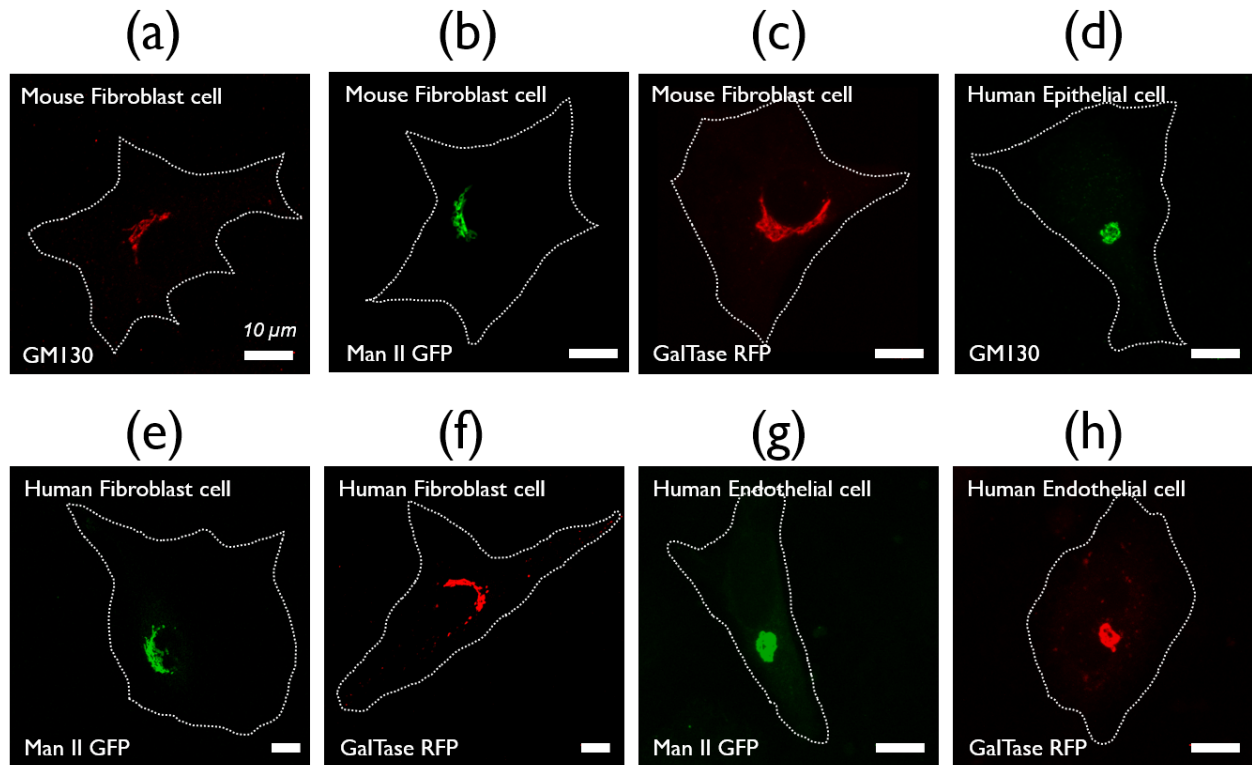


Figure 3.2 Expression/localization of Golgi markers in adherent cells. WT-MEFs **(a)** untransfected or **(b)** transfected with Man II GFP **(c)** transfected with GalTase RFP serum starved for 12 hours and fixed. Untransfected cells were immunostained with the anti-GM130 antibody. **(d)** Human normal breast epithelial cells (MCF 10A) cells fixed and immunostained with the anti-GM130 antibody. Human foreskin fibroblast cells (BJ) were transfected with **(e)** Man II GFP **(f)** GalTase RFP and serum starved for 12 hours and fixed. Human endothelial cells (EA.hy926) were transfected with **(g)** Man II GFP **(h)** GalTase RFP and serum starved for 12 hours and fixed. Representative confocal cross-sections images are shown. Scale bar in the images is set at 10 μ m.

3.2.3 Adhesion regulate Golgi organization in mouse embryonic fibroblast cells.

To access the role of adhesion on Golgi organization in mouse embryonic fibroblasts (WT-MEF) Golgi was visualized in the time points optimized earlier. Remarkably, serum starved WT-MEFs on the loss of adhesion, that is, loss of integrin-ECM connection, triggered disorganization of cis-Golgi (immunostained with anti-GM130 antibody) as represented in Figure 3.3 a. Confocal z-stacks when deconvoluted, surface rendered and 3D reconstituted revealed disorganization of cis-Golgi began as early as 5' SUSP, and this effect was further amplified by 120' SUSP. On re-adhesion to fibronectin for 5 mins, when mostly the integrin-mediated signaling has been initiated, cis-Golgi disorganized objects collapsed to form an intact organized phenotype. This observation was quantitated by calculating the number of discontinuous objects in single 3D reconstituted confocal z-stack, and found that an average number of Golgi objects were significantly less in 5'FN (~5) relative to 120'SUSP (~40) in a cell (Figure 3.3 b).

This suggests cell adhesion to the matrix (mostly through integrin engagement to ECM and hence activation/signaling) regulates Golgi organization which is a rapid and reversible process. As the number of Golgi objects varied, the total Golgi volume (Figure 3.3 c) and total Golgi surface area (Figure 3.3 d) of a suspended and re-adherent cell were compared and noted that there was a subtle increment in volume but no substantial difference in surface area. This suggested that adhesion disorganizes cis-Golgi compartment such that the structure separate out and move away, but there was no swelling in these Golgi compartment keeping the volume and area unaffected.

Golgi disorganization in response to adhesion was also observed for trans-Golgi (Figure 3.4a), which was visualized and characterized by GalTase-RFP fluorescence which re-organized rapidly on re-adhesion like cis-Golgi. Interestingly, disorganization of trans-Golgi in suspended cells was observed to a much greater extent than cis-Golgi. This is reflected in the number of discontinuous objects for GalTase in 120'SUSP (~80), which was brought down to ~10 in 5'FN time point (Figure 3.4 b). Total Golgi volume of 120'SUSP cell was significantly more than 5'SUSP, and this reverted to re-adhesion, 5' FN (Figure 3.4 c). A similar pattern was observed for the total Golgi surface area for GalTase in suspended and re-adherent cells. These results indicated that adhesion regulates trans-Golgi organization likewise cis-Golgi but to a different extent. There could be few explanation for this differential disorganization, which is discussed in the later chapter.

Golgi disorganization in response to adhesion was also observed for cis/medial-Golgi which was visualized and characterized by Man II-GFP fluorescence (Figure 3.5 a, b). This phenotype was found to be similar to cis-Golgi (GM130) regulation by adhesion.

To further ascertain the regulation of adhesion on Golgi organization on the fraction of the population of cells, percentage distribution of the organized vs disorganized trans-Golgi phenotype was determined. When compared in the cell population, confirms the disorganized phenotype to be prominent (~85 %) in suspended cells, reversed rapidly on re-adhesion (Figure 3.6 a, b). This confirmed that cell-matrix adhesion regulates Golgi organization in the majority of the cell population.

As there were differences in Golgi organization between 5' and 120' SUSP cells, the kinetics of Golgi disorganization and re-organization in WT-MEFs for all the three Golgi markers used previously were analysed in the cross-sectional images (cis, cis-medial, and trans-Golgi) (Figure 3.7 a).

Effect of loss of adhesion on Golgi disorganization could be detectable in early suspension time points, 5' SUSP, and appeared evident around 20' SUSP, as indicated by a number of Golgi objects in each time points (Figure 3.7 b). There was a subtle increase in a number of Golgi objects by 120' SUSP time point. As noted earlier, the extent of trans-Golgi disorganization was seen more than cis or cis-medial Golgi for any time point. Conversely, re-adhesion to fibronectin for 5 mins caused all three Golgi compartments to organize at a more or less similar rate (Figure 3.7 b). Post 10 mins on fibronectin, cells started to spread and that changed the shape and volume of the entire cell to be different, making it unfit to comment on Golgi organization in relation with suspended or 5'FN cells, which are close to spherical in shape. These data provided evidence that adhesion regulation on Golgi organization is a very rapid and reversible event in anchorage-dependent fibroblast cells.

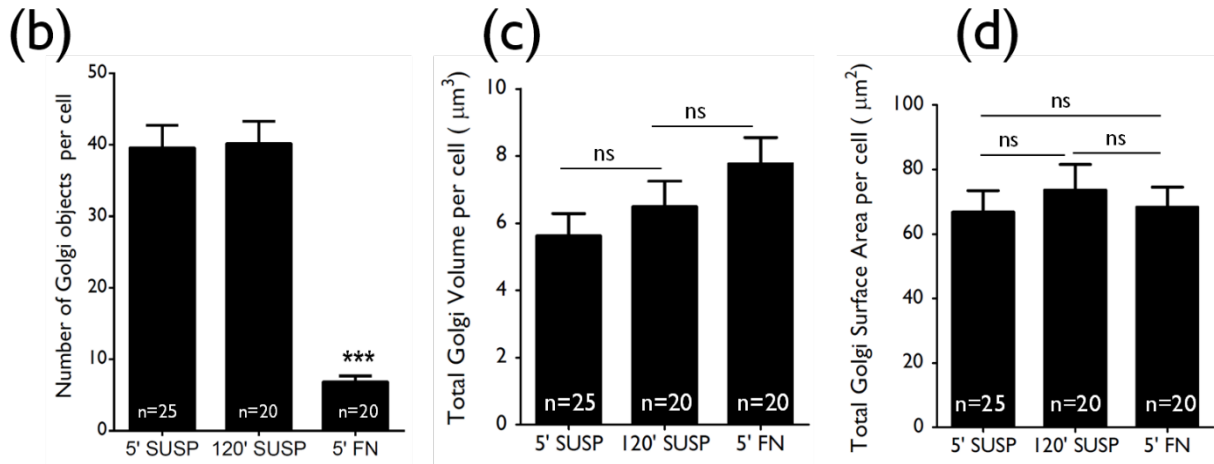
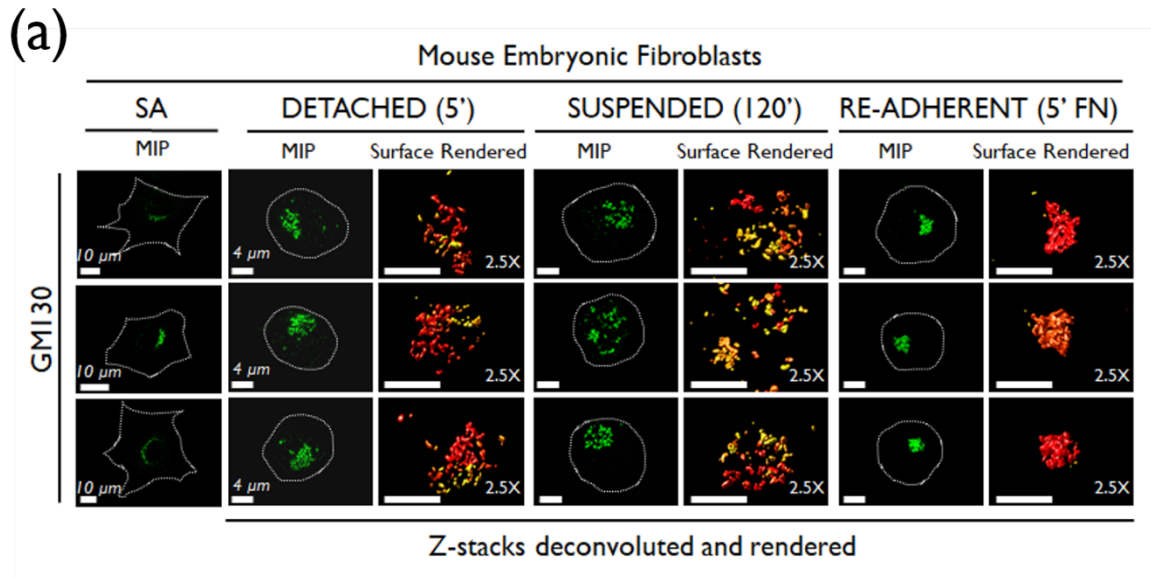


Figure 3.3 Adhesion regulates cis-Golgi organization in WT-MEFs. (a) Untransfected WT-MEFs were serum starved for 12 hours as stable adherent (SA) were detached (5') and held in suspension for 120 mins (120') and re-plated on fibronectin for 5 mins (5' FN). Their cis Golgi was detected by anti-GM130 antibody staining (GM130). Maximum intensity projections (MIP) of de-convoluted confocal images for 3 representative cells for GM130 for each time point are shown (left panel in each time point). De-convoluted confocal Z stacks were surface rendered and zoomed for clarity (2.5X) (right panel in each time point). Stable adherent cells (SA) are represented only as maximum intensity projections (MIP). (b) Following deconvolution of detached (5' SUSP), suspended (120' SUSP) and re-adherent (5' FN) cells discontinuous Golgi objects per cell detected were determined using the Huygens image analysis software. The graph represents mean \pm SE from a minimum of 20 cells and maximum of 25 cells (as indicated in each bar) from three independent experiments. Total volume (c) and total surface area (d) occupied by the cis Golgi objects detected by GM130 per cell were measured in deconvoluted Z stack images and analyzed using the Huygens image analysis software from detached (5' SUSP), suspended (120' SUSP) and re-adherent

cells (5' FN). Bars represent average data of 20-25 cells from 3 independent experiments. Statistical analysis was done using the non-parametric Kruskal-Wallis test (***) p-value <0.0001, ns represents not significant). All scale bars in images are 4 μm , except stable adherent cells set at 10 μm .

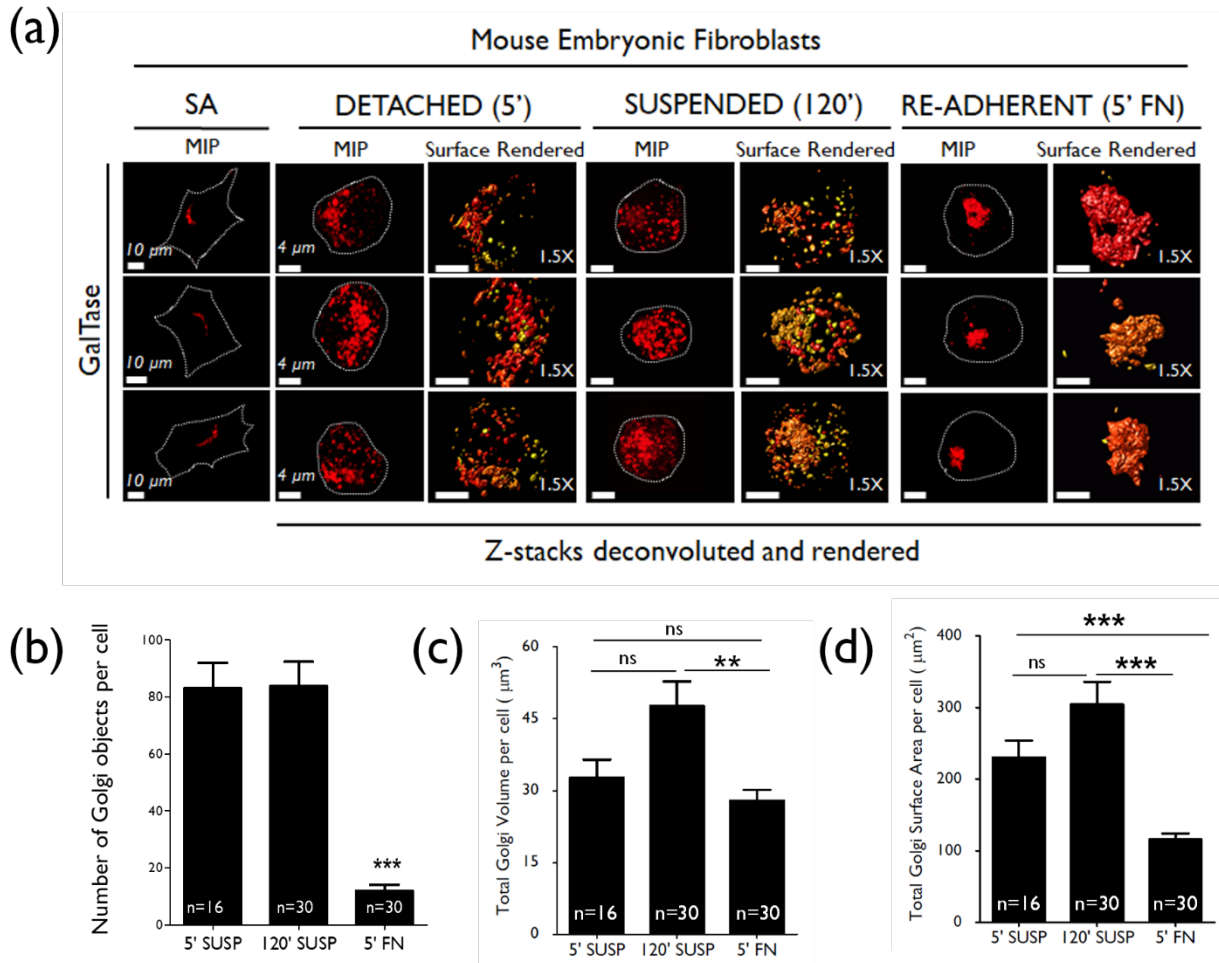


Figure 3.4 Adhesion regulates trans-Golgi organization in WT-MEFs. (a) WT-MEFs transfected with GalTase-RFP were serum starved for 12 hours as stable adherent (SA) were detached (5') and held in suspension for 120 mins (120') and re-plated on fibronectin for 5 mins (5' FN). Their trans-Golgi was detected using the GalTase RFP localization (GalTase). Maximum intensity projections (MIP) of de-convoluted confocal images for 3 representative cells for GalTase for each time point are shown (left panel in each time point). De-convoluted confocal Z stacks were surface rendered and zoomed for clarity (1.5X) (right panel in each time point). Stable adherent cells (SA) are represented only as maximum intensity projections (MIP). (b) Following deconvolution of detached (5' SUSP), suspended (120' SUSP) and re-adherent (5' FN) cells discontinuous Golgi objects per cell detected were determined using the Huygens image analysis software. The graph represents mean \pm SE from a minimum of 16 cells and maximum of 30 cells (as indicated in each bar) from three independent experiments. Total volume (c) and total surface area (d) occupied by the trans Golgi objects detected by GalTase per cell were measured in deconvoluted Z stack images and analyzed using the Huygens image analysis software from detached (5' SUSP), suspended (120' SUSP) and re-adherent cells (5' FN). Bars represent average data of 16-30 cells from 3 independent

experiments. Statistical analysis was done using the non-parametric Kruskal-Wallis test (** p-value <0.001, *** p-value <0.0001, ns represents not significant). All scale bars in images are 4 μm , except stable adherent cells set at 10 μm .

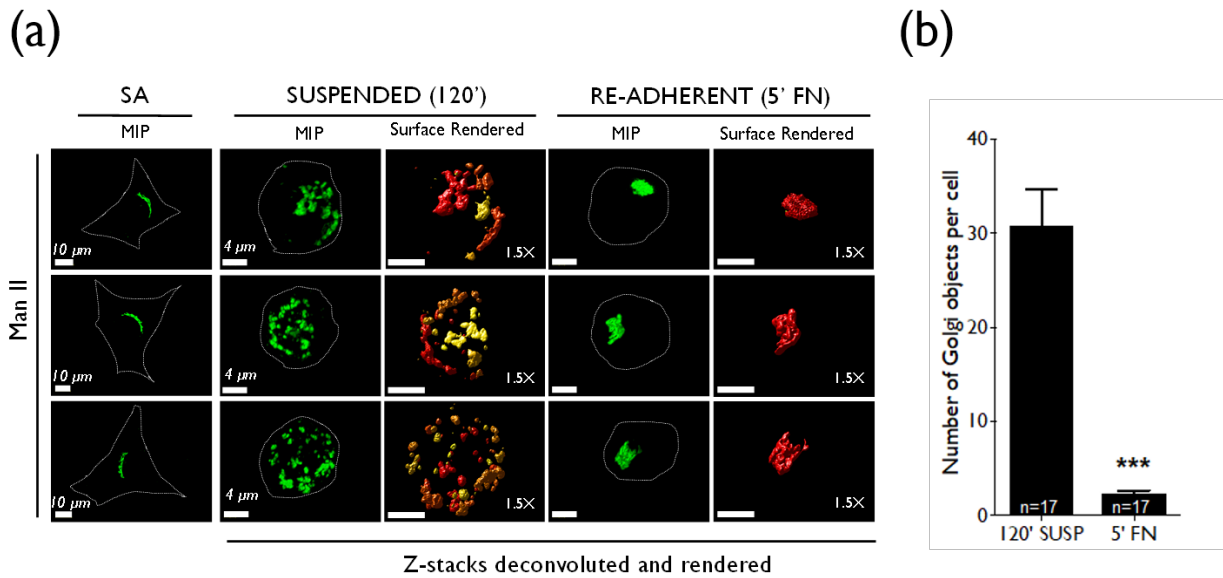


Figure 3.5 Adhesion regulates cis/medial-Golgi organization in WT-MEFs. (a) WT-MEFs transfected with Man II GFP were serum starved for 12 hours as stable adherent (SA) were detached (5') and held in suspension for 120 mins (120') and re-plated on fibronectin for 5 mins (5' FN). Their cis/medial Golgi was detected using the Man II GFP localization (Man II). Maximum intensity projections (MIP) of de-convoluted confocal images for 3 representative cells for Man II for each time point are shown (left panel in each time point). De-convoluted confocal Z stacks were surface rendered and zoomed for clarity (1.5X) (right panel in each time point). Stable adherent cells (SA) are represented only as maximum intensity projections (MIP). (b) Following deconvolution suspended (120' SUSP) and re-adherent (5' FN) cells discontinuous Golgi objects per cell detected were determined using the Huygens image analysis software. The graph represents mean \pm SE from 17 cells from three independent experiments. Statistical analysis was done using the Mann Whitney's test (***) p-value <0.0001). All scale bars in images are 4 μ m, except stable adherent cells set at 10 μ m.

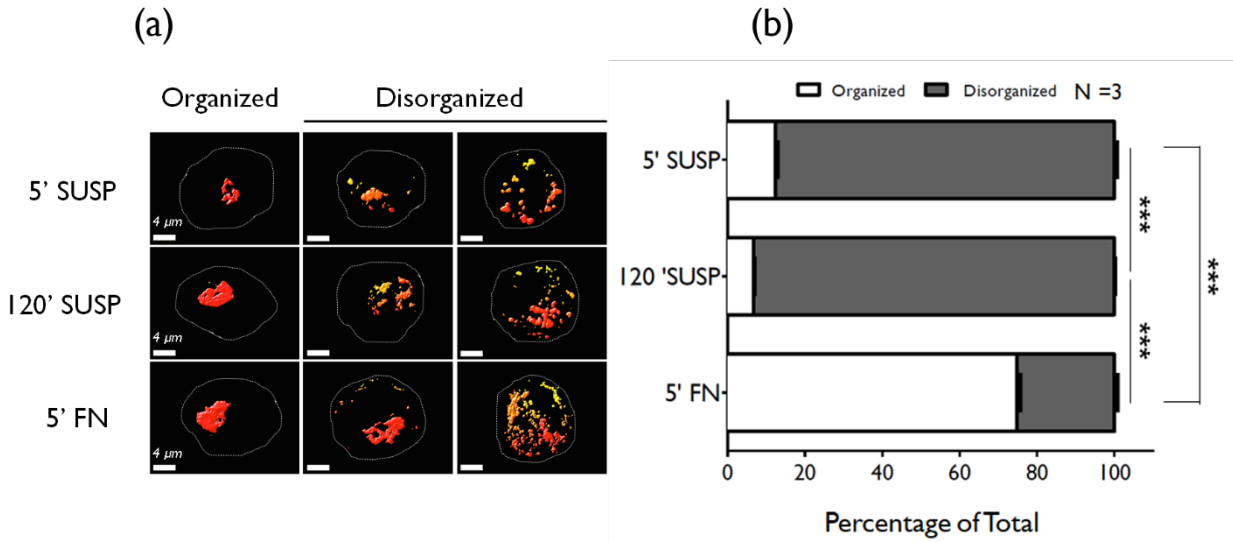


Figure 3.6 Distribution profile of Golgi phenotype in WT MEFs. The percentage distribution of cells with organized and disorganized Golgi phenotypes in WT-MEFs expressing GalTase RFP were detached (5' SUSP), held in suspension for 120 mins (120' SUSP) and re-plated on fibronectin for 5 mins (5' FN) was determined by counting 200 cells for each time point. **(a)** Representative surface rendered cross section images for the organized and disorganized phenotype at each time point. Scale bar in the images is set at 4 μm. **(b)** The graph represents mean ± SE of percentage distribution for each phenotype from 3 independent experiments. Statistical analysis comparing the change in distribution profile between all the time points were done using the Chi-Square test, two-tailed (***) p-value < 0.0001).

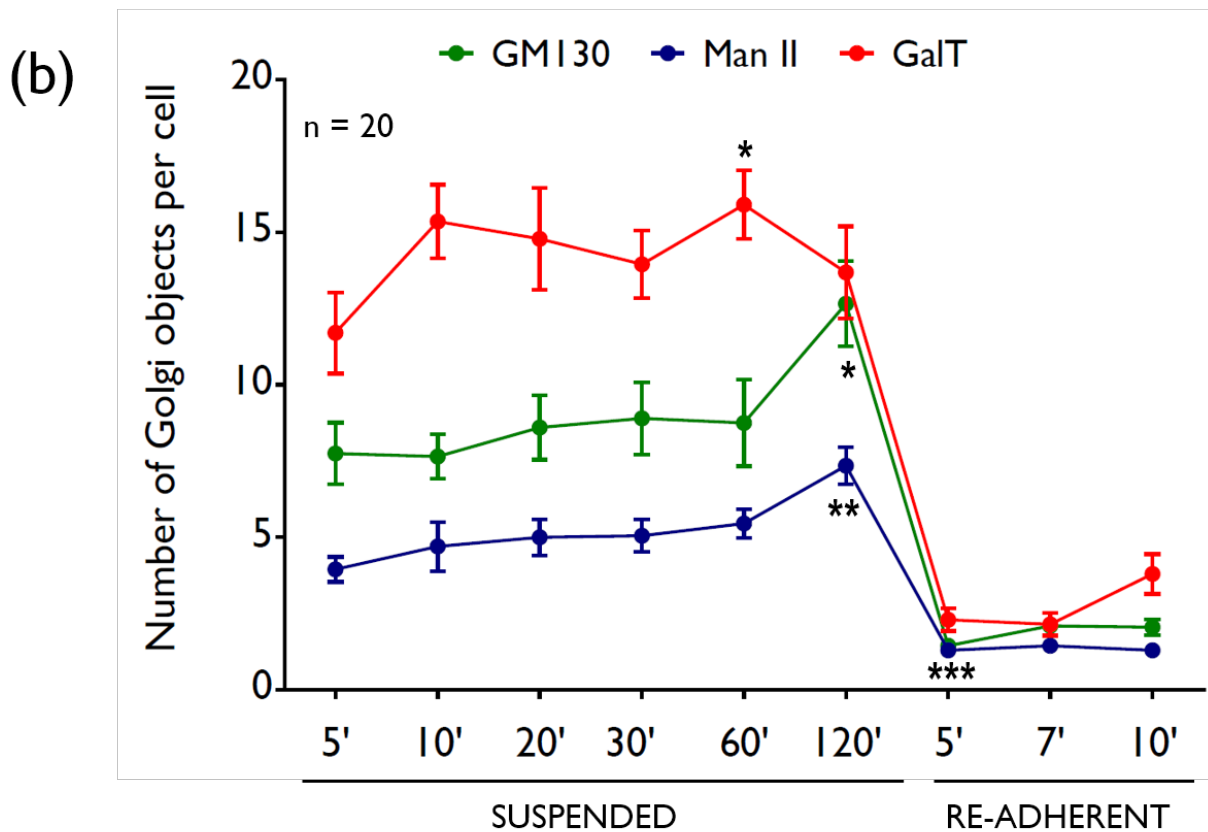
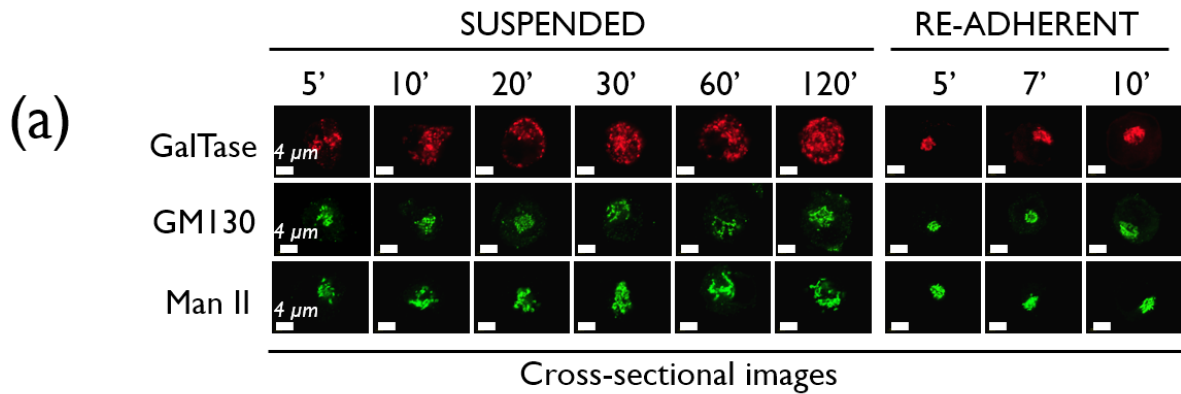


Figure 3.7 Adhesion-dependent Golgi disorganization is rapid and reversible. (a) Stable adherent WT-MEFs, expressing GalTase-RFP (top panel), ManII-GFP (lowest panel) or stained with anti-GM130 antibody (middle panel) were detached and held in suspension for increasing time points 5 mins to 120 mins (5', 10', 20', 30', 60', 120' Suspended) and then re-plated on FN for increasing times (5', 7', 10' Re-adherent). **(b)** Cross-sectional confocal images for trans-Golgi (GalTase), cis Golgi (GM130) and cis medial Golgi (Man II) were deconvoluted and discontinuous Golgi objects per cell determined using the Huygens image analysis software. Representative cross-section images for each Golgi marker across

suspension and re-adhesion time points are shown in the panel above graph. The graph represents mean \pm SE for Golgi objects in 20 cells from two independent experiments. Statistical analysis comparing object numbers in cells suspended for 5 mins to 60 mins and 120 mins was done using the Mann Whitney's test. This analysis was extended to compare the decrease in object numbers between cells suspended for 120 mins and re-adherent on fibronectin for 5 mins (* p-value <0.05, ** p-value <0.01, *** p-value <0.0001). Scale bar in all images is set to 4 μ m.

3.2.4 Adhesion regulate Golgi organization in human fibroblast, endothelial and breast epithelial cells.

It was further examined if adhesion regulates Golgi organization in anchorage-dependent cell lines of different origin like in mouse fibroblast cells. In Human foreskin fibroblast cells Golgi was visualized by expressing cis-medial Golgi marker (Man II GFP) or trans-Golgi (GalTase-RFP). Serum-starved human fibroblast cells when completely adhered and well spread, displayed organized Golgi morphology for both cis-medial or trans marker (Figure 3.8). Loss of adhesion caused cis-medial (Figure 3.8 a) and trans-Golgi disorganization (Figure 3.8 c) similar to our earlier mouse fibroblast phenotype. On re-adhesion to fibronectin, both cis-medial and trans-Golgi re-organized rapidly as is clearly evident in quantitation for the number of objects (Figure 3.8 b, d).

Further, the same question was asked in human endothelial cells (EA.hy926) cells and observed the otherwise organized cis-medial or trans-Golgi in adherent cells undergoes disorganization on loss of adhesion (5' SUSP and 120' SUSP in Figure 3.9 a, c), and re-adhesion on fibronectin for 5 mins caused disorganized Golgi objects to come back together to form a relatively compact organized phenotype (Figure 3.9 b, d).

The screen was extended by testing the hypothesis in human breast epithelial cells (MCF10A) and visualized Golgi by immunostaining for GM130 (cis-Golgi). In the same way, MCF10A cells substantiated previous observation in other cell lines. Loss of adhesion triggered Golgi to disorganize, and re-adhesion on fibronectin restores the structure (Figure 3.10 a, b). In

5'FN time point, cells were plated in such a way that there was no cell to cell contact, ensuring the effect is coming not as a result of cell-cell adherence junction.

Taken together, these data indicate that cell-matrix adhesion is a regulator of Golgi organization and is a ubiquitous feature of anchorage-dependent cells. The response occurs quickly, yet reversible in all the mammalian cells tested.

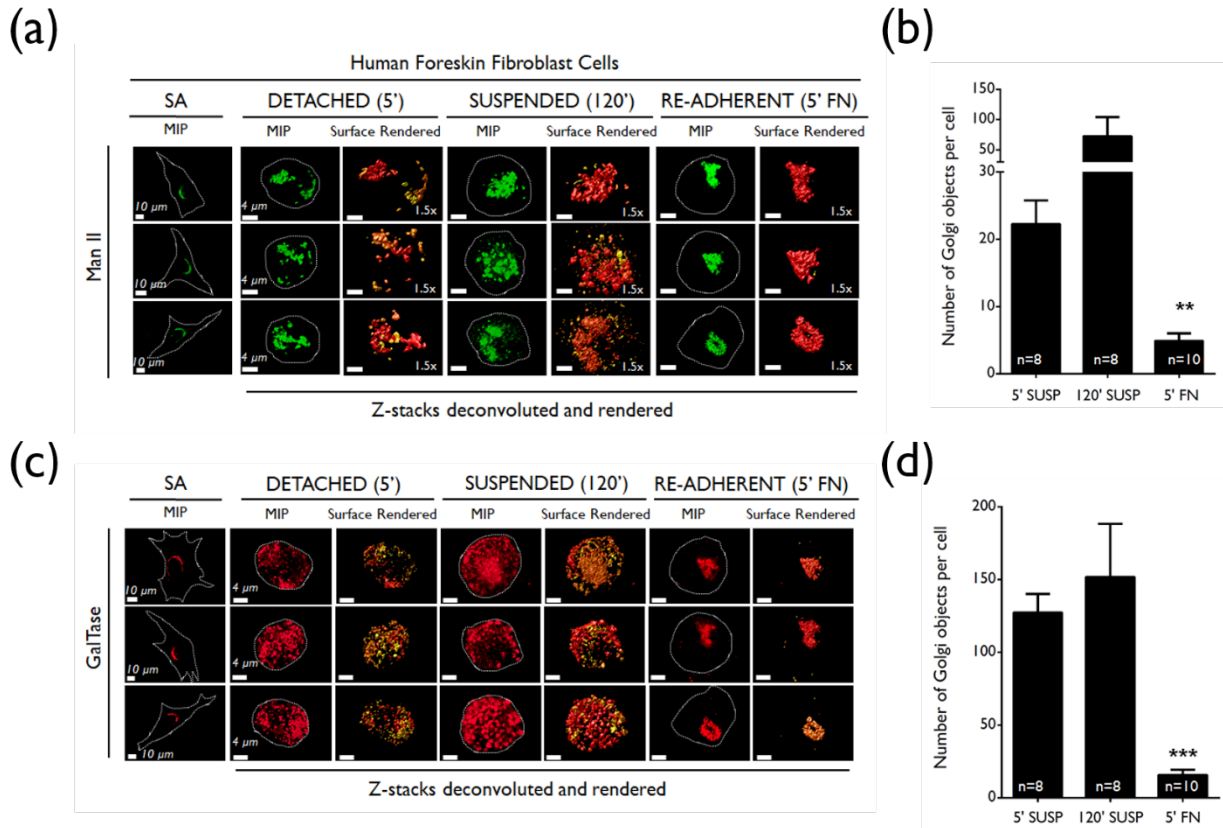


Figure 3.8 Adhesion regulates cis/medial and trans-Golgi organization in human foreskin fibroblast cells. Human foreskin fibroblasts (BJ) transfected with **(a)** cis-medial Golgi marker Man II GFP or **(c)** trans-Golgi marker GalTase RFP were detached (5' SUSP), held in suspension for 120 mins (120' SUSP) and re-plated on fibronectin for 5 mins (5' FN). Confocal Z stacks were deconvoluted and representative maximum intensity projections (MIP) and zoomed (1.5x) surface rendered images for 3 representative cells for Man II and GalTase for each time point are shown. Stable adherent cells are represented by a MIP image. Following deconvolution, discontinuous Golgi objects per cell for **(b)** Man II and **(d)** GalTase were determined using the Huygens image analysis software. The graph represents mean \pm SE from a minimum of 8 cells and maximum of 10 cells (as indicated in each bar) from two independent experiments. Statistical analysis comparing 120' SUSP and 5' FN was done using the non-parametric Kruskal-Wallis test (** p-value <0.01 , *** p-value <0.001). All scale bars in images are 4 μm , except stable adherent cells set at 10 μm .

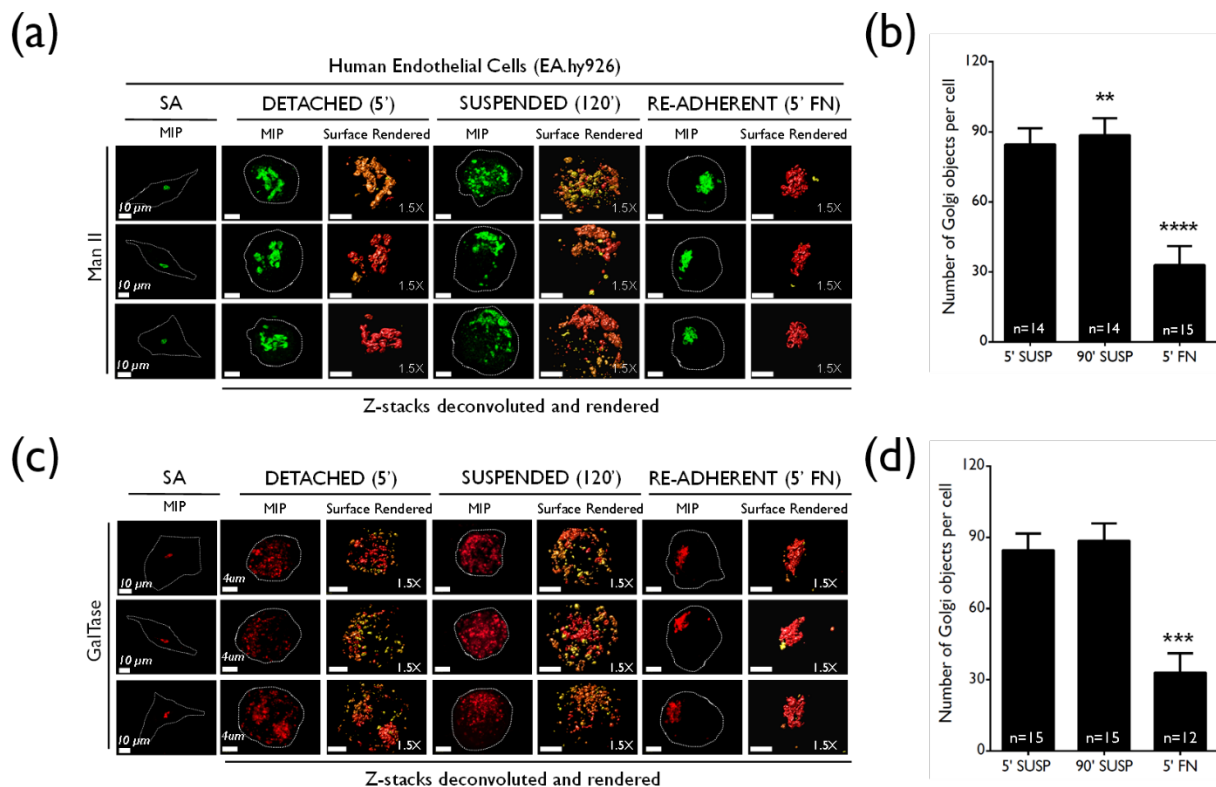


Figure 3.9 Adhesion regulates cis/medial and trans-Golgi organization in human endothelial cells (EA.hy926). Human endothelial cells (EA.hy926) transfected with (a) cis-medial Golgi marker Man II GFP or (c) trans-Golgi marker GalTase RFP were detached (5' SUSP), held in suspension for 120 mins (120' SUSP) and re-plated on fibronectin for 5 mins (5' FN). Confocal Z stacks were deconvoluted and representative maximum intensity projections (MIP) and zoomed (1.5x) surface rendered images for 3 representative cells for Man II and GalTase for each time point are shown. Stable adherent cells are represented by a MIP image. Following deconvolution, discontinuous Golgi objects per cell for (b) Man II and (d) GalTase were determined using the Huygens image analysis software. The graph represents mean \pm SE from a minimum of 12 cells and maximum of 15 cells (as indicated in each bar) from three independent experiments. Statistical analysis comparing 120' SUSP and 5' FN was done using the non-parametric Kruskal-Wallis test (** p-value <0.01, *** p-value <0.001, **** p-value <0.0001). All scale bars in images are 4 μ m, except stable adherent cells set at 10 μ m.

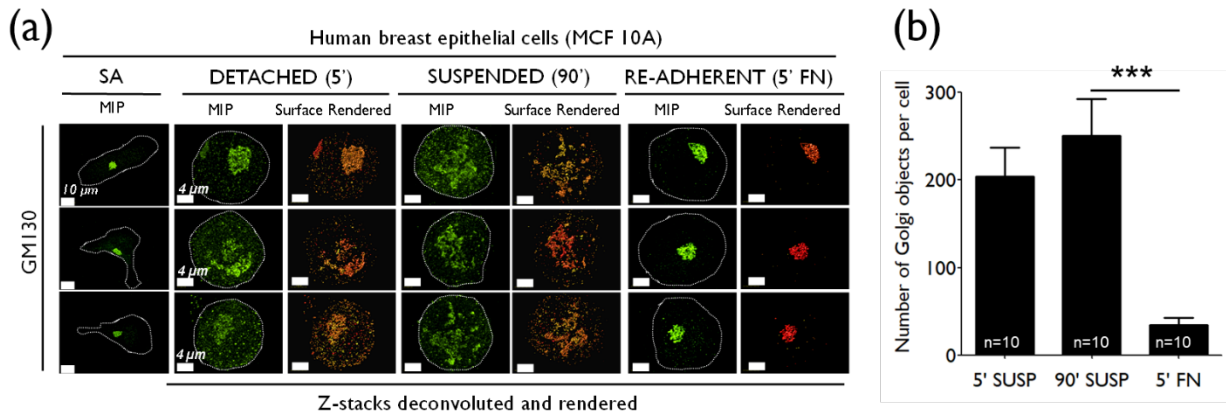


Figure 3.10 Adhesion regulates cis-Golgi organization in Breast epithelial cells (MCF10A). (a) Untransfected MCF10A were serum starved for 12 hours as stable adherent (SA) were detached (5') and held in suspension for 90 mins (90') and re-plated on fibronectin for 5 mins (5' FN). Their cis Golgi was detected by anti-GM130 antibody staining (GM130). Maximum intensity projections (MIP) of de-convoluted confocal images for 3 representative cells for GM130 for each time point are shown (left panel in each time point). De-convoluted confocal Z stacks were surface rendered (right panel in each time point). Stable adherent cells (SA) are represented only as maximum intensity projections (MIP). (b) Following deconvolution of detached (5' SUSP), suspended (90' SUSP) and re-adherent (5' FN) cells discontinuous Golgi objects per cell detected were determined using the Huygens image analysis software. The graph represents mean \pm SE of 10 cells from two independent experiments. Statistical analysis was done using the non-parametric Kruskal-Wallis test (***) p-value < 0.0001). All scale bars in images are 4 μ m, except stable adherent cells set at 10 μ m.

3.2.5 Differential regulation of Golgi compartments by adhesion.

Although all the Golgi compartments showed disorganization as a response to “loss/gain of adhesion”, a distinction between the extent of disorganization between cis/cis-medial vs. trans markers was noticed in almost all the cell lines tested. In order to further examine this difference, colocalization experiments in WT-MEF cells were set up, wherein cells were labeled with two Golgi markers at a time. These are the combination of Golgi markers used. **(a)** GM130 vs GalTase (Cis vs trans), **(b)** Man II vs GalTase (Cis-medial vs trans) and **(c)** Man II vs GM130 (Cis-medial vs Cis). Co-localization of Golgi markers in the suspended cell (120' SUSP) and re-adherent cell (5' FN) were compared by Pearson coefficient and also looking at line intensity profile across the cell. The extent of disorganization was less for both cis and cis-medial Golgi as compared to trans-Golgi in suspended cells (Figure 3.11 a, b) confirmed by qualitative and quantitative measurements. In a cell, trans-Golgi was found to be more dispersed throughout cell than both cis/cis-medial Golgi in suspension, making the co-localization Pearson's coefficient ~ 0.5 in both cases (Graph in Figure 3.11 a, b). Intensity line profile also showed very less overlap between cis/cis-medial and trans-Golgi compartments in suspension.

Nevertheless, cis and cis-Golgi compartments seem to be in the close vicinity (Pearson's coefficient ~ 0.7), but not completely co-localizing with each other in suspended cells (Figure 3.11 c). On the contrary, on re-adhesion (possibly through activation of integrin-mediated adhesion), all combination of Golgi markers seems to come to a very close vicinity (Pearson's coefficient $\sim 0.8 - 0.85$) forming the organized Golgi phenotype (5'FN in Figure 3.11 a-c).

Intensity line profile also revealed that all the combination of Golgi markers were present in very close space in 5'FN time point. This has given us an indication that loss of cell-matrix adhesion differentially regulates disorganization of Golgi compartments, and detailed mechanism and reason for this remains to be explored. Studies in later chapters looking at the regulation of such a process may provide some explanations for why this could be happening.

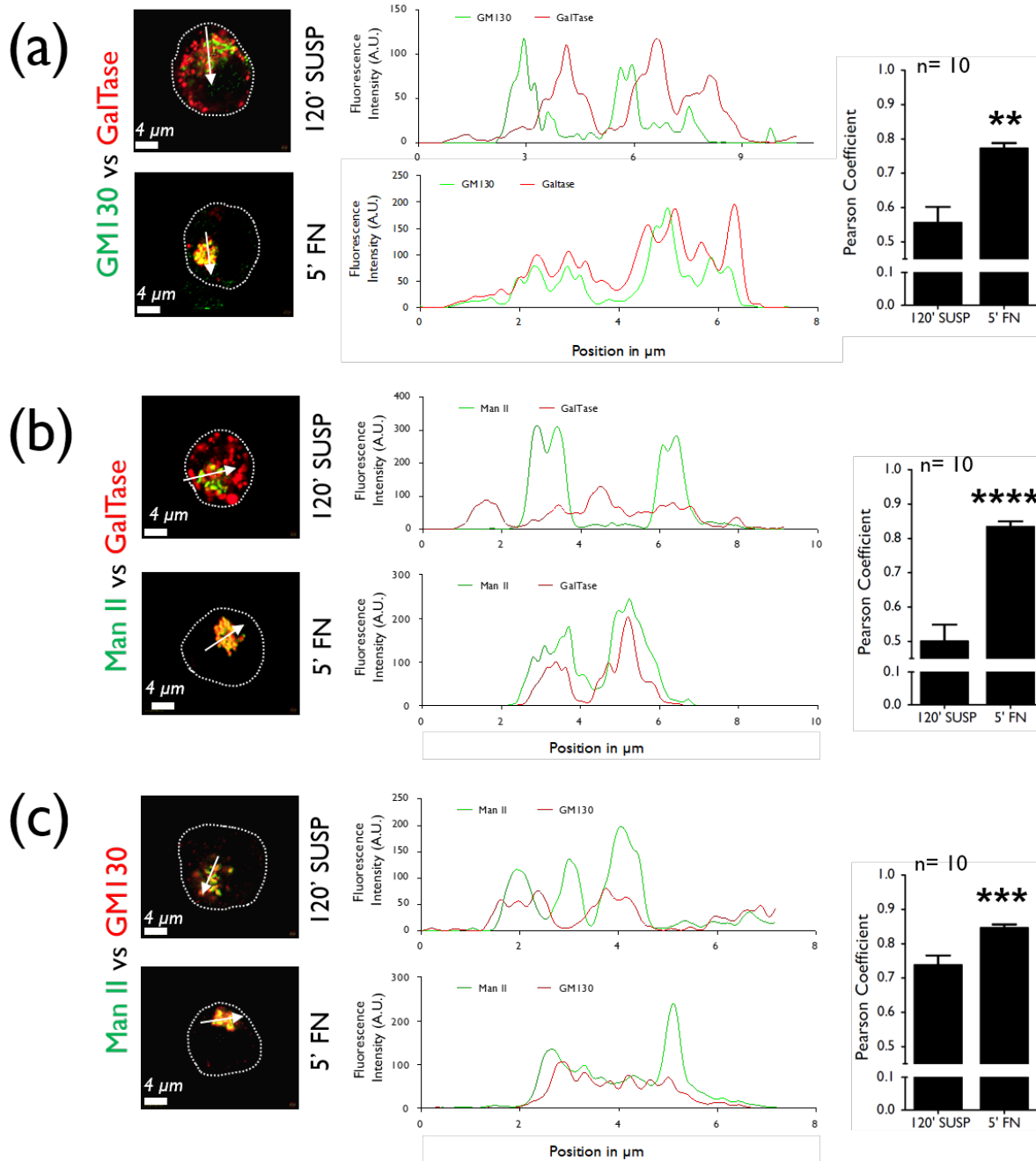


Figure 3.11 Relative localization of cis vs medial vs trans-Golgi in suspended and re-adherent cells. Serum-starved WT-MEFs transiently expressing or immunostained with a combination of Golgi markers, **(a)** GM130 vs. GalTase, **(b)** Man II vs. GalTase, and **(c)** Man II vs GM130 were held in suspension for 120 mins (120' SUSP) and re-plated on fibronectin for 5 mins (5' FN). Fluorescence intensity measurements made for these Golgi markers along a line (marked by arrow) in representative 120' SUSP and 5' FN re-adherent cell were plotted and compared. Markers labeled in green or red are represented in the line of the same color in the graph. Co-localization in the entire confocal cross-sections were determined with

Huygens software and Pearsons coefficient represented in the graph (mean \pm SE) (10 cells from one experiment). Scale bar in all images is set at 4 μ m. Statistical analysis done using the Mann Whitney's test (** p-value <0.01, *** p-value <0.0001, **** p-value <0.00001).

3.2.6 Integrin clustering/activation could restore Golgi organization in non-adherent WT-MEF.

The rapid nature of adhesion mediated regulation of the Golgi organization does suggest early adhesion events to drive the same. This leads us to test if in non-adherent serum starved WT-MEFs, binding to fibronectin (FN-Bead) vs poly-L-lysine (PLL-Bead) coated polystyrene beads affect the Golgi organization. Binding of fibronectin-coated beads on non-adherent cell surface mimic cell-to-ECM adhesion formation and have earlier shown to cause clustering and activation of β 1-integrins (Tran et al., 2002). Rapid accumulation of downstream molecules in integrin signaling pathways such as Rac1 (activation of this GTPase) (del Pozo et al., 2004b), vinculin, talin and other cytoskeletal proteins (Grinnell and Geiger, 1986; Lewis and Schwartz, 1995) occurs rapidly by induction of fibronectin-coated bead.

Fibronectin coated beads were seen to support the enrichment of GM1 labeled raft microdomains (detected with Cholera Toxin B) in cells, confirming their spatial activation of integrins (data not shown) and is in agreement with an earlier report (del Pozo et al., 2004b). This suggests there is clustering/activation of integrins and downstream signaling as a result of FN-Bead binding to the cell.

Further, fibronectin-coated beads dramatically restore the cis Golgi (GM130) (Figure 3.12 a) and trans-Golgi (GalTase) (Figure 3.12 c) organization, relative to control and poly-L-lysine coated beads. This is reflected in a significant drop in cis and trans-Golgi object numbers in FN bead-bound cells (Figure 3.12 b, d). Percentage distribution of the organized vs

disorganized trans-Golgi phenotype across cells further confirms the effect fibronectin beads have over control and PLL beads (Figure 3.13 a, b). The differential effect Fibronectin vs PLL beads have suggested variable binding and clustering of integrins and resulting downstream signaling drives the Golgi organization. PLL coated beads likely cause some integrin activation (relative to control) that reflects in a small reduction in Golgi object numbers (Figure 3.13 b, d), but is not prominent enough to affect the distribution profile for the phenotype in cells (Figure 3.13 b).

These studies provide evidence that regulation of cell-matrix adhesion on Golgi organization in anchorage-dependent cells is prominently coming as a result of integrin-ECM engagement and its downstream pathway.

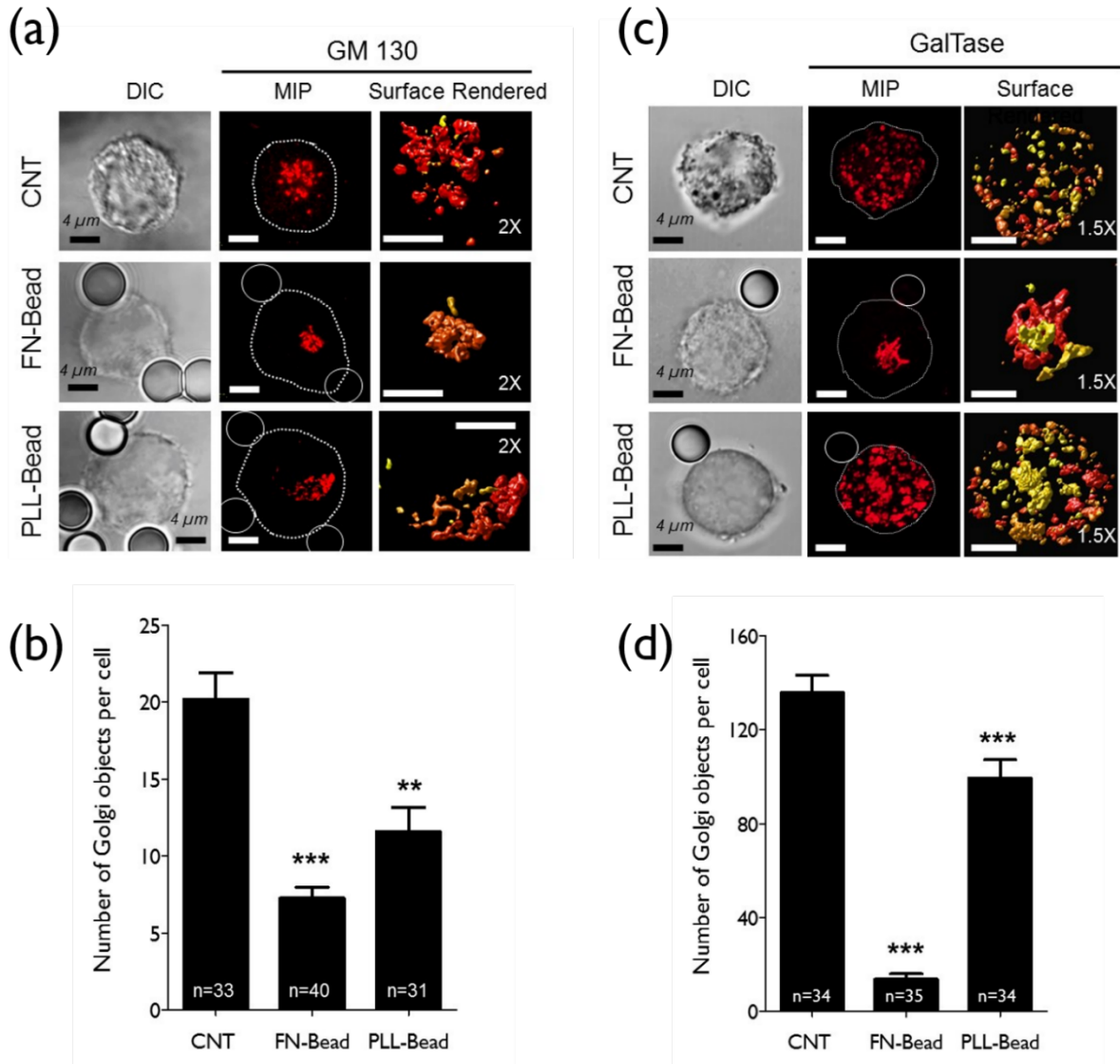


Figure 3.12 Binding to FN-coated bead restores Golgi organization in the suspended cell.

(a) WT-MEFs untransfected or (c) expressing GalTase RFP were serum starved for 12 hours were detached and held in suspension for 30 mins and incubated without beads (CNT) or with beads coated with fibronectin (FN-Bead) or poly L-Lysine (PLL-Bead) for 15 mins. DIC image of the cell shows the attached bead. Their cis-Golgi was detected using GM130 immunostaining and trans-Golgi detected using GalTase RFP (GalTase) was imaged and Z stack images deconvoluted and a representative maximum intensity projection (MIP) image shown. The cell perimeter and bead position are marked here. These images were surface rendered and zoomed for clarity (2X for GM130 and 1.5X for GalTase). Discontinuous Golgi objects per cell were determined for (b) GM130 and (b) GalTase (using the Huygens image analysis software). The graph represents mean \pm SE from a minimum of 31 cells and maximum of 40 cells (as indicated in each bar graph) from three independent experiments. Statistical analysis of this data was done using the Mann Whitney's test (** p-value <0.001 , *** p-value <0.0001). Scale bar in all images is set at 4 μ m.

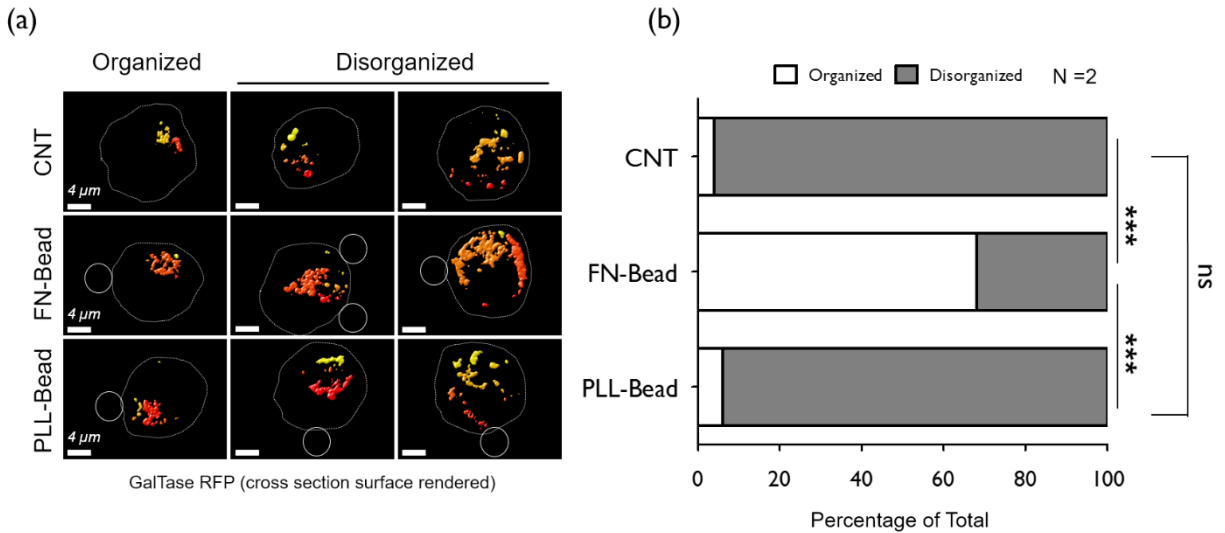


Figure 3.13 Distribution profile of Golgi phenotype in FN/PLL bead stimulated suspended WT MEFs. The percentage distribution of cells with organized and disorganized Golgi phenotypes in WT-MEFs expressing GalTase RFP incubated without (CNT) or with a bead coated with fibronectin (FN-Bead) or poly L-lysine (PLL-Bead) was determined by counting 50 cells at each time point. The left panel shows representative surface rendered cross section images for the organized and disorganized phenotype at each treatment. The graph represents percentage distribution for each phenotype in one of two comparable independent experiments. Statistical analysis comparing the change in distribution profile was done using the Chi-Square test, two-tailed (***) p-value < 0.0001). Scale bar in all the images is set at 4 μ m.

3.2.7 No spatial predisposition of Golgi organization from cell-matrix binding site.

Fibronectin coated beads bound to cells also offer a means of evaluating the spatial regulation of adhesion-dependent Golgi reorganization. Using cells bound to a single bead the orientation of cis-Golgi (GM130) and trans-Golgi (GalTase) relative to bead were compared across cells. The reorganized Golgi did not show a spatial predisposition for the FN bead (Figure 3.14 a, b) in suspended cells as it was seen to be distributed evenly through the cell from the site of attachment of the bead. The position of re-organized Golgi was also evaluated in cells re-adherent on fibronectin-coated coverslips looking at the localization of the cis-Golgi (GM130) and trans-Golgi (GalTase) (Figure 3.14 c, d) relative to the coverslip. Here again, the position of the re-organized Golgi had no correlation with the distance from the base of the cell that is attached to fibronectin (cell-matrix binding site). This result was very compelling as it does provide evidence that a very small amount of cell-matrix (fibronectin) mediated pathway very rapidly relays signal downstream in the cell to support Golgi reorganization.

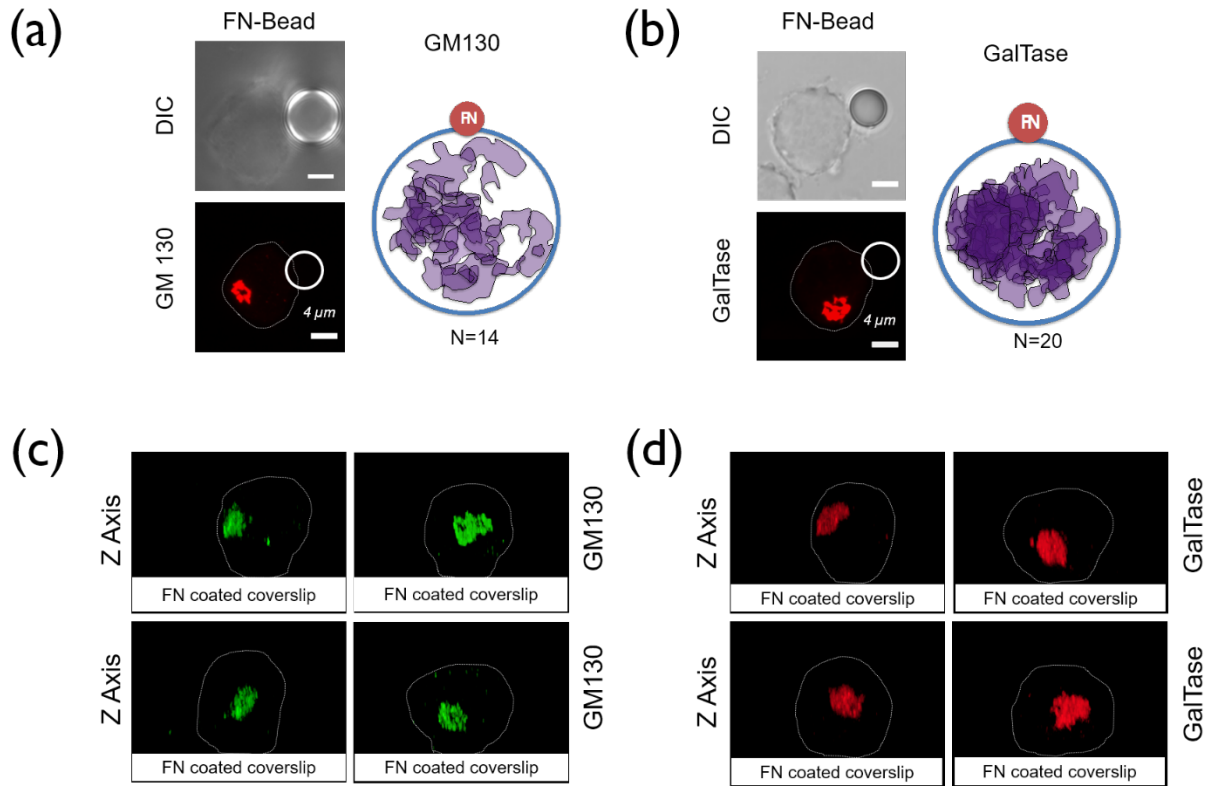


Figure 3.14 No spatial regulation by FN-bead/coverlip on Golgi organization. The position of the (a) cis Golgi (GM130) and (b) trans Golgi (GalTase) mapped as discussed in methods, relative to fibronectin bead (FN) for 14 and 20 cells respectively (from 3 independent experiments) are represented as a schematic. The position of the bead from each cell is made to overlap at one spot (represented as a single bead) (FN) with the relative position of the Golgi maintained. A representative DIC image of the cell with the attached bead and the localization of the cis and trans-Golgi respectively are shown to the left of each schematic. All scale bars in images are 4 μm. (c) cis (GM130) and (d) trans-Golgi (GalTase) of re-adherent WT-MEFs were imaged as described earlier. Confocal Z stacks were deconvoluted, 3D reconstituted and observed along their Z-Axis relative to the fibronectin (FN) coated coverslip. Four representative cells for GM130 and GalTase are represented.

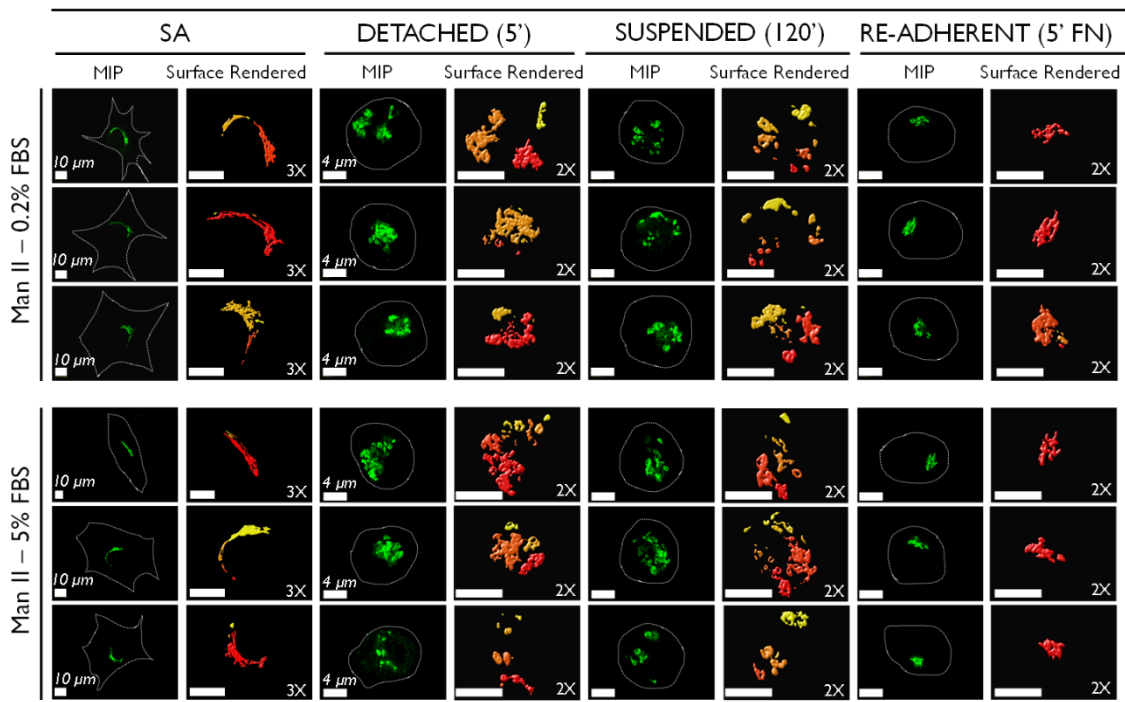
3.2.8 Cell-matrix adhesion regulated Golgi organization occurs independently of growth factors.

There are multiple mechanisms by which crosstalk between integrins and growth factors exists and is very well documented in the literature (Danen and Yamada, 2001). The objective of performing these experiments in serum-deprived conditions stems from this same reason. By depriving cells of serum growth factors, the contribution integrin signaling could be interpreted in regulating Golgi organization. However, it is of interest to ask if growth factors can influence, through known crosstalks with integrin signaling pathways, adhesion-dependent Golgi organization.

As predicted in spite of the presence of serum growth factors, cell-matrix adhesion regulated Golgi organization in WT-MEF cells. In cells with serum (5% FBS), like with cells in low serum (0.2% FBS) conditions, the cis-medial Golgi (Figure 3.15 a) and trans-Golgi (Figure 3.15 b) similarly disorganize on the loss of adhesion and recover their organization on re-adhesion. This further suggests that cell-matrix adhesion is a primary regulator of Golgi organization in mouse embryonic fibroblasts and that changes in growth factor-mediated signaling do not alter this regulatory pathway.

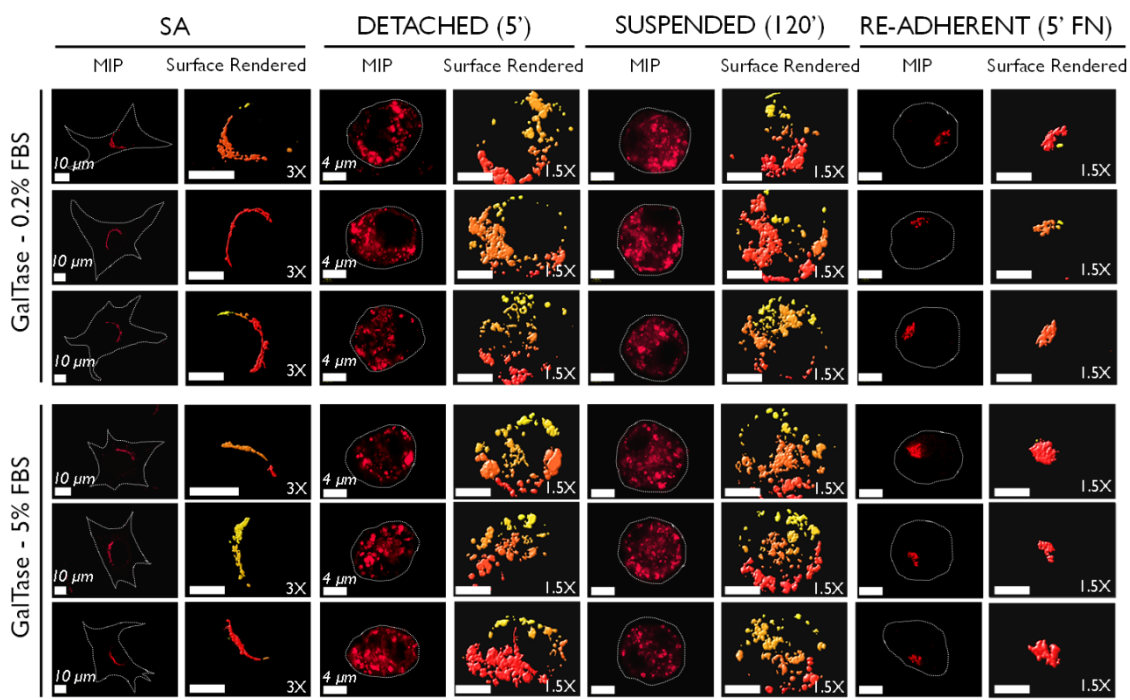
(a)

Mouse Embryonic Fibroblast Cells



(Man II GFP) Cross sections deconvoluted and rendered

(b)



(GalTase RFP) Cross sections deconvoluted and rendered

Figure 3.15 Growth factors do not influence regulation by adhesion on Golgi organization. WT-MEFs transiently expressing (a) Man II GFP and (b) GalTase-RFP were either serum starved with 0.2% FBS for 12 hours or cultured with 5% FBS. Stable adherent cells (SA) were detached (5') and held in suspension for 120 mins (120'), and re-plated on fibronectin for 5 mins (5' FN). Cross sections of deconvoluted MIP and surface rendered images which were zoomed for clarity (3X for SA for both Man II and GalTase, 2X for other time points for Man II and 1.5X for GalTase) (right panel in each time point) are represented from two independent experiments. Stable adherent cells are represented by a MIP image. Scale bar in the images is 4 μm and 10 μm for stable adherent cells.

3.3 SUMMARY.

Cell adhesion has been shown to control various cellular processes by regulating signaling pathways, migration, cell cycle progression, membrane trafficking through endocytosis and exocytosis (Caswell et al., 2009; Danen and Yamada, 2001; Huttenlocher and Horwitz, 2011; Hynes, 2002; Schwartz and Assoian, 2001b; Suzuki and Takahashi, 2003). The Golgi apparatus is a central organelle in secretory pathways and plays a major role in trafficking and processing (Lodish et al., 2000). Organization of Golgi (linked closely to its function) has been shown to undergo changes during mitosis (preceded by mitotic cell rounding). The Golgi is also seen to undergo fragmentation during cell apoptosis and in disease conditions like neurodegeneration and cancer. A role for cell-matrix adhesion in regulating Golgi organization is what this study is aiming to explore. Results from this chapter reveal cell-matrix adhesion to indeed regulate Golgi organization in anchorage-dependent cell lines of different origins. Independent of growth factors, loss of adhesion rapidly disorganizes the Golgi, restored on re-adhesion to fibronectin for 5 mins or less. Such early adhesion events in serum-deprived cells are likely mediated through integrins. The restoration of integrin-dependent Akt activation in these cells supports the same. This is further confirmed by the fact that in these cells binding to fibronectin-coated beads (but not poly-L-lysine), known to cause integrin clustering and activation, completely reorganizes the Golgi. The effect limited integrin activation at the site of bead attachment has on the Golgi is interestingly not spatially restricted. This not only suggests small changes in integrin clustering and activation can be sufficient to drive this pathway, but also raises the possibility that the signal downstream of integrins could indeed dissipate very rapidly to the Golgi. Furthermore, it's observed that adhesion regulates cis and trans-Golgi differentially, as evident in the extent of

disorganization for these compartments. They both, however, stay distinctly separated in suspended cells with the trans-Golgi undergoing a more extensive disorganization compared to the cis and cis-medial compartments. On re-adhesion, they all, however, do fall back into a compact overlapping structure. Cis vs. medial vs. trans-Golgi remains segregated in suspension, thus maintaining their identity as separate Golgi compartments. This does raise the possibility that downstream of adhesion cis and trans-Golgi compartments could indeed be regulated differently.

3.4 CONCLUSION.

Cell-matrix adhesion regulates Golgi organization in anchorage-dependent cells in a rapid and reversible manner.

Chapter 4

**Study the regulation of Golgi organization
by cell-matrix adhesion.**

4.1 RATIONALE.

Independent findings from several groups have identified multiple regulators involved in controlling Golgi organization. Various **Golgi matrix proteins** have been classified which includes GRASP (GRASP-55, GRASP-65), Golgins (GM130, p115, Golgin-84, Golgin-97, Golgin-160 etc.) (Xiang and Wang, 2011). These Golgi matrix proteins have characteristic long coiled-coil domains and they are fiber-like connections between two cisternae or between a vesicle and cisternae. *Cytoskeletal proteins, microtubules (Sandoval et al., 1984) and actin (Valderrama et al., 1998), motor proteins (Brownhill et al., 2009) are also seen to be required for the maintenance of the Golgi organization.* **Microtubule** depolymerization has a dramatic effect on the typical Golgi architecture, with Golgi elements getting fragmented and dispersed throughout the cytoplasm (Sandoval et al., 1984). **Actin** is necessary for biogenesis of Golgi-derived transport carriers and is required for maintenance of unique flat shape of Golgi cisternae (Valderrama et al., 1998). Role of **motor proteins** have also been demonstrated regulating intra-and inter-Golgi traffic, and in maintaining Golgi organization (Brownhill et al., 2009). In addition, centrosomal originated microtubule arrays along with few scaffolding proteins are necessary to keep the pericentriolar localization of the Golgi (Hurtado et al., 2011). Knowing the role cytoskeletal networks have in cell-matrix adhesion mediated regulation of cell function (Brakebusch and Fässler, 2003; Stehbens and Wittmann, 2012) and their role in Golgi organization (Sandoval et al., 1984; Valderrama et al., 1998), their role in “cell-matrix adhesion-Golgi” pathway was tested. As a first step, it was asked if the loss of adhesion affects the cytoskeletal organization.

Furthermore, the small GTPase **Arf1** is a major regulator of Golgi organization and function (Altan-Bonnet et al., 2003; Donaldson et al., 2005). Upon activation, Arf1 associates with Golgi membranes and, upon inactivation, it is released from Golgi membranes into the cytosol (Donaldson et al., 2005). This cycle of association and dissociation is regulated by Golgi-associated, guanine nucleotide exchange factors (GEFs) and GTPase activating proteins (GAPs). Arf1 binds and/or regulates adaptor, stacking, structural proteins and lipid-modifying enzymes, phospholipase D (PLD) and phosphatidylinositol 4-phosphate 5-kinase (PIP5-kinase) on the Golgi membrane (D'Souza-Schorey and Chavrier, 2006). It is hence able to influence multiple aspects of Golgi structure and function in cells. Furthermore, cell-matrix adhesion is seen to regulate Arf GTPase family member Arf6, through the Arf6-GEF ARNO, to regulate adhesion-dependent membrane exocytosis and signaling (Pawar et al., 2016). The possible role cell-matrix adhesion could have in regulating Arf1 activation to control Golgi organization remains unexplored. In addition, active Arf1 is also seen to recruit motor protein Dynein (through Golgin 160) regulate Golgi organization (Yadav et al., 2012).

In this chapter, the role of cytoskeleton downstream of cell-matrix adhesion in mediating Golgi organization was tested. Also, if adhesion could regulate Arf1 activation (like it regulates Arf6) and the impact this could have in mediating Golgi organization. Further if the Arf1-Dynein connection could act as a link that connects adhesion, Golgi and microtubule network in anchorage-dependent cells was explored.

4.2 RESULTS.

4.2.1 Cytoskeletal elements are structurally intact and functional in suspended and re-adherent cells.

There is a possibility if Golgi disorganization on loss or gain of adhesion might be a consequence of disruption of cytoskeletal elements, which normally fragments the Golgi. However, loss of adhesion and re-adhesion did not disrupt the microtubule network (top two panels), centrosomes (MTOC, green staining in the bottom panel) or the actin cytoskeletal network (bottom panel) in cells (Figure 4.1). An important point to note here is no significant change was observed between 120' SUSP and 5' FN time points.

In addition, consistent with the earlier published data (Balasubramanian et al., 2007), both cytoskeletal networks were found to also be functional in non-adherent cells, with their disruption distinctly affecting endocytic trafficking of GM1-CTxB on the loss of adhesion (Figure 4.2). On nocodazole treatment, GM1 is endocytosed into the cell cortex but not trafficked to the recycling endosome (Figure 4.2 a), while Latrunculin A treatment blocks GM1 endocytosis (Figure 4.2 b). This data indirectly provide evidence that the control suspended cells could support GM1 lipid raft endocytosis, which is dependent on intact microtubules and actin network.

Taken together, these data suggest that loss/gain of cell-matrix adhesion does not depolymerize microtubule and actin network.

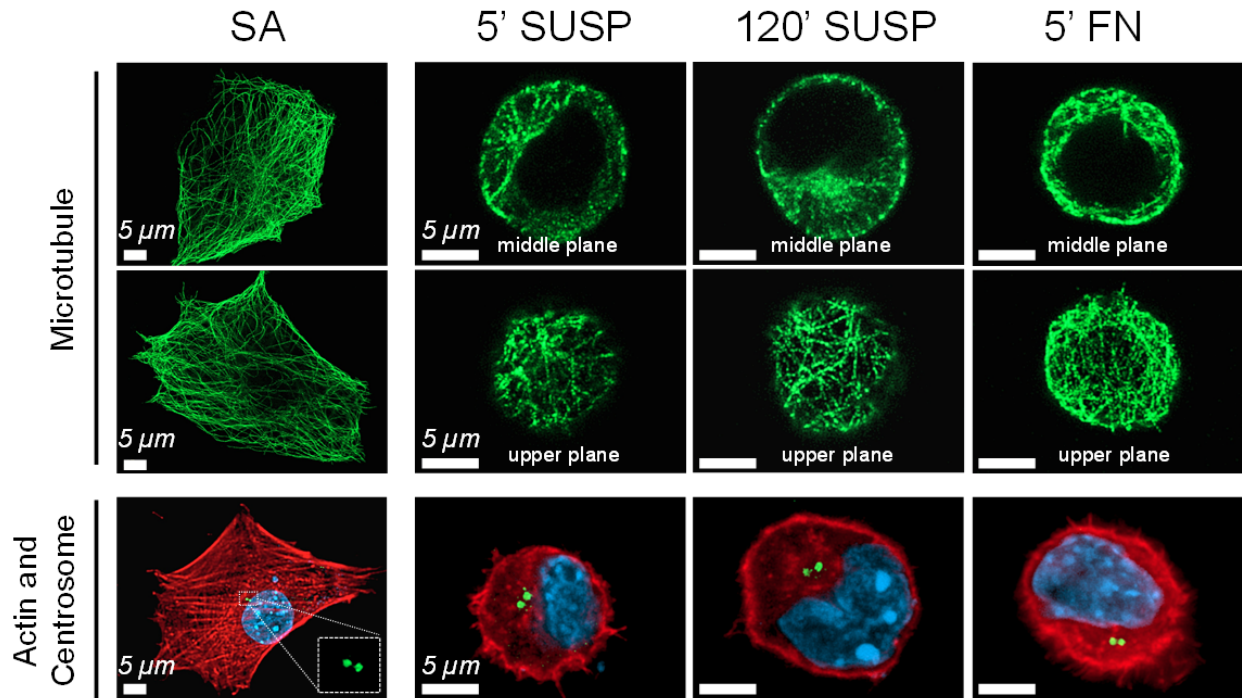


Figure 4.1 Cytoskeletal elements are structurally intact in suspended and re-adherent cells. Serum-starved stable adherent (SA) WT-MEFs detached (5' SUSP), held in suspension for 120 mins (120' SUSP) and re-plated on fibronectin for 5 mins (5' FN) were immuno-stained for β -tubulin (microtubule). Cross-sectional representative images for a middle (top panel) and upper plane (lower panel) for suspended and re-adherent cells are shown. The middle plane for two representative stable adherent (SA) cells is also shown. Cells stained for actin and γ -tubulin (to detect the centrosome) were deconvoluted and representative images for each time point shown in the lowermost panel. Images are representative of 30 cells imaged from 3 independent experiments. Scale bar in these images is set at 5 μ m.

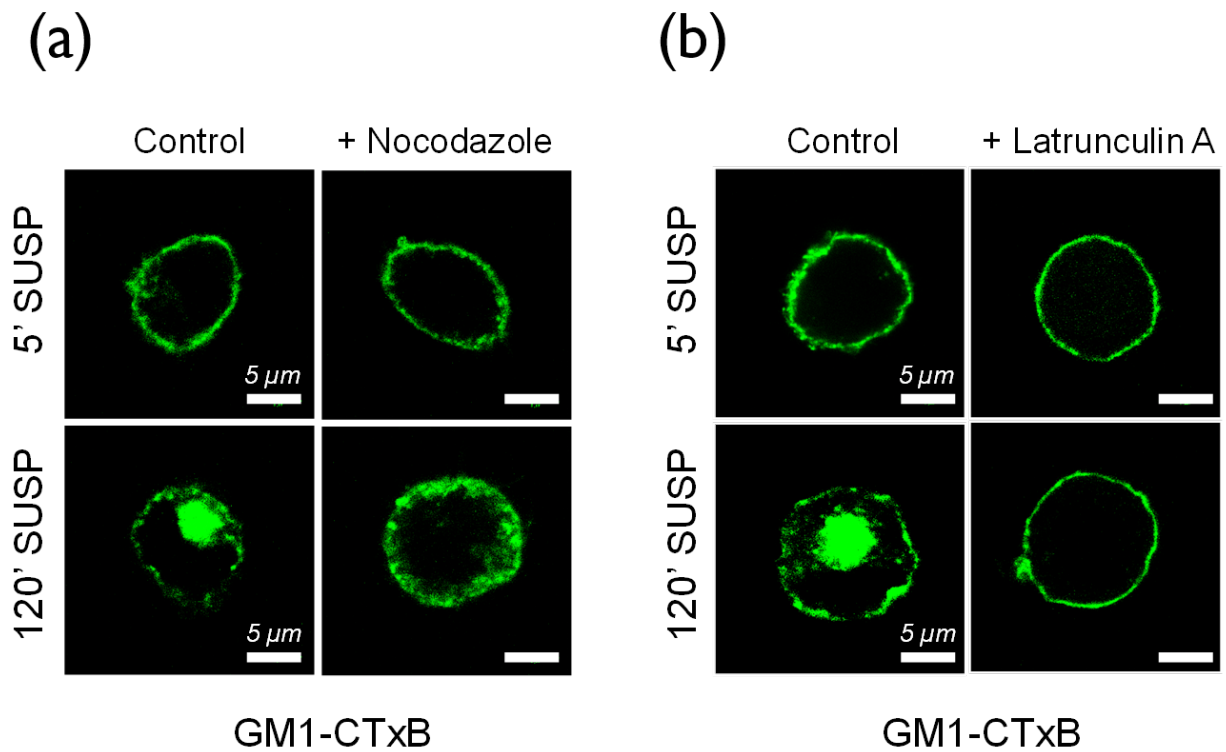


Figure 4.2 Cytoskeletal elements are functional in suspended and re-adherent cells. Stable adherent serum starved WT-MEFs, untreated (Control), pre-treated with **(a)** 10 μM Nocodazole or **(b)** 0.5 μM Latrunculin A were pre-labeled with cholera toxin B (GM1-CTxB) detached (5' SUSP) and held in suspension for 120 mins (120' SUSP). Images are representative of 20 cells (Nocodazole) and 30 cells (Latrunculin A) respectively, from 2 independent experiments. Scale bar in the images is set at 5 μm.

4.2.2 Intact microtubule and not actin network is essential for cell-matrix adhesion regulated Golgi organization.

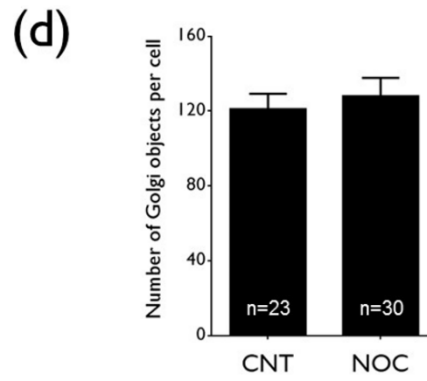
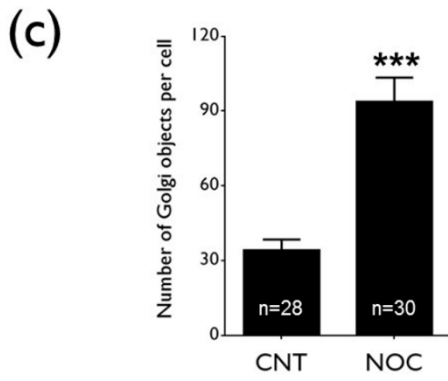
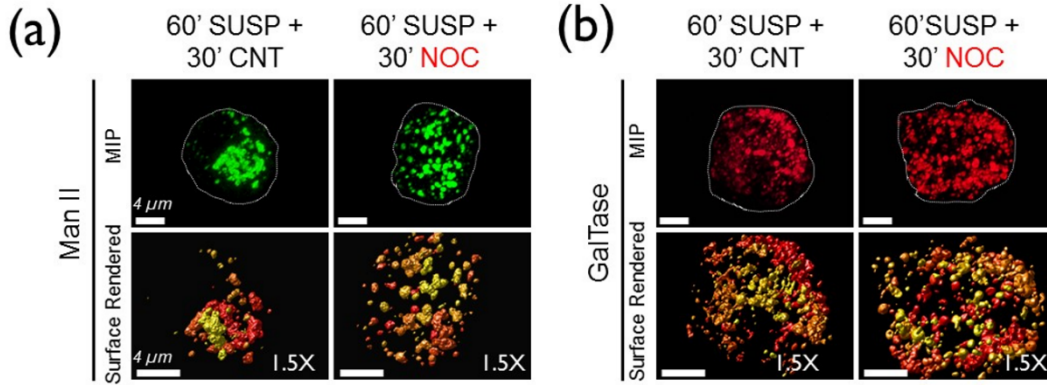
It was further examined if alternation in the microtubule or actin network affects adhesion mediated Golgi disorganization. WT-MEFs suspended for 60 mins and then treated with Nocodazole (10 μ M) exhibited the cis-medial Golgi (Man II GFP) to be further disorganized with a significant increase in the number of discontinuous Golgi objects detected per cell (Figure 4.3 a, c). The trans-Golgi (Galtase RFP), which on the loss of adhesion is already extensively disorganized, did not show any further visible change (Figure 4.3 b, d). On re-adhesion, Nocodazole-treated cells failed to reorganize both the cis-medial (Figure 4.3 e, g) and trans-Golgi (Figure 4.3 f, h).

This suggests the differential distribution of the cis vs trans-Golgi in non-adherent cells could be dependent on their relative association with the intact microtubule network. On depolymerization of microtubule network, this association was lost, hence now causing cis-medial to attain a trans-Golgi like dispersed phenotype. A complete block of re-organization of Golgi on microtubule depolymerization, in spite of cells being re-adherent was observed, which reversed the microtubule depolymerization by washing out Nocodazole (Figure 4.4 c) and found it to restore Golgi organization (Figure 4.4 a, b). This further supports the role an intact microtubule network has in cell-matrix adhesion-dependent Golgi re-organization.

Interestingly, similarly disrupting the actin cytoskeleton with Latrunculin-A, however, did not affect the Golgi organization in suspended (Figure 4.5 a-d) and re-adherent cells (Figure 4.5 e-h). A subtle decrease in cell and Golgi size on actin depolymerization was observed,

which was concomitant to reports in the literature (Valderrama et al., 1998). This suggests the adhesion-dependent regulation of the Golgi to be dependent only on the microtubule network. This does raise the prospective role is the microtubule motor proteins associated with the Golgi could have in mediating the same.

SUSPENSION



RE-ADHERENT

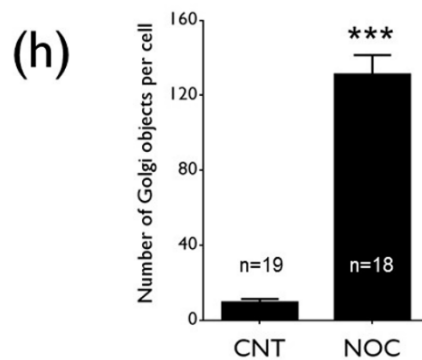
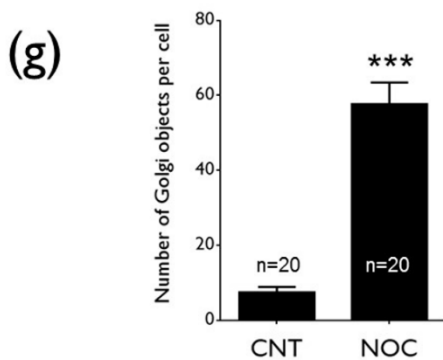
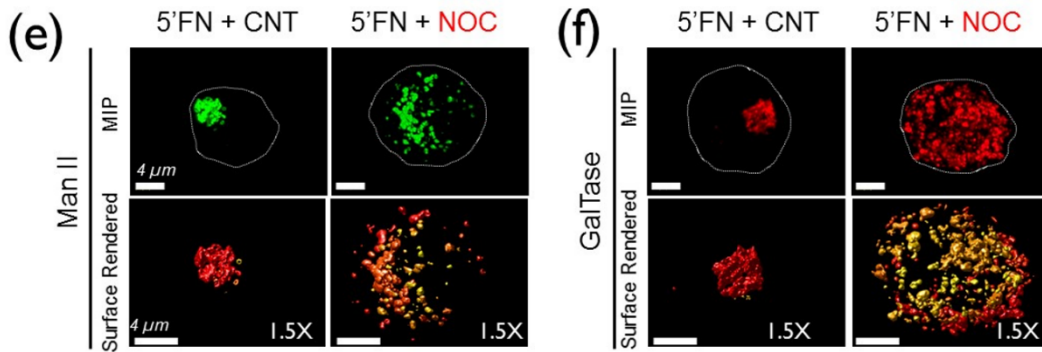


Figure 4.3 Adhesion mediated Golgi re-organization require intact microtubule network. Serum-starved WT-MEFs expressing **(a, e)** cis-medial (Man II) or **(b, f)** trans-Golgi (GalTase) marker were suspended for 60 mins (60' SUSP) and an additional 30 mins without treatment (+30' CNT) or treated with Nocodazole (+30'NOC) and re-plated on fibronectin for 5 mins without drug (5'FN+CNT) or with nocodazole (5'FN+NOC). Confocal Z stack images were deconvoluted, represented as maximum intensity projections (MIP) (top panel) and surface rendered images zoomed 1.5X for clarity (bottom panel for each cell). **(c, d, g, h)** Discontinuous Golgi objects per cell for Man II and GalTase were determined using the Huygens image analysis software. The graph represents mean \pm SE (18-30 cells from three independent experiments). Statistical analysis was done using the Mann Whitney's test (***) p-value <0.001). Scale bar in the images is set at 4 μ m.

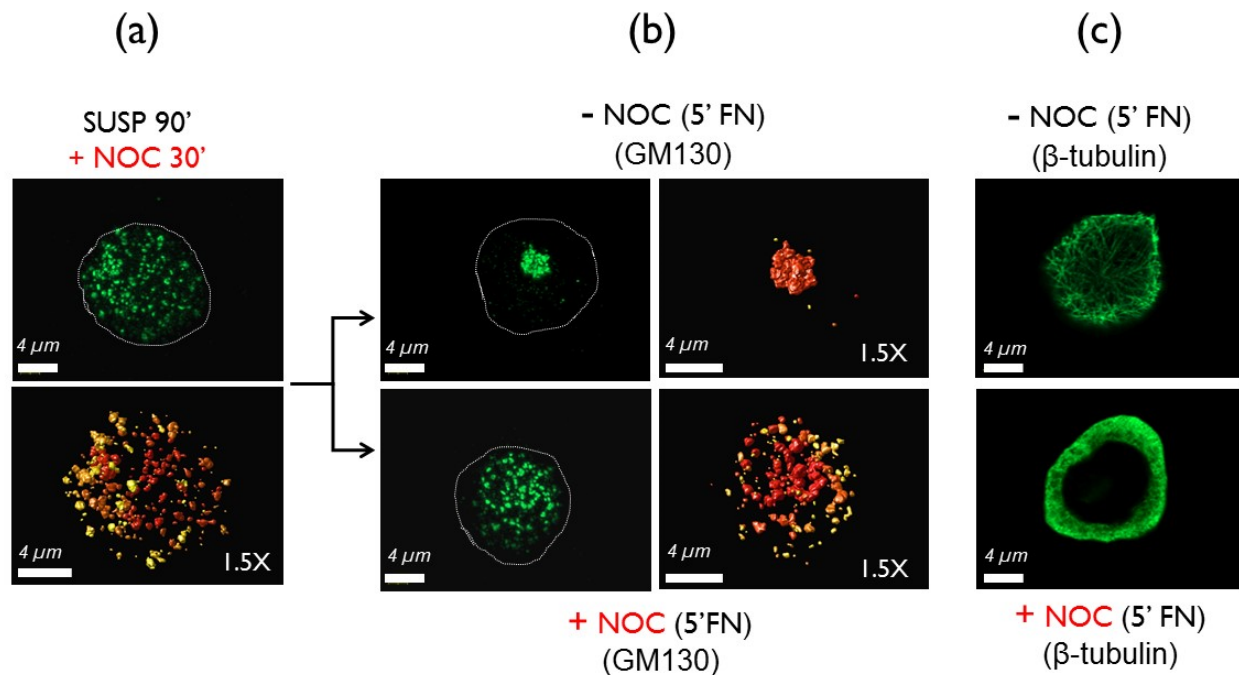
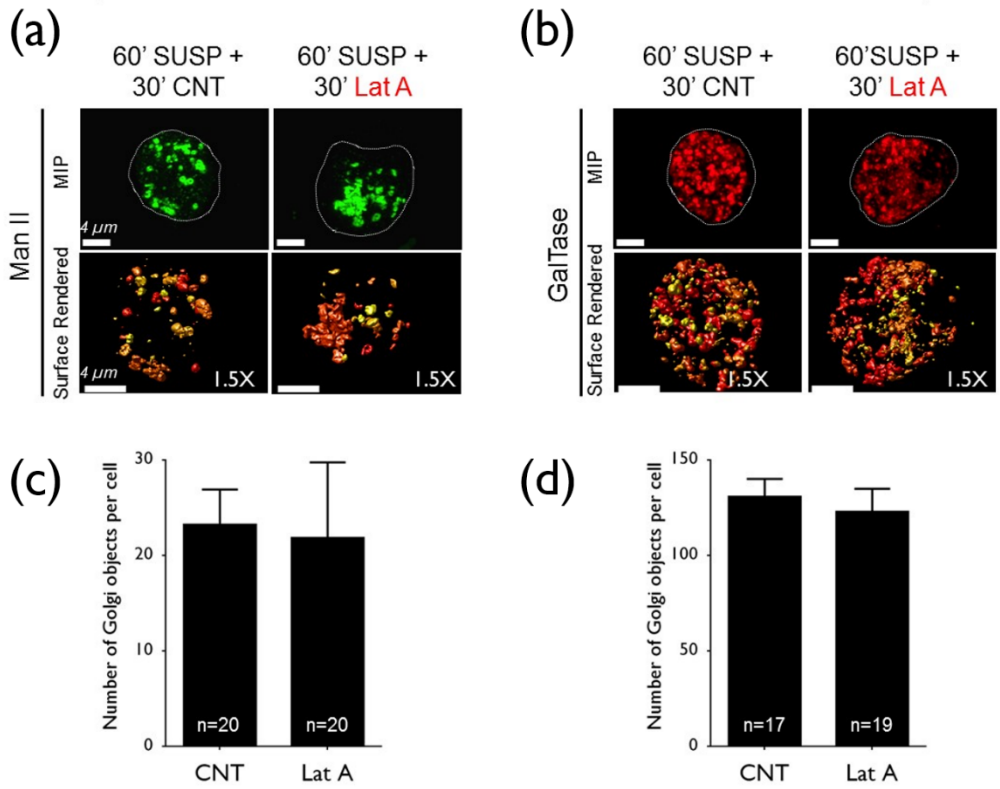


Figure 4.4 Washout of Nocodazole triggers adhesion mediated Golgi re-organization. Untransfected serum starved WT-MEFs were detached and held in suspension for 90 mins and then incubated with (a) 10 μ M Nocodazole for another 30 mins (SUSP 120' + NOC), and either washed without Nocodazole and (b) re-plated on fibronectin (WASH FN8'), or in presence of 10 μ M Nocodazole and re-plated on fibronectin containing nocodazole (NOC + FN8'). These cells were then immunostained with GM130 and deconvoluted confocal z stacks are represented. (c) Fibronectin re-adherent (WASH FN8') or (NOC + FN8') were also stained with β -tubulin (microtubule). Representative confocal cross-sectional images are shown. Scale bar in all images is set at 4 μ m.

SUSPENSION



RE-ADHERENT

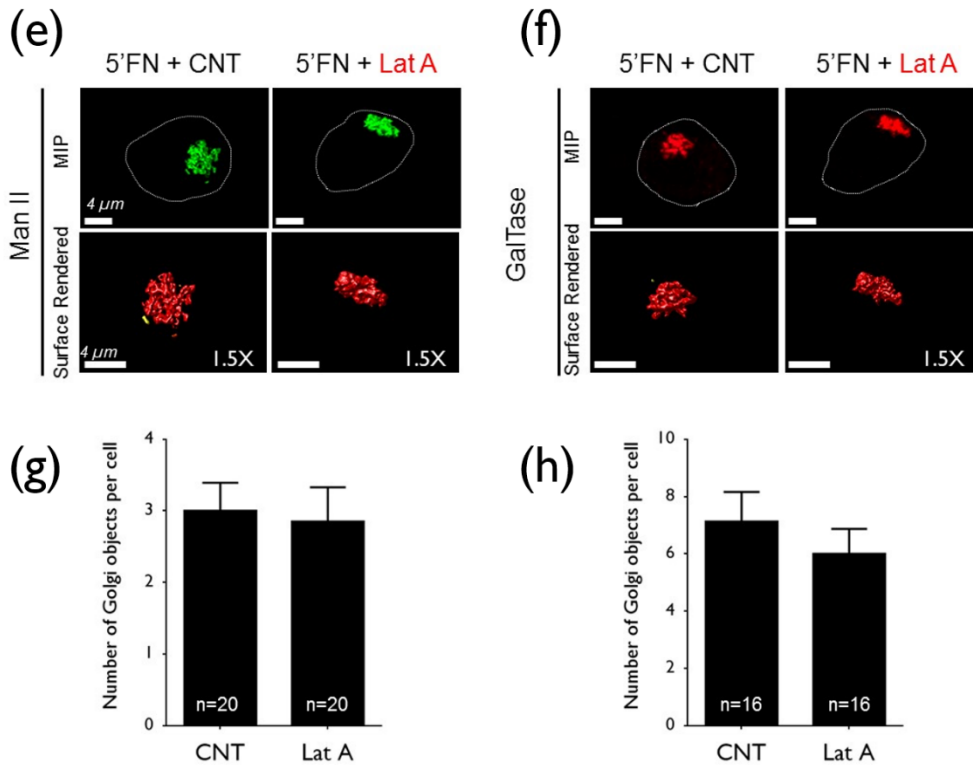


Figure 4.5 Adhesion mediated Golgi re-organization does not require intact actin network. Serum-starved WT-MEFs expressing (a) cis-medial (Man II) or (a) trans Golgi (GalTase) marker were suspended for 60 mins (60' SUSP) and an additional 30 mins without treatment (+30' CNT) or treated with Latrunculin A (+30' LatA) and re-plated on fibronectin for 5 mins (e, f) without drug (5' FN+CNT) or with Latrunculin A (5' FN+LatA). Confocal Z stack images were deconvoluted, represented as maximum intensity projections (MIP) (top panel) and surface rendered images zoomed 1.5X for clarity (bottom panel for each cell). (c, d, g, h) Discontinuous Golgi objects per cell for Man II and GalTase were determined using the Huygens image analysis software. The graph represents mean \pm SE (16-20 cells from two independent experiments). Statistical analysis was done using the Mann Whitney's test and p-values were not significant. Scale bar in the images is set at 4 μ m.

4.2.3 Cell-matrix adhesion regulate activation of small GTPase Arf1.

Next, the regulator downstream of cell-matrix adhesion that is to driving the rapid change in Golgi organization was explored. **First**, during mitotic Golgi fragmentation Arf1 inactivation (GDP bound form) leads to release Golgi proteins in the cytosol that drives Golgi to disassemble (Altan-Bonnet et al., 2003). **Second**, cell-matrix adhesion regulates Arf family member, Arf6 activation (Balasubramanian et al., 2007). Together these observations led us to ask what happens to Arf1 activation on loss and gain of cell-matrix adhesion.

Towards this end, as a first step the specificity of monoclonal Arf1 antibody was checked by performing siRNA mediated knockdown of Arf1 in WT-MEFs (Figure 4.6 a). Active Arf1 pulled down using GST conjugated GGA3 effector binding domain reveals loss of adhesion to significantly reduce Arf1 activation (by ~60%), rapidly restored on re-adhesion to fibronectin (Figure 4.6 b). Net Arf1 levels do not change under these conditions (Figure 4.6 c).

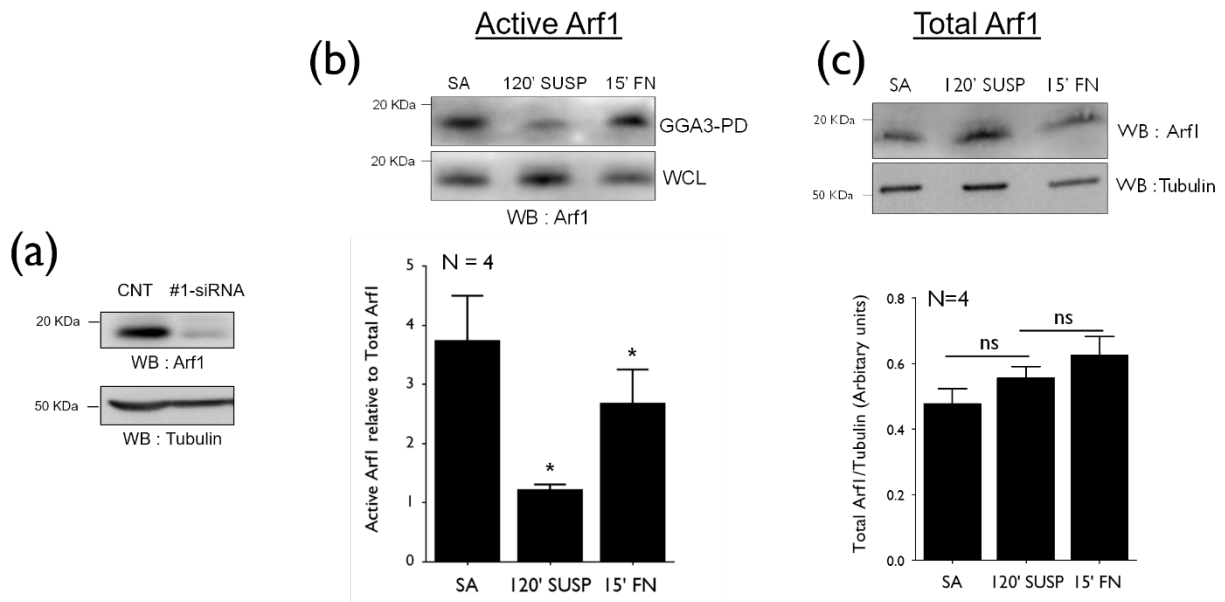


Figure 4.6 Adhesion regulate activation of Arf1. (a) Representative blots showing knockdown of endogenous Arf1 with respect to Tubulin as loading control demonstrating the specificity of the Arf1 antibody (Clone 1D9) for western blot detection. (b) Western blot detection of (b) active Arf1 in GST-GGA3 pull-down (GGA3 PD) and (c) total Arf1 in whole cell lysate (WCL) of serum-starved WT-MEFs stable adherent (SA), suspended for 120 mins (120' SUSP) and re-adherent on fibronectin for 15 mins (15' FN). The graph represents mean \pm SE from four independent experiments.

4.2.4 Cell matrix adhesion dependent Arf1 activation controls Golgi organization.

To test if this drop in active Arf1 levels has a role in mediating Golgi disorganization it was disrupted the same by expressing GFP tagged constitutively active Arf1 (Q71L) in WT-MEFs (Figure 4.7 a) and found it prevents disorganization of the trans-Golgi (Galtase-RFP) in suspended cells (Figure 4.7 d). GFP-WT-Arf1 expressing MEFs behave like un-transfected control cells, with a distinctly disorganized Golgi phenotype. This is further reflected in a significant decrease in the number of trans-Golgi objects per cell in suspended Q71L Arf1 expressing cells relative to WT Arf1 and control (Figure 4.7 e).

The distribution profile of organized versus disorganized phenotype in suspended and re-adherent WT-Arf1 and Q71L-Arf1 expressing cell populations further confirm this regulation (Figure 4.7 b, c).

In order to strengthen the observation, the same experiments to probe restoration of cis-Golgi (GM130) was repeated. HA-tagged constitutively active Arf1 (Q71L) in WT-MEFs (Figure 4.8 a, b) was expressed and likewise, the cis-Golgi organization was also restored in suspended cells (Figure 4.8 c). Untransfected CNT cells and HA-WT-Arf1 expressing MEFs exhibited disorganized Golgi phenotype. This is further reflected in a significant decrease in the number of cis-Golgi objects per cell in suspended Q71L Arf1 expressing cells relative to WT Arf1 and control (Figure 4.8 d).

The result is in agreement with earlier published data that inactivation of Arf1 leads to Golgi fragmentation during mitotic Golgi disassembly and expression of active Arf1 mutant blocked

this phenotype and along with arrested cells in mitotic phase of cell cycle (Altan-Bonnet et al., 2003).

Based on our finding that cell-matrix re-adhesion (to fibronectin) activates Arf1, and an active mutant of Arf1 restores Golgi organization in suspended cells, next question was what happens during re-adhesion if Arf1 activation gets blocked. This was tested by inhibiting Arf1 using a dominant negative mutant GFP tagged T31N-Arf1 (Figure 4.7 a) and HA-tagged T31N-Arf1 (Figure 4.8 a). Localization of the constructs revealed the cytosolic presence of T31N-Arf1 (both GFP and HA-tagged), as reported in the literature (Vasudevan et al., 1998). Presence of this mutant does not allow Arf1 to become active, “GTP bound” form. In suspension, there was no significant change in disorganization of cis-Golgi (GM130) or trans-Golgi (Galtase) as evident in the images and quantitation for the number of objects (Figure 4.9). Re-organization of both cis and trans-Golgi was completely abrogated in 5'FN time points. There was no effect on cell attachment (5'FN) in cells expressing T31N-Arf1 mutant, suggesting early adhesion events did trigger, but it failed to drive re-organize Golgi as active Arf1 was not present. This is evidently reflected in Golgi object numbers in re-adherent cells being comparable to those seen in suspended cells (Figure 4.9 b, d). These results provide evidence that Arf1 activation is a part of the molecular machinery that is downstream of adhesion in regulating Golgi organization.

In order to further establish the role of Arf1 downstream of adhesion, fibronectin-coated bead experiments were performed in the background of inhibited Arf1. Binding of fibronectin-

coated beads to suspended BFA treated cells (BFA+FN-Bead) failed to restore Golgi organization unlike untreated cells bound to FN beads (Figure 4.10 c, d).

Golgi object numbers accordingly stayed significantly high in BFA+ FN-Bead treated cells (Figure 4.10 d). The distribution profile of the organized versus disorganized phenotype in FN-Bead vs BFA+ FN-Bead treated cells further confirming this (Figure 4.10 a, b). Taken together, these studies clearly demonstrate that cell-matrix adhesion regulates Small GTPase Arf1 activity to control Golgi organization. Loss of adhesion leads to inactivation of Arf1 and re-adhesion strongly activate Arf1.

With known overlap in regulation and function of Arf family members and the known regulation of Arf6 by cell adhesion, it was tested if Arf6 can have an effect on the “adhesion-Golgi pathway”. Towards this end, HA-tagged fast cycling mutant Arf6 (HA-T157A-Arf6) and constitutively active Arf1 (HA-Q71L-Arf1) in WT-MEFs were expressed. Western blotting shows relative expression of both the mutants were comparable in the cells (Figure 4.11 a). As expected, active Arf1 expressing suspended cells (middle panel) could block cis-Golgi (GM130) disorganization. On the contrary active Arf6 (T157A) expressing suspended cells (rightmost panel) did not have this effect and displayed Golgi their Golgi to be disorganized like CNT cells (Figure 4.11 b). This further confirmed that adhesion uses Arf1 specifically to regulate Golgi organization.

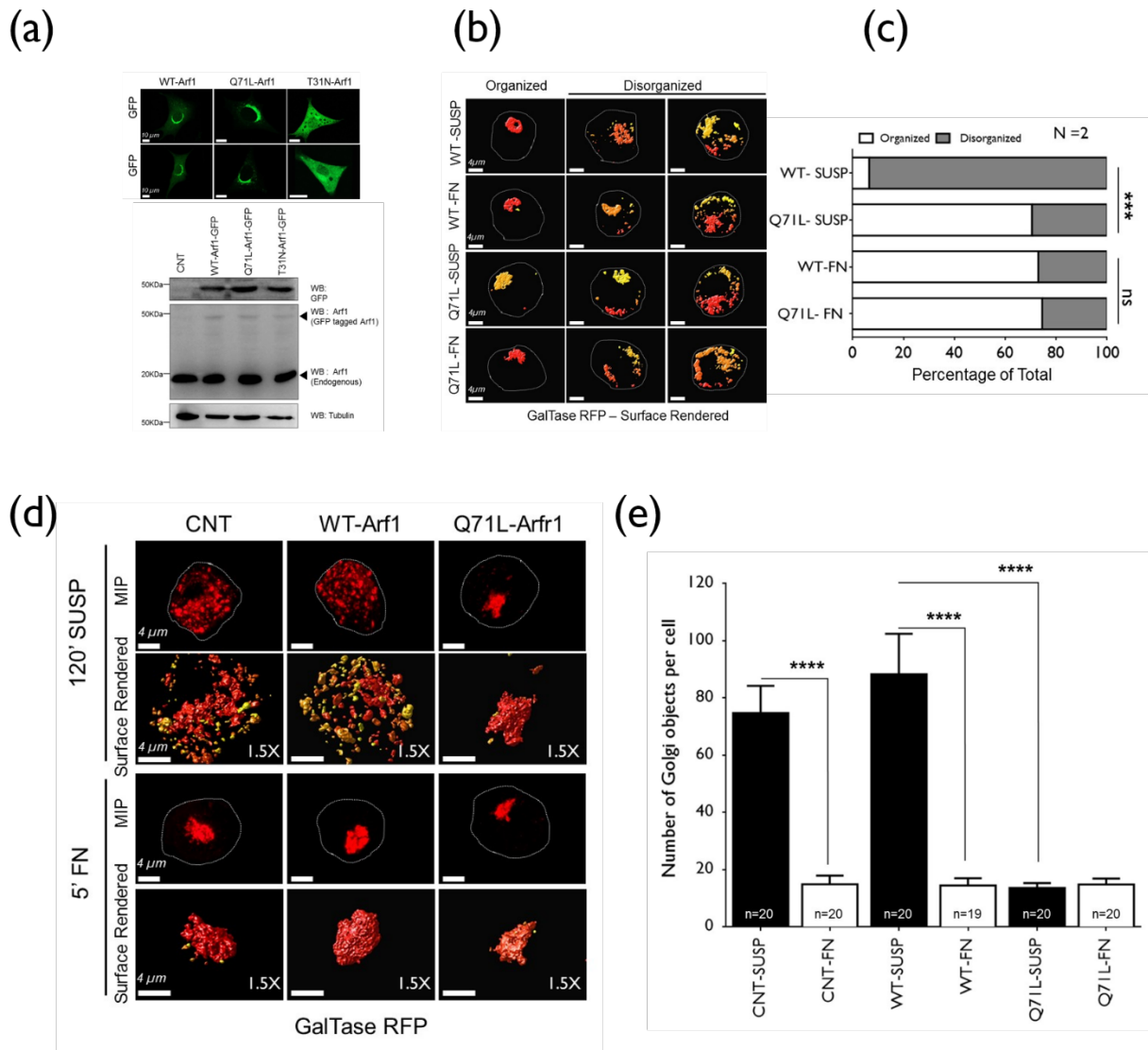


Figure 4.7 Adhesion-dependent Arf1 activation regulates trans-Golgi organization. (a) Localization of GFP tagged wild-type (WT-Arf1), constitutively active Arf1 (Q71L Arf1) and dominant negative Arf1 (T31N Arf1) in serum-starved stable adherent WTMEFs (top panel). These cells along with un-transfected control (CNT) were lysed and whole cell lysates probed with anti-GFP (WB: GFP), anti Arf1 antibody (WB: Arf1) to detect the endogenous Arf1 (Endogenous Arf1) and overexpressed Arf1 (GFP tagged Arf1) and compared to tubulin (WB: tubulin). **(b)** The percentage distribution of cells with organized and disorganized Golgi phenotypes in WT-MEFs expressing GalTase RFP and GFP tagged wild-type Arf1 (WT-Arf1) or active Arf1 (Q71L Arf1) suspended for 120 mins (WT-SUSP, Q71L-SUSP) and re-adherent on fibronectin for 5 mins (WT-FN, Q71L-FN) was determined. Representative surface rendered cross section images for the organized and disorganized phenotype for each treatment. **(c)** The graph represents percentage distribution for each phenotype in one of two

comparable but independent experiments. 100 cells were counted for each time point in an experiment. Statistical analysis comparing the change in distribution profile was done using the Chi-Square test, two-tailed (***) p-value < 0.0001). **(d)** Serum-starved WT-MEFs transfected with GalTase RFP alone (CNT) or along with GFP wild-type Arf1 (WT-Arf1) or active Arf1 (Q71L Arf1) were detached, held in suspension for 120 mins (120' SUSP) and replated on fibronectin for 5 mins (5'FN). Confocal Z stack images were deconvoluted, represented as maximum intensity projections (MIP) (top panel) and surface rendered images zoomed 1.5X for clarity (bottom panel for each cell). **(e)** Discontinuous Golgi objects per cell determined using Huygens is represented in the graph as mean \pm SE from a minimum of 19 and maximum of 20 cells from two independent experiments. Statistical analysis was done using the Mann Whitney's test (**** p-value <0.0001). Scale bar in the images is set at 4 μ m.

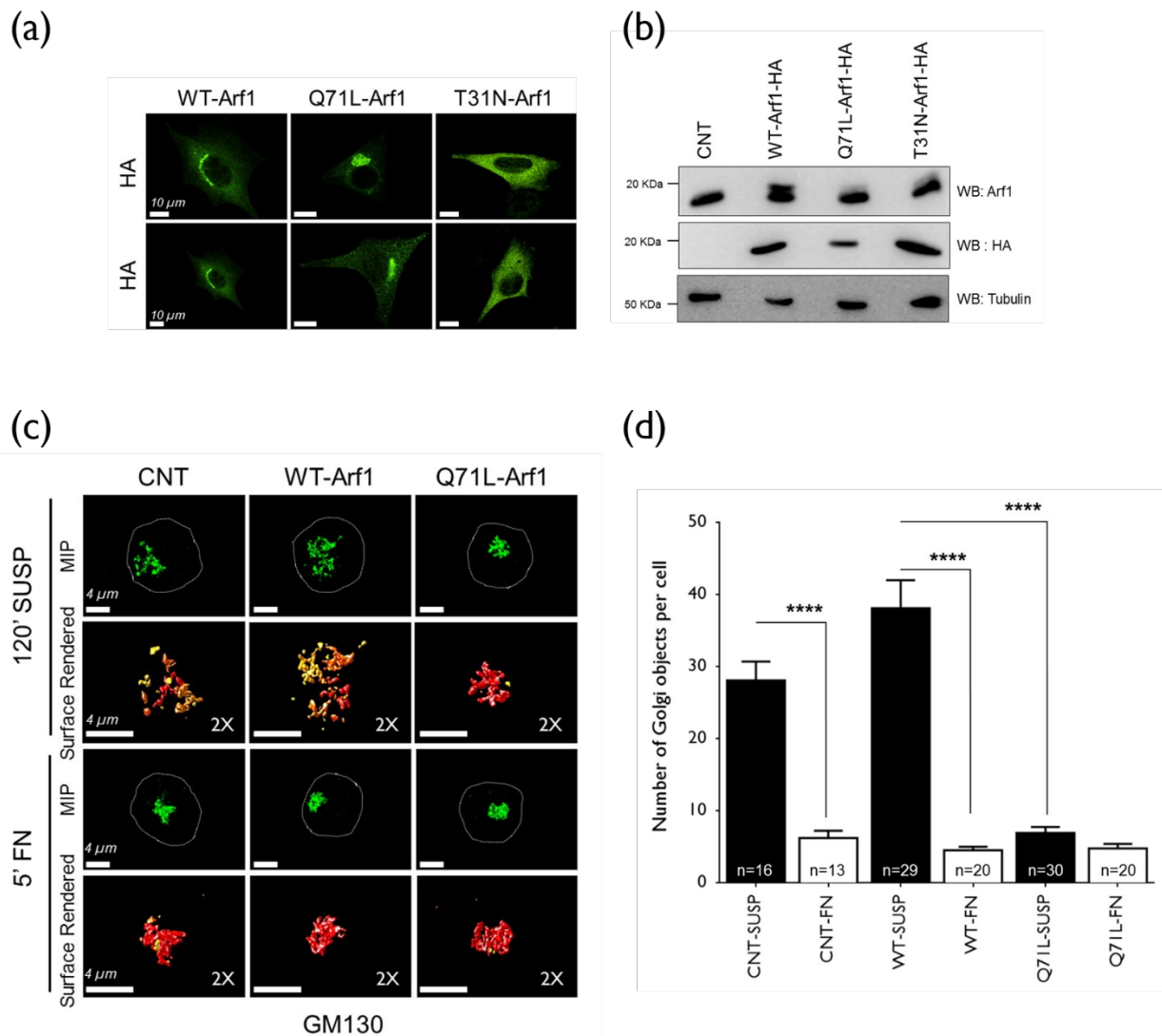
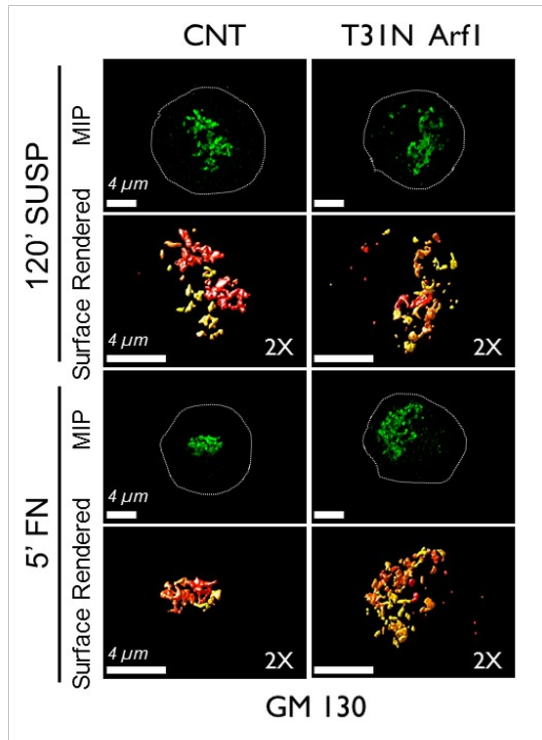
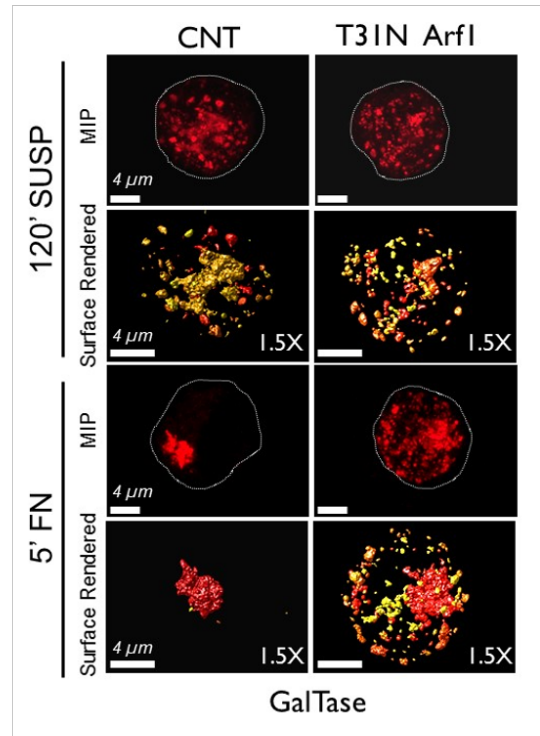


Figure 4.8 Adhesion-dependent Arf1 activation regulates cis Golgi organization. (a) Localization of HA-tagged wild-type (WT-Arf1), constitutively active Arf1 (Q71L Arf1) and dominant negative Arf1 (T31N Arf1) in serum-starved stable adherent WT-MEFs (left panel). **(b)** These cells along with un-transfected control (CNT) were lysed and whole cell lysates probed with an anti Arf1 antibody (WB: Arf1), anti-HA (WB: HA), and compared to tubulin (WB: tubulin). **(c)** Serum-starved untransfected WT-MEFs (CNT) or along with HA wild-type Arf1 (WT-Arf1), active Arf1 (Q71L Arf1) were detached, held in suspension for 120 mins (120' SUSP) and re-plated on fibronectin for 5 mins (5'FN). In all of the above confocal Z stacks were deconvoluted and representative maximum intensity projection (MIP) and surface rendered the zoomed image (1.5X) are shown. **(d)** Discontinuous Golgi objects per cell determined using Huygens is represented in the graph as mean \pm SE from a minimum of 13 and maximum of 30 cells from three independent experiments. Statistical analysis was done using the Mann Whitney's test (**** p-value < 0.0001). Scale bar in all images is set at 4 μm .

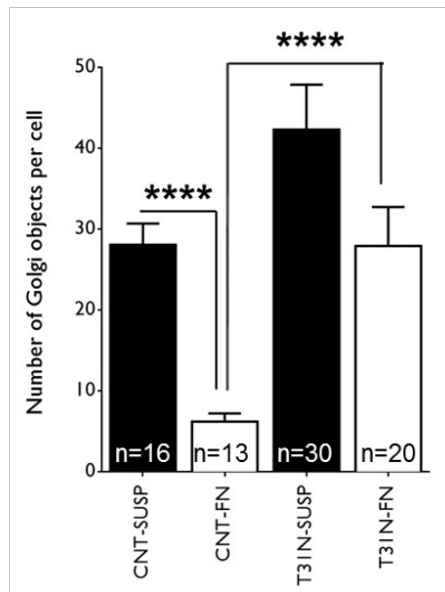
(a)



(c)



(b)



(d)

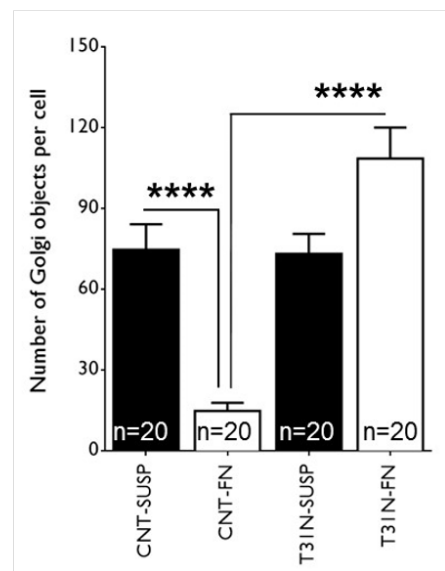


Figure 4.9 Active Arf1 is necessary for the adhesion-dependent Golgi organization. (a) Serum-starved untransfected WT-MEFs (CNT) or with HA dominant negative Arf1 (T31N-Arf1), were detached, held in suspension for 120 mins (120' SUSP) and re-plated on

fibronectin for 5 mins (5'FN). Cells were fixed and immunostained with anti-GM130 antibody to detect cis-Golgi. **(c)** Serum-starved WT-MEFs transfected with GalTase RFP alone (CNT) or along with GFP dominant negative Arf1 (T31N Arf1) were detached, held in suspension for 120 mins (120' SUSP) and re-plated on fibronectin for 5 mins (5'FN). In all of the above confocal Z stacks were deconvoluted and representative maximum intensity projection (MIP) and surface rendered zoomed image (2.5X for GM130 and 1.5X for GalTase) are shown. Discontinuous Golgi objects per cell determined for **(b)** GM130 and **(d)** GalTase using Huygens. The graph represents mean \pm SE from a minimum of 13 cells and maximum of 30 cells (as indicated in each bar) from (b) three and (d) two independent experiments respectively. Statistical analysis comparing was done using the Mann Whitney's test (**** p-value <0.0001). Scale bar in all images is set at 4 μ m.

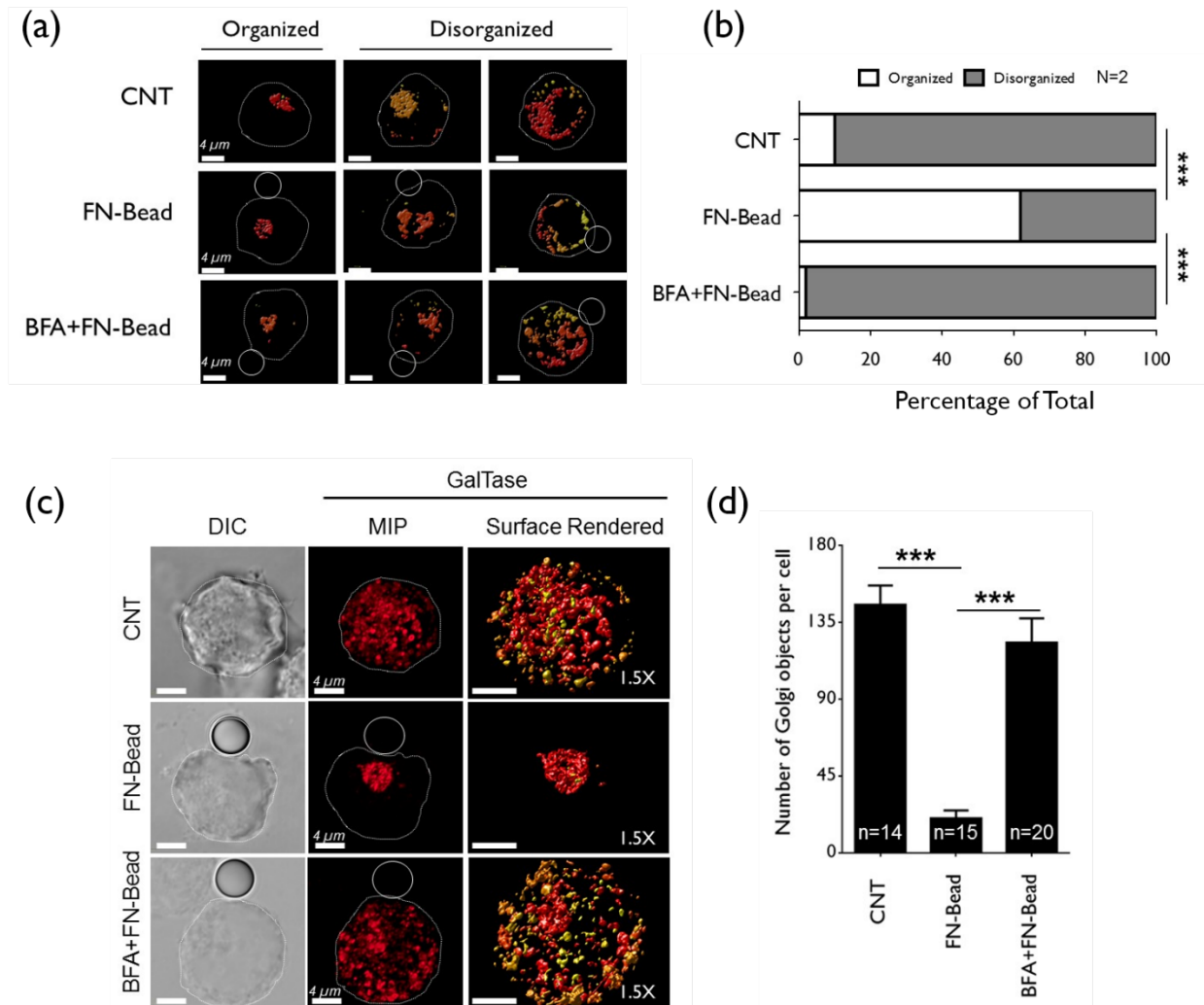


Figure 4.10 Active Arf1 is necessary for integrin activation mediated restoration of Golgi organization. Control and BFA treated suspended cells (30 mins) incubated with beads coated with fibronectin (FN-Bead) and (BFA+FN-Bead) for 15 mins or MeOH as mock (CNT). **(a)** The percentage distribution of cells with organized and disorganized Golgi phenotypes in WT-MEFs expressing GalTase RFP without a bead (CNT), incubated with fibronectin-coated (FN-Bead) or fibronectin bead in presence of BFA (BFA+FN-Bead) was determined. The left panel shows representative surface rendered cross section images for the organized and disorganized phenotype at each treatment. **(b)** The graph represents percentage distribution for each phenotype in one of two comparable independent experiments. 50 cells were counted for each time point in an experiment. Statistical analysis comparing the change in distribution profile was done using the Chi-Square test, two-tailed (*** p-value < 0.0001). **(c)** In all of the above confocal Z stacks were deconvoluted and representative maximum intensity projection (MIP) and surface rendered the zoomed image (1.5X) are shown. **(d)** Discontinuous Golgi objects per cell determined using Huygens is represented in the graph as

mean \pm SE from a minimum of 15 and maximum of 29 cells from two independent experiments. Statistical analysis comparing object numbers was done using the Mann Whitney's test (***) p-value <0.0001). All scale bars in images are set at 4 μ m.

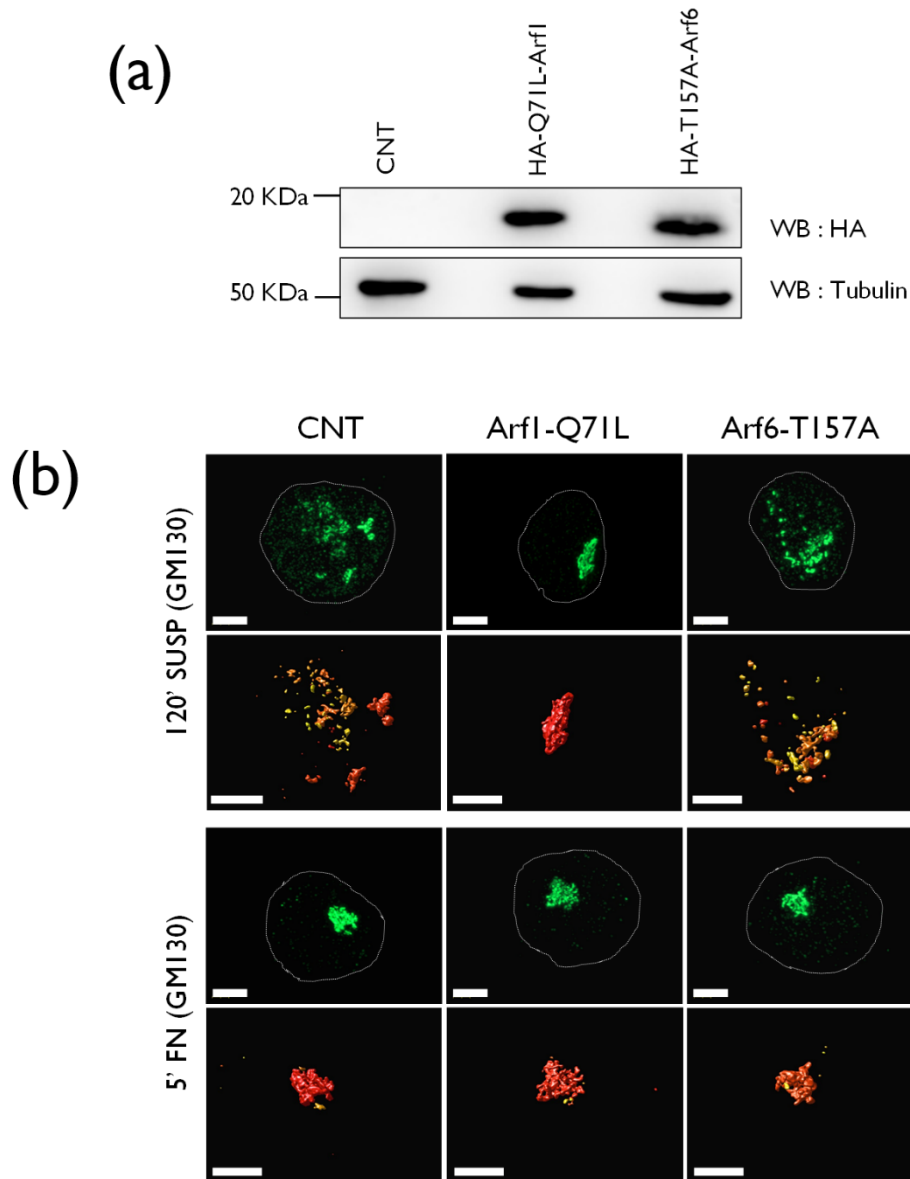


Figure 4.11 Adhesion specifically uses Arf1, and not Arf6 to regulate Golgi organization.

(a) Western blot detection for expression of untransfected serum starved stable adherent WT-MEFs (CNT), HA-tagged constitutively active Arf1 (HA-Q71L-Arf1) and HA-tagged fast cycling Arf6 (HA-T157A-Arf6). These cells were lysed and whole cell lysates probed with anti-HA (WB: HA) and tubulin (WB: tubulin). **(b)** Serum-starved untransfected WT-MEFs (CNT) or transfected with HA-Arf1 Q71L), and HA-Arf6-T157A were detached, held in suspension for 120 mins (120' SUSP) and re-plated on fibronectin for 5 mins (5'FN). These cells were immunostained with anti GM130 antibody and imaged. In all of the above confocal Z stacks were deconvoluted and representative maximum intensity projection (MIP) and surface rendered the zoomed image (1.5X) are shown. Scale bar in all images is set at 4 μ m.

4.2.5 BIG1/2 is the predominant Arf1 specific GEF downstream adhesion mediated Golgi organization.

In exploring further the adhesion-Arf1-Golgi pathway, it was asked how is Arf1 activated downstream of cell-matrix adhesion. Arf1 activation downstream of multiple stimuli is regulated by specific Arf1 GEFs (Guanine exchange factors), that accelerate the conversion of inactive to the active form of Arf1. The large ARF-GEFs Golgi-specific BFA resistance factor 1 (**GBF1**) and BFA-inhibited GEFs (**BIGs**) localize to the Golgi but show a very limited overlap with each other. GBF1 primarily localizes at *cis-Golgi* whereas BIGs at trans-Golgi compartment (Zhao et al., 2002).

Brefeldin-A (BFA) which is a non-competitive inhibitor of Arf1 GEF, BIG1/2 and GBF1 and Golgicide-A (GCA) as an inhibitor of GBF1 (Golgi-specific Brefeldin A-resistance factor 1) were used. While BFA blocked Golgi reorganization dramatically GCA only had a minor effect on the same, reflected in their distribution profiles (Figure 4.12 a, b). Confocal z-stacks also revealed the Golgi organization in BFA treated cells to be completely disorganized as opposed to CNT or GCA, where it was observed to be organized (figure 4.12 c). This suggests BIG1/2 is the prominent GEF working downstream of adhesion to regulate Arf1 activation and Golgi organization. This also provides an explanation of the difference in the extent of disorganization between cis vs trans-Golgi by adhesion. Cell-matrix adhesion prominently affects BIGs, thereby inactivating Arf1 at trans-Golgi and hence more disorganization than cis-Golgi.

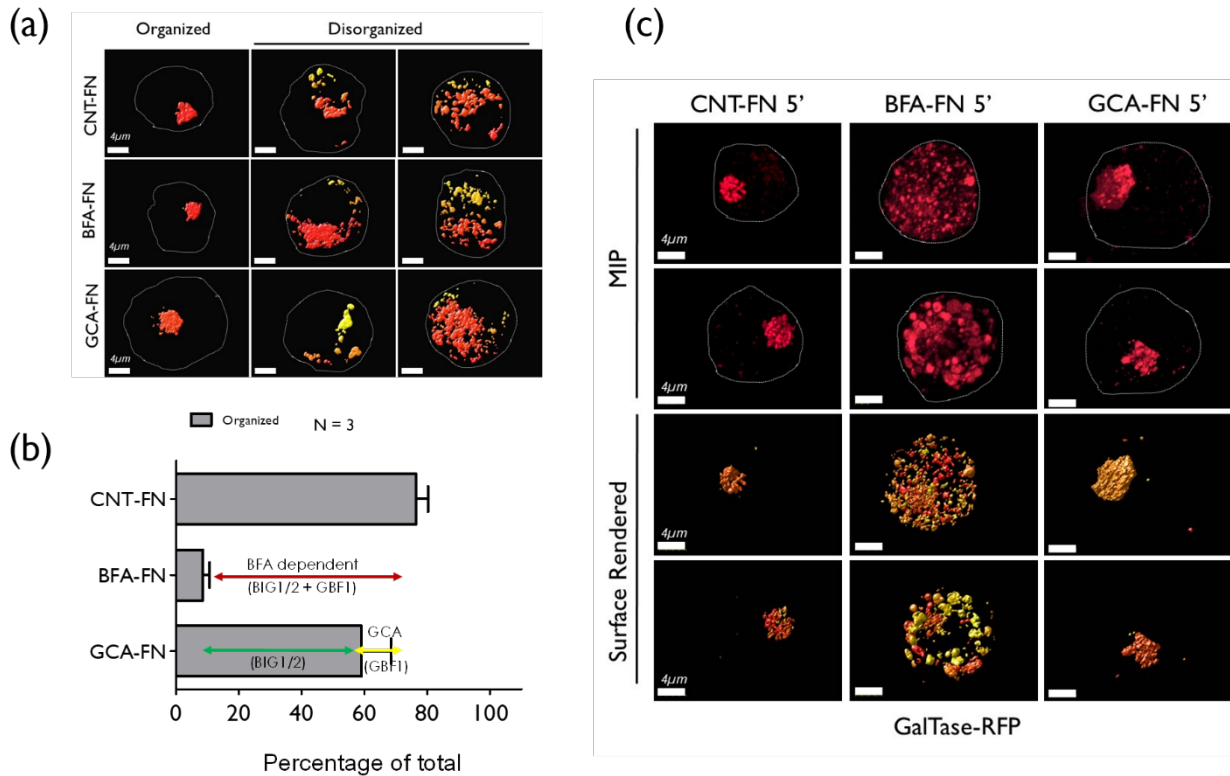


Figure 4.12 BIG1/2 is the predominant Arf1 specific GEF downstream adhesion mediated Golgi organization. (a) Cells expressing GalTase-RFP held in suspension for 90 mins and treated with DMSO (mock) brefeldin A (BFA, 10 μg/ml) or Golgicide-A (GCA, 10 μM in DMSO) for additional 30 mins (120' SUSP) were re-plated on fibronectin for 5 mins (5'FN) without drug (CNT FN-5') or with BFA (BFA FN-5') or with GCA (GCA FN-5'). Percentage distribution of cells with organized and disorganized Golgi phenotypes determined and representative surface rendered cross section images shown. (b) The graph represents mean ± SE from 3 independent experiments. Statistical analysis was done using the two-tailed Chi-Square test (***) p-value <0.0001). (c) In all of the above confocal Z stacks were deconvoluted and representative maximum intensity projection (MIP) and surface rendered the zoomed image (1.5X) are shown. All scale bars in images are set at 4 μm.

4.2.6 Microtubule depolymerization does not affect Arf1 activity to block adhesion-mediated Golgi re-organization.

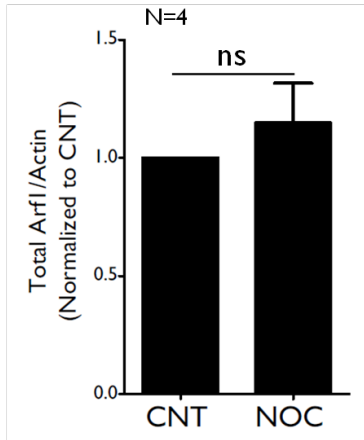
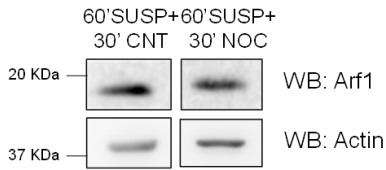
As cell-matrix adhesion regulate Arf1 activation and also require intact microtubule to control Golgi organization, it was further investigated if microtubule depolymerization affects Arf1 activity. In this regard, Total Arf1 levels and Arf1 activity in control and Nocodazole treated suspended cells were evaluated. Nocodazole treatment did not affect net Arf1 levels (Figure 4.13 a) nor did it altered Arf1 activation status in suspended cells.

During re-adhesion, where microtubule depolymerization inhibited Golgi re-organization (Figure 4.3 e-h), there could be a possibility if this effect is because depolymerization is hindering Arf1 activation. Total Arf1 levels did not differ between control and Nocodazole treated FN re-adherent cells (Figure 4.13 c). Very interestingly, there were not any significant difference Arf1 activity on nocodazole treatment in re-adherent cells. This confirms that in these cells in response to re-adhesion, Arf1 is getting activated like control cells, but because of lack of intact microtubule network Golgi re-organization was blocked. This confirms that nocodazole-induced microtubule depolymerization does not alter Arf1 activity to block Golgi reorganization on re-adhesion.

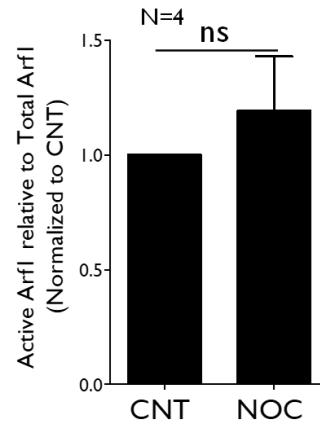
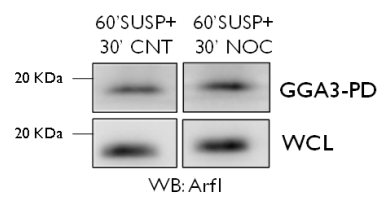
These studies provide evidence that cell-matrix adhesion regulates Arf1 activation and require intact microtubule network for maintaining Golgi organization in anchorage-dependent cells.

SUSPENSION (120' SUSP)

(a) Total Arf1 levels

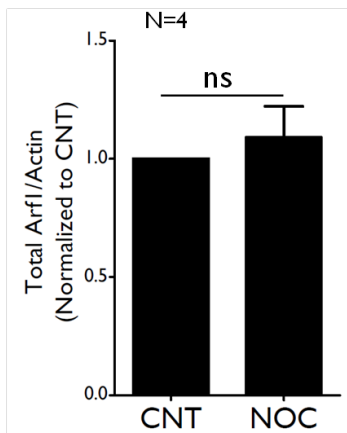
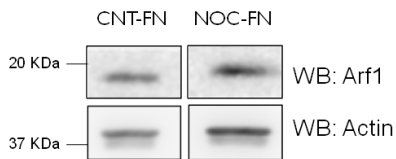


(b) Active Arf1



RE-ADHERENT (15' FN)

(c) Total Arf1 levels



(d) Active Arf1

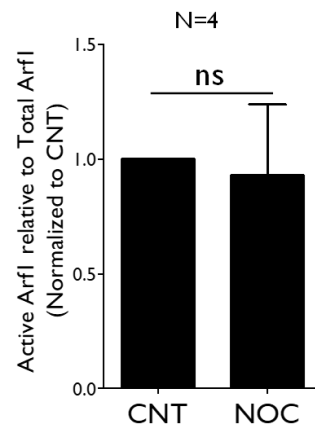
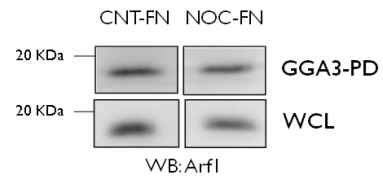


Figure 4.13 Microtubule depolymerization does not affect Arf1 activity to block adhesion-mediated Golgi re-organization. (a) Western blot detection of total Arf1 and Actin in whole cell lysate (WCL) of serum-starved WT-MEFs suspended for 120 mins with DMSO (CNT) or 10 μ M Nocodazole (NOC). The ratio of the densitometric measurement of band intensities of Total Arf1/Actin is represented in the Graph (mean \pm SE) from four independent experiments. (b) Western blot detection of active Arf1 in GST-GGA3 pulldown (GGA3 PD) serum starved WT-MEFs suspended for 120 mins either treated with DMSO (CNT) or 10 μ M Nocodazole (NOC). Graph (mean \pm SE) from four independent experiments. (c) Western blot detection of total Arf1 and Actin in whole cell lysate (WCL) of serum-starved WT-MEFs re-adherent on fibronectin for 15 mins either in presence of DMSO (CNT) or 10 μ M Nocodazole (NOC). The ratio of the densitometric measurement of band intensities of Total Arf1/Actin is represented in the Graph (mean \pm SE) from four independent experiments. (d) Western blot detection of active Arf1 in GST-GGA3 pulldown (GGA3 PD) serum starved WT-MEFs re-adherent on fibronectin for 15 mins either in presence of DMSO (CNT) or 10 μ M Nocodazole (NOC). Graph (mean \pm SE) from four independent experiments. Statistical analysis was done using the one sample t-test and p-values “ns” denotes not significant.

4.2.7 Adhesion-dependent activation of Arf1 recruits motor protein dynein for Golgi organization.

Activation of Arf1 is seen to be dependent on its localization at the Golgi, which could, in turn, mediate recruitment of the minus end motor protein dynein (Yadav et al., 2012). It was hence tested if differential Arf1 activation could regulate its binding and recruitment of the dynein in suspended vs re-adherent cells driving the observed Golgi phenotype. It was observed that pull down of active Arf1 with GST-GGA3 beads does bring down dynein with it (Figure 4.14 a), and further inhibition of Arf1 with BFA affects the same (Figure 4.14 b). As clear from the western blot result in total Arf1 or dynein levels did not change in control and BFA treated adherent cells. This suggests that active Arf1 present in cells controls the amount of dynein recruited/bound to it.

Next, it was tested if there is a differential dynein binding to active Arf1 levels as a result of loss/gain of adhesion. Remarkably, loss of adhesion mediated drop in active Arf1 (Figure 4.14 c) also significantly reduces the amount of dynein that is brought down with it, re-adhesion restoring active Arf1 and bound dynein levels (Figure 4.14 d). This suggests adhesion-dependent Arf1 activation can differentially recruit dynein to drive Golgi reorganization.

Based on two of the observations, **(1)** Cell-matrix re-adhesion activates Arf1 and **(2)** this activated Arf1 recruits Dynein to drive movement of disorganized Golgi towards minus end of the cell, which results in Golgi organization, the role of inhibiting dynein function on Golgi organization was explored. Accordingly, ciliobrevin-D (CB) mediated inhibition of dynein

without affecting suspended cells, blocks re-adhesion mediated Golgi organization as reflected in the distribution profile (Figure 4.15 a, b). Next comparison of confocal z-stacks and observed Golgi object numbers to be significantly high in ciliobrevin treated re-adherent cells relative to control (Figure 4.15 c). Furthermore, Ciliobrevin-D did not affect adhesion-dependent Arf1 activation (relative to untreated control) (Figure 4.15 e) or Arf1 levels (Figure 4.15 d), suggesting the inhibition of dynein downstream of Arf1 is what affects Golgi reorganization here.

Taken together this reveals the presence of an adhesion-Arf1-Dynein-Microtubule pathway mediating Golgi organization in anchorage-dependent cells.

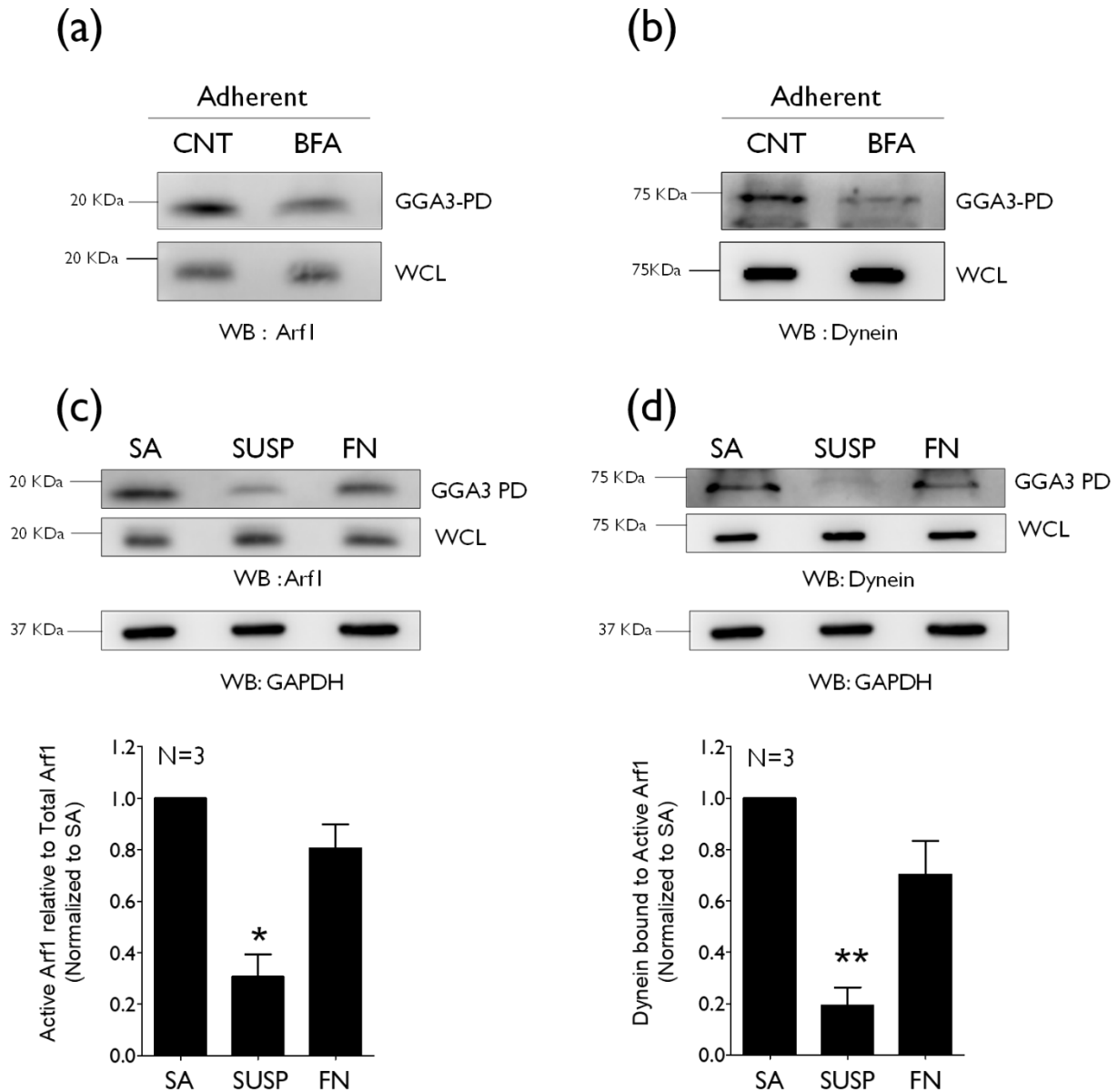


Figure 4.14 Adhesion-dependent activation of Arf1 recruits dynein for Golgi organization. (a) Western blot detection of active Arf1 and (b) dynein (right panel) in GST-GGA3 pull-down (GGA3 PD) and total Arf1 & dynein in whole cell lysate (WCL) of serum-starved WT-MEFs stable adherent (SA), suspended for 120 mins (120' SUSP) and re-adherent on fibronectin for 15 mins (15' FN). The ratio of densitometric band intensities of Arf1 and dynein in pull-down relative to their levels in the WCL are represented in the graph as mean \pm SE from three independent experiments. (c) Western blot detection of active Arf1 (WB: Arf1) and dynein (WB: Dynein) in GST-GGA3 pull-down (GGA3 PD) and total Arf1 in whole cell lysate (WCL) of serum-starved WT-MEFs stable adherent treated with DMSO (CNT) or 10 μ g/mL BFA (BFA). The graph is representative of one of three comparable independent experiments. Statistical analysis was done using one sample t-test (***) p-value <0.0001).

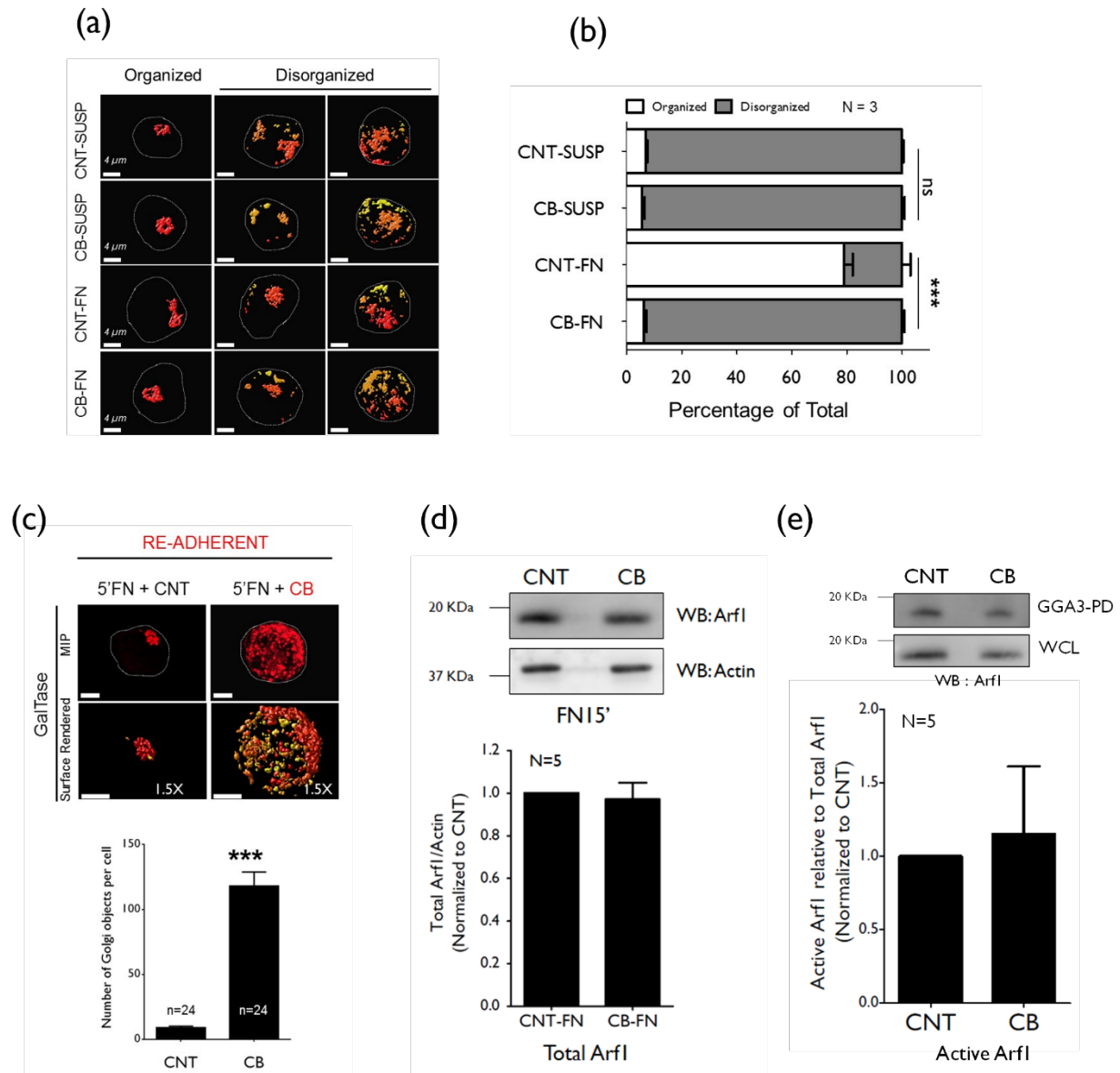


Figure 4.15 Inhibition of Dynein activity hinders adhesion mediated Golgi re-organization. Cells expressing GalTase RFP were held in suspension for 90 mins (CNT) and treated with Ciliobrevin-D (CB, 20 μ M in DMSO) for additional 30 mins and re-plated on fibronectin for 5 mins without (5'FN+CNT) or with CB (5'FN+CB). **(a)** The percentage distribution of re-adherent cells on fibronectin for 5 mins with organized and disorganized Golgi phenotypes in WT-MEFs expressing GalTase RFP with DMSO (CNT-FN) or incubated with Ciliobrevin (CB-FN) was determined. Representative surface rendered cross section images for the organized and disorganized phenotype at each treatment are shown. 100 cells were counted for each time point in an experiment. **(b)** The graph represents mean \pm SE of percentage distribution for each phenotype from 3 independent experiments. Statistical analysis comparing the change in distribution profile was done using the Chi-Square test, two-tailed (***) p-value < 0.0001). **(c)** Representative (5'FN+CNT) or (5'FN+CB)

Confocal Z stacks deconvoluted and representative maximum intensity projection (MIP) and surface rendered zoomed image (1.5X) shown. Discontinuous Golgi objects per cell determined using Huygens represented in the graph. Mean \pm SE from three independent experiments. Statistical analysis comparing object numbers was done using the Mann Whitney's test (***) p-value <0.0001). All scale bars in images are set at 4 μ m. **(d)** Western blot detection of active Arf1 using GST-GGA3 pulldown (GGA3 PD) and total Arf1 in whole cell lysate (WCL) of serum-starved WT-MEFs suspended for 120 mins and re-adherent on fibronectin for 15 mins (FN 15') without (CNT) or with ciliobrevin (CB). The ratio of densitometric band intensities of Arf1 in the pulldown relative to their levels in the WCL is represented in the graph as mean \pm SE from five independent experiments. **(e)** Western blot detection of total Arf1 (WB: Arf1) and Actin (WB: Actin) in whole cell lysate (WCL) of serum-starved WT-MEFs suspended for 120 mins and re-adherent on fibronectin for 15 mins (15' FN) with DMSO (CNT) or Ciliobrevin (CB). The ratio of densitometric band intensities of Total Arf1/Actin is represented in the Graph (mean \pm SE) from five independent experiments.

4.3 SUMMARY.

Having established the role of cell-matrix adhesion in regulating Golgi organization, next it was explored how adhesion could be regulating this pathway in mouse embryonic fibroblasts. It was observed that cytoskeletal elements are structurally intact and functional at suspended and re-adherent cells when their Golgi organization was seen to be distinctly different. This does rule out the possibility that disorganization of Golgi is a result of cytoskeletal elements being structurally de-polymerized on the loss of adhesion. Next it was confirmed that presence of intact microtubule network is essential for adhesion-mediated Golgi re-organization. This regulation is interestingly independent of an intact actin network. Further it has been demonstrated that cell-matrix adhesion regulates small GTPase Arf1 activation, which could contribute to Golgi organization. It was indeed found that adhesion-dependent Arf1 activation is necessary to maintain Golgi organization. It was also observed that downstream of cell-matrix adhesion, BIG1/2 (Arf1 specific GEF) to be the prominent GEF working along this pathway. Loss of adhesion mediated decrease in Arf1 activation, which results in reduced binding of motor protein dynein to it, controls Golgi disorganization. On re-adhesion to fibronectin, Arf1 becomes active, recruiting the minus end motor protein dynein to drive re-organization of the Golgi along an intact microtubule network.

4.4 CONCLUSION.

Cell-matrix adhesion activates Arf1, which recruits motor protein dynein to drive Golgi organization along microtubule network in anchorage-dependent mouse embryonic fibroblast cells.

Chapter 5

**Compare loss of adhesion mediated
Golgi disorganization to
Golgi fragmentation.**

5.1 RATIONALE.

In a mitotic mammalian cell, the fate of Golgi apparatus had been an area of debate for many years concerning the nature of Golgi (structurally and functionally) and the mechanism of secretory protein transport. The forward flow of cargo from ER to Golgi (anterograde transport) is balanced by recycling of components back to Golgi and ER (retrograde transport). This balance is lost in a dividing cell as ER and Golgi undergo structural re-arrangements. One of the question in this debate has been centered whether Golgi retains its own identity with enzymes rapidly recycling to and fro from ER or collapse into ER.

In recent years, many of these questions have been addressed by the use of advanced fluorescence microscopic techniques that led detection of Golgi enzymes in a live cell. Various studies have commented on the quantitative measurements for Golgi enzyme localization, the rate of anterograde and retrograde traffic between ER and Golgi, and also their diffusion rates between these compartments. Based on this researchers have come to a consensus that during mitosis, Golgi is partially absorbed into ER, which is primarily dependent on Arf1 activity (Pecot and Malhotra, 2004; Villeneuve et al., 2017), and expression of dominant negative Sar1 GTPase or treatment with BFA (to inhibit Arf1 GTPase) caused the Golgi to completely collapse into ER membranes (Fujiwara et al., 1988; Lippincott-Schwartz et al., 1989). This led us to ask in the observed “cell-matrix adhesion-Golgi” pathway if on the loss of adhesion the disorganized Golgi falls back into the ER to mimic fragmentation?

5.2 RESULT.

5.2.1 Cell-matrix mediated disorganized Golgi remains separate from Endoplasmic reticulum.

It was observed that on the loss of adhesion the disorganized cis Golgi (GM130) did not show any significant overlap with the ER (KDEL-RFP) in WT-MEFs. Interestingly, this overlap did not decrease in re-adherent cells as shown by Pearson's coefficient values measured from the confocal z-stacks for the entire imaged frame (Figure 5.1 a, b). Analysis of line fluorescence intensity profile for cis-Golgi and ER marker also confirms that there is negligible overlap in these two compartments in suspended or re-adherent cells (Figure 5.1 c). This suggests that the disorganized Golgi in non-adherent cells did not fall back into ER and making the cell-matrix regulated Golgi “disorganization” phenotype distinct from known Golgi “fragmentation”. This could be mediated by their relative active Arf1 status.

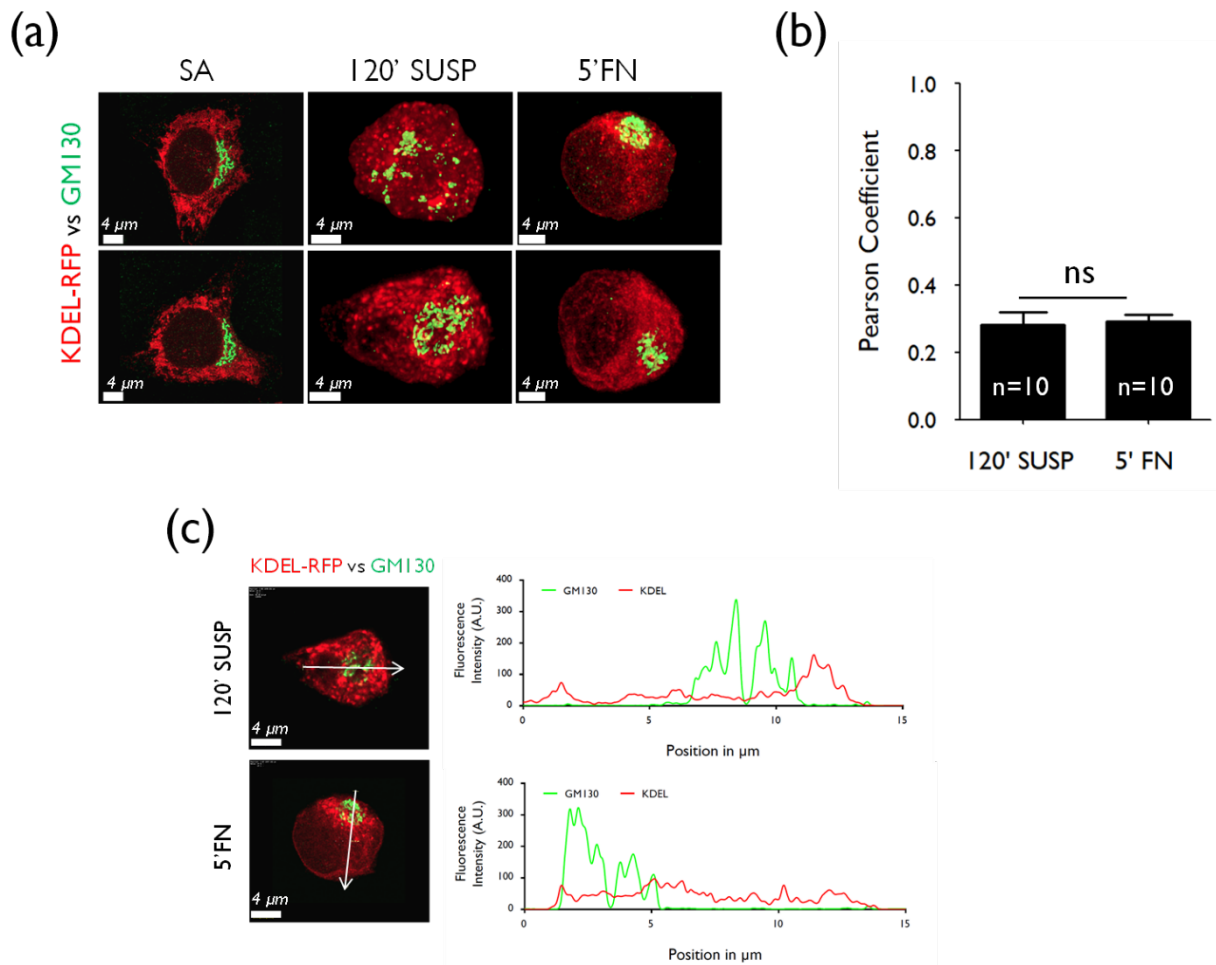


Figure 5.1 Disorganized Golgi remains separate from the endoplasmic reticulum in WT-MEFs. (a) Representative images of serum-starved WT-MEFs expressing ER marker KDEL (KDEL-RFP) were stable adherent (SA), held in suspension for 120 mins (120' SUSP), re-plated on fibronectin for 5 mins (5' FN) and cis Golgi stained with the anti GM130 antibody (GM130). (b) Co-localization for ER (KDEL-RFP) and Golgi (GM130) in the entire confocal cross-sections were determined with Huygens software and Pearsons coefficient represented in graph (mean \pm SE) (c) Colocalization was also assessed in a representative 120' SUSP and 5' FN re-adherent cell, using a line plot across the cell (marked by arrow) for each marker using Huygens image analysis software. Fluorescence intensity measurements obtained were plotted for both the markers and their profiles compared. Scale bars in images are set at 4 μ m.

5.2.2 BFA mediated Arf1 inhibition results in fragmentation of Golgi, which is structurally distinct from Golgi disorganization.

Next, Arf1 was completely inhibited using Brefeldin-A (BFA) in order to find what happens to adhesion mediated disorganized Golgi. BFA mediated inhibition of Arf1 in earlier studies has been shown to cause β COPI mediated fall back of the cis/medial Golgi membrane to the ER, leading to Golgi fragmentation.

Next, quantitative changes in the number of Golgi objects upon BFA treatment on cis/medial-Golgi in both suspended and re-adherent mouse embryonic fibroblast cells were determined. BFA treatment in suspended cells did cause the cis-medial Golgi, Man II GFP, (Figure 5.2 a, b) to fragment completely. Cis/medial Golgi upon BFA treatment seems to appear to have fallen back into ER. This suggests cell-matrix adhesion could be regulating cis/medial and trans-Golgi differently, as evident from the extent of disorganization. This observation could be coming as result of 40% Arf1 remaining in “active form”, suggesting bound to the Golgi. BFA inhibits Arf1 further in the suspended cell over the loss of adhesion effect, triggering now the complete fragmentation of cis/medial Golgi. Active Arf1 levels in suspended cells accordingly drop from ~40% to ~15% on BFA treatment. Quantitation show that BFA does not affect the total Arf1 levels in suspended (Figure 5.3 a) vs re-adherent cells (Figure 5.3 c), but affects only its activation status (Figure 5.3 b, d).

Similar results were observed with cis/medial-Golgi on BFA treatment in Human endothelial cells (Figure 5.4) and human foreskin fibroblast (Figure 5.5). Inhibition of Arf1 by BFA has a

similar effect on cis-Golgi (GM130) in normal breast epithelial cells (Figure 5.6). Here again, cis Golgi was completely fragmented on BFA addition in suspended MCF10A cells, and abrogated the Golgi re-organization on re-adhesion to fibronectin.

MOUSE EMBRYONIC FIBROBLAST

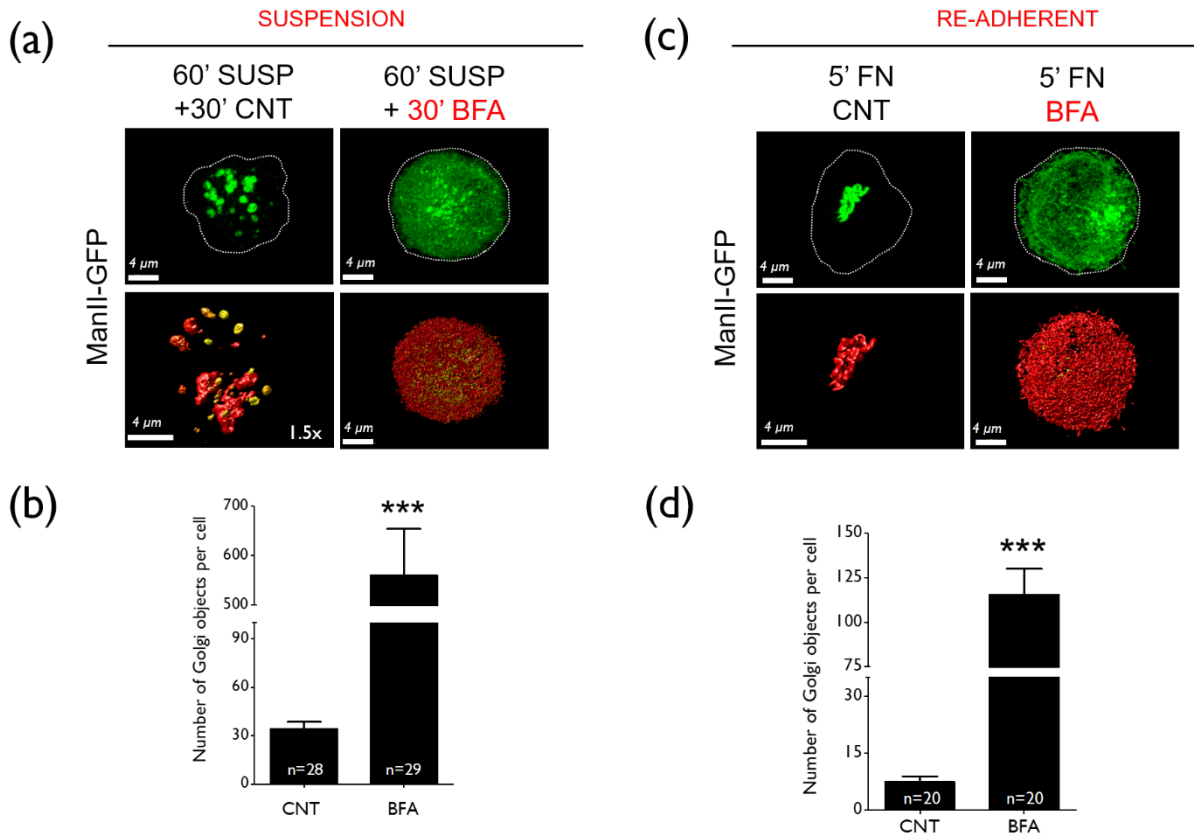


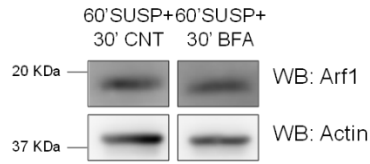
Figure 5.2 BFA mediated inactivation of Arf1 causes fragmentation of disorganized Golgi phenotype in WT-MEFs. (a) Serum-starved WT-MEFs expressing cis-medial (Man II) marker were suspended for 60 mins (60' SUSP) and an additional 30 mins without treatment (+30' CNT) or treated with Brefeldin A (+30'BFA) and (c) re-plated on fibronectin for 5 mins without drug (5'FN+CNT) or with Brefeldin A (5'FN+BFA). Confocal Z stack images were deconvoluted, represented as maximum intensity projections (MIP) (top panel) and surface rendered images zoomed 1.5X for clarity (bottom panel for each cell). (b, d) Discontinuous Golgi objects per cell for Man II and GalTase were determined using the Huygens image analysis software. The graph represents mean \pm SE (19-29 cells from three independent experiments). Statistical analysis was done using the Mann Whitney's test (***) p-value <0.0001). Scale bar in the images is set at 4 μ m.

(a)

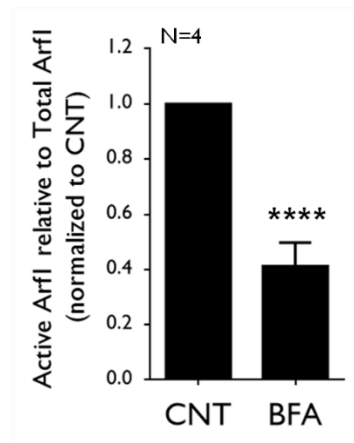
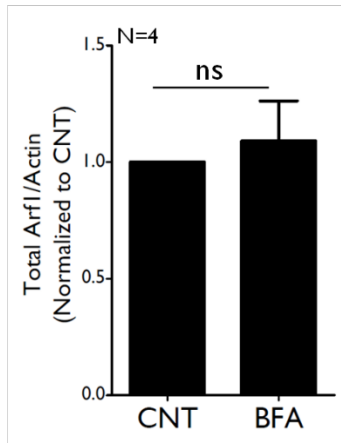
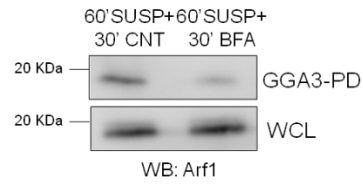
SUSPENSION (90' SUSP)

(b)

Total Arf1 levels



Active Arf1

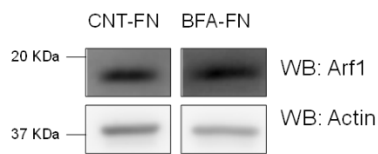


(c)

RE-ADHERENT (15' FN)

(d)

Total Arf1 levels



Active Arf1

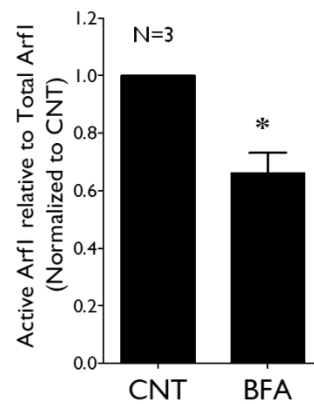
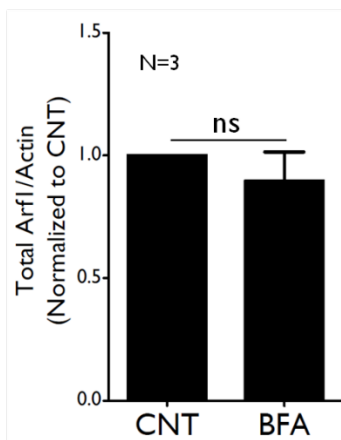
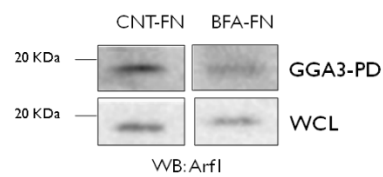


Figure 5.3 BFA inhibits Arf1 activity in suspended and re-adherent WT-MEFs (a) Western blot detection of total Arf1 and Actin in whole cell lysate (WCL) of serum-starved WT-MEFs suspended for 60 mins and additional 30 mins with DMSO (CNT) or 10 $\mu\text{g}/\text{mL}$ Brefeldin-A (BFA). The ratio of densitometric measurement of band intensities of Total Arf1/Actin are represented in the Graph represents mean \pm SE from four independent experiments. (b) Western blot detection of active Arf1 in GST-GGA3 pulldown (GGA3 PD) serum starved WT-MEFs suspended for 90 (60+30) mins either treated with DMSO (CNT) or 10 $\mu\text{g}/\text{mL}$ Brefeldin A (BFA). The graph represents mean \pm SE from four independent experiments. (c) Western blot detection of total Arf1 and Actin in whole cell lysate (WCL) of serum-starved WT-MEFs re-adherent on fibronectin for 15 mins either in presence of DMSO (CNT-FN) or 10 $\mu\text{g}/\text{mL}$ Brefeldin A (BFA-FN). The ratio of the densitometric measurement of band intensities of Total Arf1/Actin is represented in the Graph (mean \pm SE) from three independent experiments. (d) Western blot detection of active Arf1 in GST-GGA3 pulldown (GGA3 PD) serum starved WT-MEFs re-adherent on fibronectin for 15 mins either in presence of DMSO (CNT) or Brefeldin-A (BFA). Graph (mean \pm SE) from three independent experiments. Statistical analysis was done using the one sample t-test (***) p-value <0.0001, ^{ns} p = not significant).

HUMAN ENDOTHELIAL CELLS

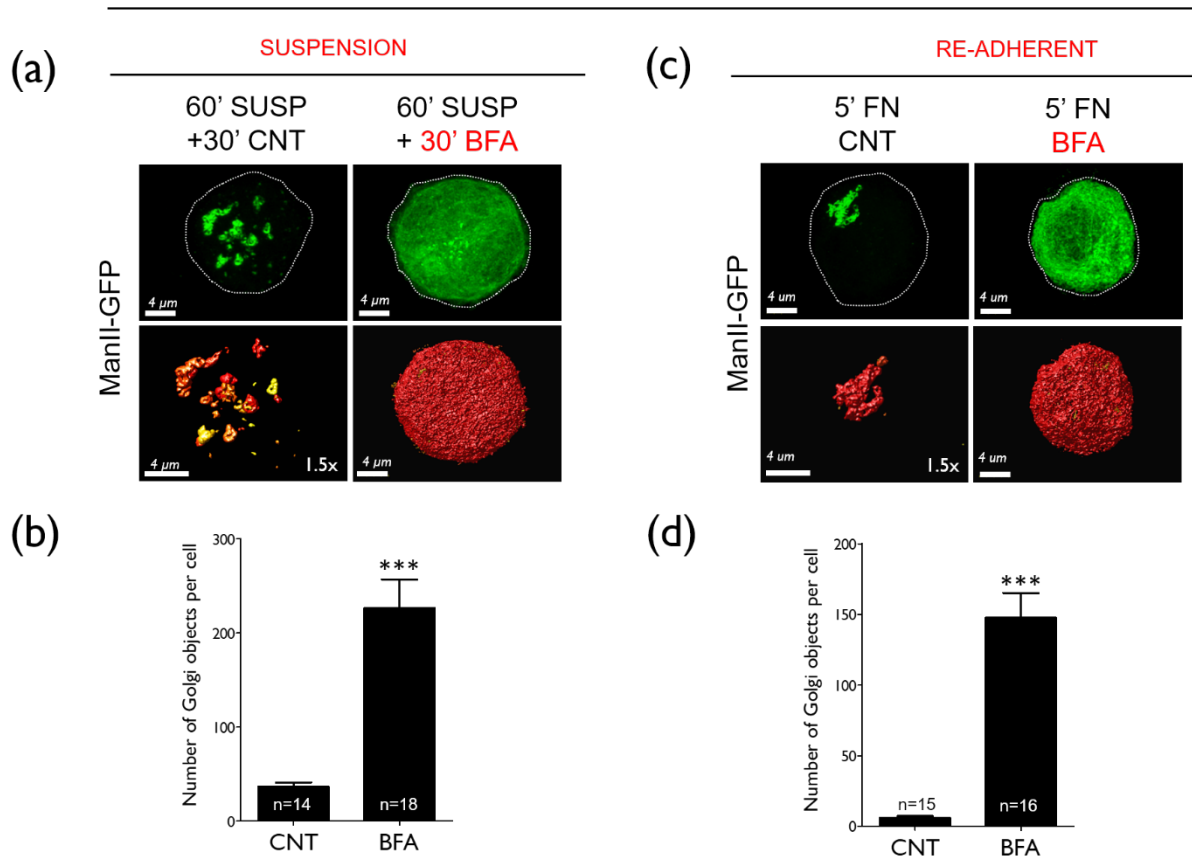


Figure 5.4 BFA mediated inactivation of Arf1 causes fragmentation of disorganized Golgi phenotype in Human endothelial cells (EA.hy926). (a) Serum-starved endothelial cells expressing cis-medial (Man II) marker were suspended for 60 mins (60' SUSP) and an additional 30 mins without treatment (+30' CNT) or treated with Brefeldin A (+30'BFA) and (c) re-plated on fibronectin for 5 mins without drug (5'FN+CNT) or with Brefeldin A (5'FN+BFA). Confocal Z stack images were deconvoluted, represented as maximum intensity projections (MIP) (top panel) and surface rendered images zoomed 1.5X for clarity (bottom panel for each cell). (b, d) Discontinuous Golgi objects per cell for Man II and GalTase were determined using the Huygens image analysis software. The graph represents mean \pm SE from 12-18 cells from three independent experiments. Statistical analysis was done using the Mann Whitney's test (***) p-value <0.0001). Scale bar in the images is set at 4 μ m.

HUMAN EPITHELIAL CELLS

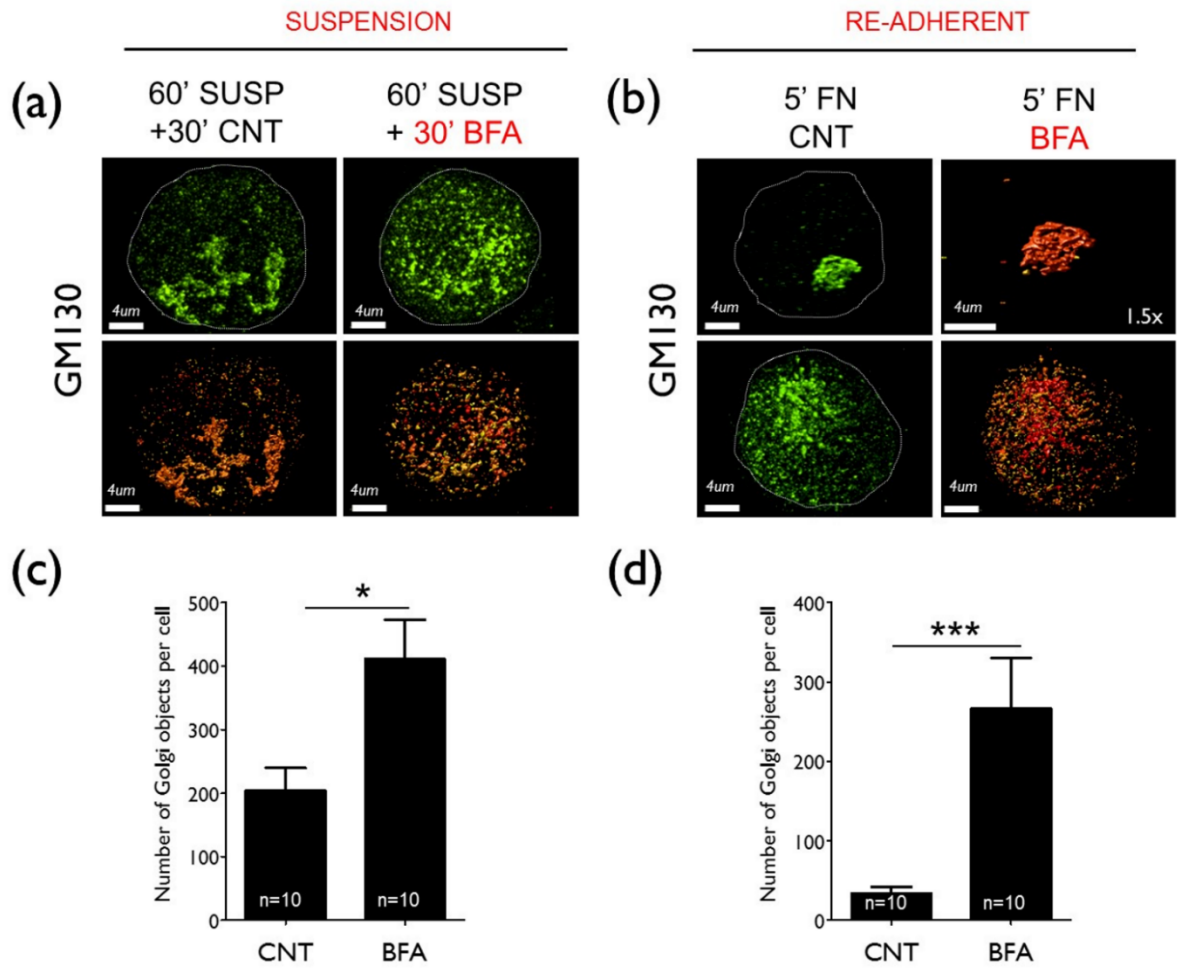


Figure 5.5 BFA mediated inactivation of Arf1 causes fragmentation of disorganized Golgi phenotype in human breast epithelial cells (MCF10A). Untransfected MCF10A cells were (a) suspended for 60 mins (60' SUSP) and an additional 30 mins without treatment (+30' CNT) or treated with Brefeldin A (+30'BFA) and (b) re-plated on fibronectin for 5 mins without drug (5'FN+CNT) or with Brefeldin A (5'FN+BFA). Cells were immunostained with anti-GM130 antibody and Confocal Z stack images were deconvoluted, represented as maximum intensity projections (MIP) (top panel) and surface rendered images zoomed 1.5X for clarity (bottom panel for each cell). (c, d) Discontinuous Golgi objects per cell for GM130 were determined using the Huygens image analysis software. The graph represents mean \pm SE from 10 cells from two independent experiments. Statistical analysis were done using the Mann Whitney's test (* p-value < 0.01, *** p-value < 0.0001). Scale bar in the images is set at 4 μ m.

5.2.3 BFA inhibited Arf1 in suspended cells causes the disorganized Golgi to fall back into Endoplasmic reticulum.

Further, it was asked what is the fate of disorganized Golgi (in suspended cells) if the Arf1 activity is inhibited by brefeldin A (BFA). It was observed that cis/medial Golgi (Man II GFP) showed very less colocalization (Pearson's coefficient) with ER (KDEL-RFP) in suspended cells (Figure 5.6 a). Microtubule depolymerization by Nocodazole, which does not affect Arf1 activity (as discussed in Chapter 4, Figure 4.13), but fragments the cis-medial disorganized Golgi further, did not cause it fall back into ER (Figure 5.6 b). However, BFA mediated inhibition of Arf1 in suspended cells caused cis/medial Golgi to completely fragment now showing a strong co-localization with the endoplasmic reticulum (Figure 5.6 c). This is reflected in a significant increase in their co-localization along line plots (Figure 5.7 a) and in cellular Pearson's coefficient of entire z-stacks (Figure 5.7 b). While on the loss of adhesion Arf1 activity drops by ~60% (relative to stable adherent cells) (Figure 4.6 b), BFA treatment of suspended cells reduces it further by ~60% (Figure 5.7 c), causing a net ~85% drop (relative to stable adherent cells). These data suggest the differential effect on Arf1 activation likely makes the loss of adhesion mediated Golgi disorganization distinctly different from BFA mediated Golgi fragmentation. This led us to ask if the loss of adhesion does affect Golgi function and how BFA treatment impacts the same, and this is discussed in Chapter 6.

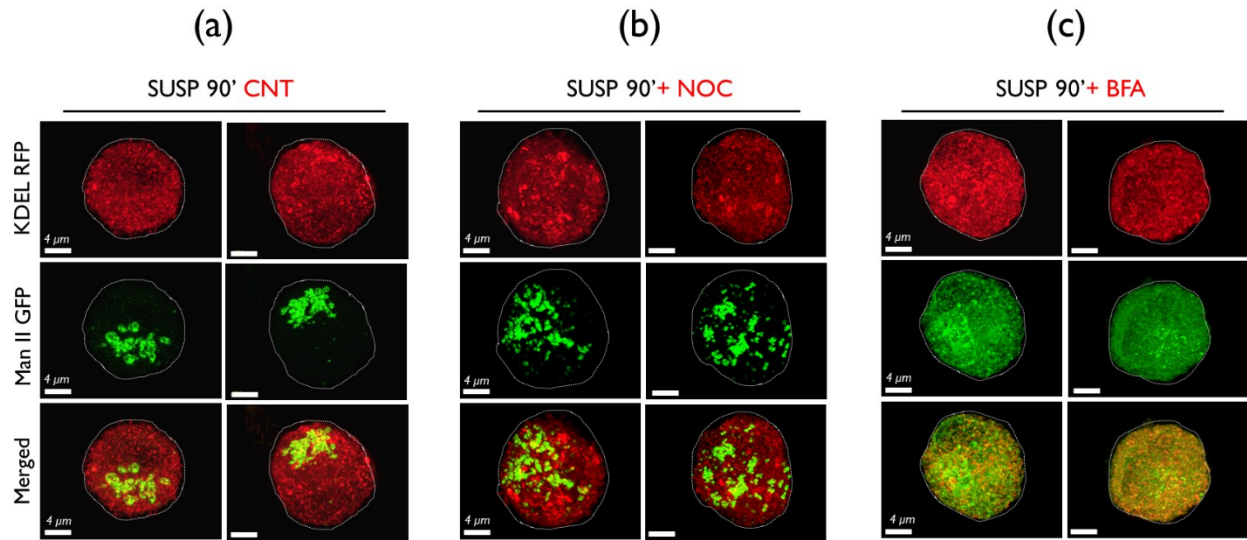


Figure 5.6 BFA mediated Arf1 inactivation causes fragmentation of disorganized Golgi and into collapses to the endoplasmic reticulum in WT-MEFs. Serum-starved WT-MEFs expressing ER marker KDEL (KDEL-RFP) and Golgi marker Mannosidase GFP (Man II GFP) were suspended for 60 mins plus additional 30 mins without **(a)** (SUSP 90' CNT) or with **(b)** Nocodazole (SUSP 90'+NOC) and **(c)** brefeldin A (SUSP 90'+BFA) and. Confocal Z stack images were deconvoluted and represented as maximum intensity projections (MIP) for ER, Golgi and merged image. Data is representative of 30 cells from three independent experiments. Scale bars in images are set at 4 μ m.

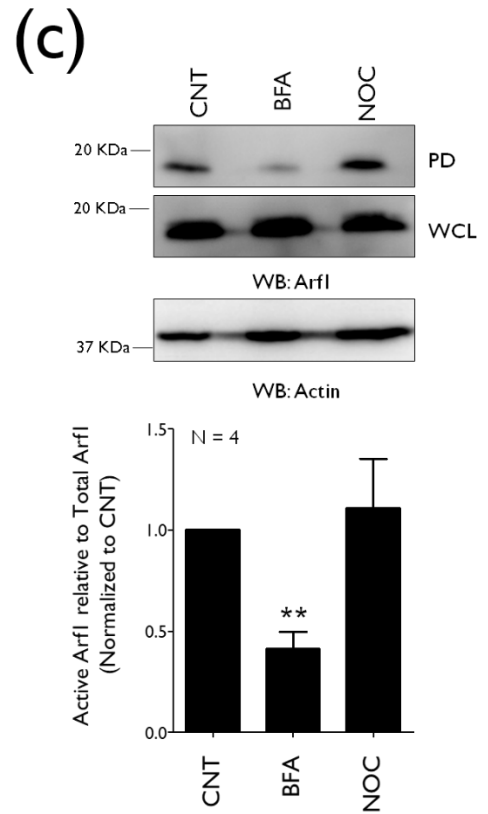
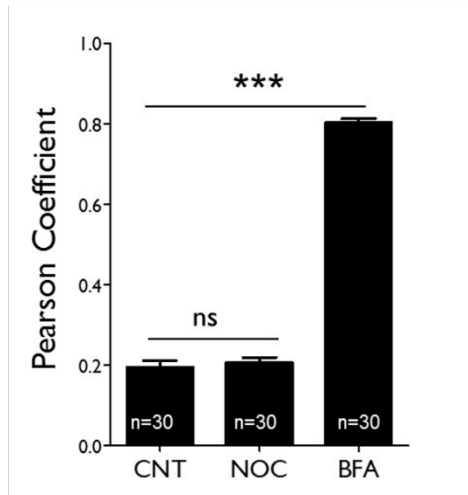
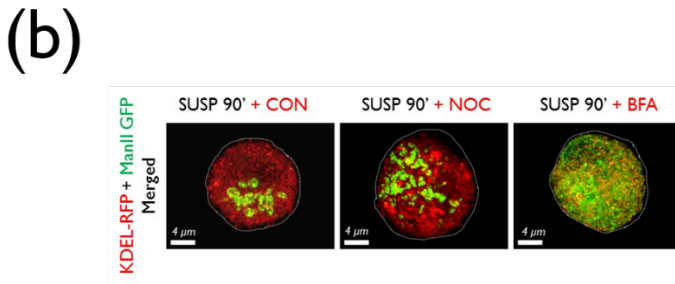
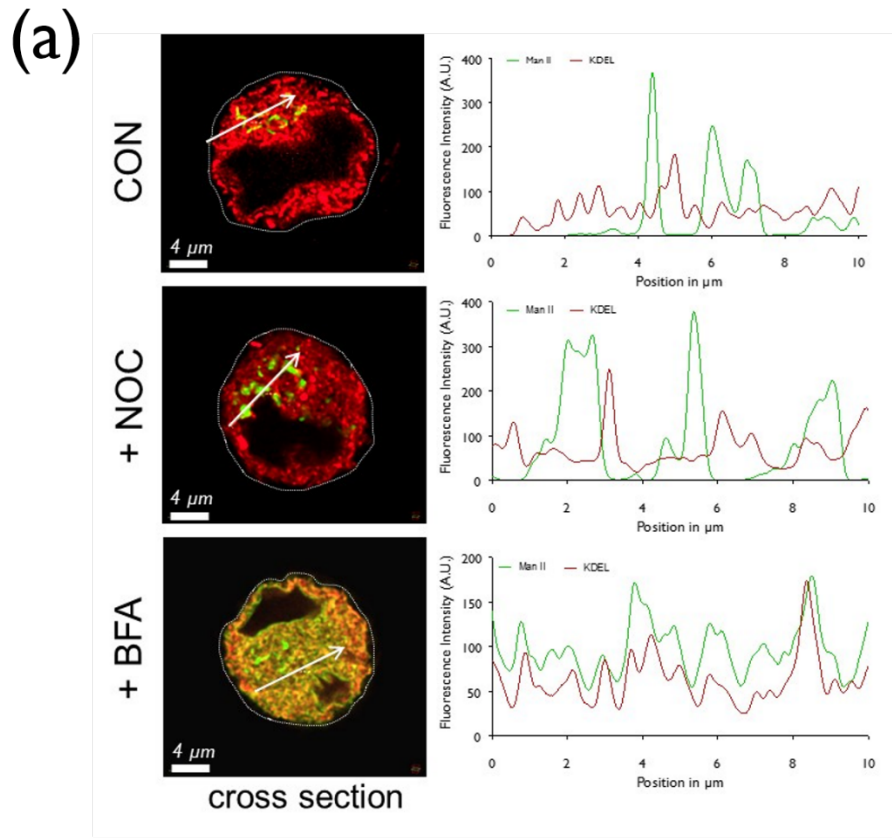


Figure 5.7 Colocalization analysis of disorganized and fragmented Golgi with ER in WT-MEFs. (a) The colocalization between ER (KDEL RFP) and cis-medial Golgi (ManII GFP) in WT-MEFs held in suspension for 90 mins without drug (CNT) and with Brefeldin (+BFA) or Nocodazole (+NOC) were compared using a line plot across the cell for each marker using Huygens image analysis software. Fluorescence intensity measurements obtained were plotted for ManII GFP (green line) and KDEL RFP (red line) and their profiles compared to CNT vs BFA /NOC treated cells. **(b)** Cells expressing KDEL-RFP and Mannosidase GFP (Man II GFP) were suspended for 60 mins (60' SUSP) plus 30 mins without (+30'CNT) or with brefeldin A (+30'BFA). Co-localization in confocal z-stack determined with Huygens software and Pearson's coefficient represented in the graph (mean \pm SE) (30 cells from three independent experiments. Statistical analysis was done using the Mann Whitney's test (*** p-value <0.0001). Scale bar in all images are set at 4 μ m. **(c)** Active Arf1 from suspended CNT, BFA, and NOC treated suspended cells pulled down by GST-GGA3 (GGA3 PD), equated to total Arf1 in whole cell lysate (WCL) and normalized to CNT. The graph represents mean \pm SE from four independent experiments. Statistical analysis was done using the one sample t-test (** p-value <0.001).

5.3 SUMMARY.

Cell-matrix adhesion regulated disorganized Golgi remains segregated from endoplasmic reticulum as a minimal overlap observed between these two compartments were observed. This is evident from quantitative measurements showing the extent of colocalization (Pearson's coefficient) and line intensity profile of cis/medial-Golgi vs. ER of suspended and re-adherent cells. Additionally, inhibition of Arf1 activity in suspended cells by BFA robustly fragments the disorganized and increases the colocalization of Golgi with ER. Also, further inhibition of Arf1 activity with BFA in suspended WT-MEF results in fragmentation of cis/medial Golgi (Man II GFP). A similar result with human foreskin fibroblast, human endothelial cells, and human epithelial cells was observed, strengthening the observation. BFA inhibited Arf1 resulted in cis-medial Golgi to fall back into endoplasmic reticulum in Mouse embryonic fibroblast cells.

Results from earlier chapters demonstrate that cis/cis-medial Golgi is partially disorganized as opposed to trans-Golgi which undergoes complete disorganization. One explanation for differential regulation by cell-matrix adhesion on "cis/cis-medial" and "trans' Golgi compartment could be because cell-adhesion regulates BIG1/2 Arf1 GEF prominently which localizes to trans-Golgi, hence inactivating Arf1 more at trans than cis-medial allowing differences in disorganization. This is supported by the fact that BFA inhibition of suspended cells (which results in almost ~85% inactivation of Arf1) caused cis-medial Golgi to completely disorganize and collapse into ER. However, more evidence is needed in support of this speculation. This further led us to ask if "disorganized Golgi" is functionally similar or dissimilar than a "fragmented Golgi" and that is discussed in the next chapter.

5.4 CONCLUSION.

Cell-matrix adhesion regulated Golgi disorganization is different from BFA mediated Golgi fragmentation phenotype and remains separate from the endoplasmic reticulum.

Chapter 6

**Study the effect of adhesion-dependent
Golgi disorganization on
Golgi function.**

6.1 RATIONALE.

A major post-translational modification of proteins and lipids that occurs in the Golgi is their Glycosylation (Wilson et al., 2011). Accurate glycosylation of proteins and lipids are vital for many cellular functions such as correct protein folding, cell signaling, immunological recognition and defense, cell adhesion and motility (Stanley, 2011). Golgi compartments host a variety of enzymes, such as glycosyltransferases, glycosidases, which carry out the transfer of glycan molecules to proteins and lipids, in an ordered manner, which eventually exits trans-Golgi network to its destination. Various reports have documented multiple factors that regulate glycosylation including the luminal Golgi environment (Golgi pH) (Kellokumpu et al., 2002; Maeda and Kinoshita, 2010), Golgi organization (Koreishi et al., 2013), expression and correct functioning of enzymes catalyzing glycosylation (Freeze and Schachter, 2009) and proteins of conserved oligomeric Golgi (COG) complex (which act as a scaffold for Golgi membrane structure and tethering of retrograde vesicles) (Pokrovskaya et al., 2011). Additionally, in many cancer types, Golgi is distinctly fragmented (Egea et al., 1993; Migita and Inoue, 2012; Petrosyan, 2015) and accompanied by altered glycosylation (increased sialylation and decreased sulfation) on the cell surface (shorter and less branched carbohydrate chains) (Petrosyan, 2015).

In summary, Golgi sorts and traffic several proteins and lipid cargoes glycosylate them and regulate their correct pick-up and delivery to different destinations within the cell, including the plasma membrane. Any change in Golgi organization due to mutation/depletion/non-

functioning of Golgi proteins in disease conditions or physiological changes like cell division affects glycosylation levels and patterns.

This study so far was focused on elucidating the role and regulation of cell-matrix adhesion-dependent Golgi organization in anchorage-dependent cell lines. With known association between Golgi organization and its function it was checked if changes in adhesion and resulting Golgi organization can affect cell surface glycosylation (known to be a direct reflection of Golgi function). Using fluorescently tagged lectin markers that bind glycosylated residues changes in cell surface glycosylation levels in non-adherent WT-MEFs by flow cytometry was examined. Using active Arf1 (that restores Golgi organization in suspended cells) it was also tested how changes in Golgi organization in non-adherent cells contribute to changes in glycosylation observed in these cells.

6.1 RESULTS.

6.2.1 Loss of cell-matrix adhesion increases global cell surface glycosylation in WT-MEFs.

Four classes of lectins were selected which display different specificity towards glycan modification on proteins such as mannose, Galactose, Sialic acid, and fucose to investigate the effect of adhesion in regulating cell surface glycosylation. Figure 6.1 a lists the fluorescently tagged lectins used in the study and their glycan specificity Concanavalin A (**ConA**) (mannose-binding), wheat germ agglutinin (**WGA**) (Galactose/N-acetylgalactosamine binding), peanut agglutinin (**PNA**) (N-acetylglucosamine binding) and Ulex europaeus agglutinin (**UEA**) (Fucose binding).

It was validated that treatment with accutase also results in similar adhesion mediated Golgi disorganization for both ManII and GalTase marker (Figure 6.1a) Cells held in suspension for 120 mins (Blue color histogram) show a significant increase in cell surface binding of all four lectins as indicated with a right shift of fluorescence intensity histograms when compared to just detached cells 5' SUSP (red color histogram) (Figure 6.1 c). This change was also quantitated and plotted as average median fluorescence intensity (black bars) relative to their basal levels when detached and normalized to 100% (grey bars) (Figure 6.1 d). An increase in surface glycosylation was observed post 120 mins suspension (~ 45% for WGA/UEA and ~100% fold for ConA and PNA. It is to this effect that a time kinetics profile of changes in ConA surface binding was compared over increasing suspension time points (5mins to 120 mins). Interestingly, on the loss of adhesion, there is subtle, but steady increase in surface

ConA binding, which peaks around 120 mins suspension (Figure 6.1 e, f). Cells treated with cycloheximide (thereby blocking protein synthesis) also showed the similar increase in ConA surface levels in 120 mins (Figure 6.1 g). This suggests a loss of adhesion promotes Golgi processing and/or trafficking to increase membrane glycosylation levels. Typically, a cargo like VSVG could take around 10-15 mins to reach plasma membrane and 150-200 mins to complete trafficking from ER to PM (Hirschberg et al., 1998). As an increase in glycosylation as early as 20 mins in suspension and also when synthesis of new proteins were blocked, it is speculated that this change is mostly coming through an increased rate of trafficking to the cell surface. Studies have shown synthesis in the ER, post-translational modification and delivery to the cell surface of a protein could take around 2 hours (Hirschberg et al., 1998).

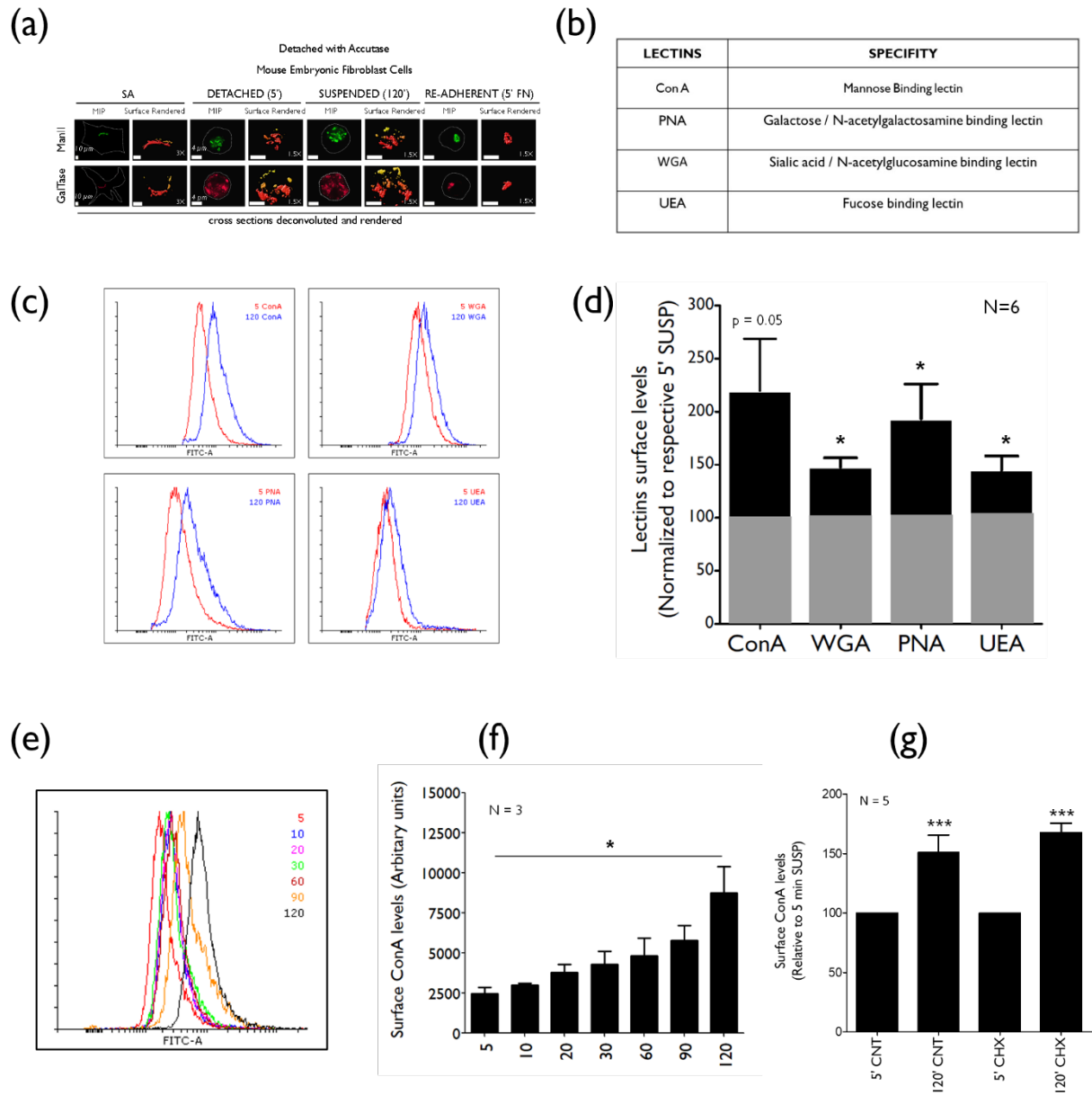


Figure 6.1 Loss of adhesion results in an increase in cell surface glycosylation. (a) WT-MEFs transiently expressing (top panel) Man II GFP and (bottom panel) GalTase-RFP were either serum starved with 0.2% FBS for 12 hours or cultured with 5% FBS. Stable adherent cells (SA) were detached with Accutase (5') and held in suspension for 120 mins (120'), and re-plated on fibronectin for 5 mins (5' FN). Cross sections of deconvoluted MIP and surface rendered images which were zoomed for clarity (3X for SA, 1.5X for other time points for Man II and GalTase) (right panel in each time point) are represented from three independent experiments. Stable adherent cells are represented by a MIP image. Scale bar in the images is 4 μ m and 10 μ m for stable adherent cells. **(b)** List of fluorescently tagged lectin probes with

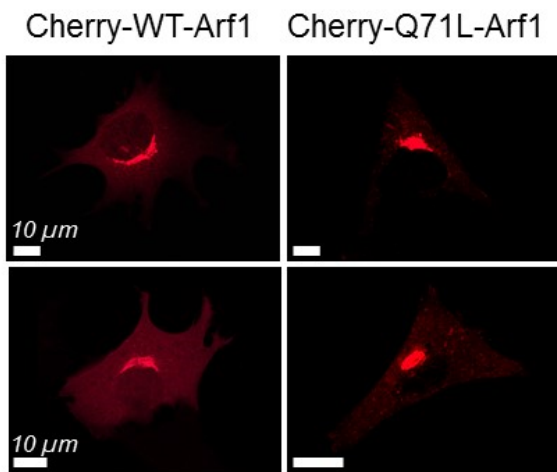
their carbohydrate specificity. Serum-starved WT-MEFs detached with Accutase (5' SUSP) and held in suspension for 120 mins (120' SUSP), labeled with Alexa-488 conjugated ConA, WGA, PNA and FITC-UEA lectin. **(c)** Cell surface-bound lectin fluorescence was measured by flow cytometry and represented as histograms. **(d)** The median fluorescence intensity of 120' SUSP cells (black bar) was normalized to their respective 5' SUSP cells (equated to 100 and represented as a grey bar). The graph represents mean \pm SE from 6 independent experiments. Statistical analysis was done using the one sample t-test (** p-value <0.001). **(e)** Serum-starved WT-MEFs were detached and labeled with ConA-Alexa-488 at 5, 10, 20, 30, 60, 90 and 120 mins. Representative histogram of flow cytometry measurements of all time points is shown. **(f)** Median fluorescence intensity is represented in the graph (mean \pm SE) from three independent experiments. Statistical analysis was done using the two-tailed Mann Whitney's test (* p-value <0.01). **(g)** Serum-starved WT-MEFs untreated (CNT) or treated with cycloheximide (CHX) were detached and labeled with ConA-Alexa-488 at 5 and 120 mins. Median fluorescence intensity is represented in the graph (mean \pm SE) from five independent experiments. Statistical analysis was done using the column statistics (***) p-value <0.0001).

6.2.2 Restoration of Golgi organization in non-adherent cells abolishes the increase in surface glycosylation.

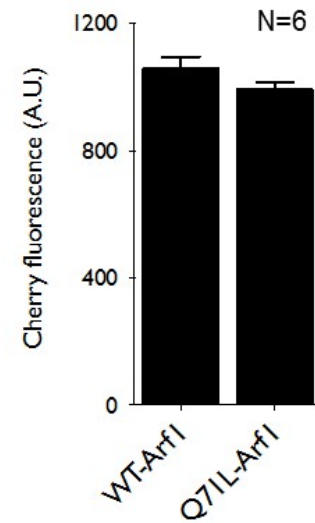
To confirm if the increase in surface glycosylation is indeed the result of the disorganized Golgi phenotype on the loss of adhesion it was tested if active Arf1 mediated restoration of Golgi organization in suspended cells could prevent this glycosylation change. Cherry tagged wild-type (WT-Arf1) and active (Q71L-Arf1) Arf1 expressing cells (Figure 6.2 a) showed comparable Arf1 expression (Figure 6.2 b) and only a modest change in basal cell surface ConA (Figure 6.2 c) and UEA (Figure 6.2 d) binding when detached (5' SUSP). This data confirms that on a similar amount of wild-type or active Arf1 exogenous expression, there is very modest, but insignificant increase in basal cell surface glycosylation (*i.e.*, 5' SUSP).

Suspended cells with active Arf1 expression did block the increase in cell surface glycosylation observed in untransfected control and WT-Arf1 expressing cells. This was seen for ConA (Figure 6.3 a-d) and UEA labeling (Figure 6.3 e-h). This strongly suggests cell-matrix adhesion-dependent regulation of Arf1 and resulting Golgi disorganization indeed affects Golgi function and net surface glycosylation levels.

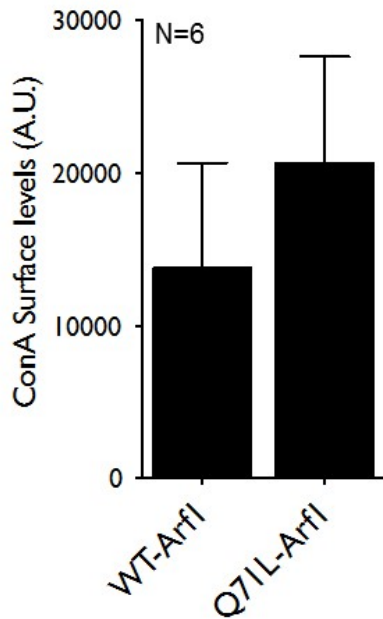
(a)



(b)



(c)



(d)

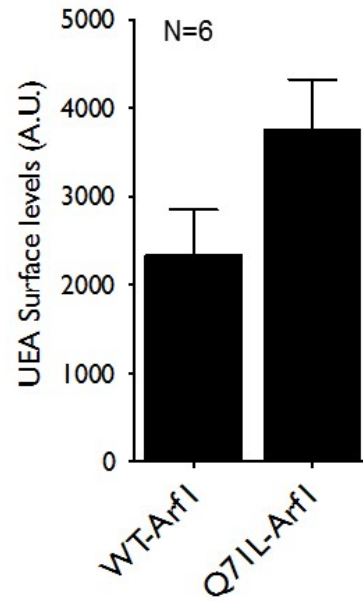


Figure 6.2 Exogenous expression of Cherry tagged Arf1 does not affect basal ConA and UEA cell surface levels. (a) The localization of Cherry tagged wild-type Arf1 (WT-Arf1) or active Arf1 (Q71L Arf1) in serum-starved WT-MEFs was confirmed. Scale bar in images set

at 10 μm . **(b)** The fluorescence intensity and hence expression of both cherry constructs in cells was analyzed by flow cytometry and average median fluorescence intensity represented as arbitrary units (A.U.) in the graph (mean \pm SE) from six independent experiments. **(c, d)** Serum-starved WT-MEFs expressing Cherry tagged wild-type Arf1 (WT-Arf1) or active Arf1 (Q71L Arf1) were detached using Accutase and surface labeled with **(c)** ConA-Alexa 488 or **(d)** UEA-FITC lectin. Fluorescence intensity of cell surface bound lectins were measured by flow cytometry in population gated for cherry tagged Arf1 expression and average median fluorescence intensity represented in the graph (mean \pm SE). Data from six independent experiments.

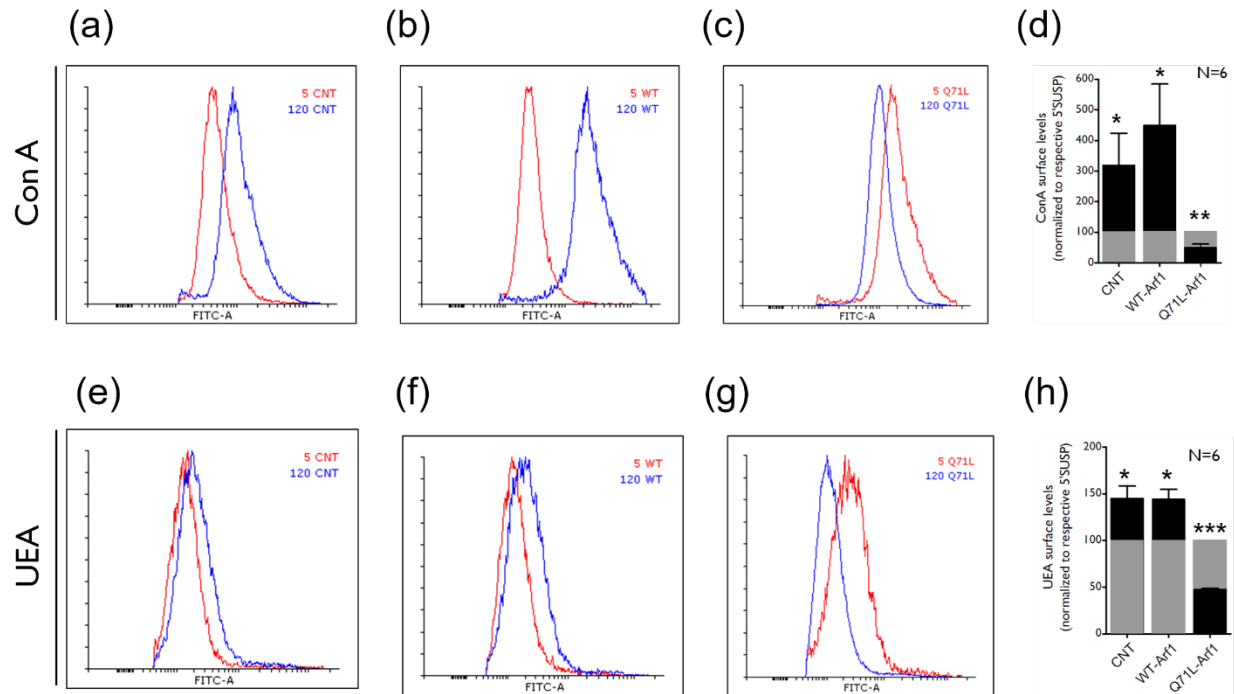


Figure 6.3 Active Arf1 rescues loss of adhesion regulated increase in cell surface glycosylation. WT-MEFs expressing (a, e) cherry-N1 (CNT), (b, f) wild-type Arf1-Cherry-N1 (WT-Arf1) or (c, g) active Arf1-Cherry-N1 (Q71L Arf1) were detached (5' SUSP) and held in suspension (120' SUSP) and labelled with (a-d) ConA-Alexa488 and (e-h) UEA-FITC. Surface-bound lectin fluorescence in cell population gated for cherry tagged Arf1 expression was measured by flow cytometry and median fluorescence intensity at 120' SUSP (black bar) normalized to their respective 5' SUSP cells (equated to 100 and represented as a grey bar). The graph represents mean \pm SE of 6 independent experiments. Statistical analysis was done using the one sample t-test (* p-value <0.01, ** p-value <0.001, *** p-value <0.0001).

6.2.3 Golgi disorganization is functionally different from Golgi fragmentation.

As described in chapter 5, cell-matrix adhesion regulated Golgi disorganization does seem to be structurally different from BFA or Nocodazole mediated Golgi breakup. It was hence asked if there is a functional difference between these as well. This was determined by treating suspended cells with BFA or Nocodazole and comparing cell surface ConA binding in these cells.

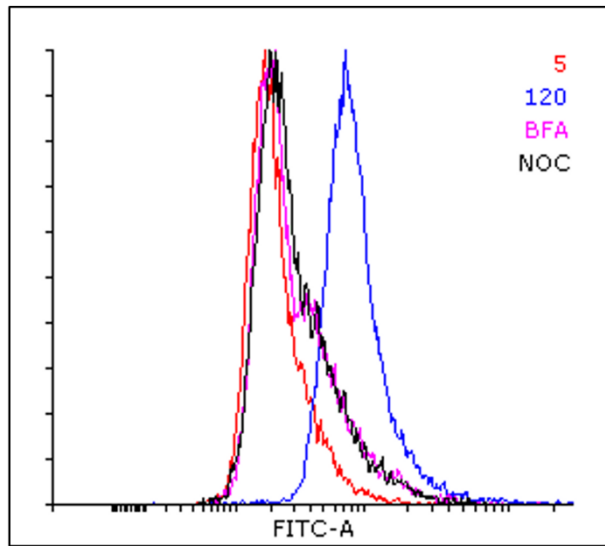
Serum-starved WT-MEFs were held in suspension for 90 mins and then either treated with DMSO (CNT) or with 10 μ M Nocodazole (NOC) or with 10 μ g/ml Brefeldin-A (BFA) for additional 30 mins. A right shift in histogram was observed between for 120' SUSP (Blue color histogram) relative to 5' SUSP (Red color histogram) in control (Figure 6.4 a). Control suspended cells for 90 mins (which showed increase in ConA surface levels relative to 5 mins) were treated with Nocodazole or BFA (after cells are held in suspension for 90 mins) resulted in reversal of increase in cell surface glycosylation. Quantitative measurement as average median fluorescence intensity displays the same observation (Figure 6.4 b).

Both BFA and NOC treatment did not freeze the cell surface glycosylation levels at what was observed after cells are suspended for 90 mins, but instead reversed the increment. This likely reflects a combined effect of the change in trafficking to the cell membrane with the rate at which surface glycosylated proteins and lipids are removed from the cell surface, possibly by their endocytosis. Loss of adhesion is known to dramatically affect endocytosis rates of plasma membrane lipids in earlier studies (Balasubramanian et al., 2007).

BFA mediated Golgi fragmentation affects Golgi trafficking (Lippincott-Schwartz et al., 1990) and hence will disrupt the delivery of glycosylated cargo to cell surface. Interestingly, BFA does not affect loss of adhesion mediated endocytosis in our studies (unpublished data). Thus a combined effect of disrupting exocytosis with continuing endocytosis could cause a drop in net surface glycosylation levels in BFA treated cells. Since both endocytosis and exocytosis are dependent on microtubule network, Nocodazole treatment will similarly disrupt exocytosis. Endocytosis from the plasma membrane does however continue in the presence of nocadazole, though this cargo stays trapped in the actin cortex (Balasubramanian et al., 2007) but is lost from the plasma membrane. This will hence (similar to BFA mediated disruption of trafficking) affect exocytosis without changing cell surface endocytosis causing a net drop in surface glycosylation levels.

Together this data does support the increase in cell surface glycosylation on the loss of adhesion to mostly likely be the result of an increase in possible rate of trafficking of cargoes to the plasma membrane and only marginally affected by an increase in actual glycosylation rates in the Golgi.

(a)



(b)

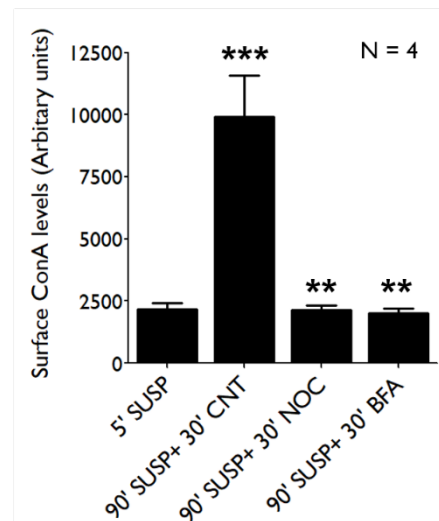


Figure 6.4 Effect of BFA and Nocodazole on non-adherent cell surface glycosylation. (a) Serum-starved WT-MEFs detached (5' SUSP) and suspended for 90 mins plus 30 mins without (90'SUSP+30'CNT) or with BFA (90'SUSP+30'BFA) or with NOC (90'SUSP+30'NOC) were labeled with ConA-Alexa 488. Representative histogram of flow cytometry measurements of all treatments. **(b)** Median fluorescence intensity is represented in the graph (mean \pm SE) from four independent experiments. Statistical analysis was done using the two-tailed Mann Whitney's test (** p-value <0.01, *** p-value <0.001).

6.3 SUMMARY.

In this chapter, it was tested how the loss of adhesion mediated Golgi disorganization regulates Golgi function, reflected in glycosylation changes. Adherent cells when detached have a basal level of surface glycosylation (detected by surface lectin binding), which increases as cells are held in suspension. This does suggest that this is not likely to be a result of the new synthesis of proteins, as on an average synthesis of protein from ER to final delivery to plasma membrane could take ~ 2 hours in a cell (Hirschberg et al., 1998). A gradual increase in cell surface glycosylation and similar increase when new synthesis of proteins were blocked could be attributed to disorganized Golgi in suspended cells triggering accelerated rate of trafficking of glycosylated proteins to the cell surface.

To gain further insights into this regulation, it was tested if active Arf1 mediated restoration of Golgi organization could influence the elevated surface glycosylation observed on the loss of adhesion. Indeed active Arf1 expressing cells with an organized Golgi when suspended did not show the increase in surface glycosylation observed in wild-type Arf1 expressing cells with a disorganized Golgi. This suggests elevated surface glycosylation to be a result of the disorganized Golgi, which could possibly be reversed by the restoration of Golgi integrity.

Next, it was demonstrated that BFA and Nocodazole mediated fragmented Golgi functions differently than a loss of adhesion disorganized Golgi. This is reflected by their ability to reverse the increase in surface glycosylation. BFA mediated inhibition of Arf1 disrupts the trafficking between Golgi-ER and leading to its restoration to the ER. This suggests disorganized or fragmented Golgi could have a differential function in the cell as

demonstrated by differences in surface glycosylation. Trafficking of cargoes will dramatically slow down if microtubule network is absent in a cell, and hence Nocodazole-treated cells display less surface glycosylation. As both BFA and NOC treatment resulted in a reversal of the increased glycosylation from the cell surface, it strongly suggests that loss of cell-matrix adhesion triggers exocytosis to the cell surface. This could further be supported by the dramatic endocytosis that loss of adhesion is known to support (del Pozo et al., 2005) which is not affected by microtubule disruption (Balasubramanian et al., 2007) or BFA treatment (unpublished data). Results from Chapter 5 and 6 hence do provide evidence that adhesion mediated Golgi disorganization is structurally and functionally different from BFA mediated Golgi fragmentation

6.4 CONCLUSION.

Loss of adhesion mediated Golgi disorganization affects cell surface Golgi glycosylation.

Chapter 7

Study Adhesion dependent regulation of Golgi organization in anchorage-independent cancer cells.

7.1 RATIONALE.

Cultured cancer cells exhibit anchorage-independent growth, and can proliferate in the absence of adhesion to extracellular matrix (Schwartz, 1997). The colony forming capacity in the semi-solid medium of cancer cells have been linked to *in vivo* tumorigenic and metastatic potential and is utilized as a marker for *in vitro* transformation (Mori et al., 2009). Among other variety of ways, anchorage-independent activation of specific pathways is employed by cancer cells to proliferate in an anchorage-independent manner (Freedman and Shin, 1974). Furthermore, reports from our lab have shown that cell-matrix adhesion regulates Arf6 and RalA/B signaling pathways in anchorage-dependent mouse fibroblast, that is deregulated in bladder cancer cells T24 to regulate Erk signaling and attaining anchorage-independence (Pawar et al., 2016).

Furthermore, Golgi fragmentation has been reported during many physiological and pathological conditions, although the exact mechanism and significance of this breakup remains particularly unclear in disease conditions (Machamer, 2003; Nakagomi et al., 2008; Petrosyan, 2015). Presence of a fragmented Golgi was reported quite some time back in electron microscopic images of cultured mucin-producing colon cancer cells (Egea et al., 1993). Furthermore, in cancer cells fragmentation of Golgi has also been correlated with mislocalization of the glycosyltransferase, thus, leading to the formation of cancer-specific epitopes (Petrosyan et al., 2014).

Having established the presence of an adhesion-Arf1-Golgi pathway in normal mouse fibroblasts that controls Golgi function, next it was investigated if adhesion-Arf1 pathways exist/de-regulated in cancer cells and if it has any role in Golgi organization.

To test this Golgi organization in cancer cell lines of different origin were screened. pancreatic cancer cell lines Mia-PaCa-2 and CFPAC-1, fibrosarcoma cell line HT-1080 and bladder cancer cell line T-24 were used for the studies. Golgi organization was visualized with a trans-Golgi marker and all the studies were done in presence of serum growth factors.

7.2 RESULTS.

7.2.1 Golgi organization in cancer cell lines.

In adherent conditions pancreatic cancer cell lines Mia-PaCa-2 and CFPAC-1, fibrosarcoma cell line HT-1080 cancer cell lines showed a fragmented Golgi which is completely dispersed throughout the cell (Figure 7.1 top 3 panels). However, one of the cancer cell line tested, bladder cancer cell line (T24), displayed an organized Golgi (Figure 7.1 bottom panel). This led us to ask if the adhesion-dependent regulation of the Golgi observed in mouse fibroblasts exists or it is deregulated in these cells. In non-adherent conditions, the disrupted Golgi phenotype in Mia-PaCa-2 and CFPAC-1, fibrosarcoma cell line HT-1080 cancer cell lines was retained (Figure 7.2). T24 cells which interestingly had an organized Golgi when adherent, failed to disorganize their Golgi when detached and held in suspension. The data in MEFs had revealed cell-adhesion regulates Arf1 activity to control Golgi organization (Refer chapter 4). Additionally, it's reported from our lab that in T24 cells Arf6 is activated in an anchorage-independent manner (Pawar et al., 2016) which is regulated by cell-matrix adhesion in MEFs (Balasubramanian et al., 2007). These led us to test if the activation status of Arf1 in adherent vs non-adherent T24 cells is deregulated to achieve its anchorage independent Golgi phenotype.

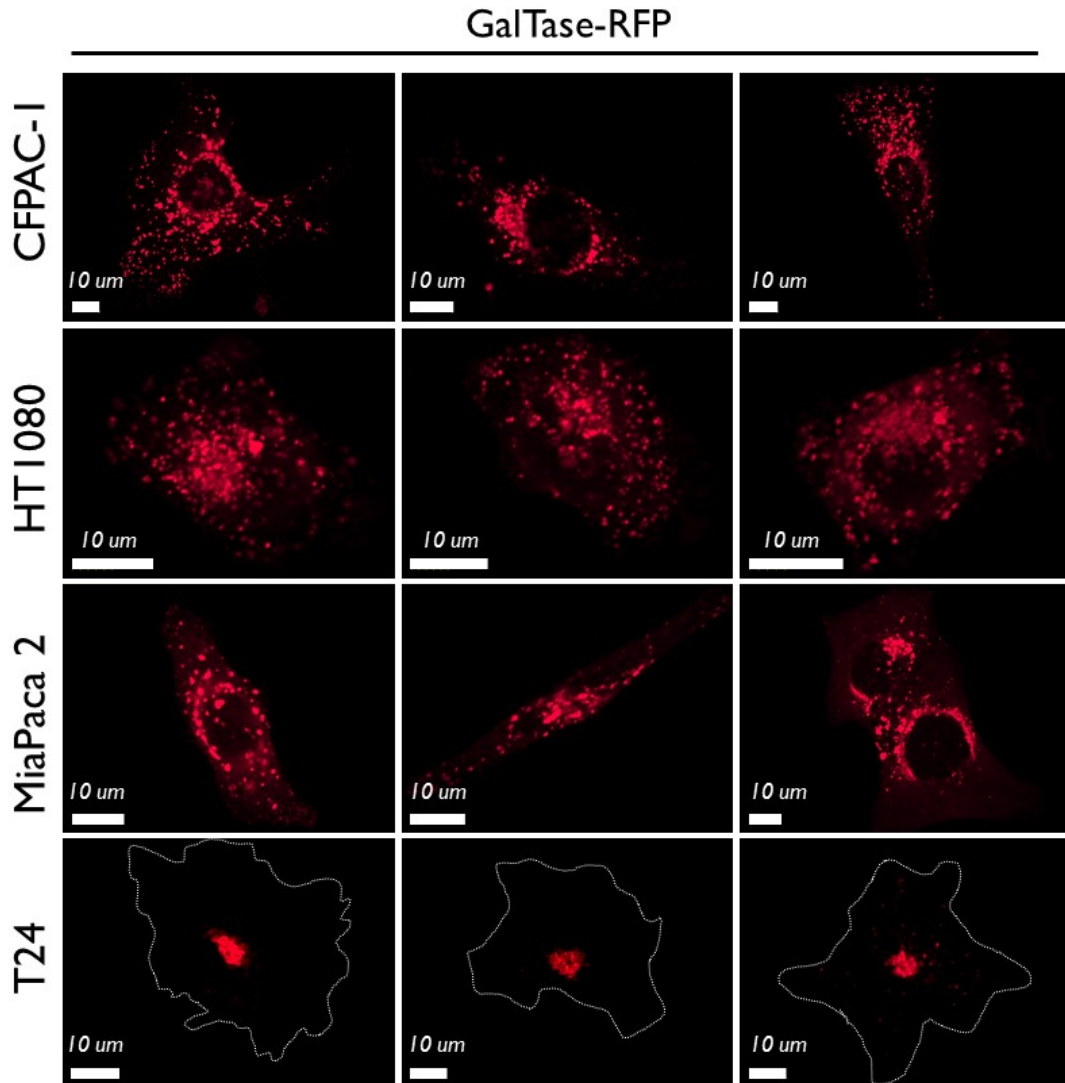


Figure 7.1 Golgi organization in adherent cancer cell lines. Three Representative images demonstrating organization of Golgi by expressing GalTase-RFP in pancreatic cancer cell lines Mia-PaCa-2 and CFPAC-1, fibrosarcoma cell line HT-1080 and bladder cancer cell line T-24. Scale bar in all the images is set to 10 μ m.

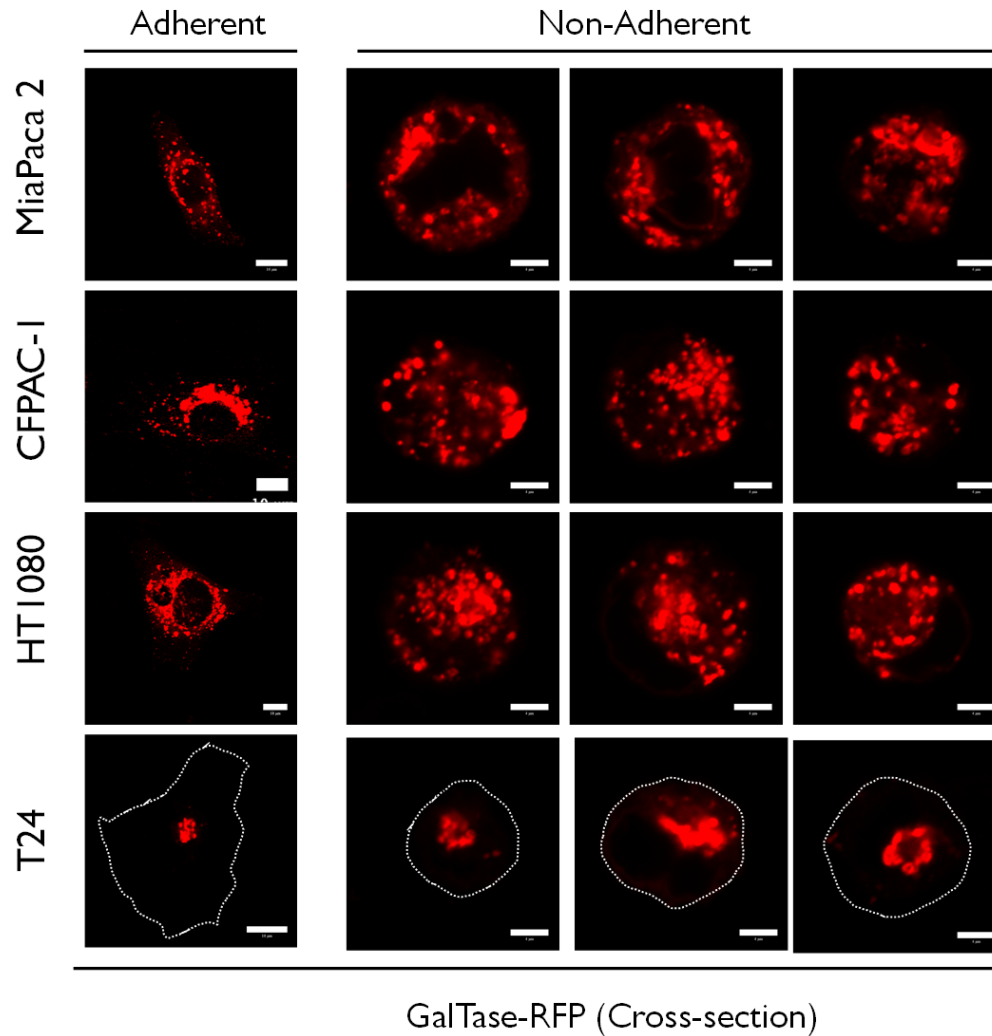


Figure 7.2 Golgi organization is anchorage-independent in cancer cell lines. Representative images demonstrating organization of Golgi in adherent and non-adherent cells by expressing GalTase-RFP in pancreatic cancer cell lines Mia-PaCa-2 and CFPAC-1, fibrosarcoma cell line HT-1080 and bladder cancer cell line T-24. Scale bar in all the images is set to 10 μm for adherent and 4 μm for non-adherent.

7.2.2 Anchorage-independent activation of Arf1 retains an organized Golgi in non-adherent T24 cells.

Anchorage-independent activation of Arf1 in T24 cells was detected, as pulled down active Arf1 did not show any change when the cells were held in suspension (Figure 7.3 a). Further examination of 3D reconstitutions demonstrating organization of Golgi in non-adherent T24 cells was done and it was observed that Golgi remains organized. This was unaffected when the cells were re-plated on fibronectin (Figure 7.3 b). Based on our observation in MEFs and T24 cells it's a speculation that anchorage independence of Arf1 activation in T24 cells is the cause of Golgi retaining its structural identity in non-adherent cells.

In order to elucidate the role of Arf1 in the anchorage-independent Golgi organization, Arf1 activity was inhibited by Brefeldin-A (BFA) and Golgicide-A (GCA). Remarkably, inhibition of Arf1 by both BFA (Figure 7.4 b) and GCA (Figure 7.4 c) activity indeed resulted in Golgi to disorganize in the anchorage-independent T24 cells. Also, the effect of these inhibitors was similar (Figure 7.4 d, e), shifting the distribution profile to ~90 % of the cell population with disorganized Golgi in non-adherent T24 cells. As there was similar extent of change in distribution profile with BFA and GCA, both BIG1/2 and GBF1 plays a role in keeping Arf1 active in an anchorage-independent manner in T24 cells.

Arf1 was also inhibited by expressing GFP tagged dominant negative Arf1 mutant (T31N-Arf1-GFP) and found that cells expressing this mutant have a disorganized Golgi, while untransfected cells in the same frame retain organized Golgi in non-adherent T24 cells (Figure 7.5 a, b).

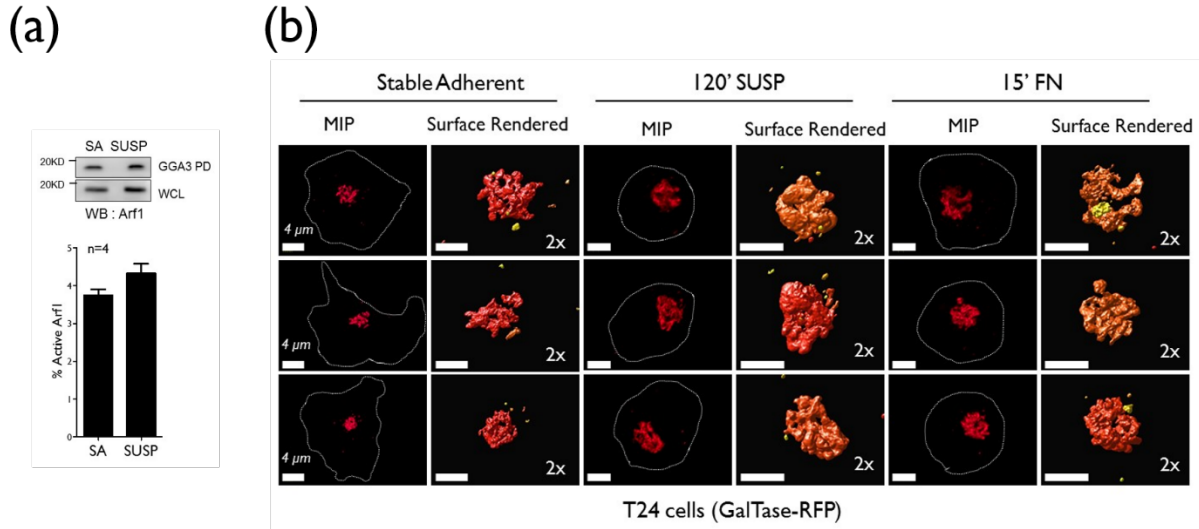


Figure 7.3 Anchorage-independent activation of Arf1 retains an organized Golgi in non-adherent T24 cells. (a) Western blot detection of active Arf1 in GST-GGA3 pulldown (GGA3 PD) and total Arf1 in whole cell lysate (WCL) of T24 stable adherent (SA) and suspended for 120 mins (SUSP). Graph represents mean \pm SE from four independent experiments. (b) T24 cells transfected with GalTase-RFP were detached and held in suspension for 120 mins (120' SUSP) and re-plated on fibronectin for 15 mins (15' FN) or 4 hours as stable adherent (SA). Their trans-Golgi was detected using the GalTase RFP localization (GalTase). Maximum intensity projections (MIP) of de-convoluted confocal images for three representative cells for GalTase for each time point are shown (left panel in each time point). De-convoluted confocal Z stacks were surface rendered and zoomed for clarity (2X) (right panel in each time point). All scale bars in images are set at 4 μ m.

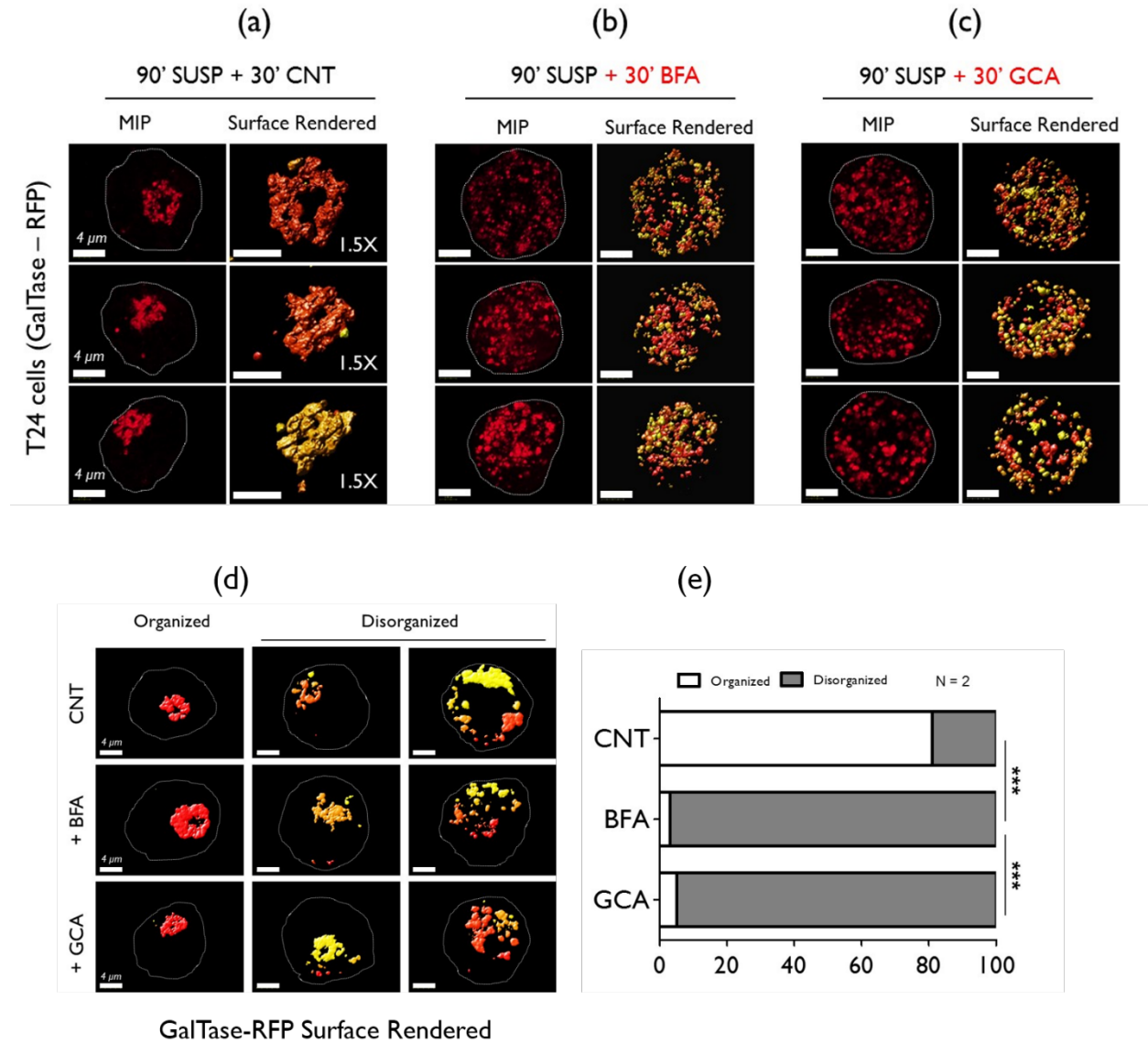


Figure 7.4 Brefeldin-A or Golgicide-A mediated Arf1 inactivation causes Golgi disorganization in the non-adherent T24 cell line. T24 cells expressing trans Golgi (GalTase) marker were suspended for 90 mins (60' SUSP) and an additional 30 mins without treatment (a) (90' SUSP+30' CNT) or treated with Brefeldin A (b) (90' SUSP+30'BFA) or (c) Golgicide A (90' SUSP+30'GCA). Confocal Z stack images were deconvoluted, represented as maximum intensity projections (MIP) and surface rendered images zoomed 1.5X for clarity (only for CNT). (d) The percentage distribution of cells with organized and disorganized Golgi phenotypes in T24 cells expressing GalTase RFP suspended for 90 mins and an additional 30 mins without (CNT) or with brefeldin A (+BFA) or Golgicide A (+GCA). Representative surface rendered cross section images for the organized and disorganized phenotype at each treatment are shown. (e) 100 cells were counted for each time point in an

experiment. Graph represents mean percentage distribution for each phenotype of one of the two comparable independent experiments. Statistical analysis comparing the change in distribution profile was done using the Chi-Square test, two-tailed (***) p-value < 0.0001). Scale bar in all images are set at 4 μ m.

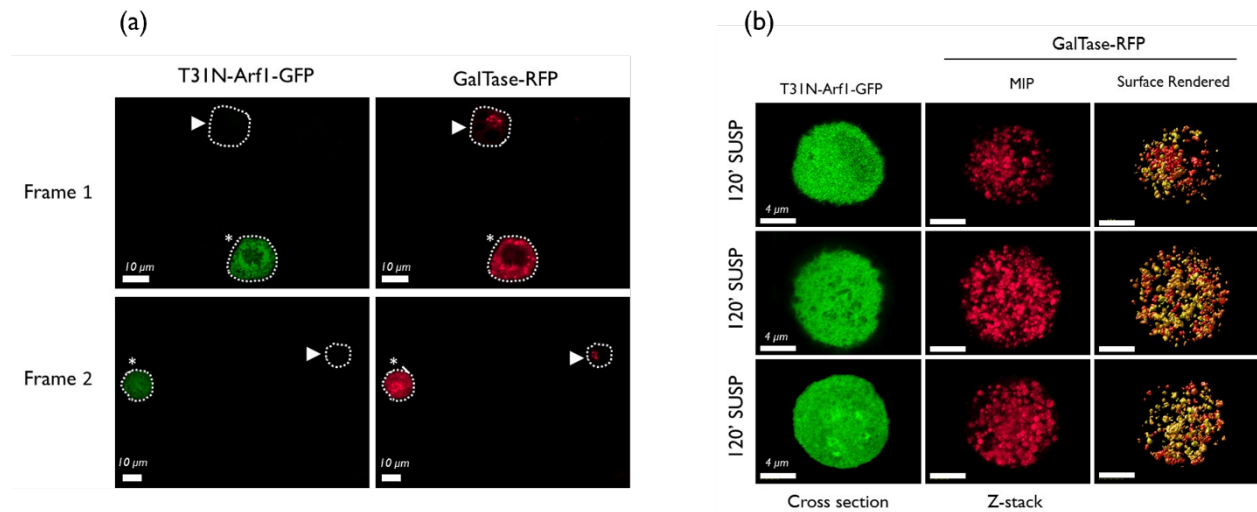


Figure 7.5 Dominant negative T31N-Arf1-GFP causes Golgi disorganization in the non-adherent T24 cell line. T24 cells expressing trans-Golgi (GalTase-RFP) and GFP tagged dominant negative Arf1 mutant (T31N-Arf1-GFP) were suspended for 120 mins. **(a)** Arrowheads highlight non-adherent T24 cells with organized Golgi phenotype present in untransfected cells; Asterisk indicates the disorganized Golgi morphology present in T31N-Arf1-GFP transfected cells. Scale bars in the images are set at 10 μ m. **(b)** Confocal Z stack images were deconvoluted, represented as maximum intensity projections (MIP) and surface rendered images for Golgi (GalTase-RFP). T31N-Arf1-GFP expression in the same cells is also shown. Images are representative of 30 cells from three independent experiments. Scale bar in all images are set at 4 μ m.

7.3 SUMMARY.

Cancer cells have the ability to grow and proliferate in an anchorage-independent manner, and thereby keep many pathways active even when the cells are not adherent. This property is utilized by cancer cells during tumorigenesis and metastasis. Furthermore, many cancer cells display a fragmented Golgi, although the mechanism remains largely unexplored. Knowing the existence of an adhesion-Arf1-Golgi pathway in anchorage-dependent mouse embryonic fibroblasts, it was then asked if this regulatory pathway exists in cancer cells and whether it is de-regulated. It was observed that MiA-PaCa-2, CFPAC-1, and HT-1080 cancer cells have a fragmented Golgi in adherent state and also retain this organization when non-adherent. However, in T24 bladder cancer cells, the Golgi is seen to be organized when adherent and non-adherent suggesting it is able to bypass the anchorage-dependent regulation of the Golgi seen in normal WTMEFs. Anchorage-independent activation of Arf1 is responsible for this Golgi phenotype in non-adherent T24 cells. This further supports the adhesion-Arf1-golgi pathway, by highlighting how a cancer cell is able to use anchorage independent Arf1 activation to bypass this regulation. Understanding how cancer cells mediate this activation of Arf1 and the functional significance of this deregulation is an open question the lab is now trying to address.

7.4 CONCLUSION.

Stable adherent T24 cells with an organized Golgi use anchorage-independent active Arf1 to overcome the loss of adhesion mediated Golgi disorganization.

Chapter 8: Discussion

The work presented in this thesis discusses a novel regulation by cell-matrix adhesion in regulating Golgi organization and function, in anchorage-dependent mouse embryonic fibroblast cells. These findings will have implications for the regulation of Golgi organization in various cellular events, such as mitosis, as well as in disease conditions like cancer.

8.1. A novel regulation of Golgi organization by cell-matrix adhesion.

Extracellular matrix (ECM) is a complex mixture of glycoproteins (fibronectin, collagen, laminins etc.) and non-matrix protein that include growth factors present in all tissues and organs (Hynes, 2004). Integrins are the primary cell-matrix adhesion receptors that mediate signal transduction and thereby controls cell attachment, spreading, proliferation, cytoskeletal organization, membrane trafficking (endocytosis and exocytosis), and also plasma membrane order (Balasubramanian et al., 2007b; Caswell et al., 2009; Huttenlocher and Horwitz, 2011). Cell-matrix has been implicated in regulating many cellular events like cell division (LaFlamme et al., 2008a), apoptosis (Meredith and Schwartz, 1997), and pathological conditions like cancer (Desgrosellier and Cheresch, 2010) and neurodegeneration (Wu and Reddy, 2012). Interestingly, in these cellular processes changes in Golgi organization leading to its fragmentation is observed and thought to contribute to its regulation and function. This regulation of Golgi organization is at times reversible or irreversible.

This thesis discusses a regulatory crosstalk between cell-matrix adhesion and Golgi organization and its functional consequence in normal mouse embryonic fibroblasts and other anchorage-dependent cell lines.

Detachment of serum-starved anchorage-dependent mouse embryonic fibroblast cells from the extracellular matrix results in rapid disorganization of Golgi (cis, cis-medial and trans-Golgi). This regulation was also observed in human fibroblast, human endothelial, human breast epithelial cells. This process was found to be reversed rapidly, 5-10 mins of re-adhesion to ECM, driving Golgi re-organization. The rapid nature of this regulation on re-adhesion of suspended cells to fibronectin in the absence of serum growth factors supports a role for integrin-mediated adhesion in mediating the same. Furthermore, a small amount of integrin clustering/activation by fibronectin-coated beads (and not poly-L-Lysine coated beads) on non-adherent MEFs also rescues Golgi integrity, establishing this regulation. Although extreme end points of adhesion, loss of adhesion and re-adhesion was studied to establish the phenotype, this pathway could be controlled by the extent of adhesion and the effect this could have on Golgi organization. While this remains to be tested but could mean that changes in adhesion may reflect on Golgi organization status and hence function.

Integrin-ligand binding has been classified into different groups, based on the type of molecular interaction (RGD, Collagen, Laminin-binding integrins). Fibronectin binds to following integrins ($\alpha 2\beta 1$, $\alpha 3\beta 1$, $\alpha 4\beta 1$, $\alpha 4\beta 7$, $\alpha 5\beta 1$, $\alpha 8\beta 1$, $\alpha v\beta 1$, $\alpha v\beta 3$, $\alpha v\beta 5$, $\alpha v\beta 6$, $\alpha v\beta 8$, $\alpha IIb\beta 3$) to mediate signaling downstream of the cell (Hynes, 1987; Plow et al., 2000). It will be important to study which integrin(s) play a significant role in the adhesion-Golgi pathway. Furthermore, investigating how other extra-cellular matrix proteins regulate Golgi organization becomes an interesting open question.

So far the hypothesis was tested in 2-dimensional (2D) cell cultures, however, in physiology cells experience 3-dimensional microenvironment. Additionally, integrin engagement and downstream signaling pathways are known to be different in cells which are embedded in a 3D matrix as compared to a 2D microenvironment (Baker and Chen, 2012). Hence, comparing 2D and 3D micro-environment on the role of adhesion in regulating Golgi organization remains will provide an important insight into how this pathway and its role in vivo.

In physiology indeed many cellular responses affect the organization of the Golgi, but cell-adhesion to extracellular matrix being able to regulate an organelle like the Golgi could have implications for various secretory and trafficking pathways involved in physiological processes that are particularly regulated by adhesion. Cell division is one such cellular event where Golgi fragmentation has been studied in detail (Colanzi and Corda, 2007; Colanzi et al., 2003) and is also seen to be affected by cell adhesion (LaFlamme et al., 2008b). Mitotic Golgi fragmentation is a reversible stepwise disassembly-reassembly process which enables its inheritance into newly formed daughter cells and also acts as a checkpoint for cell-cycle progression (Corda et al., 2012). Independent researchers have contributed to finding the regulators that drive Golgi fragmentation during mitosis, which includes Membrane fission molecules (CtBP/BARS), kinases (Cdk1, MEK1, ERK, and Plk1) (Preisinger et al., 2005), which act on Golgi structural proteins like (GRASP-55/65) (Tang et al., 2010) and GM130 (Marra et al., 2001). Small GTPase Arf1 has been implicated in dissociation of Golgi matrix proteins leading up to disassembly of Golgi stack (Altan-Bonnet et al., 2003). Furthermore, dividing adherent cells undergo “mitotic cell rounding” in which a flat interphase cell adopts

a spherical shape during mitosis. De-adhesion (loosening of cell-substrate connection) and increase in RhoA (GTPase) activity results in cell cortex retraction and rigidity leading up to actin re-arrangement in the cell when it enters a mitotic phase (Maddox and Burridge, 2003; Théry and Bornens, 2008).

Taken together cell rounding precede Golgi fragmentation during cell division. This study that adhesion regulates Golgi organization when considered with the observation of mitotic cell-rounding and Golgi fragmentation during mitosis, supports the possibility that changing cell-matrix adhesion that controls rounding of cells could support Golgi disorganization to leading eventually to Golgi fragmentation. In future, investigating role and regulation of different classes of integrins (and their ligand) during cell division in regulating Golgi organization becomes an open question in the field.

8.2 Adhesion-dependent differential regulation of the cis vs trans-Golgi.

The major criterion for differentiating Golgi compartments into cis, cis-medial and trans has been the polarized distribution of Golgi processing enzymes residing at a specific location within a stack (Stanley, 2011). Further, differences in morphological and protein/lipid composition between cis vs. medial vs. trans-Golgi-compartment has been demonstrated (Klumperman, 2011). Small GTPase and their regulators also show differences in their cis vs trans Golgi localization (Baschieri and Farhan, 2012). Although dynamic intra-Golgi traffic is noted, little is known about the differential regulation of these compartments. A challenge in studying this crosstalk in live cells has been the proximity in which these compartments sit in live cells.

While establishing the regulatory role of adhesion on Golgi organization, a differential effect on the cis/cis-medial and trans-Golgi was observed. In response to the loss of adhesion, trans-Golgi seems to disorganize significantly more than cis or cis-medial Golgi. Earlier reports with BFA induced Golgi fragmentation in adherent cells (Alcalde et al., 1992) describes trans-compartment takes more time to completely fragment, while the presence of re-assembled cis/medial structure was necessary for trans-Golgi to start re-constructing on the removal of BFA (Alcalde et al., 1992)s. These studies indicate that cis/medial compartment could act as a template for reassembly of a trans-compartment. However, the presence and reason for such differential regulation in a cellular context remain unexplored.

While such a regulation by a physiological cue remains largely unknown, our observations reveal cell-matrix adhesion by differentially affecting the cis/cis-medial and trans-Golgi could hence provide a system to visualize them as distinct compartments by diffraction limited confocal imaging. This could hence allow us now to study differential role cis vs trans-Golgi compartments could play in trafficking and processing in a cell. Reorganization of both cis and trans-Golgi on re-adhesion occur rapidly, however, there is a subtle difference in their kinetics of re-organization.

Cis, medial and Trans-Golgi maintains polarity which is necessary for stepwise trafficking and processing of cargo through these sub-compartments for efficient delivery and sorting (Glick and Luini, 2011; Rios and Bornens, 2003; Rodriguez-Boulan and Musch, 2005; Stanley, 2011). An important question then such differentially disorganized Golgi

compartments raises would be, if and how their functional polarity is affected by this disorganization in non-adherent cells?

Cell-matrix adhesion (through integrins) controls cell migration in normal and disease condition through a continuous formation and disassembly of focal adhesion complexes and cytoskeletal rearrangements (Huttenlocher and Horwitz, 2011). Furthermore, the positioning of Golgi near centrosome-based microtubule organizing center (MTOC) is a dynamic process which is regulated during the process of cell migration (Yadav and Linstedt, 2011). This study do raise the question if adhesion-Golgi pathway could contribute to regulating the Golgi organization and possibly function in a migrating cell.

8.3 Regulators of the adhesion-dependent Golgi organization.

As discussed previously different class of proteins is required for maintaining Golgi organization which includes cytoskeleton, associated motor proteins, Golgi matrix proteins, and Small GTPases. After establishing the rapid and reversible regulation cell-matrix adhesion have on the Golgi organization, regulation of this pathway was investigated. As a first step, it was probed and found that no significant differences in the structural arrangement of the microtubule, actin networks, and centrosome between suspended and re-adherent cells. Furthermore, studies involving depolymerization of microtubule revealed that adhesion-Golgi pathway works along with an intact microtubule network. However, an intact actin network is not a necessary requirement for this regulation. It was also noticed that in the absence of intact microtubule network, cis/cis-medial Golgi opened up further in a suspended

cell. On re-adhesion to fibronectin, both cis-medial and trans-Golgi re-organization was not supported in the absence of microtubule network.

As adhesion controls Golgi organization very rapidly it suggests that these Golgi objects likely stay associated with the microtubule network and hence disorganize and re-organize quickly. Additionally, there could also be a possibility that there exists a differential active regulation by microtubule network through motor proteins of the cis/medial vs trans-Golgi compartment, resulting in a difference in their extent of disorganization.

Depolymerization of actin and suppression of associated proteins (m-Dia1, cortactin, Myosin18A) causes Golgi compaction (Gurel et al., 2014). It has been speculated that actin and associated protein provide a tensile force and help expand Golgi, hence depolymerization results in compaction of the organelle. Also, Arp2/3 and myosin II play a role in transport and sorting of vesicles from TGN, which gets affected by actin-disrupting agent (Gurel et al., 2014). Our findings are in agreement with the previously reported role of depolymerization of microtubule (fragmentation of Golgi) (Sandoval et al., 1984) and actin network (compaction of Golgi) (Egea et al., 2006; Valderrama et al., 1998) in maintaining Golgi organization. Rapid nature of disorganization and re-organization as a result of loss/gain of adhesion indicates that disorganized Golgi objects are actively regulated by microtubules.

Next, the molecule that could be working downstream of cell-matrix adhesion was explored. Arf1, Class I small GTPase, localized on Golgi membranes when in active GTP bound state, is an important regulator of Golgi organization during mitosis and in retrograde trafficking

(D'Souza-Schorey and Chavrier, 2006; Donaldson et al., 2005). There is evidence describing inactivation of Arf1 and hence dissociating from Golgi membranes leads to mitotic Golgi fragmentation (Altan-Bonnet et al., 2003). Based on this literature and also on the fact that adhesion does regulate the activity of a member of Arf superfamily, Arf6 (Balasubramanian et al., 2007b), the possibility of Arf1 working downstream of cell-matrix adhesion in controlling Golgi organization was explored.

It was found that cell-matrix adhesion indeed does regulate Arf1 activity in serum-starved WT-MEFs. Loss of adhesion results in a decrease of cellular Arf1-GTP levels (without affecting total Arf1 (GDP + GTP) levels), which re-adhesion to fibronectin could restore. Presence of a constitutively active Arf1 mutant (Q71L-Arf1) could override loss of adhesion phenotype, suggesting Arf1-GTP form is necessary downstream of cell-matrix adhesion. Role of Arf1 was also confirmed in re-adhesion time point, and it was noticed that in spite of re-adhesion to fibronectin, which results in integrin activation, the absence of Arf1-GTP in the cells completely abolishes the Golgi re-organization. Similarly, integrin clustering/activation in non-adherent cells by addition of fibronectin-coated bead, could not restore Golgi integrity when Arf1 activation is blocked. This study provides a preliminary evidence that BIG1/2 is the prominent Arf1 specific GEF (and GBF1 has a minor role) regulated downstream of adhesion to control Arf1 activity in regulating rapid re-organization of Golgi. Arf1 GEF BIG1/2 which predominantly localizes to trans-Golgi compartment and is also used by cell-matrix adhesion to regulate Arf1 activity. This provides a possible explanation for the differential extent of cis vs trans-Golgi compartment. Loss of cell-matrix adhesion could potentially be re-localizing BIG1/2 resulting more Arf1 inactivation at trans-Golgi than cis-

Golgi, and hence complete disorganization of trans as opposed to cis Golgi. Does that mean Arf1 activation could indeed be different in Golgi compartments depending on the stimulus the cells remains an open question to be tested? With no Arf1 activity sensor being available, being able to visualize the activation of Arf1 in a cell and the Golgi real-time remains a challenge. Such a sensor could allow for us to track Arf1 activation in non-adherent cells to test the above hypothesis.

How cell adhesion regulates Arf1 GEFs remains unexplored and will be an open question for future investigation. Integrins engagement with ECM triggers an increase in cytosolic Ca^{2+} levels in several cell types (Balasubramanian et al., 2007a; Sjaastad and Nelson, 1997). Integrin-induced calcium signaling requires focal adhesion proteins paxillin, talin, Src, and FAK and intact cytoskeletal elements, microtubules and Actin (Clark and Brugge, 1995; Wu et al., 2001). Also, calcium acts as a fundamental regulator of membrane fusion events in a cell (Hay, 2007). This coupled with the fact that calcium signal can be dissipated rapidly through the cell and calcium does modulate Arf1 function via calcium sensor (NCS1) (Haynes et al., 2005) raises the possibility that cell-adhesion mediated regulation of calcium signaling could contribute to the regulation of Arf1 dependent Golgi organization and function.

8.4 Arf1 activation-dependent regulation of Golgi disorganization and fragmentation.

There has been a disagreement for a long time regarding the identity of Golgi as a separate independent organelle in a cell. It was proposed that Golgi emerges from the endoplasmic reticulum (ER), and structurally/functionally dependent on the ER status in a cell (Altan-Bonnet et al., 2006; Miles et al., 2001; Ward et al., 2001). However, many reports have

confirmed that indeed there is the dynamic transport of cargoes and enzymes between Golgi and ER, only a fraction of Golgi is collapsed into ER during the onset of mitosis and remains segregated otherwise (Pecot and Malhotra, 2004, 2006; Villeneuve et al., 2017). However, BFA mediated fragmentation of Golgi, which occurs because of complete inhibition of Arf1 activity, affects COPI mediated retrograde transport and eventually results in absorption of Golgi into ER (Fujiwara et al., 1988; Lippincott-Schwartz et al., 1989; Storrie et al., 1998). This led us to investigate if the disorganized Golgi in suspended cells also falls back into ER. In this study there was no significant overlap between Golgi and ER in non-adherent cells as the Golgi disorganizes. This suggests, on the loss of adhesion disorganized Golgi remains separate from the endoplasmic reticulum. This is indeed distinctly different from Golgi fragmentation observed also on BFA mediated inhibition of Arf1 activation. Could this be the result of how the loss of adhesion and BFA affect Arf1 activation?

It was hence asked if BFA further inhibits Arf1 activity in suspended cells (which is around ~ 40 %), and would it now lead to complete fragmentation of Golgi? Indeed further 60 % decrease of Arf1 in suspended cells by addition of BFA, caused cis-medial Golgi (Man II) to display a complete disorganized phenotype, in suspended cell. Correspondingly, BFA mediated inhibition of Arf1 activation during re-adhesion of cells could completely block the re-organization of both cis-medial-Golgi. This data suggest that depending on active Arf1 levels in a cell, which mostly represents a fraction of Arf1 associated with Golgi, the organization and hence function of the Golgi could be regulated. These results raise further interesting questions such if “adhesion mediated disorganization” could act as an intermediary to “mitotic or BFA mediated fragmentation”?

8.5 Role microtubule-associated motor protein dynein in the adhesion-dependent Golgi organization.

Despite the importance of the role of motor proteins in Golgi positioning in a cell, mechanism describing this phenomenon has now begun to unravel. Earlier studies have shown active Arf1 to recruit the minus-end motor protein dynein through Golgin-160 to the Golgi to control its organization (Yadav et al., 2012). It was hence asked if dynein is involved in the adhesion-Arf1-Golgi pathway that was explored so far. Consistent with the speculation, adhesion regulates the amount of dynein bound to active Arf1, thereby regulating Golgi organization. Loss of adhesion mediated drop in active Arf1 levels and active Arf1 bound dynein from the Golgi causes it to now walk away from the MTOC acquiring the disorganized phenotype. This coupled with the fact that on re-adhesion inhibiting dynein function affects re-organization of Golgi does confirm a role for dynein along this pathway. The fact that on the loss of active Arf1 bound dynein the Golgi fragments do walk away towards the plus ends of the microtubule network does suggest that a plus end kinesin motor proteins (like kinesin KIFC-3) could also be actively bound and regulate Golgi organization. A possible competition between kinesin and dynein motors could hence mediate the relative position of the Golgi in non-adherent cells. Does that mean the cis/cis-medial and trans-Golgi differentially bind plus and minus end motor proteins that mediate their differential localization downstream of adhesion remains an open question?

8.6 Adhesion mediated Golgi Disorganization affects Golgi function.

The effect of loss of adhesion mediated Golgi disorganization on Golgi function was tested. Golgi performs several functions in a cell, primary being post-translational modification,

(glycosylation). In literature, various reports link the Golgi organization to function, in terms of fragmentation of Golgi and its effect on trafficking of a particular cargo (Reynders et al., 2011). To begin with, changes in total cell surface glycosylation was explored, which could be narrowed it down to the regulation of one or more cell surface proteins in future. Quantitative flow cytometric measurements of fluorescently tagged lectin probes reveal a gradual increase in cell surface glycosylation of non-adherent cells, where Golgi disorganization was observed earlier. Furthermore, the possibility that increase in surface glycosylation is indeed a result of the loss of adhesion mediated disorganized Golgi was explored. It was found that active Arf1 expressing cells that have an organized Golgi could inhibit the increase in cell surface glycosylation confirming this regulation to be adhesion-Golgi mediated (Figure 8.1).

The elevation on the loss of adhesion could be a result of the elevated rate of trafficking of glycosylated cargo to the cell surface, and/or increased rate of post-translational modification in a disorganized Golgi. A gradual increase in surface glycosylation could be more likely be coming from the faster delivery of processed cargo to the cell surface with the possible contribution of the change in the processing machinery over time. Studies have shown synthesis, post-translational modification and delivery to the cell surface of a protein could take around 2 hours (Hirschberg et al., 1998). Additionally, similar increase in cell surface glycosylation was observed when new protein synthesis was blocked. This suggest increased cell surface glycosylation is most likely a result of accelerated rate of trafficking.

As it was previously demonstrated in thesis “disorganized” Golgi in non-adherent cells to be structurally different from BFA inhibited “fragmented” Golgi, in terms of their organization and association with ER membranes, it was hence asked if there is a functional difference as well. It was observed that cells with fragmented Golgi (BFA or NOC) reverses the increased levels of glycosylation as seen in control cells with disorganized Golgi (loss of adhesion). It is possible that in suspended cells there is a balance between adhesion-triggered endocytosis + accelerated rate of trafficking to the cell surface, resulting in more cell surface glycosylation being observed. On BFA treatment, the rate of endocytosis is not affected (unpublished studies) but it could affect exocytosis and hence net surface glycosylation levels. The fact that nocodazole similarly affects net surface glycosylation also supports the possibility that disrupting trafficking to the cell membrane can indeed affect the same. It will, however, be important to establish the reason why a suspended cell display more surface protein/lipids with glycosylation? If and how net proteins cell surface levels are affected by the loss of adhesion also remains to be confirmed. How adhesion mediated Golgi disorganization in physiological cellular events like cell-division and migration affects cell surface glycosylation is an open question.

Eukaryotic cells display an array of glycosylated proteins and lipids, which also are components of the extracellular matrix and secreted soluble molecules (Varki et al., 2009). Glycosylation is important for protein structure, function and stability and protein-protein interaction such as seen in receptor-ligand interaction (J., 2012). Hence regulation of glycosylation is vital in determining the cellular response by extra-cellular cues. It is possible that an organized Golgi (in adherent cells) ensures regulated delivery of glycosylated cargo at

the cell surface in a way that is distinctly different from that seen when the Golgi is disorganized. This could be mediated by the regulation of trafficking and sorting of these cargoes. On loss of adhesion, such a change in glycosylation could affect proteins to support cell-matrix adhesion and restore anchorage-dependent signaling and function. This speculation could be tested by evaluating anchorage-dependent signaling in non-adherent cells with an intact Golgi like it has been seen in some cancers.

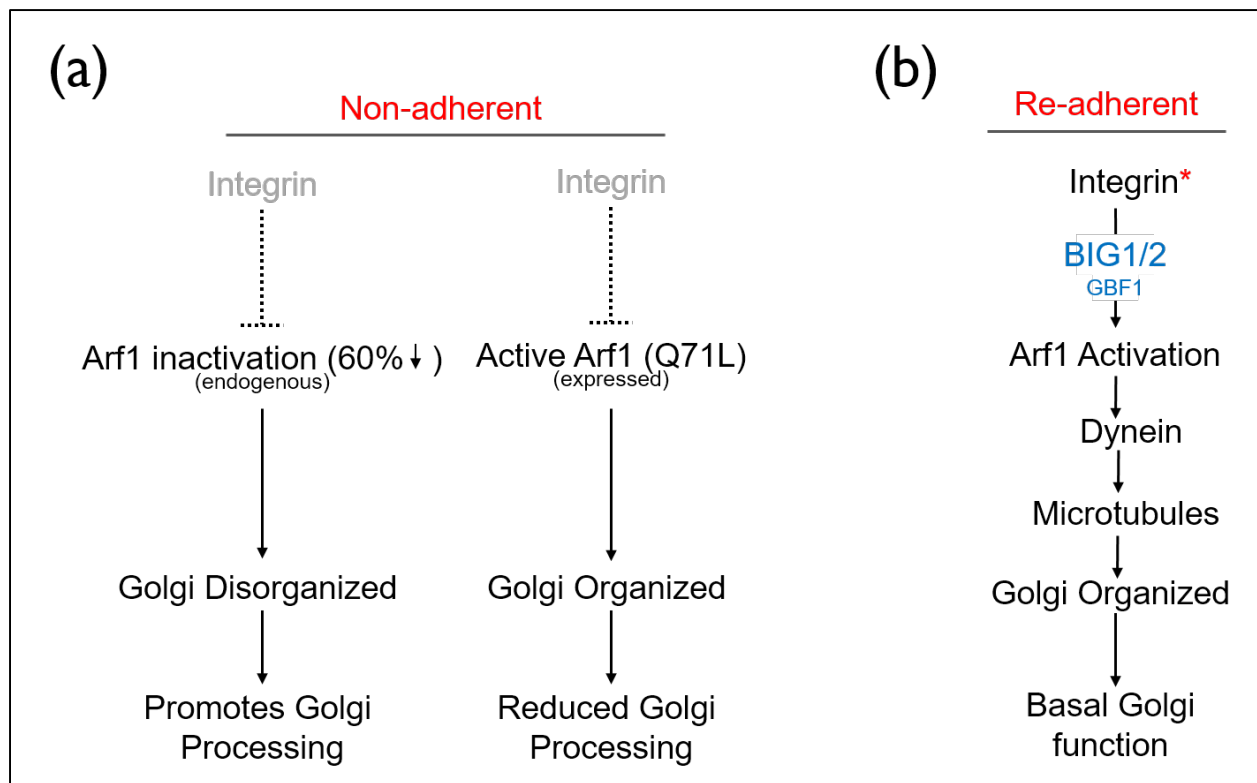


Figure 8.1 Schematic of the proposed model of cell-matrix adhesion regulation on Golgi organization and function. Schematic represents regulation by cell-matrix adhesion on Arf1 through BIG1/2, that allows for the recruitment of dynein which along the microtubule network regulates Golgi organization and function in **(a)** Non-adherent MEFs **(b)** Re-adherent MEFs

8.7 Deregulation of adhesion dependent Golgi organization in cancer cells.

In literature, reports do suggest that in many cancer cell types, Golgi is fragmented (Petrosyan, 2015). Cancer cells also show distinct changes in surface glycosylation that is thought to contribute to their function (Schultz et al., 2012). Having established the adhesion-Arfl-Golgi pathway and its effect on glycosylation in normal fibroblast cells, it made looking at the regulation of this pathway in cancers and the contribution this could have on glycosylation changes of much interest. While cancer cells tested mostly carried a broken up Golgi, there were cancer cells like T24 cells where the Golgi was intact and did not undergo loss of adhesion mediated Golgi disorganization. The fact that anchorage-independent activation of Arfl in T24 cells sustains the Golgi phenotype further supports the role this pathway has in cells. How does it affect glycosylation and functioning of T24 cells is something that remains to be explored? It is also of much interest to determine if the broken up Golgi in cancer cells mimic changes loss of adhesion mediated Golgi disorganization.

Potential mechanism of integrin mediated adhesion regulation of Golgi organization.

The rapid and spatially independent nature of cell-matrix adhesion dependent Golgi reorganization suggests a role for a secondary messenger like calcium (Ca^{2+}) downstream of integrins. Integrins engagement with ECM triggers an increase in cytosolic Ca^{2+} levels in several cell types (Jude et al., 2008; Sjaastad and Nelson, 1997). Integrin-induced calcium signaling requires focal adhesion proteins paxillin, talin, Src, and FAK (Clark and Brugge, 1995; Wu et al., 2001) and intact cytoskeletal elements, microtubules and Actin (Balasubramanian et al., 2007; Maniotis et al., 1997; Wu et al., 2001). FN-Bead attachment in renal vascular smooth muscle sparks cytosolic Ca^{2+} , which gets inhibited on microtubule

or actin depolymerization (Balasubramanian et al., 2007). Intracellular Ca^{2+} which acts as a second messenger in the cell, regulates various processes. One of the many its functions involves regulating vesicle targeting and fusion of endo-membranes in a cell. An increase in cytosolic calcium triggers the fusion of secretory granules and synaptic vesicles with the plasma membrane (Hay, 2007). A regulatory role for Ca^{2+} is also seen in constitutive trafficking from endoplasmic reticulum (ER)-to-Golgi, intra-Golgi transport, endosome and lysosome fusion (Hay, 2007).

Arf1 (Class I Arf), is associated with Golgi and its active form is an important regulator of mitotic Golgi fragmentation (Donaldson and Jackson, 2011). Arf1 protein has been shown to interact with a novel calcium sensor protein, Neuronal calcium sensor-1 (NCS-1, expressed in many cell types), both localize to Golgi and interact in a Ca^{2+} dependent manner. The NCS-1-ARF1 interaction provides evidence for functional cross-talk between Ca^{2+} dependent and ARF-dependent pathways in TGN to plasma membrane traffic and Golgi structure (Haynes et al., 2005). Also, downstream of integrins calcium could regulate the recruitment of a Arf1-GEF BIG2, as seen in TNFR1 exosome-like vesicles (Islam et al., 2008).

These literature and adhesion-Golgi pathway studied in this thesis led us to speculate the possible role of calcium downstream of integrins in regulating Arf1-GEF, Arf1 activation and thereby Golgi organization. This remains an open question and need to be investigated.

CONCLUSION.

The work presented in this thesis demonstrate the existence of a cell-matrix adhesion-Golgi pathway regulated by the adhesion-dependent regulation of small GTPase Arf1. Further, active Arf1 controls recruitment of the microtubule minus-end motor protein Dynein to regulate this pathway in normal mouse embryonic fibroblasts. This thesis also provide insight into the functional consequence such a regulation has on Golgi trafficking and/or processing to affect cell surface membrane glycosylation. This thesis hence raises the possibility that such a regulatory pathway could have a role in Golgi dependent cellular function in normal and disease conditions.

REFERENCES.

- Alcalde, J., Bonay, P., Roa, A., Vilaro, S., and Sandoval, I. V** (1992). Assembly and disassembly of the Golgi complex: two processes arranged in a cis-trans direction. *J. Cell Biol.* *116*, 69–83.
- Altan-Bonnet, N., Phair, R.D., Polishchuk, R.S., Weigert, R., and Lippincott-Schwartz, J.** (2003). A role for Arf1 in mitotic Golgi disassembly, chromosome segregation, and cytokinesis. *Proc. Natl. Acad. Sci. U. S. A.* *100*, 13314–13319.
- Altan-Bonnet, N., Sougrat, R., Liu, W., Snapp, E.L., Ward, T., and Lippincott-Schwartz, J.** (2006). Golgi inheritance in mammalian cells is mediated through endoplasmic reticulum export activities. *Mol. Biol. Cell* *17*, 990–1005.
- Appenzeller-Herzog, C., Hauri, H.-P., Andersson, H., and Appenzeller, C.** (2006). The ER-Golgi intermediate compartment (ERGIC): in search of its identity and function. *J. Cell Sci.* *119*, 2173–2183.
- De Arcangelis, A., and Georges-Labouesse, E.** (2000). **Integrin and ECM functions: roles in vertebrate development.** *Trends Genet.* *16*, 389–395.
- Arnaout, M.A., Mahalingam, B., and Xiong, J.-P.** (2005). INTEGRIN STRUCTURE, ALLOSTERY, AND BIDIRECTIONAL SIGNALING. *Annu. Rev. Cell Dev. Biol.* *21*, 381–410.
- Baker, B.M., and Chen, C.S.** (2012). Deconstructing the third dimension – how 3D culture microenvironments alter cellular cues. *J. Cell Sci.* *125*, 3015–3024.
- Balasubramanian, L., Ahmed, A., Lo, C.-M., Sham, J.S.K., and Yip, K.-P.** (2007a). Integrin-mediated mechanotransduction in renal vascular smooth muscle cells: activation of calcium sparks. *Am. J. Physiol. Integr. Comp. Physiol.* *293*, R1586–R1594.
- Balasubramanian, N., Scott, D.W., Castle, J.D., Casanova, J.E., and Schwartz, M.A.** (2007b). Arf6 and microtubules in adhesion-dependent trafficking of lipid rafts. *Nat. Cell Biol.* *9*, 1381–1391.
- Balasubramanian, N., Meier, J.A., Scott, D.W., Norambuena, A., White, M.A., and Schwartz, M.A.** (2010). RalA-Exocyst Complex Regulates Integrin-Dependent Membrane Raft Exocytosis and Growth Signaling. *Curr. Biol.* *20*, 75–79.
- Bannykh, S.I., and Balch, W.E.** (1997). Membrane dynamics at the endoplasmic reticulum-Golgi interface. *J. Cell Biol.* *138*, 1–4.
- Bannykh, S.I., Nishimura, N., and Balch, W.E.** (1998). Getting into the Golgi. *Trends Cell Biol.* *8*, 21–25.
- Barczyk, M., Carracedo, S., and Gullberg, D.** (2010). Integrins. *Cell Tissue Res.* *339*, 269–280.
- Barinaga-Rementeria Ramirez, I., and Lowe, M.** (2009). Golgins and GRASPs: Holding the Golgi together. *Semin. Cell Dev. Biol.* *20*, 770–779.
- Barlowe, C.** (2003). Signals for COPII-dependent export from the ER: what’s the ticket out? *Trends Cell Biol.* *13*, 295–300.
- Barlowe, C., Orci, L., Yeung, T., Hosobuchi, M., Hamamoto, S., Salama, N., Rexach, M.F., Ravazzola, M., Amherdt, M., and Schekman, R.** (1994). COPII: A membrane coat formed by Sec proteins that drive vesicle budding from the endoplasmic reticulum. *Cell* *77*, 895–907.
- Baschieri, F., and Farhan, H.** (2012). Crosstalk of small GTPases at the Golgi apparatus. *Small GTPases* *3*, 80–90.
- Baumann, O., and Walz, B.** (2001). Endoplasmic reticulum of animal cells and its organization into structural and functional domains. *Int. Rev. Cytol.* *205*, 149–214.
- Becker, B., and Melkonian, M.** (1996). The secretory pathway of protists: spatial and functional organization and evolution. *Microbiol. Rev.* *60*, 697–721.
- Ben-Tekaya, H., Miura, K., Pepperkok, R., and Hauri, H.-P.** (2005). Live imaging of bidirectional traffic from the ERGIC. *J. Cell Sci.* *118*, 357–367.
- Ben-Ze’ev, A., and Raz, A.** (1981). Multinucleation and inhibition of cytokinesis in suspended cells: reversal upon reattachment to a substrate. *Cell* *26*, 107–115.

Benaud, C.M., and Dickson, R.B. (2001). Adhesion-regulated G1 cell cycle arrest in epithelial cells requires the downregulation of c-Myc. *Oncogene* 20, 4554–4567.

Berrier, A.L., and Yamada, K.M. (2007). Cell–matrix adhesion. *J. Cell. Physiol.* 213, 565–573.

Bisel, B., Wang, Y., Wei, J.-H., Xiang, Y., Tang, D., Miron-Mendoza, M., Yoshimura, S., Nakamura, N., and Seemann, J. (2008). ERK regulates Golgi and centrosome orientation towards the leading edge through GRASP65. *J. Cell Biol.* 182, 837–843.

Bonifacino, J.S., and Rojas, R. (2006a). Retrograde transport from endosomes to the trans-Golgi network. *Nat. Rev. Mol. Cell Biol.* 7, 568–579.

Bonifacino, J.S., and Rojas, R. (2006b). Retrograde transport from endosomes to the trans-Golgi network. *Nat. Rev. Mol. Cell Biol.* 7, 568–579.

Bottanelli, F., Kilian, N., Ernst, A.M., Rivera-Molina, F., Schroeder, L.K., Kromann, E.B., Lessard, M.D., Erdmann, R.S., Schepartz, A., Baddeley, D., et al. (2017). A novel physiological role for ARF1 in the formation of bidirectional tubules from the Golgi. *Mol. Biol. Cell* 28, 1676–1687.

Brakebusch, C., and Fässler, R. (2003). NEW EMBO MEMBER’S REVIEW: The integrin-actin connection, an eternal love affair. *EMBO J.* 22, 2324–2333.

Bresalier, R.S., Niv, Y., Byrd, J.C., Duh, Q.Y., Toribara, N.W., Rockwell, R.W., Dahiya, R., and Kim, Y.S. (1991). Mucin production by human colonic carcinoma cells correlates with their metastatic potential in animal models of colon cancer metastasis. *J. Clin. Invest.* 87, 1037–1045.

Brownhill, K., Wood, L., and Allan, V. (2009). Molecular motors and the Golgi complex: Staying put and moving through. *Semin. Cell Dev. Biol.* 20, 784–792.

Burkhardt, J.K. (1998a). The role of microtubule-based motor proteins in maintaining the structure and function of the Golgi complex. *Biochim. Biophys. Acta* 1404, 113–126.

Campbell, I.D., and Humphries, M.J. (2011). Integrin structure, activation, and interactions. *Cold Spring Harb. Perspect. Biol.* 3.

Cancino, J., and Luini, A. (2013). Signaling Circuits on the Golgi Complex. *Traffic* 14, 121–134.

Caswell, P.T., and Norman, J.C. (2006). Integrin Trafficking and the Control of Cell Migration. *Traffic* 7, 14–21.

Caswell, P.T., Vadrevu, S., and Norman, J.C. (2009). Integrins: masters and slaves of endocytic transport. *Nat. Rev. Mol. Cell Biol.* 10, 843–853.

Cherfils, J., and Zeghouf, M. (2013). Regulation of Small GTPases by GEFs, GAPs, and GDIs. *Physiol. Rev.* 93, 269–309.

Chia, J., Goh, G., Racine, V., Ng, S., Kumar, P., and Bard, F. (2012a). RNAi screening reveals a large signaling network controlling the Golgi apparatus in human cells. *Mol. Syst. Biol.* 8, 629.

Chiu, V.K., Bivona, T., Hach, A., Sajous, J.B., Silletti, J., Wiener, H., Johnson, R.L., Cox, A.D., and Philips, M.R. (2002). Ras signalling on the endoplasmic reticulum and the Golgi. *Nat. Cell Biol.* 4, 343–350.

Clark, E.A., and Brugge, J.S. (1995). Integrins and signal transduction pathways: the road taken. *Science* 268, 233–239.

Colanzi, A., and Corda, D. (2007). Mitosis controls the Golgi and the Golgi controls mitosis. *Curr. Opin. Cell Biol.* 19, 386–393.

Colanzi, A., Suetterlin, C., and Malhotra, V. (2003). Cell-cycle-specific Golgi fragmentation: how and why? *Curr. Opin. Cell Biol.* 15, 462–467.

Cole, N.B., Sciaky, N., Marotta, A., Song, J., and Lippincott-Schwartz, J. (1996). Golgi dispersal during microtubule disruption: regeneration of Golgi stacks at peripheral endoplasmic reticulum exit sites. *Mol. Biol. Cell* 7, 631–650.

Collinet, C., Stöter, M., Bradshaw, C.R., Samusik, N., Rink, J.C., Kenski, D., Habermann, B., Buchholz, F., Henschel, R., Mueller, M.S., et al. (2010). Systems survey of endocytosis by

multiparametric image analysis. *Nature* 464, 243–249.

Corda, D., Barretta, M.L., Cervigni, R.I., and Colanzi, A. (2012). Golgi complex fragmentation in G2/M transition: An organelle-based cell-cycle checkpoint. *IUBMB Life* 64, 661–670.

Corthésy-Theulaz, I., Pauloin, A., and Pfeffer, S.R. (1992). Cytoplasmic dynein participates in the centrosomal localization of the Golgi complex. *J. Cell Biol.* 118, 1333–1345.

Cox, E.A., Sastry, S.K., and Huttenlocher, A. (2001). Integrin-mediated adhesion regulates cell polarity and membrane protrusion through the Rho family of GTPases. *Mol. Biol. Cell* 12, 265–277.

D'Souza-Schorey, C., and Chavrier, P. (2006). ARF proteins: roles in membrane traffic and beyond. *Nat. Rev. Mol. Cell Biol.* 7, 347–358.

Dalton, A.J., and Felix, M.D. (1954). Cytologic and cytochemical characteristics of the Golgi substance of epithelial cells of the epididymis-in situ, in homogenates and after isolation. *Am. J. Anat.* 94, 171–207.

DALTON, A.J., and FELIX, M.D. (1956). A comparative study of the Golgi complex. *J. Biophys. Biochem. Cytol.* 2, 79–84.

Danen, E.H.J., and Yamada, K.M. (2001). Fibronectin, integrins, and growth control. *J. Cell. Physiol.* 189, 1–13.

Day, K.J., Staehelin, L.A., and Glick, B.S. (2013). A three-stage model of Golgi structure and function. *Histochem. Cell Biol.* 140, 239–249.

DeMali, K.A., Wennerberg, K., and Burridge, K. (2003). Integrin signaling to the actin cytoskeleton. *Curr. Opin. Cell Biol.* 15, 572–582.

Desgrosellier, J.S., and Cheresch, D.A. (2010a). Integrins in cancer: biological implications and therapeutic opportunities. *Nat. Rev. Cancer* 10, 9–22.

Donaldson, J.G., and Jackson, C.L. (2000). Regulators and effectors of the ARF GTPases. *Curr. Opin. Cell Biol.* 12, 475–482.

Donaldson, J.G., Honda, A., and Weigert, R. (2005). Multiple activities for Arf1 at the Golgi complex. *Biochim. Biophys. Acta - Mol. Cell Res.* 1744, 364–373.

Duden, R., and Schekman, R. (1997). Insights into Golgi function through mutants in yeast and animal cells. In *The Golgi Apparatus*, (Basel: Birkhäuser Basel), pp. 219–246.

Egea, G., Francí, C., Gambús, G., Lesuffleur, T., Zweibaum, A., and Real, F.X. (1993). cis-Golgi resident proteins and O-glycans are abnormally compartmentalized in the RER of colon cancer cells. *J. Cell Sci.* 105 (Pt 3), 819–830.

Egea, G., Lázaro-Diéguéz, F., and Vilella, M. (2006). Actin dynamics at the Golgi complex in mammalian cells. *Curr. Opin. Cell Biol.* 18, 168–178.

Ezratty, E.J., Partridge, M.A., and Gundersen, G.G. (2005). Microtubule-induced focal adhesion disassembly is mediated by dynamin and focal adhesion kinase. *Nat. Cell Biol.* 7, 581–590.

Farber-Katz, S.E., Dippold, H.C., Buschman, M.D., Peterman, M.C., Xing, M., Noakes, C.J., Tat, J., Ng, M.M., Rahajeng, J., Cowan, D.M., et al. (2014). DNA Damage Triggers Golgi Dispersal via DNA-PK and GOLPH3. *Cell* 156, 413–427.

Farhan, H., and Hsu, V.W. (2016). Cdc42 and Cellular Polarity: Emerging Roles at the Golgi. *Trends Cell Biol.* 26, 241–248.

Farmaki, T., Ponnambalam, S., Prescott, A.R., Clausen, H., Tang, B.L., Hong, W., and Lucocq, J.M. (1999). Forward and retrograde trafficking in mitotic animal cells. ER-Golgi transport arrest restricts protein export from the ER into COPII-coated structures. *J. Cell Sci.* 112 (Pt 5), 589–600.

Farquhar, M.G. (1985). Progress in Unraveling Pathways of Golgi Traffic. *Annu. Rev. Cell Biol.* 1, 447–488.

Farquhar, M.G., and Palade, G.E. (1981). The Golgi apparatus (complex)-(1954-1981)-from artifact to center stage. *J. Cell Biol.* 91, 77s–103s.

- Feinstein, T.N., and Linstedt, A.D.** (2007). Mitogen-activated protein kinase kinase 1-dependent Golgi unlinking occurs in G2 phase and promotes the G2/M cell cycle transition. *Mol. Biol. Cell* *18*, 594–604.
- Freedman, V.H., and Shin, S.I.** (1974). Cellular tumorigenicity in nude mice: correlation with cell growth in semi-solid medium. *Cell* *3*, 355–359.
- Freeze, H.H., and Schachter, H.** (2009). *Genetic Disorders of Glycosylation* (Cold Spring Harbor Laboratory Press).
- Fujiwara, T., Oda, K., Yokota, S., Takatsuki, A., and Ikehara, Y.** (1988). Brefeldin A causes disassembly of the Golgi complex and accumulation of secretory proteins in the endoplasmic reticulum. *J. Biol. Chem.* *263*, 18545–18552.
- Gaus, K., Le Lay, S., Balasubramanian, N., and Schwartz, M.A.** (2006). Integrin-mediated adhesion regulates membrane order. *J. Cell Biol.* *174*, 725–734.
- Geiger, B., and Yamada, K.M.** (2011). Molecular Architecture and Function of Matrix Adhesions. *Cold Spring Harb. Perspect. Biol.* *3*, a005033–a005033.
- Geiger, B., Bershadsky, A., Pankov, R., and Yamada, K.M.** (2001a). Transmembrane crosstalk between the extracellular matrix and the cytoskeleton. *Nat. Rev. Mol. Cell Biol.* *2*, 793–805.
- Geiger, B., Spatz, J.P., and Bershadsky, A.D.** (2009). Environmental sensing through focal adhesions. *Nat. Rev. Mol. Cell Biol.* *10*, 21–33.
- Geuze, H.J., and Morré, D.J.** (1991). Trans-Golgi reticulum. *J. Electron Microsc. Tech.* *17*, 24–34.
- Girod, A., Storrle, B., Simpson, J.C., Johannes, L., Goud, B., Roberts, L.M., Lord, J.M., Nilsson, T., and Pepperkok, R.** (1999). Evidence for a COP-I-independent transport route from the Golgi complex to the endoplasmic reticulum. *Nat. Cell Biol.* *1*, 423–430.
- Glick, B.S., and Luini, A.** (2011). Models for Golgi traffic: a critical assessment. *Cold Spring Harb. Perspect. Biol.* *3*, a005215.
- Golgi, C., Bentivoglio, M., and Swanson, L.** (2001). On the fine structure of the pes Hippocampi major (with plates XIII-XXIII). 1886. *Brain Res. Bull.* *54*, 461–483.
- Gonatas, N.K., Stieber, A., and Gonatas, J.O.** (2006). Fragmentation of the Golgi apparatus in neurodegenerative diseases and cell death. *J. Neurol. Sci.* *246*, 21–30.
- Grinnell, F., and Geiger, B.** (1986). Interaction of fibronectin-coated beads with attached and spread fibroblasts. Binding, phagocytosis, and cytoskeletal reorganization. *Exp. Cell Res.* *162*, 449–461.
- Gurel, P.S., Hatch, A.L., and Higgs, H.N.** (2014). Connecting the cytoskeleton to the endoplasmic reticulum and Golgi. *Curr. Biol.* *24*, R660–R672.
- Haase, G., and Rabouille, C.** (2015). Golgi Fragmentation in ALS Motor Neurons. *New Mechanisms Targeting Microtubules, Tethers, and Transport Vesicles. Front. Neurosci.* *9*, 448.
- Harada, A., Takei, Y., Kanai, Y., Tanaka, Y., Nonaka, S., and Hirokawa, N.** (1998). Golgi vesiculation and lysosome dispersion in cells lacking cytoplasmic dynein. *J. Cell Biol.* *141*, 51–59.
- Hawes, C.** (2004). Cell biology of the plant Golgi apparatus. *New Phytol.* *165*, 29–44.
- Hay, J.C.** (2007). Calcium: a fundamental regulator of intracellular membrane fusion? *EMBO Rep.* *8*, 236–240.
- Hirschberg, K., Miller, C.M., Ellenberg, J., Presley, J.F., Siggia, E.D., Phair, R.D., and Lippincott-Schwartz, J.** (1998a). Kinetic analysis of secretory protein traffic and characterization of golgi to plasma membrane transport intermediates in living cells. *J. Cell Biol.* *143*, 1485–1503.
- Humphries, M.J., Symonds, E.J.H., and Mould, A.P.** (2003). Mapping functional residues onto integrin crystal structures. *Curr. Opin. Struct. Biol.* *13*, 236–243.
- Hurtado, L., Caballero, C., Gavilan, M.P., Cardenas, J., Bornens, M., and Rios, R.M.** (2011). Disconnecting the Golgi ribbon from the centrosome prevents directional cell migration and ciliogenesis. *J. Cell Biol.* *193*, 917–933.

- Huttenlocher, A., and Horwitz, A.R.** (2011). Integrins in cell migration. *Cold Spring Harb. Perspect. Biol.* 3, a005074.
- Hynes, R.O.** (1987). Integrins: a family of cell surface receptors. *Cell* 48, 549–554.
- Hynes, R.O.** (2002). Integrins: bidirectional, allosteric signaling machines. *Cell* 110, 673–687.
- Hynes, R.O.** (2004). The emergence of integrins: a personal and historical perspective. *Matrix Biol.* 23, 333–340.
- J., B.** (2012). The Role of Glycosylation in Receptor Signaling. In *Glycosylation*, (InTech), p.
- Jékely, G.** (2007). Origin of Eukaryotic Endomembranes: A Critical Evaluation of Different Model Scenarios. In *Eukaryotic Membranes and Cytoskeleton*, (New York, NY: Springer New York), pp. 38–51.
- Johannes, L., and Popoff, V.** (2008). Tracing the retrograde route in protein trafficking. *Cell* 135, 1175–1187.
- Joshi, G., Chi, Y., Huang, Z., and Wang, Y.** (2014). A β -induced Golgi fragmentation in Alzheimer's disease enhances A β production. *Proc. Natl. Acad. Sci.* 111, E1230–E1239.
- Kanada, M., Nagasaki, A., and Uyeda, T.Q.P.** (2005). Adhesion-dependent and contractile ring-independent equatorial furrowing during cytokinesis in mammalian cells. *Mol. Biol. Cell* 16, 3865–3872.
- Kellokumpu, S., Sormunen, R., and Kellokumpu, I.** (2002). Abnormal glycosylation and altered Golgi structure in colorectal cancer: dependence on intra-Golgi pH. *FEBS Lett.* 516, 217–224.
- Klopfenstein, D.R., Klumperman, J., Lustig, A., Kammerer, R.A., Oorschot, V., and Hauri, H.P.** (2001). Subdomain-specific localization of CLIMP-63 (p63) in the endoplasmic reticulum is mediated by its luminal alpha-helical segment. *J. Cell Biol.* 153, 1287–1300.
- Klumperman, J.** (2011). Architecture of the mammalian Golgi. *Cold Spring Harb. Perspect. Biol.* 3, a005181.
- Klute, M.J., Melançon, P., and Dacks, J.B.** (2011). Evolution and diversity of the Golgi. *Cold Spring Harb. Perspect. Biol.* 3, a007849.
- Koivisto, L., Heino, J., Häkkinen, L., and Larjava, H.** (2014). Integrins in Wound Healing. *Adv. Wound Care* 3, 762–783.
- Koreishi, M., Gniadek, T.J., Yu, S., Masuda, J., Honjo, Y., and Satoh, A.** (2013). The Golgin Tether Giantin Regulates the Secretory Pathway by Controlling Stack Organization within Golgi Apparatus. *PLoS One* 8, e59821.
- Kragl, M., and Lammert, E.** (2010). Basement Membrane in Pancreatic Islet Function. In *Advances in Experimental Medicine and Biology*, pp. 217–234.
- Ladinsky, M.S., Mastronarde, D.N., McIntosh, J.R., Howell, K.E., and Staehelin, L.A.** (1999). Golgi structure in three dimensions: functional insights from the normal rat kidney cell. *J. Cell Biol.* 144, 1135–1149.
- Ladinsky, M.S., Wu, C.C., McIntosh, S., McIntosh, J.R., and Howell, K.E.** (2002). Structure of the Golgi and distribution of reporter molecules at 20 degrees C reveals the complexity of the exit compartments. *Mol. Biol. Cell* 13, 2810–2825.
- LaFlamme, S.E., Nieves, B., Colello, D., and Reverte, C.G.** (2008a). Integrins as regulators of the mitotic machinery. *Curr. Opin. Cell Biol.* 20, 576–582.
- Lawson, C., and Schlaepfer, D.D.** (2012a). Integrin adhesions: who's on first? What's on second? Connections between FAK and talin. *Cell Adh. Migr.* 6, 302–306.
- Lawson, C., Lim, S.-T., Uryu, S., Chen, X.L., Calderwood, D.A., and Schlaepfer, D.D.** (2012). FAK promotes recruitment of talin to nascent adhesions to control cell motility. *J. Cell Biol.* 196, 223–232.
- Lee, J.O., Rieu, P., Arnaut, M.A., and Liddington, R.** (1995). Crystal structure of the A domain from the alpha subunit of integrin CR3 (CD11b/CD18). *Cell* 80, 631–638.

- Levine, T., and Rabouille, C.** (2005). Endoplasmic reticulum: one continuous network compartmentalized by extrinsic cues. *Curr. Opin. Cell Biol.* *17*, 362–368.
- Lewis, J.M., and Schwartz, M.A.** (1995). Mapping in vivo associations of cytoplasmic proteins with integrin beta 1 cytoplasmic domain mutants. *Mol. Biol. Cell* *6*, 151–160.
- LI, Y., KELLY, W.G., LOGSDON, J.M., SCHURKO, A.M., HARFE, B.D., HILL-HARFE, K.L., and KAHN, R.A.** (2004). Functional genomic analysis of the ADP-ribosylation factor family of GTPases: phylogeny among diverse eukaryotes and function in *C. elegans*. *FASEB J.* *18*, 1834–1850.
- Lingwood, D., and Simons, K.** (2010). Lipid Rafts As a Membrane-Organizing Principle. *Science* (80-.). *327*, 46–50.
- Lippincott-Schwartz, J., Yuan, L.C., Bonifacino, J.S., and Klausner, R.D.** (1989). Rapid redistribution of Golgi proteins into the ER in cells treated with brefeldin A: evidence for membrane cycling from Golgi to ER. *Cell* *56*, 801–813.
- Lippincott-Schwartz, J., Donaldson, J.G., Schweizer, A., Berger, E.G., Hauri, H.P., Yuan, L.C., and Klausner, R.D.** (1990). Microtubule-dependent retrograde transport of proteins into the ER in the presence of brefeldin A suggests an ER recycling pathway. *Cell* *60*, 821–836.
- Lippincott-Schwartz, J., Presley, J.F., Cole, N.B., Schroer, T.A., Hirschberg, K., and Zaal, K.J.M.** (1997). ER-to-Golgi transport visualized in living cells. *Nature* *389*, 81–85.
- Lippincott-Schwartz, J., Roberts, T.H., and Hirschberg, K.** (2000). Secretory Protein Trafficking and Organelle Dynamics in Living Cells. *Annu. Rev. Cell Dev. Biol.* *16*, 557–589.
- Lodish, H., Berk, A., Zipursky, S.L., Matsudaira, P., Baltimore, D., and Darnell, J.** (2000). Overview of the Secretory Pathway.
- Losev, E., Reinke, C.A., Jellen, J., Strongin, D.E., Bevis, B.J., and Glick, B.S.** (2006). Golgi maturation visualized in living yeast. *Nature* *441*, 1002–1006.
- Lowe, M.** (2002). Golgi Complex: Biogenesis de novo? *Curr. Biol.* *12*, R166–R167.
- Lowe, M., Gonatas, N.K., and Warren, G.** (2000). The mitotic phosphorylation cycle of the cis-Golgi matrix protein GM130. *J. Cell Biol.* *149*, 341–356.
- Machamer, C.E.** (2003). Golgi disassembly in apoptosis: cause or effect? *Trends Cell Biol.* *13*, 279–281.
- Maddox, A.S., and Burridge, K.** (2003a). RhoA is required for cortical retraction and rigidity during mitotic cell rounding. *J. Cell Biol.* *160*, 255–265.
- Maeda, Y., and Kinoshita, T.** (2010). The Acidic Environment of the Golgi Is Critical for Glycosylation and Transport. In *Methods in Enzymology*, pp. 495–510.
- Malhotra, V., and Campelo, F.** (2011). PKD regulates membrane fission to generate TGN to cell surface transport carriers. *Cold Spring Harb. Perspect. Biol.* *3*.
- Marra, P., Maffucci, T., Daniele, T., Tullio, G. Di, Ikehara, Y., Chan, E.K.L., Luini, A., Beznoussenko, G., Mironov, A., and De Matteis, M.A.** (2001). The GM130 and GRASP65 Golgi proteins cycle through and define a subdomain of the intermediate compartment. *Nat. Cell Biol.* *3*, 1101–1113.
- Marre, M.L., Petnicki-Ocwieja, T., DeFrancesco, A.S., Darcy, C.T., and Hu, L.T.** (2010). Human Integrin $\alpha 3\beta 1$ Regulates TLR2 Recognition of Lipopeptides from Endosomal Compartments. *PLoS One* *5*, e12871.
- Marsh, B.J., Mastrorade, D.N., Buttle, K.F., Howell, K.E., and McIntosh, J.R.** (2001). Organellar relationships in the Golgi region of the pancreatic beta cell line, HIT-T15, visualized by high resolution electron tomography. *Proc. Natl. Acad. Sci. U. S. A.* *98*, 2399–2406.
- Martchenko, M., Jeong, S.-Y., and Cohen, S.N.** (2010). Heterodimeric integrin complexes containing $\beta 1$ -integrin promote internalization and lethality of anthrax toxin. *Proc. Natl. Acad. Sci.* *107*, 15583–15588.
- Matsuura-Tokita, K., Takeuchi, M., Ichihara, A., Mikuriya, K., and Nakano, A.** (2006). Live

imaging of yeast Golgi cisternal maturation. *Nature* 441, 1007–1010.

De Matteis, M.A., and Luini, A. (2008a). Exiting the Golgi complex. *Nat. Rev. Mol. Cell Biol.* 9, 273–284.

Meredith, J.E., and Schwartz, M.A. (1997). Integrins, adhesion and apoptosis. *Trends Cell Biol.* 7, 146–150.

Migita, T., and Inoue, S. (2012). Implications of the Golgi apparatus in prostate cancer. *Int. J. Biochem. Cell Biol.* 44, 1872–1876.

Miles, S., McManus, H., Forsten, K.E., and Storrie, B. (2001). Evidence that the entire Golgi apparatus cycles in interphase HeLa cells. *J. Cell Biol.* 155, 543–556.

Millarte, V., and Farhan, H. (2012a). The Golgi in Cell Migration: Regulation by Signal Transduction and Its Implications for Cancer Cell Metastasis. *Sci. World J.* 2012, 1–11.

Mogelsvang, S., Marsh, B.J., Ladinsky, M.S., and Howell, K.E. (2004). Predicting Function from Structure: 3D Structure Studies of the Mammalian Golgi Complex. *Traffic* 5, 338–345.

Van De Moortele, S., Picart, R., Tixier-Vidal, A., and Tougard, C. (1993). Nocodazole and taxol affect subcellular compartments but not secretory activity of GH3B6 prolactin cells. *Eur. J. Cell Biol.* 60, 217–227.

Mori, S., Chang, J.T., Andrechek, E.R., Matsumura, N., Baba, T., Yao, G., Kim, J.W., Gatza, M., Murphy, S., and Nevins, J.R. (2009). Anchorage-independent cell growth signature identifies tumors with metastatic potential. *Oncogene* 28, 2796–2805.

Mowbrey, K., and Dacks, J.B. (2009). Evolution and diversity of the Golgi body. *FEBS Lett.* 583, 3738–3745.

Moyer, B.D., Allan, B.B., and Balch, W.E. (2001). Rab1 interaction with a GM130 effector complex regulates COPII vesicle cis-Golgi tethering. *Traffic* 2, 268–276.

Mukherjee, S., Chiu, R., Leung, S.-M., and Shields, D. (2007). Fragmentation of the Golgi Apparatus: An Early Apoptotic Event Independent of the Cytoskeleton. *Traffic* 8, 369–378.

Munro, S. (2005). The Golgi apparatus: defining the identity of Golgi membranes. *Curr. Opin. Cell Biol.* 17, 395–401.

Munro, S. (2011). The golgin coiled-coil proteins of the Golgi apparatus. *Cold Spring Harb. Perspect. Biol.* 3, a005256.

Nakagomi, S., Barsoum, M.J., Bossy-Wetzel, E., Sütterlin, C., Malhotra, V., and Lipton, S.A. (2008). A Golgi fragmentation pathway in neurodegeneration. *Neurobiol. Dis.* 29, 221–231.

Nakamura, N., Lowe, M., Levine, T.P., Rabouille, C., and Warren, G. (1997). The vesicle docking protein p115 binds GM130, a cis-Golgi matrix protein, in a mitotically regulated manner. *Cell* 89, 445–455.

Orci, L., Perrelet, A., and Rothman, J.E. (1998). Vesicles on strings: morphological evidence for processive transport within the Golgi stack. *Proc. Natl. Acad. Sci. U. S. A.* 95, 2279–2283.

Ortega-Velazquez, R., Gonzalez-Rubio, M., Ruiz-Torres, M.P., Diez-Marques, M.L., Iglesias, M.C., Rodriguez-Puyol, M., and Rodríguez-Puyol, D. (2004). Collagen I upregulates extracellular matrix gene expression and secretion of TGF- β 1 by cultured human mesangial cells. *Am. J. Physiol. Physiol.* 286, C1335–C1343.

Palazzo, A.F., Eng, C.H., Schlaepfer, D.D., Marcantonio, E.E., and Gundersen, G.G. (2004). Localized Stabilization of Microtubules by Integrin- and FAK-Facilitated Rho Signaling. *Science* (80-.). 303, 836–839.

Pan, L., Zhao, Y., Yuan, Z., and Qin, G. (2016). Research advances on structure and biological functions of integrins. *Springerplus* 5, 1094.

Papanikou, E., and Glick, B.S. (2009). The yeast Golgi apparatus: Insights and mysteries. *FEBS Lett.* 583, 3746–3751.

Papanikou, E., and Glick, B.S. (2014). Golgi compartmentation and identity. *Curr. Opin. Cell Biol.* 29, 74–81.

- Park, S.-Y., Yang, J.-S., Schmider, A.B., Soberman, R.J., and Hsu, V.W.** (2015). Coordinated regulation of bidirectional COPI transport at the Golgi by CDC42. *Nature* *521*, 529–532.
- Patterson, G.H., Hirschberg, K., Polishchuk, R.S., Gerlich, D., Phair, R.D., and Lippincott-Schwartz, J.** (2008). Transport through the Golgi Apparatus by Rapid Partitioning within a Two-Phase Membrane System. *Cell* *133*, 1055–1067.
- Pawar, A., Meier, J.A., Dasgupta, A., Diwanji, N., Deshpande, N., Saxena, K., Buwa, N., Inchanalkar, S., Schwartz, M.A., and Balasubramanian, N.** (2016). Ral-Arf6 crosstalk regulates Ral dependent exocyst trafficking and anchorage independent growth signalling. *Cell. Signal.* *28*, 1225–1236.
- Payne, C., and Schatten, G.** (2003). Golgi dynamics during meiosis are distinct from mitosis and are coupled to endoplasmic reticulum dynamics until fertilization. *Dev. Biol.* *264*, 50–63.
- Pearse, B.M.F., and Robinson, M.S.** (1990). Clathrin, Adaptors, and Sorting. *Annu. Rev. Cell Biol.* *6*, 151–171.
- Pecot, M.Y., and Malhotra, V.** (2004). Golgi Membranes Remain Segregated from the Endoplasmic Reticulum during Mitosis in Mammalian Cells. *Cell* *116*, 99–107.
- Pecot, M.Y., and Malhotra, V.** (2006). The Golgi apparatus maintains its organization independent of the endoplasmic reticulum. *Mol. Biol. Cell* *17*, 5372–5380.
- Pelkmans, L., Fava, E., Grabner, H., Hannus, M., Habermann, B., Krausz, E., and Zerial, M.** (2005a). Genome-wide analysis of human kinases in clathrin- and caveolae/raft-mediated endocytosis. *Nature* *436*, 78–86.
- Pellinen, T., Tuomi, S., Arjonen, A., Wolf, M., Edgren, H., Meyer, H., Grosse, R., Kitzing, T., Rantala, J.K., Kallioniemi, O., et al.** (2008). Integrin Trafficking Regulated by Rab21 Is Necessary for Cytokinesis. *Dev. Cell* *15*, 371–385.
- Petrosyan, A.** (2015a). Onco-Golgi: Is Fragmentation a Gate to Cancer Progression? *Biochem. Mol. Biol. J.* *1*.
- Petrosyan, A., Holzappel, M.S., Muirhead, D.E., and Cheng, P.-W.** (2014a). Restoration of Compact Golgi Morphology in Advanced Prostate Cancer Enhances Susceptibility to Galectin-1-Induced Apoptosis by Modifying Mucin O-Glycan Synthesis. *Mol. Cancer Res.* *12*, 1704–1716.
- Pfeffer, S.R.** (1999). Transport-vesicle targeting: tethers before SNAREs. *Nat. Cell Biol.* *1*, E17–E22.
- Plow, E.F., Haas, T.A., Zhang, L., Loftus, J., and Smith, J.W.** (2000). Ligand Binding to Integrins. *J. Biol. Chem.* *275*, 21785–21788.
- Pokrovskaya, I.D., Willett, R., Smith, R.D., Morelle, W., Kudlyk, T., and Lupashin, V. V.** (2011). Conserved oligomeric Golgi complex specifically regulates the maintenance of Golgi glycosylation machinery. *Glycobiology* *21*, 1554–1569.
- del Pozo, M.A., Alderson, N.B., Kiosses, W.B., Chiang, H.-H., Anderson, R.G.W., and Schwartz, M.A.** (2004a). Integrins Regulate Rac Targeting by Internalization of Membrane Domains. *Science* (80-.). *303*, 839–842.
- del Pozo, M.A., Balasubramanian, N., Alderson, N.B., Kiosses, W.B., Grande-García, A., Anderson, R.G.W., and Schwartz, M.A.** (2005a). Phospho-caveolin-1 mediates integrin-regulated membrane domain internalization. *Nat. Cell Biol.* *7*, 901–908.
- Preisinger, C., Körner, R., Wind, M., Lehmann, W.D., Kopajtich, R., and Barr, F.A.** (2005). Plk1 docking to GRASP65 phosphorylated by Cdk1 suggests a mechanism for Golgi checkpoint signalling. *EMBO J.* *24*, 753–765.
- Pugacheva, E.N., Roegiers, F., and Golemis, E.A.** (2006). Interdependence of cell attachment and cell cycle signaling. *Curr. Opin. Cell Biol.* *18*, 507–515.
- Rabouille, C., and Klumperman, J.** (2005). The maturing role of COPI vesicles in intra-Golgi transport. *Nat. Rev. Mol. Cell Biol.* *6*, 812–817.
- Radi, Z.A., Kehrl, M.E., and Ackermann, M.R.** Cell adhesion molecules, leukocyte trafficking,

- and strategies to reduce leukocyte infiltration. *J. Vet. Intern. Med.* *15*, 516–529.
- Rambourg, A., and Clermont, Y.** (1997). Three-dimensional structure of the Golgi apparatus in mammalian cells. In *The Golgi Apparatus*, (Basel: Birkhäuser Basel), pp. 37–61.
- Rendón, W.O., Martínez-Alonso, E., Tomás, M., Martínez-Martínez, N., and Martínez-Menárguez, J.A.** (2013a). Golgi fragmentation is Rab and SNARE dependent in cellular models of Parkinson's disease. *Histochem. Cell Biol.* *139*, 671–684.
- Reverte, C.G., Benware, A., Jones, C.W., and LaFlamme, S.E.** (2006). Perturbing integrin function inhibits microtubule growth from centrosomes, spindle assembly, and cytokinesis. *J. Cell Biol.* *174*, 491–497.
- Reynders, E., Foulquier, F., Annaert, W., and Matthijs, G.** (2011). How Golgi glycosylation meets and needs trafficking: the case of the COG complex. *Glycobiology* *21*, 853–863.
- Ridley, A.J.** (2011). Life at the Leading Edge. *Cell* *145*, 1012–1022.
- Rios, R.M., and Bornens, M.** (2003). The Golgi apparatus at the cell centre. *Curr. Opin. Cell Biol.* *15*, 60–66.
- Rismanchi, N., Soderblom, C., Stadler, J., Zhu, P.-P., and Blackstone, C.** (2008). Atlantin GTPases are required for Golgi apparatus and ER morphogenesis. *Hum. Mol. Genet.* *17*, 1591–1604.
- Robin, P., Rossignol, B., and Raymond, M.N.** (1995). Effect of microtubule network disturbance by nocodazole and docetaxel (Taxotere) on protein secretion in rat extraorbital lacrimal and parotid glands. *Eur. J. Cell Biol.* *67*, 227–237.
- Rodriguez-Boulan, E., and Müsch, A.** (2005). Protein sorting in the Golgi complex: Shifting paradigms. *Biochim. Biophys. Acta - Mol. Cell Res.* *1744*, 455–464.
- Rottner, K., and Stradal, T.E.** (2011). Actin dynamics and turnover in cell motility. *Curr. Opin. Cell Biol.* *23*, 569–578.
- Sandoval, I. V., Bonifacino, J.S., Klausner, R.D., Henkart, M., and Wehland, J.** (1984). Role of microtubules in the organization and localization of the Golgi apparatus. *J. Cell Biol.* *99*, 113s–118s.
- Scales, S.J., Pepperkok, R., and Kreis, T.E.** (1997). Visualization of ER-to-Golgi transport in living cells reveals a sequential mode of action for COPII and COPI. *Cell* *90*, 1137–1148.
- Schultz, M.J., Swindall, A.F., and Bellis, S.L.** (2012). Regulation of the metastatic cell phenotype by sialylated glycans. *Cancer Metastasis Rev.* *31*, 501–518.
- Schwartz, M.A.** (1997). Integrins, oncogenes, and anchorage independence. *J. Cell Biol.* *139*, 575–578.
- Schwartz, M.A.** (2001). Integrin signaling revisited. *Trends Cell Biol.* *11*, 466–470.
- Schwartz, M.A., and Assoian, R.K.** (2001a). Integrins and cell proliferation: regulation of cyclin-dependent kinases via cytoplasmic signaling pathways. *J. Cell Sci.* *114*, 2553–2560.
- Schwartz, M.A., and Ginsberg, M.H.** (2002). Networks and crosstalk: integrin signalling spreads. *Nat. Cell Biol.* *4*, E65–E68.
- Seguin, L., Desgrosellier, J.S., Weis, S.M., and Cheresch, D.A.** (2015). Integrins and cancer: regulators of cancer stemness, metastasis, and drug resistance. *Trends Cell Biol.* *25*, 234–240.
- Shima, D.T., Haldar, K., Pepperkok, R., Watson, R., and Warren, G.** (1997). Partitioning of the Golgi apparatus during mitosis in living HeLa cells. *J. Cell Biol.* *137*, 1211–1228.
- Shorter, J., and Warren, G.** (1999). A role for the vesicle tethering protein, p115, in the post-mitotic stacking of reassembling Golgi cisternae in a cell-free system. *J. Cell Biol.* *146*, 57–70.
- Shorter, J., and Warren, G.** (2002). Golgi Architecture and Inheritance. *Annu. Rev. Cell Dev. Biol.* *18*, 379–420.
- Sjaastad, M.D., and Nelson, W.J.** (1997). Integrin-mediated calcium signaling and regulation of cell adhesion by intracellular calcium. *BioEssays* *19*, 47–55.

- Slusarewicz, P., Nilsson, T., Hui, N., Watson, R., and Warren, G.** (1994). Isolation of a matrix that binds medial Golgi enzymes. *J. Cell Biol.* *124*, 405–413.
- Smith, R.D., Willett, R., Kudlyk, T., Pokrovskaya, I., Paton, A.W., Paton, J.C., and Lupashin, V. V.** (2009). The COG Complex, Rab6 and COPI Define a Novel Golgi Retrograde Trafficking Pathway that is Exploited by SubAB Toxin. *Traffic* *10*, 1502–1517.
- Stanley, P.** (2011). Golgi glycosylation. *Cold Spring Harb. Perspect. Biol.* *3*.
- Stehbens, S., and Wittmann, T.** (2012). Targeting and transport: how microtubules control focal adhesion dynamics. *J. Cell Biol.* *198*, 481–489.
- Stinchcombe, J.C., Nomoto, H., Cutler, D.F., and Hopkins, C.R.** (1995). Anterograde and retrograde traffic between the rough endoplasmic reticulum and the Golgi complex. *J. Cell Biol.* *131*, 1387–1401.
- Storrie, B., White, J., Röttger, S., Stelzer, E.H., Suganuma, T., and Nilsson, T.** (1998). Recycling of golgi-resident glycosyltransferases through the ER reveals a novel pathway and provides an explanation for nocodazole-induced Golgi scattering. *J. Cell Biol.* *143*, 1505–1521.
- Stupack, D.G., and Cheresch, D.A.** (2002). Get a ligand, get a life: integrins, signaling and cell survival. *J. Cell Sci.* *115*, 3729–3738.
- Sütterlin, C., and Colanzi, A.** (2010). The Golgi and the centrosome: building a functional partnership. *J. Cell Biol.* *188*, 621–628.
- Sütterlin, C., Hsu, P., Mallabiabarrena, A., and Malhotra, V.** (2002). Fragmentation and dispersal of the pericentriolar Golgi complex is required for entry into mitosis in mammalian cells. *Cell* *109*, 359–369.
- Suzuki, K., and Takahashi, K.** (2003). Reduced cell adhesion during mitosis by threonine phosphorylation of $\beta 1$ integrin. *J. Cell. Physiol.* *197*, 297–305.
- Tamkun, J.W., DeSimone, D.W., Fonda, D., Patel, R.S., Buck, C., Horwitz, A.F., and Hynes, R.O.** (1986). Structure of integrin, a glycoprotein involved in the transmembrane linkage between fibronectin and actin. *Cell* *46*, 271–282.
- Tang, D., Yuan, H., and Wang, Y.** (2010). The Role of GRASP65 in Golgi Cisternal Stacking and Cell Cycle Progression. *Traffic* *11*, 827–842.
- Tang, D., Yuan, H., Vielemeyer, O., Perez, F., and Wang, Y.** (2012). Sequential phosphorylation of GRASP65 during mitotic Golgi disassembly. *Biol. Open* *1*, 1204–1214.
- Théry, M., and Bornens, M.** (2008). Get round and stiff for mitosis. *HFSP J.* *2*, 65–71.
- Tran, H., Pankov, R., Tran, S.D., Hampton, B., Burgess, W.H., and Yamada, K.M.** (2002). Integrin clustering induces kinectin accumulation. *J. Cell Sci.* *115*, 2031–2040.
- Trucco, A., Polishchuk, R.S., Martella, O., Pentima, A. Di, Fusella, A., Giandomenico, D. Di, Pietro, E.S., Beznoussenko, G. V., Polishchuk, E. V., Baldassarre, M., et al.** (2004). Secretory traffic triggers the formation of tubular continuities across Golgi sub-compartments. *Nat. Cell Biol.* *6*, 1071–1081.
- Tucker, K.L., Sage, T., Stevens, J.M., Jordan, P.A., Jones, S., Barrett, N.E., St-Arnaud, R., Frampton, J., Dedhar, S., and Gibbins, J.M.** (2008). A dual role for integrin-linked kinase in platelets: regulating integrin function and α -granule secretion. *Blood* *112*, 4523–4531.
- Valderrama, F., Babià, T., Ayala, I., Kok, J.W., Renau-Piqueras, J., and Egea, G.** (1998). Actin microfilaments are essential for the cytological positioning and morphology of the Golgi complex. *Eur. J. Cell Biol.* *76*, 9–17.
- Valderrama, F., Durán, J.M., Babià, T., Barth, H., Renau-Piqueras, J., and Egea, G.** (2001). Actin microfilaments facilitate the retrograde transport from the Golgi complex to the endoplasmic reticulum in mammalian cells. *Traffic* *2*, 717–726.
- Varki, A., Cummings, R.D., Esko, J.D., Freeze, H.H., Stanley, P., Bertozzi, C.R., Hart, G.W., and Etzler, M.E.** (2009). *Essentials of Glycobiology* (Cold Spring Harbor Laboratory Press).
- Vasudevan, C., Han, W., Tan, Y., Nie, Y., Li, D., Shome, K., Watkins, S.C., Levitan, E.S.,**

and Romero, G. (1998). The distribution and translocation of the G protein ADP-ribosylation factor 1 in live cells is determined by its GTPase activity. *J. Cell Sci.* *111* (Pt 9), 1277–1285.

Villeneuve, J., Duran, J., Scarpa, M., Bassaganyas, L., Van Galen, J., and Malhotra, V. (2017a). Golgi enzymes do not cycle through the endoplasmic reticulum during protein secretion or mitosis. *Mol. Biol. Cell* *28*, 141–151.

Volpicelli-Daley, L.A., Li, Y., Zhang, C.-J., and Kahn, R.A. (2005). Isoform-selective Effects of the Depletion of ADP-Ribosylation Factors 1-5 on Membrane Traffic. *Mol. Biol. Cell* *16*, 4495–4508.

Wang, X., Zhang, Z., and Yao, C. (2011). Targeting integrin-linked kinase increases apoptosis and decreases invasion of myeloma cell lines and inhibits IL-6 and VEGF secretion from BMSCs. *Med. Oncol.* *28*, 1596–1600.

Ward, T.H., Polishchuk, R.S., Caplan, S., Hirschberg, K., and Lippincott-Schwartz, J. (2001). Maintenance of Golgi structure and function depends on the integrity of ER export. *J. Cell Biol.* *155*, 557–570.

Wickström, S.A., and Fässler, R. (2011). Regulation of membrane traffic by integrin signaling. *Trends Cell Biol.* *21*, 266–273.

Wideman, J.G., Leung, K.F., Field, M.C., and Dacks, J.B. (2014). The Cell Biology of the Endocytic System from an Evolutionary Perspective. *Cold Spring Harb. Perspect. Biol.* *6*, a016998–a016998.

Wilson, C., Venditti, R., Rega, L.R., Colanzi, A., D’Angelo, G., and De Matteis, M.A. (2011a). The Golgi apparatus: an organelle with multiple complex functions. *Biochem. J.* *433*, 1–9.

Wu, X., and Reddy, D.S. (2012). Integrins as receptor targets for neurological disorders. *Pharmacol. Ther.* *134*, 68–81.

Wu, X., Davis, G.E., Meininger, G.A., Wilson, E., and Davis, M.J. (2001). Regulation of the L-type Calcium Channel by $\alpha_5\beta_1$ Integrin Requires Signaling between Focal Adhesion Proteins. *J. Biol. Chem.* *276*, 30285–30292.

Xiang, Y., and Wang, Y. (2011). New components of the Golgi matrix. *Cell Tissue Res.* *344*, 365–379.

Xiang, Y., Zhang, X., Nix, D.B., Katoh, T., Aoki, K., Tiemeyer, M., and Wang, Y. (2013). Regulation of protein glycosylation and sorting by the Golgi matrix proteins GRASP55/65. *Nat. Commun.* *4*, 1659.

Yadav, S., and Linstedt, A.D. (2011a). Golgi Positioning. *Cold Spring Harb. Perspect. Biol.* *3*, a005322–a005322.

Yadav, S., Puri, S., and Linstedt, A.D. (2009). A Primary Role for Golgi Positioning in Directed Secretion, Cell Polarity, and Wound Healing. *Mol. Biol. Cell* *20*, 1728–1736.

Yadav, S., Puthenvedu, M.A., and Linstedt, A.D. (2012). Golgin160 Recruits the Dynein Motor to Position the Golgi Apparatus. *Dev. Cell* *23*, 153–165.

Yin, Y.X., Shen, F., Pei, H., Ding, Y., Zhao, H., Zhao, M., and Chen, Q. (2012). Increased expression of Rab25 in breast cancer correlates with lymphatic metastasis. *Tumor Biol.* *33*, 1581–1587.

van Zanten, T.S., Cambi, A., Koopman, M., Joosten, B., Figdor, C.G., and Garcia-Parajo, M.F. (2009). Hotspots of GPI-anchored proteins and integrin nanoclusters function as nucleation sites for cell adhesion. *Proc. Natl. Acad. Sci. U. S. A.* *106*, 18557–18562.

Zhang, L., and Ten Hagen, K.G. (2010). Dissecting the biological role of mucin-type O-glycosylation using RNA interference in Drosophila cell culture. *J. Biol. Chem.* *285*, 34477–34484.

Zhao, X., Lasell, T.K.R., and Melançon, P. (2002). Localization of large ADP-ribosylation factor-guanine nucleotide exchange factors to different Golgi compartments: evidence for distinct functions in protein traffic. *Mol. Biol. Cell* *13*, 119–133.

Zhu, J., Motejlek, K., Wang, D., Zang, K., Schmidt, A., and Reichardt, L.F. (2002). beta8

integrins are required for vascular morphogenesis in mouse embryos. *Development* 129, 2891–2903.